

PROCESS DESIGN AND EVALUATION OF VALUE-ADDED CHEMICAL PRODUCTION FROM
CRUDE GLYCEROL OBTAINED FROM BIODIESEL INDUSTRY



A Dissertation Submitted in Partial Fulfillment of the Requirements
for the Degree of Doctor of Engineering in Chemical Engineering
Department of Chemical Engineering
Faculty Of Engineering
Chulalongkorn University
Academic Year 2023

การออกแบบและประเมินกระบวนการผลิตสารเคมีมูลค่าเพิ่มจากกลีเซอรอลดิบที่ได้จาก
อุตสาหกรรมไบโอดีเซล



วิทยานิพนธ์นี้เป็นส่วนหนึ่งของการศึกษาตามหลักสูตรปริญญาวิศวกรรมศาสตรดุษฎีบัณฑิต
สาขาวิชาวิศวกรรมเคมี ภาควิชาวิศวกรรมเคมี
คณะวิศวกรรมศาสตร์ จุฬาลงกรณ์มหาวิทยาลัย
ปีการศึกษา 2566

Thesis Title	PROCESS DESIGN AND EVALUATION OF VALUE-ADDED CHEMICAL PRODUCTION FROM CRUDE GLYCEROL OBTAINED FROM BIODIESEL INDUSTRY
By	Miss Piyawan Thanahiranya
Field of Study	Chemical Engineering
Thesis Advisor	Professor SUTTICHAJ ASSABUMRUNGRAT, Ph.D.
Thesis Co Advisor	Assistant Professor PONGTORN CHAROENSUPPANIMIT, Ph.D.

Accepted by the FACULTY OF ENGINEERING, Chulalongkorn University in
Partial Fulfillment of the Requirement for the Doctor of Engineering

..... Dean of the FACULTY OF
ENGINEERING
(Professor SUPOT TEACHAVORASINSKUN, D.Eng.)

DISSERTATION COMMITTEE

..... Chairman
(Associate Professor Worapon Kiatkittipong, D.Eng.)

..... Thesis Advisor
(Professor SUTTICHAJ ASSABUMRUNGRAT, Ph.D.)

..... Thesis Co-Advisor
(Assistant Professor PONGTORN CHAROENSUPPANIMIT,
Ph.D.)

..... Examiner
(Dr. AKAWAT SRIRISUK, Ph.D.)

..... Examiner
(Associate Professor PATTARAPORN KIM, Ph.D.)

..... Examiner
(Associate Professor AMORNCHAI ARPORNWICHANOP,
D.Eng.)

ปิยวรรณ ณะหิรัญญา : การออกแบบและประเมินกระบวนการผลิตสารเคมีมูลค่าเพิ่มจากกลีเซอรอลดิบที่ได้จากอุตสาหกรรมไบโอดีเซล. (PROCESS DESIGN AND EVALUATION OF VALUE-ADDED CHEMICAL PRODUCTION FROM CRUDE GLYCEROL OBTAINED FROM BIODIESEL INDUSTRY) อ.ที่ปรึกษาหลัก : ศ. ดร.สุทธิชัย อัสสะบารุจรัตน์, อ.ที่ปรึกษาร่วม : ผศ. ดร.พงศ์ธร เจริญคุณนิมิตร

กลีเซอรอลที่เป็นผลพลอยได้จากอุตสาหกรรมไบโอดีเซลได้ถูกนำไปใช้เป็นวัตถุดิบตั้งต้นในการผลิตสารเคมีที่มีมูลค่าเพิ่มมากขึ้น การศึกษานี้มีวัตถุประสงค์เพื่อจำลองการผลิตสารเคมีมูลค่าเพิ่มผ่านกระบวนการหมักของกลีเซอรอลไปเป็นกรดโพรพิโอนิก กรดซักซินิก และไดไฮดรอกซีอะซิโตน กรณีการผลิตกรดโพรพิโอนิก งานนี้ได้พิจารณาการเลือกสารเจือจาง สารสกัด รวมถึงเทคนิคในขั้นตอนการสกัดกลับ ขณะที่เทคนิคของกระบวนการสกัดแบบมีปฏิกิริยาและการตกผลึกโดยตรง รวมถึงการใช้ไดเมทิลซัลฟอกไซด์เป็นตัวรับอเล็กตรอนสำหรับการผลิตกรดซักซินิกก็ถูกดำเนินการเช่นกัน นอกจากนี้ยังมีการตรวจสอบผลกระทบของประเภทแหล่งคาร์บอนและประเภทกลีเซอรอลต่อผลผลิตไดไฮดรอกซีอะซิโตน โดยสถานการณ์ทั้งหมดได้รับการประเมินทั้งในด้านของการใช้กลีเซอรอล ประสิทธิภาพทางเศรษฐศาสตร์ การใช้พลังงาน และผลกระทบต่อสิ่งแวดล้อม จากผลการจำลองกระบวนการพบว่าการใช้ออกทานอลเป็นสารเจือจางสามารถนำไปสู่การผลิตกรดโพรพิโอนิกได้อย่างมีประสิทธิภาพ ส่งผลให้ประหยัดต้นทุนได้ประมาณ 5.45 ล้านเหรียญสหรัฐต่อปี และลดการปล่อยก๊าซคาร์บอนไดออกไซด์ได้ถึง 34% เมื่อเทียบกับการผลิตจากปิโตรเลียม นอกจากนี้ผลลัพธ์ที่ได้บ่งชี้ว่าการเติม DMSO ในการหมักเป็นกุญแจสำคัญสำหรับการผลิตกรดซักซินิกทางชีวภาพ โดยทำกำไรดีที่สุดที่ DPV 190 ล้านเหรียญสหรัฐ DCFROR 33.3% และระยะเวลาคืนทุน 4.48 ปี อีกทั้งการศึกษานี้ยังเผยให้เห็นว่าการเติมซอร์บิทอลเพื่อเป็นแหล่งคาร์บอนทุติยภูมิสำหรับการผลิตไดไฮดรอกซีอะซิโตนเป็นวิธีที่คุ้มค่าที่สุดและเป็นมิตรต่อสิ่งแวดล้อม โดยการออกแบบเครือข่ายพลังงานเพื่อปรับปรุงกระบวนการผลิตไดไฮดรอกซีอะซิโตนทางชีวภาพช่วยประหยัดพลังงานโดยรวมได้ถึง 52-58%

สาขาวิชา วิศวกรรมเคมี
ปีการศึกษา 2566

ลายมือชื่อนิสิต
ลายมือชื่อ อ.ที่ปรึกษาหลัก
ลายมือชื่อ อ.ที่ปรึกษาร่วม

6171442121 : MAJOR CHEMICAL ENGINEERING

KEYWORD: Glycerol utilization, Process design, Sustainability assessment

Piyawan Thanahiranya : PROCESS DESIGN AND EVALUATION OF VALUE-ADDED CHEMICAL PRODUCTION FROM CRUDE GLYCEROL OBTAINED FROM BIODIESEL INDUSTRY. Advisor: Prof. SUTTICHAJ ASSABUMRUNGRAT, Ph.D. Co-advisor: Asst. Prof. PONGTORN CHAROENSUPPANIMIT, Ph.D.

Excessive glycerol, a major by-product of biodiesel industry, has been increasingly utilized as a platform chemical feedstock for production of value-added chemicals. Accordingly, this study aims to simulate the productions of propionic acid (PA), succinic acid (SA), and dihydroxyacetone (DHA) from glycerol via fermentation. For PA production, diluents and extractants as well as techniques in the back-extraction are investigated, whereas the techniques of reactive extraction and direct crystallization, as well as the use of dimethyl sulfoxide (DMSO) as an electron acceptor for SA production are investigated. Meanwhile, the effects of carbon source types and glycerol types on the DHA productivity are investigated. All scenarios are evaluated based on glycerol utilization, economic performance, energy utilization, and environmental impacts. According to the simulated results, using 2-octanol as diluent can lead to the efficient production of PA. This results in cost savings of about 5.45 million USD/y and a significant reduction of CO₂ emissions by 34% compared to petroleum-based production. Furthermore, the obtained results indicate that the addition of DMSO in the fermentation is key for the bio-based SA production – the best profit of 190 million USD of DPV, 33.3% of DCFROR, and 4.48 years of DPP are estimated. In addition, this study reveals that the addition of sorbitol as the secondary carbon source for DHA production was the most cost-effective and environmentally friendly. The heat integration is also investigated to improve the bio-based DHA production, which increases the total energy savings by 52–58%.

Field of Study: Chemical Engineering

Student's Signature

Academic Year: 2023

Advisor's Signature

Co-advisor's Signature

ACKNOWLEDGEMENTS

I take this opportunity to express my sincere gratitude to every support and guidance for this thesis. First, I am extremely grateful to my thesis advisor, Prof. Suttichai Assabumrungrat and co-advisor, Asst. Prof. Pongtorn Charoensuppanimit for their invaluable advice, continuous support, and patience throughout my years of study and through the process of researching and writing this thesis. Their expertise and encouragement helped me to complete this research. Without their assistance and dedicated involvement in every step throughout the process, this project would have never been accomplished.

Moreover, I would like to extend my sincere thanks to Prof. Jhuma Sadhukhan for sharing expertise, and sincere and valuable guidance and encouragement extended to me throughout my research at the University of Surrey.

I am also thankful to the chairman, Assoc. Prof. Worapon Kiatkittipong and committee members, Dr. Akawat Sirisuk, Assoc. Prof. Pattaraporn Kim, and Assoc. Prof. Amornchai Arpornwichanop for their insightful comments and suggestions.

I gratefully acknowledge the funding received towards my PhD from the Thailand Science Research and Innovation Fund, Chulalongkorn University. I also would like to acknowledge the Thailand Science Research and Innovation (TSRI), and the Graduate School Chulalongkorn University with the Faculty of Engineering for financial support. I also would like to acknowledge the NSRF via the Program Management Unit from Human Resources & Institutional Development, Research and Innovation.

Thanks to my friends for their encouragement all through my studies.

Most importantly, none of this could have happened without my parents, who endured this long process with me, always offering support and love.

Piyawan Thanahiranya

TABLE OF CONTENTS

	Page
.....	iii
ABSTRACT (THAI).....	iii
.....	iv
ABSTRACT (ENGLISH).....	iv
ACKNOWLEDGEMENTS	v
TABLE OF CONTENTS.....	vi
LIST OF TABLES.....	xi
LIST OF FIGURES	xiv
LIST OF NOMENCLATURE	xvi
CHAPTER 1 INTRODUCTION	1
1.1 Background and problem statement.....	1
1.2 Research objective.....	7
1.3 Scope of research.....	7
1.4 Expected outcomes.....	8
CHAPTER 2 FUNDAMENTAL THEORY AND LITERATURE REVIEWS.....	9
2.1 Fundamentals.....	9
2.1.1 Biodiesel	9
2.1.1.1 Overview of biodiesel.....	9
2.1.1.2 Biodiesel production via transesterification	11
2.1.2 Glycerol.....	12
2.1.2.1 Glycerol grades	13

2.1.2.2 Refining of crude glycerol.....	14
2.1.2.3 Applications of glycerol.....	16
2.1.3 Propionic acid (PA).....	24
2.1.4 Succinic acid (SA).....	26
2.1.5 Dihydroxyacetone (DHA).....	29
2.2 Literature reviews.....	31
2.2.1 Propionic acid (PA).....	32
2.2.2 Succinic acid (SA).....	33
2.2.3 Dihydroxyacetone (DHA).....	36
2.2.4 Sustainability assessment.....	37
CHAPTER 3 METHODOLOGY.....	40
3.1 Process simulation.....	40
3.2 Process evaluation.....	43
3.2.1 Glycerol and carbon utilization efficiencies.....	44
3.2.2 Economic performance.....	44
3.2.3 Energy utilization.....	47
3.2.4 Exergy analysis.....	47
3.2.5 Environmental impacts.....	50
CHAPTER 4 SUSTAINABLE PROCESS DESIGN OF PROPIONIC ACID PRODUCTION FROM GLYCEROL: A COMPARATIVE STUDY OF BIO-BASED AND PETROLEUM-BASED TECHNOLOGIES.....	52
4.1 Process description of propionic acid production.....	52
4.1.1 Scenario I (extractant: TOA, diluent: MIBK and back-extraction: temperature-swing regeneration).....	54

4.1.2 Scenario II (extractant: TOA, diluent: MIBK, back-extraction: utilization of TMA)	57
4.1.3 Scenario III (extractant: TOA, diluent: 2-octanol, back-extraction: utilization of TMA)	58
4.1.4 Scenario IV (propionic acid production from the petroleum-based feedstock).....	59
4.2 Process evaluation	60
4.2.1 Representation of selected thermodynamic model	60
4.2.2 Glycerol utilization.....	61
4.2.3 Energy utilization.....	62
4.2.4 Economic performance	63
4.2.5 CO ₂ equivalent emissions	66
4.3 Process sensitivity.....	68
CHAPTER 5 SUCCINIC ACID PRODUCTION FROM GLYCEROL BY <i>ACTINOBACILLUS SUCCINOGENES</i> : TECHNO-ECONOMIC, ENVIRONMENTAL, AND EXERGY ANALYSES	
5.1 Process description of succinic acid production.....	69
5.1.1 Scenario I: SA purification using direct crystallization (no addition of DMSO)	70
5.1.2 Scenario II: SA purification using reactive extraction (no addition of DMSO)	72
5.1.3 Scenario III: SA purification using direct crystallization (addition of DMSO)	73
5.1.4 Scenario IV: SA purification using reactive extraction (addition of DMSO)	74
5.2 Process evaluation	74
5.2.1 Glycerol and carbon utilization	74
5.2.2 Economic performance	75

5.2.3 Energy utilization.....	77
5.2.4 Exergy analysis.....	78
5.2.5 Greenhouse gas emissions	80
5.3 Comparison between bio-based and petroleum-based SA production.....	81
5.4 Process sensitivity.....	82
5.4.1 Effect of feedstock and product prices on DPV	82
5.4.2 Effect of SA production capacity on economic indicators.....	83
CHAPTER 6 SUSTAINABILITY ASSESSMENT OF DIHYDROXYACETONE (DHA) PRODUCTION FROM GLYCEROL: A COMPARATIVE STUDY BETWEEN BIOLOGICAL AND CATALYTIC OXIDATION ROUTES.....	
6.1 Process description of dihydroxyacetone production.....	85
6.1.1 Biological route	87
6.1.2 Chemical route (catalytic oxidation).....	91
6.2 Process evaluation.....	92
6.2.1 Glycerol and carbon utilization efficiencies	92
6.2.2 Energy utilization efficiency	93
6.2.3 Economic performance	94
6.2.4 Environmental impacts.....	96
6.3 Heat integration	98
6.4 Process sensitivity.....	102
CHAPTER 7 CONCLUSIONS AND RECOMMENDATIONS	
7.1 Conclusions	104
7.1.1 Propionic acid production.....	104
7.1.2 Succinic acid production	105

7.1.3 Dihydroxyacetone production.....	105
7.2 Recommendations for future works.....	106
REFERENCES	108
APPENDIX A GROSS PROFIT MARGIN ANALYSIS.....	130
APPENDIX B SUPPLEMENTARY INFORMATION OF CHAPTER 4	132
APPENDIX C SUPPLEMENTARY INFORMATION OF CHAPTER 5	168
APPENDIX D SUPPLEMENTARY INFORMATION OF CHAPTER 6	207
VITA.....	257



LIST OF TABLES

	Page
Table 2.1 Biodiesel production ranking and major feedstock in 2022 [63].....	10
Table 2.2 Biodiesel price of using different feedstocks [64]	10
Table 2.3 Chemical compositions of crude glycerol from various feedstocks [66] ...	13
Table 2.4 Properties of the different glycerol grades [44, 64, 68]	13
Table 2.5 Comparison of four deep refining technologies [66].....	15
Table 2.6 List of chemicals from glycerol by different chemical reactions.....	19
Table 2.7 List of chemicals from glycerol by fermentation process with different microorganisms	21
Table 2.8 Global overview of the state of production facilities of different chemicals [76, 109].....	22
Table 2.9 Properties of propionic acid [116]	24
Table 2.10 Propionic acid from different carbon sources and microbial strains	26
Table 2.11 Properties of succinic acid [116].....	27
Table 2.12 Succinic acid from different carbon sources and microbial strains.....	29
Table 2.13 Properties of dihydroxyacetone [116]	30
Table 2.14 Dihydroxyacetone produced from different carbon sources and microbial strains	31
Table 2.15 Biomass ranking in terms of feasibility on a commercial scale [139]	33
Table 3.1 General investment parameters for economic analysis	45
Table 3.2 Summary of the prices of utilities	45
Table 3.3 Summary of raw material and product prices	46
Table 4.1 Key attributes in Scenarios I to IV for propionic acid production	53

Table 4.2 Summary of optimum diluent [181]	58
Table 4.3 Summary of reactions involved in petroleum-based production of propionic acid.....	60
Table 4.4 Summary of glycerol utilization for propionic acid production scenarios ..	61
Table 4.5 Summary of energy utilization for propionic acid production scenarios	62
Table 4.6 Summary of economic performance for propionic acid production scenarios.....	64
Table 4.7 Comparison of hotspots for propionic acid production scenarios	65
Table 4.8 Summary of total capital investment for propionic acid production scenarios.....	65
Table 4.9 Summary of emissions of CO ₂ equivalence (cradle to gate) for propionic acid production.....	67
Table 5.1 Key attributes in Scenarios I to IV of glycerol-based production.....	70
Table 5.2 Summary of glycerol utilization for bio-based production scenarios.....	75
Table 5.3 Summary of carbon utilization for bio-based production scenarios.....	75
Table 5.4 Summary of economic performance for bio-based production scenarios.	76
Table 5.5 Comparison of the most expensive equipment in each scenario.....	77
Table 5.6 Summary of energy utilization for bio-based production scenarios	77
Table 5.7 Summary of exergy analysis for Scenario III	79
Table 5.8 Summary of emission of CO ₂ equivalence (cradle to gate) for bio-based production scenarios.....	80
Table 5.9 Comparison between glycerol-based and petroleum-based SA production	81
Table 5.10 The economic indicators with a different succinic acid capacity of Scenario III	84
Table 6.1 Overview of Scenarios I to VI for DHA production	86

Table 6.2 Summary of reactions involved in catalytic oxidation.....	91
Table 6.3 Summary of glycerol utilization for DHA production scenarios	92
Table 6.4 Summary of carbon utilization for DHA production scenarios	93
Table 6.5 Summary of energy utilization for DHA production scenarios	94
Table 6.6 Summary of economic performance for DHA production scenarios	95
Table 6.7 Comparison of hotspot in each scenario for DHA production	96
Table 6.8 Summary of environmental impacts (Cradle to gate).....	98
Table 6.9 Summary of energy utilization after HEN.....	100
Table 6.10 Summary of economic performance after HEN	101
Table 6.11 Summary of environmental impacts after HEN.....	101



LIST OF FIGURES

	Page
Figure 1.1 Potential chemicals producible from glycerol	2
Figure 2.1 Schematic diagram for biodiesel production.....	11
Figure 2.2 Transesterification of triglyceride with methanol [64]	11
Figure 2.3 Simplified flow chart of biodiesel and glycerol [67]	12
Figure 2.4 A general refining process of crude glycerol	14
Figure 2.5 Chemical structures and prices of propionic acid derivatives [27]	25
Figure 2.6 Some chemicals produced from succinic acid [14]	27
Figure 3.1 Superstructure for the production of value-added chemicals from glycerol including propionic acid, succinic acid, and dihydroxyacetone.....	41
Figure 3.2 Simulation of the reactive extraction unit in Aspen Plus	42
Figure 3.3 Aspen simulation of the crystallizer model.....	43
Figure 3.4 Aspen simulation of RadFrac model	43
Figure 3.5 The “Equipment Selection” window to modify the equipment type.....	45
Figure 3.6 Utilities related to equipment	47
Figure 3.7 Exergy calculation in the “Property Sets” folder	49
Figure 3.8 Select property sets in the “Report Options” menu	50
Figure 3.9 Life cycle assessment of chemical production.....	50
Figure 3.10 The life cycle inventory data in SimaPro	51
Figure 4.1 The shift of PA feed composition after the temperature-swing-regeneration applied.....	54
Figure 4.2 General block flow diagram of bio-based PA production.....	55
Figure 4.3 General block flow diagram of petroleum-based PA production	59

Figure 4.4 Representation of propionic acid/water vapor-liquid equilibrium system using UNIFAC model	61
Figure 4.5 Diagram with relevant parameters of glycerol-based process.....	66
Figure 4.6 Diagram with relevant parameters of petroleum-based process.....	66
Figure 4.7 Effect of the price of Scenario III on DPV for propionic acid production....	68
Figure 5.1 General block flow diagram of bio-based SA production.....	71
Figure 5.2 Effect of the utility duty of the bio-based succinic acid production: (a) Scenario I, (b) Scenario II, (c) Scenario III, and (d) Scenario IV	78
Figure 5.3 Effect of the price of Scenario III on DPV for succinic acid production	83
Figure 6.1 Overview of the framework in the design of DHA production.....	86
Figure 6.2 General block flow diagram of DHA production.....	88
Figure 6.3 Process flow diagram of DHA production.....	89
Figure 6.4 Diagram with relevant parameters of the glycerol-based DHA production	97
Figure 6.5 The composite curve of Scenario V	99
Figure 6.6 Heat integration of DHA production via the fermentation process	100
Figure 6.7 Summary of all assessments of DHA production	102
Figure 6.8 Effect of the price of Scenario V on DPV.....	103
Figure 6.9 Effect of the origins of glycerol on environmental impacts.....	103

LIST OF NOMENCLATURE

Symbols/Parameters

A^-	anion of acid
CF	cash flow
$CO_{2\text{-eq}}$	CO_2 equivalence
E	degree of extraction
ex	specific exergy (kJ/kg)
$\dot{E}x$	exergy flow rate (kW)
$\dot{E}x_d$	exergy destruction (kW)
HA	carboxylic acid
H^+	proton
h	specific enthalpy (kJ/kg)
K_D	distribution coefficient
K_E	extraction equilibrium constant
\dot{m}	mass flow rate (kg/h)
\dot{Q}	heat transfer rate (kW)
R	gas constant (kJ/kmol K)
R_3N	tertiary amine
s	specific entropy (kJ/kg K)
\dot{W}	work transfer rate (kW)
y_D	irreversibility (%)
y_j	mole fraction of component j
Ψ	exergy efficiency (%)

Abbreviations

AA	acetic acid
CAGR	compounded annual growth rate
DCFROR	discounted cash flow rate of return
DHA	dihydroxyacetone
DMF	dimethylformamide
DPP	discounted payback period
DPV	discounted present value
GCA	glycolic acid
GHG	greenhouse gas emissions
HEN	heat exchanger network
LCA	life cycle assessment
MIBK	methyl isobutyl ketone
MONG	matter organic non-glycerol
MT	mega tonne
NP	nickel propionate
OXA	oxalic acid
PA	propionic acid
SA	succinic acid
SACRYS	succinic acid (solid form)
SEC	specific energy consumption
TOA	trioctylamine
TMA	trimethylamine

CHAPTER 1

INTRODUCTION

1.1 Background and problem statement

Renewable energy is gaining attention as a consequence of the ever-increasing global energy demand and greenhouse gas emissions from the combustion of fossil fuels [1]. To reduce reliance on imports of fossil fuels, industries are attempting to develop and use domestically produced renewable energy, especially in the transportation sector [2]. In Thailand, the target for reducing CO₂ emissions from the energy and transportation sectors has been anticipated to be reduced to 113 million tonnes of CO₂ by 2035 [3]. One important strategy to accomplish CO₂ emissions reduction is the utilization of biofuels. Most of the existing technologies are mainly focused on the production of fatty acid methyl ester (FAME) or biodiesel since it causes less environmental impact compared to fossil fuels [4-6].

The world production capacity of biodiesel is about 41 billion liters in 2019 and is anticipated to increase to about 50 billion liters by 2030 [7]. Thailand is an agricultural country with advantages in raw materials such as palm oil, which can be used as feedstock for the production of biodiesel [4]. Biodiesel production has piqued the interest of entrepreneurs in the palm oil sector. In addition, the Thai government has a policy to promote the production and use of biodiesel [8]. Therefore, the development of the biodiesel industry plays an important role in increasing the economic benefits.

Biodiesel is commonly produced through the transesterification process of either animal or vegetable fats [9]. The main by-product from this process is glycerol which is typically obtained at approximately 1 kg of glycerol per 10 kg of biodiesel produced [10]. The size of the global glycerol market, which is at 2.8 MT in 2020, is expected to reach 4 MT by 2027 [11]. Given the high volume of biodiesel production, a large amount of glycerol is produced. Currently, the size of the glycerol market

cannot support the large surplus of glycerol [12]. This is one of the major issues in biodiesel production that still requires wise management to improve its sustainability.

Glycerol has a wide range of applications. It is traditionally used in the pharmaceutical, cosmetic, personal care products, and food industries [13, 14]. Many researchers have paid attention to glycerol management through the synthesis of valuable chemicals via biological, thermochemical, and catalytic conversion pathways as given in Figure 1.1. In general, the thermochemical conversion pathway could deal with a large amount of excessive glycerol. However, the thermal degradation of glycerol could lead to emissions of toxic gases that are harmful to the environment [12]. Regarding the catalytic conversion pathway, it offers higher conversion of glycerol and higher selectivity of valuable products, compared to the other pathways. Nevertheless, the extreme operating conditions could lead to safety and environmental concerns [15-21]. Alternatively, glycerol conversion via the biological conversion pathway could be attractive given its milder operating conditions (about the atmospheric condition) and its better eco-friendliness due to less CO₂ emissions [12]. Accordingly, glycerol conversion via the biological pathway was the focus in our work.

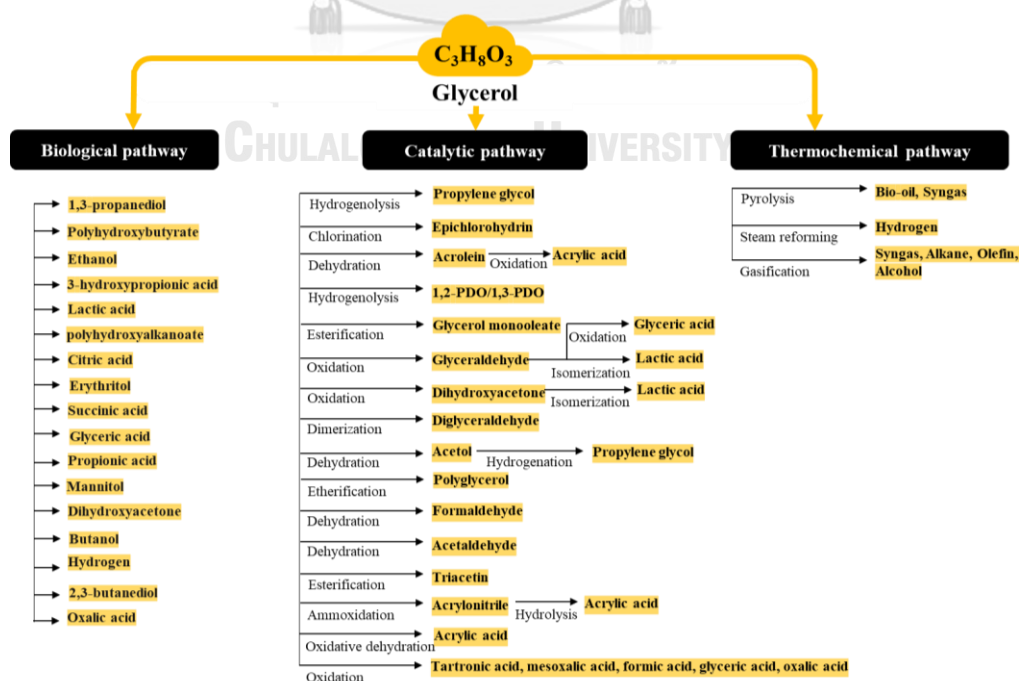


Figure 1.1 Potential chemicals producible from glycerol

Glycerol could be used as a raw material in fermentation and anaerobic digestion to produce valuable chemicals since microorganisms could use glycerol as their carbon and energy sources. The utilization of glycerol also offers other advantages including, 1) glycerol is readily available and the pretreatment process of refined glycerol is not as complex as those pretreatments found in the lignocellulosic biomass (2nd generation feedstock), and 2) the utilization of glycerol does not engage in the food-fuel competition as faced by the 1st generation feedstock. Accordingly, sugars, e.g., glucose, xylose, and sorbitol that can be attained from the first and second generation feedstocks could be replaced with glycerol to produce valuable chemicals via fermentation [22, 23].

Regarding the fermentation of glycerol, a wide range of chemicals can be synthesized by this process such as 1,3-propanediol, lactic acid, propionic acid, succinic acid, etc. [6, 24-26]. These chemicals are used in a broad variety of industries. Chemicals that have the potential to be produced from glycerol must be feasible for their production and have the potential to replace products from the petrochemical industry. The selection of the appropriate chemicals produced from glycerol depends on the technological know-how, market demand, application, and production cost. Initially, we calculated the gross profit margin of each alternative, as present in Appendix A. From the analysis results, there are three chemicals with high gross profit margins, including propionic acid, succinic acid, and dihydroxyacetone.

Ranked as one of the top thirty platform chemicals [27], propionic acid (PA) and its derivatives could be converted into valuable chemicals and biomaterials [28]. Currently, the existing technology of PA synthesis employs petroleum-based feedstock. Although the petroleum-based technology provides a higher conversion of glycerol and a higher selectivity of PA, this technology depends on the non-renewable feedstock which is not sustainable in long term. Thus, to align with the attempt to replace the petroleum-based feedstock, PA should be produced alternatively via fermentation of glycerol.

The fermentation of glycerol for the PA production is influenced by several factors. Among all types of bacteria, *Propionibacterium* [29] exhibited the highest

efficacy to produce PA which had been shown promising for industrial applications. Apart from the fermentation technology, acid-recovery technologies also play key roles in the production of carboxylic acids (e.g., propionic acid, succinic acid, and lactic acid) [30, 31]. Specific to PA production, the recovery of PA containing in the fermentation broth (about 2 wt% of PA) could not be undertaken by conventional techniques. For example, the conventional distillation could not be utilized since PA and water form a minimum-boiling azeotrope [32].

Therefore, advanced techniques for the acid recovery are required to recover PA effectively, which directly affects the overall process economics [33, 34]. Regarding the acid recovery process, there are several methods for the efficient recovery of dilute propionic acids in aqueous solutions. Such methods include an electrodialysis, a reverse osmosis, an adsorption, an anion exchange, as well as a reactive extraction [33, 35]. Among these technologies, the reactive extraction has received the most attention for the recovery of organic acids [10, 36-38].

In the reactive extraction, there are two steps involved: the forward and the backward steps. Initially, an extractant and a diluent were present in the organic phase whereas a propionic acid and other by-products were present in the aqueous phase. In the forward step, the extractant (generally organic compounds such as amines) reacts with the propionic acid to form the organic complex that can dissolve in the organic phase. The organic phase containing the organic complex is sent to the backward step. In this step, the organic complex is cleaved using various back-extraction techniques, including a utilization of NaOH, a temperature-swing regeneration, a diluent-swing regeneration, and a utilization of trimethylamine (TMA) to recover the reusable extractant and the salable propionic acid [36, 37, 39].

In fact, the appropriate selection of diluent and extractant pair as well as the back-extraction technique in the reactive extraction are especially important when the reactive extraction is considered for upscaling to a commercial level. To facilitate the selection that accounts for these factors, a process simulation is employed in this work.

Meanwhile, the conversion of glycerol to succinic acid (SA) has received growing attention [26, 30, 40, 41] due to its versatility and its intriguing market growth [42]. SA is a crucial chemical since it is typically used in a variety of industrial processes including the production of biodegradable plastics, food, pharmaceuticals, and chemical industries [43-45]. Nowadays, petroleum is the primary source of SA production through the hydrogenation of maleic anhydride [31]. However, bacterial fermentation provides various advantages over the petroleum pathway, including milder operating conditions, a greener approach, and lower GHG emissions [46].

Glycerol can be used as a substrate for the SA production. However, the redox imbalance during cell growth hindered the application of microorganisms in the production of SA. To increase the rate, the addition of external electron acceptors was found effective as evidenced in *A. succinogenes* according to Carvalho et al. [23]. Dimethyl sulfoxide (DMSO) was found to be a highly effective electron acceptor, leading to a significant boost in both SA synthesis and glycerol consumption [23]. Furthermore, DMSO is a non-toxic commercial organic solvent. Its usage has increased for pharmaceutical and electronics manufacturing purposes [47]. Additionally, DMSO is inexpensive as it is a by-product of kraft paper manufacturing [48]. The price of DMSO is about 0.267 USD per kg [49]. Therefore, the addition of DMSO in SA production could be cost-effective and environmentally friendly.

In addition to the upstream process, the separation and purification of SA obtained from the fermentation broth also needs careful investigation. According to Cok et al. [50] and Morales et al. [31], the two promising technologies of SA purification, e.g., reactive extraction and direct crystallization were proposed. To assess this, the simulation of bio-based SA production is developed in this work along with the sustainability assessment tools to identify hotspots of the bio-based SA such that further enhancement could be undertaken.

Moreover, the conversion of glycerol to 1,3-dihydroxyacetone (DHA) is focused in this work due to the attractive market growth and the high price of DHA [51, 52]. DHA is a specialty chemical, used as an effective ingredient in sunless tanning products [53]. DHA also serves as a building block for chemicals synthesis

such as lactic acid [30]. DHA can be produced from glycerol using either chemical (catalytic oxidation) or biological routes [54]. Commercial synthesis of DHA is preferred via the biological route as compared to the chemical route due to the nature of their microorganisms and the mild process environment [55, 56]. Although the biological route can give excellent DHA selectivity, they have some limitations. The main challenge of DHA production is the inhibitory effect on bacterial growth due to the high concentrations of glycerol, leading to the low DHA production capacity [57, 58].

To improve the bacterial growth rate, recent studies attempted to add secondary carbon sources such as sugars. According to Lu et al. [55] and Liebminger's work [59], the growth efficiency of *Gluconobacter* strains was greatly enhanced by growing the strains in a medium, containing glucose and sorbitol as the secondary carbon sources. By considering these works, it can be inferred that the addition of secondary carbon sources can be beneficial for cost reduction. To prove this inference, process simulation is needed.

Given the useful properties of these three chemicals, their biological synthesis can be a promising candidate for the development of a sustainable process that can help solve the problem of glycerol surplus. Nevertheless, approaches and technologies for using glycerol to produce these chemicals are still lacking. Also, their purification is a challenge in biological processes. This is because the purification requires high energy and costs, making it an economic disadvantage compared to the chemical processes [33, 34]. Consequently, the concept of process design and comparing it to existing processes is an excellent tool for increasing the profitability of the biodiesel industry.

As mentioned above, this study aims to identify the promising technology for the productions of value-added chemicals from glycerol. This study has been divided into three parts including 1) sustainable process design of propionic acid production by *Propionibacterium acidipropionici*, 2) succinic acid production from glycerol by *Actinobacillus succinogenes*: techno-economic, environmental, and exergy analyses,

and 3) process design and evaluation of the production of dihydroxyacetone. The optimum scenarios of each process are compared with the conventional process.

The process model of glycerol-derived biochemical processes is expected to serve as a guideline for reassurance to the biodiesel plants for further investment in the development of by-products. It is also expected that this process model could be used to assist entrepreneurs in selecting technologies developed from this work to increase their competitiveness and enhance the economy of the industry.

1.2 Research objective

To design and evaluate the productions of value-added chemicals from glycerol, including propionic acid, succinic acid, and dihydroxyacetone as sustainable alternatives for biodiesel industry using computer-aided tools.

1.3 Scope of research

- 1.3.1 Design possible processes for the productions of value-added chemicals from glycerol based on research data related to production technologies.
- 1.3.2 Create a process model to assist in decision-making for optimal process selection using the Aspen Plus® program.
- 1.3.3 Assess the economic performance of the designed processes in terms of discounted present value (DPV), discounted payback period (DPP), and discounted cash flow rate of return (DCFROR).
- 1.3.4 Assess the energy utilization of the designed processes in terms of specific energy consumption (SEC).
- 1.3.5 Assess the environmental impact of the designed processes in terms of CO₂ equivalent emission.
- 1.3.6 Improve the designed processes by enhancing the process efficiencies which can be conducted by identifying hotspots for further improvement.

1.4 Expected outcomes

- 1.4.1 To assist industry in decision-making the best alternatives for the designs of value-added biochemical productions from glycerol obtained from biodiesel industry.
- 1.4.2 To increase the competitiveness of the industry and lead to the development of the sustainable biodiesel industry in the future.
- 1.4.3 The development of the biodiesel industry by valorization of glycerol to the production of chemicals can reduce the environmental burden and disposal problem.



CHAPTER 2

FUNDAMENTAL THEORY AND LITERATURE REVIEWS

This chapter provides the necessary theory and the basic knowledge of value-added chemicals production from glycerol including background of biodiesel production, glycerol grades, refining of crude glycerol, applications of glycerol, propionic acid production, succinic acid production, and dihydroxyacetone production. It also provides literature reviews related to the development of chemical production for both upstream and downstream processing. Moreover, sustainability assessments are also reviewed to gain more understanding.

2.1 Fundamentals

2.1.1 Biodiesel

Biodiesel is an alternative fuel for fossil fuels. The ability to release air pollution in small quantities makes it more environmentally friendly than petroleum fuels [4]. Recently, Thailand has implemented the Renewable and Alternative Energy Development Plan with the objective of reducing dependence on conventional fuels [3]. There is a strategy to develop biofuels that can replace petroleum diesel, especially biodiesel from oil palm [60].

2.1.1.1 Overview of biodiesel

The global biodiesel production is around 41 billion liters in 2019 and is expected to be approximately 50 billion liters by 2030 [61]. In Thailand, biodiesel production is 1.4 billion liters in 2014 and is expected to be approximately 1.85 billion liters by 2027 [7]. Biodiesel can be produced from a variety of raw materials. Oleaginous crops are the most commonly utilized raw materials as shown in Table 2.1. In Europe, rapeseed is the main feedstock, whereas in the USA, Argentina, and Brazil, soybeans are the main feedstock. Palm oil also has a significant market in this biofuel from Indonesia, Colombia, and Thailand [62, 63].

Table 2.1 Biodiesel production ranking and major feedstock in 2022 [63]

Country	Production ranking (base period)	Major feedstock
United States	2 (18.3%)	Used cooking oils, soybean oil
European Union	1 (32.2%)	Rapeseed oil /Palm oil/ used cooking oils
Brazil	4 (12.3%)	Soybean oil
China	5 (3.6%)	Used cooking oils
India	15 (0.4%)	Used cooking oils
Canada	12 (0.7%)	Canola oil / used cooking oil/soybean oil
Indonesia	3 (17.6%)	Palm oil
Argentina	6 (3.3%)	Soybean oil
Thailand	7 (3.0%)	Palm oil
Colombia	10 (1.2%)	Palm oil
Paraguay	17 (0.02%)	Soybean oil

According to Table 2.2, the cost of biodiesel production is strongly reliant on raw material costs. The challenge of high raw material costs could be handled by using lower-cost feedstocks such as waste cooking oils [64].

The widespread use of biofuels in the future depends on the development of new production technologies to produce high quality transportation fuels from various agricultural feedstocks.

Table 2.2 Biodiesel price of using different feedstocks [64]

Feedstock	Oil Concentration (%w/w)	Price of Crude Feedstock (\$/ton)	Price of B100 Biodiesel (\$/ton)
Soybean	15–20	735	800–805
Rapeseed	38–46	815–829	940–965
Palm oil	45–55	610	720–750
Jatropha curcas	Seed 35–40 Kernel 50–60	-	400–500
Waste cooking oil	-	224–360	600

2.1.1.2 Biodiesel production via transesterification

Figure 2.1 depicts the schematic diagram for biodiesel production. The important steps in biodiesel production are oil extraction and transesterification. In oil extraction step, oleaginous crops are subjected to physical, chemical, or enzymatic treatments to extract the oil. The main product obtained is crude oil that is used as the main feedstock for biodiesel production through transesterification [65].

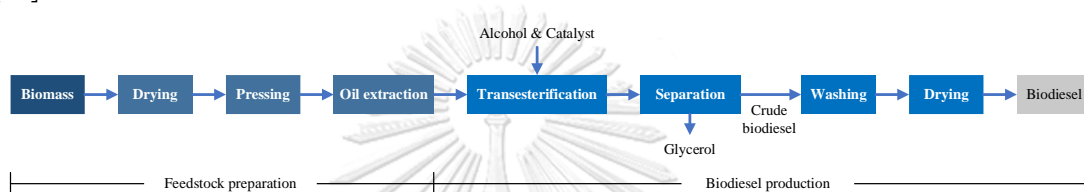


Figure 2.1 Schematic diagram for biodiesel production

Transesterification of triglycerides, as shown in Figure 2.2, is the most common method for biodiesel production from a variety of raw materials [9]. When triglycerides react with alcohol in the presence of a catalyst, biodiesel is produced as the main product and glycerol as a by-product. The most common types of alcohol used are ethanol or methanol, in particular methanol, which generally is less expensive and has a better reaction. Although the reaction requires three moles of alcohol per one mole of triglycerides, excess alcohol is required to shift the equilibrium towards products and achieve a high yield [14]. In general practice, the most recommended mole ratio is 6:1 of methanol to oil. After the reaction is completed, the excess methanol is recovered and recycled in the reaction process. The crude biodiesel is washed and dried under vacuum to achieve low moisture content of the final product [9].

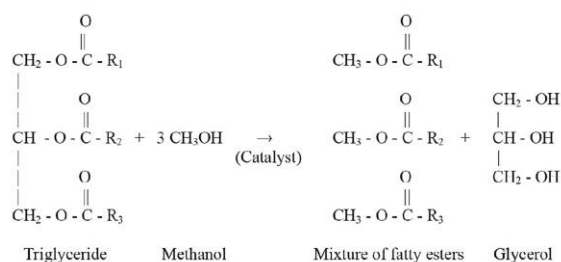


Figure 2.2 Transesterification of triglyceride with methanol [64]

2.1.2 Glycerol

Glycerol, also known as glycerin, is a by-product from the production of biodiesel through transesterification [44, 64]. Figure 2.3 shows the flow chart of biodiesel and glycerol production. Generally, for every three moles of methyl ester, one mole of glycerol is generated, which is approximately 10 wt% [64]. Glycerol is a colorless, odorless, viscous liquid soluble in different polar liquids, such as methanol, ethanol, isopropanol, and insoluble in fatty oils, hydrocarbons, and chlorinated solvents such as hexane, benzene and chloroform [45]. Crude glycerol is a mixture of glycerol and other contaminants such as water, methanol, soap, and matter organic nonglycerol (MONG). The components of crude glycerol vary depending on the feedstock, the process used for biodiesel production, and the post-treatment methods used [66]. Table 2.3 provides glycerol contents ranging from 20.0% to over 85.0% (w/w).

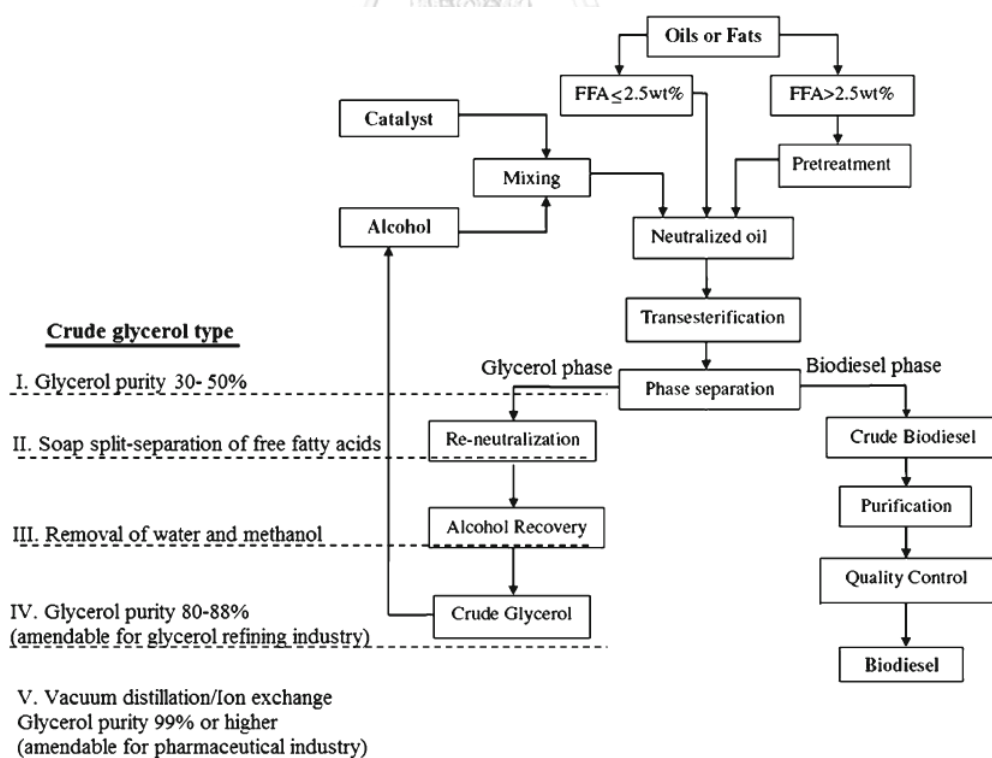


Figure 2.3 Simplified flow chart of biodiesel and glycerol [67]

Table 2.3 Chemical compositions of crude glycerol from various feedstocks [66]

Sources of crude glycerol		Glycerol	Methanol	Soap	MONG
Feedstock	Catalyst (w/w)	(w/w)	(w/w)	(w/w)	(w/w)
Soybean oil	KOH	62.0%	12.8%	25.2%	n/a
Chicken fat /soybean oil (50/50, w/w)	KOH	62.3%	14.4%	23.2%	n/a
Canola oil	NaOH	56.5%	28.3%	15.3%	n/a
Sunflower oil	0.5% NaOH	75.0%	1.0%	9.3%	n/a
Sunflower oil	0.5% NaOH	90.0%	<1.0%	n.d.	n/a
Seed oils	3.8-4.2% NaOCH ₃	62.5-76.6%	n/a	n/a	n/a
Soybean oil	n/a	63.0%	6.2%	n.d.	n.d.
Soybean oil	n/a	22.9%	10.9%	26.2%	23.5%
Soybean oil	n/a	33.3%	12.6%	26.1%	22.3%
Waste vegetable oil	n/a	27.8%	8.6%	20.5%	38.8%
Jatropha oil	n/a	18.0-22.0%	14.5%	29.0%	11.0-21.0%
Palm oil	n/a	80.5%	0.5%	n/a	<2.0%

Notes: n/a: not available; n.d.: not detected

2.1.2.1 Glycerol grades

The industry divides between different grades of glycerol, based on its purity (by wt%). Many grades of glycerol are available in the market. Glycerol can be categorized into three main types – crude glycerol, technical glycerol, and refined glycerol. An overview of the different glycerol grades is summarized in Table 2.4.

Table 2.4 Properties of the different glycerol grades [44, 64, 68]

Properties	Crude glycerol	Technical glycerol	Refined glycerol (USP & FCC grade)
Market price (USD/kg)	0.14	0.66	0.895
Glycerol (wt%)	78 wt% min	95 wt% min	99.7 wt% min
Methanol (wt%)	0.3 wt% max	0.1 wt% max	-
Water (wt%)	12 wt% max	5 wt% max	0.5 wt% max
Ash (wt%)	2 wt% max	-	-
Moisture (wt%)	1.5-6.5 wt%	2 wt% max	0.3 wt% max
Soap (wt%)	3-5 wt%	0.56 wt%	-
Chlorides (ppm)	-	10 ppm max	10 ppm max
Color (APHA)	-	34-45	1.8-10.3
pH	9.8-11.2	6.7-6.9	6.7-6.8

From this table, crude glycerol generated from biodiesel production is sold with methanol concentration of 0.3% (max) and glycerol concentration of 80-88% purity (min) for lower grade applications. In the current market, crude glycerol produced from biodiesel is the form most commonly sold by biodiesel producers [44]. Due to various impurities, crude glycerol has very little economic worth. However, it can be further purified in a wide variety of purification processes to increase purity and reach higher market levels (see Figure 2.4). Technical glycerol grade with glycerol concentration of 95% purity (min) is used as a chemical building block while United States Pharmacopeia (USP) and Food Chemicals Codex (FCC) grade with glycerol concentration of 99.7% purity (min) are suitable for use in cosmetics, pharmaceuticals, and food [64].

2.1.2.2 Refining of crude glycerol

The refining process or purification of crude glycerol consists of three stages: 1) neutralization to remove non-glycerol compounds, soaps and salts, 2) evaporation to eliminate methanol and water, and 3) deep refining to obtain required purity through vacuum distillation, ion exchange, membrane separation and activated carbon adsorption [66].

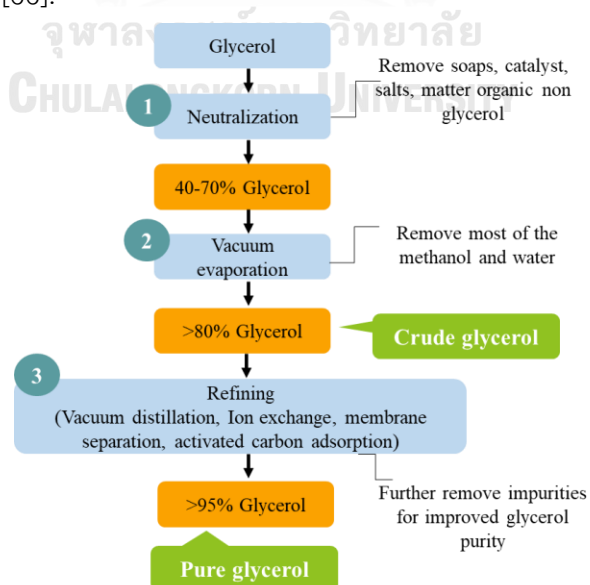


Figure 2.4 A general refining process of crude glycerol

Table 2.5 summarizes and compares advantages, disadvantages, and performance of four deep refining technologies. Currently, vacuum distillation is the most popular method of glycerol purification. Glycerol is operated under a vacuum because it is susceptible to high temperatures. The use of this technique avoids the polymerization or dehydration of glycerol [69]. Purification processes of crude glycerol generally require significant energy input, are high in chemical consumption, and have high production costs. The development of cheap and efficient purification processes that can be deployed at scale is essential to the biodiesel industry.

Table 2.5 Comparison of four deep refining technologies [66]

Technology	Advantages	Disadvantages	Purity of refined glycerol (w/w)
Vacuum distillation	<ul style="list-style-type: none"> - Simple and wide adaptability - Applicable for small to large-scale continuous operation - High quality glycerol 	<ul style="list-style-type: none"> - Intensive energy requirement - Temperature sensitive to feed steam variations 	94–96.6%
Ion exchange	<ul style="list-style-type: none"> - Low energy input - Suitable for small- and medium-sized plants 	<ul style="list-style-type: none"> - Generation of pollutant wastewater - Strict requirement for salt content in crude glycerol - High cost for resin reuse 	95–99% (Technical grade)
Membrane separation	<ul style="list-style-type: none"> - Low energy requirement - Easy to control and set up unit - Environment compatibility - Various membrane materials 	<ul style="list-style-type: none"> - Fouling and durability issues of membranes - Lack of suitable membranes for specific operations 	99.0% (Technical grade)
Activated carbon adsorption	<ul style="list-style-type: none"> - Easy to operate; efficient color reduction 	<ul style="list-style-type: none"> - Inefficient for the removal of other impurities, such as oleic acid and stearic acid 	99.7% (USP & FCC-grade)

Notes: Food Chemical Codes (FCC); United States Pharmacopeia (USP); Technical grade has not been exactly defined, mostly >96.0%.

In recent years, the emerging purification technology of glycerol is membrane separation which offers both economic and environmental benefit [70]. The combination of more than one method can enhance the process and increase the purity level. However, the purification process of crude glycerol to its pure form is an

expensive process which is unfeasible for small and medium. Thus, developing strategies for efficient use of crude glycerol may be possible for manufacturers.

2.1.2.3 Applications of glycerol

Glycerol is widely used in foods and beverages, which acts as a sweetener and preservative. It may indirectly be used as an emulsifier and stabilizer in many food products. Besides, it is used in pharmaceuticals, personal care products and animal feed [13]. Glycerol is considered as a building block to produce bio-based products for example, 1,2-propanediol, 1,3-propanediol, acrolein, dihydroxyacetone, glycerol carbonate, polyglycerols, etc. [71-74] During the forecast period of 2019–2027, the biochemical market is expected at a compound annual growth rate CAGR) of 16.67% [75]. In fact, the production of biochemical is a viable alternative for reducing the dependence on petroleum by lowering CO₂ emissions [71].

Glycerol can be converted into value-added chemicals by two main routes which are chemical and biological processes. These processes produce many chemical compounds with different properties and applications. The list of chemicals from glycerol via the chemical process is summarized in Table 2.6. Glycerol is a significant by-product of biodiesel production. The large glycerol availability (overproduction) has prompted chemical manufacturers to investigate methods for converting it to chemical building blocks [76].

For instance, Sánchez et al. [77] developed the catalyst for the production of allyl alcohol from glycerol deoxydehydration. Using ZSM5-supported iron catalysts, modified by rubidium deposition, as stable materials achieved a 99.9% conversion and 11.9% selectivity at 340°C, 1 bar, 35 wt% glycerol, GHSV 100 h⁻¹. Allyl alcohol derivatives are used in the preparation of perfume, medicine, and food. This wide range of uses causes allyl alcohol to have a higher commercial value than other products such as acrolein.

El Roz et al. [78] studied the effect of supports (SiO₂, ZSM-5, TiO₂, γ -Al₂O₃) for glycerol oxidation to glyceraldehyde. The results showed that the best selectivity

was obtained with Pt/ SiO₂ and found that γ -Al₂O₃ was not suitable for glycerinaldehyde because it obtained glyceric acid, the main by-product from glycerinaldehyde production, with high selectivity.

Wang et al. [79] examined zirconia supported noble metal catalysts (Ru, Rh, Pt, Pd) for propylene glycol production via glycerol hydrogenolysis. Ru tended to accelerate the cleavage of C-C bonds, which led to the ethylene glycol and methane formation, while Pd showed the highest selectivity with 90.5%.

Glycerol is an attractive alternative carbon source in biological processes because glycerol is readily available and inexpensive. It also has a higher degree of reduction of carbon atoms in glycerol compared to sugar [22, 80, 81]. In this way, glycerol may be used as a replacement for traditional carbohydrates, such as glucose, sucrose, and starch in the fermentation process [5]. Fermentation using glycerol as a carbon source has been of great interest for the productions of various chemicals, such as propionic acid, 2,3-butanediol, succinic acid, and others. List of chemicals from glycerol by fermentation process are summarized in Table 2.7.

For example, Tabah et al. [82] used glycerol for 1,3-propanediol production via anaerobic fermentation by *Saccharomyces cerevisiae*. It produced with a maximum yield of 0.423 g/g. Global production of 1,3-propanediol is continuously growing at around 45,300 tonnes per year [13]. It is an important chemical intermediate in manufacture. 1,3-propanediol can be produced via chemical process and fermentation. The fermentation of glycerol to 1,3-propanediol is more environment-friendly than chemical process, and generally, it has advantage because of milder conditions and less energy requirements [82].

Acetol can be produced from dehydration of glycerol or dehydrogenation of propylene glycol, but these processes are costly [83]. Acetol is used as an intermediate in the chemical industry, as a substitute for sodium dithionite in the textile industry, as an ingredient in the cosmetic industry, and as aroma for foods [84]. Zhu et al. [83] performed acetol production from glycerol fermentation using *Escherichia coli* Lin43 strain. The highest yield reached was 0.37 g/g, and production concentration was 5.38 g/L in 21 h at 28°C.

Cybulski et al. [85] screened *Yarrowia lipolytica* strains for glycerol fermentation to pyruvic acid, and identified that the *Y. lipolytica* SKO6 strain was the best producer and suit for pyruvic acid production at industrial scale with process yield of 0.63 g/g and volumetric production rate of 1.18 g/L/h. *Yarrowia lipolytica* is one of the most widely studied microorganisms. It is commonly used in industry as a robust producer [40].

Yarrowia lipolytica was also applied by Gao et al. [40] to study succinic acid from glycerol. Using the fed-batch system and *Y. lipolytica* PGC01003 strain produced yield and productivity of succinic acid with 0.4 g/g and 0.4 g/L/h, respectively. Succinic acid is one of the most important building block chemicals and has various applications. As a result, the global SA market is growing rapidly and expected to reach 97,099 tonnes by 2024 [86].

Nowadays, the valorization of glycerol has been successfully implemented in the commercial scale, such as the production of 1,3-PDO via bacterial fermentation [87, 88]. Table 2.8 provides the global overview of plant status for each chemical. Key attributes, enabling the success include 1) the versatility of 1,3-PDO – it is used as a coating agent, a solvent and a starting material to produce a polyester [89], 2) the high yield of 1,3-PDO in the biological platform – 0.729 g of PDO is produced per 1 g of converted glycerol [89], 3) the increasing demand of 1,3-PDO – the compounded annual growth rate (CAGR) of 7% during the forecast period of 2021 to 2026 [90], and 4) the high sale price of PDO comparing to glycerol. Thus, value-added chemicals that have similar attributes should be perceived as the potential chemicals for the sustainable valorization of glycerol.

However, some chemicals have a complicated manufacturing process or may produce the required substance in small quantities, resulting in a non-profitable production process. Therefore, it is necessary to find out the suitability of production and the economic cost-effectiveness.

Table 2.6 List of chemicals from glycerol by different chemical reactions

Chemicals	Reactions	Catalyst	Condition	Conversion (%)	Selectivity (%)	Ref.
1,2-Propanediol	hydrogenolysis	Cu-ZnO	200°C, H ₂ 20 bar, 16 h, 20 wt.% glycerol, catalyst weight 1.2 g (6%)	34	93	[74]
1,3-Dichloropropanol	hydrochlorination	malonic acid	110°C, 3 h, reactant molar ratio glycerol to HCl=1:24	43.09	-	[91]
1,3-Propanediol	hydrogenolysis	Pt/WOx/AlOOH	180°C, H ₂ 5 MPa, H ₂ O solvent, 12 h, glycerol 1 mmol, water 3 mL, catalyst 0.1 g (Pt 0.9 mol%)	100	66	[92]
1-Propanol	hydrogenolysis	ZrP and Ru/SiO ₂ layer	315°C, H ₂ 2 MPa flow rate of glycerol (10% wt) 0.04 mL/min, flow rate of H ₂ 30 mL/min	100	77	[93]
Acetol	dehydration	Ni/Si-Al ₂ O ₃	240°C, 98 kPa, flow rate of glycerol 33.33 g/h	92.71	58.11	[94]
Acrolein	dehydration	Q6-SiW-30	275°C, 1 bar, catalyst weight 0.3 g, flow rate of glycerol 1.8 mmol/h	100	74	[95]
Allyl alcohol	deoxydehydration	HZSM5/Fe/Rb	340°C, 1 bar, 35 wt% glycerol, GHSV 100 h ⁻¹	99.9	11.9	[77]
Dihydroxyacetone	Photocatalytic oxidation	TiO ₂ in acetonitrile	300 min, 1 g/L catalyst loading, 4 mM initial glycerol concentration	96.8	17.8	[96]
Formic acid	selective oxidation	HPMoV ₃	150°C, O ₂ 2 MPa, 3 h, 1 %wt glycerol, catalyst 0.1 mmol	100	60	[97]
Formic acid	selective oxidation	HPMoV ₃	150°C, O ₂ 4 MPa, 3 h, 50 %wt glycerol, catalyst 0.1 mmol	94.8	51.3	[97]

Table 2.6 List of chemicals from glycerol by different chemical reactions (cont.)

Chemicals	Reactions	Catalyst	Condition	Conversion (%)	Selectivity (%)	Ref.
Glyceraldehydes	oxidation	Pt/SiO ₂	80°C, O ₂ 2 bar, 1 h, catalyst 0.5 g, 200 cm ³ of an aqueous 0.1M glycerol	10	74	[78]
Glyceraldehydes	oxidation	Pt/ZSM-5	80°C, O ₂ 2 bar, 1 h catalyst 0.5 g, 200 cm ³ of an aqueous 0.1M glycerol	14	69	[78]
Glyceraldehydes	oxidation	Pt/TiO ₂	80°C, O ₂ 2 bar, 1 h, catalyst 0.5 g, 200 cm ³ of an aqueous 0.1M glycerol	25	51	[78]
Glyceraldehydes	oxidation	Pt/γ-Al ₂ O ₃	80°C, O ₂ 2 bar, 1 h, catalyst 0.5 g, 200 cm ³ of an aqueous 0.1M glycerol	37	37	[78]
Glycerol carbonate	carbonylation	NaAlO ₂	30°C, 2 h, catalyst amount 30 wt%	85	100	[98]
Hydrogen	aqueous-phase reforming	1Cu-12Ni/MMNT	240°C, 40 bar, flow rate of glycerol (1wt%) 0.05 mL/min, catalyst 150 mg	84	86	[99]
Methanol	supercritical water reforming	Cu/HZSM-5	500°C, 1 atm, 4 h	100	-	[100]
Polyglycerols	Etherification	Li/MK10	260°C, 1 atm	90	40	[101]
Propylene glycol	hydrogenolysis	Ru/m-ZrO ₂	200°C, H ₂ 6.0 MPa, 3 h, 10 wt% glycerol	22.9	45.7	[79]
Propylene glycol	hydrogenolysis	Ru/γ-Al ₂ O ₃	200°C, H ₂ 6.0 MPa, 3 h, 10 wt% glycerol	18.7	14.3	[79]
Propylene glycol	hydrogenolysis	Rh/m-ZrO ₂	200°C, H ₂ 6.0 MPa, 3 h, 10 wt% glycerol	22.8	65.6	[79]
Propylene glycol	hydrogenolysis	Pt/m-ZrO ₂	200°C, H ₂ 6.0 MPa, 3 h, 10 wt% glycerol	20.4	85.7	[79]
Propylene glycol	hydrogenolysis	Pd/m-ZrO ₂	200°C, H ₂ 6.0 MPa, 3 h, 10 wt% glycerol	21	90.5	[79]
Triacetin	Acetylation	Amberlyst-15	50°C, ratio of acetic acid to glycerol of 3:1	98.51	8.98	[102]

Table 2.7 List of chemicals from glycerol by fermentation process with different microorganisms

Chemicals	Applications	Microorganisms	Yield	Ref.
1,3-Propanediol	used in the preparation of polyester fibers, and coatings, used in the textile industry, food packaging, lubricants, and medicine	<i>Saccharomyces cerevisiae</i>	0.423 g/g	[82]
2,3-Butanediol	applications in the food, pharmaceutical, and synthetic rubber industries	<i>Raoultella ornithinolytica</i> B6	0.42 g/g	[80]
Acetol	intermediate used to produce polyols and acrolein, used as a reduced dye in the textile industry and as a skin tanning agent in the cosmetic industry	<i>Escherichia coli</i> Lin43	0.37 g/g	[83]
Butanol	biofuel, as an industrial intermediate for production of various compounds used in polymer technology	<i>Clostridium pasteurianum</i> CH4	0.31 g/g	[103]
Dihydroxyacetone (DHA)	ingredient of sunless tanning products, used in cosmetic preparations, use in polymer synthesis	<i>Gluconobacter oxydans</i> ZJB09112	161.9 g/L	[58]
Erythritol	sweetener with applications in food and pharmaceuticals; food additives	<i>Yarrowia lipolytica</i> K1	170 g/L	[104]
Ethanol	biofuel, as a solvent and chemical intermediate	<i>Escherichia coli</i>	0.47 g/g	[105]
lactic acid	applications in the food, pharmaceutical, and polymer industries	<i>Escherichia coli</i>	50.1 g/L	[25]
Mannitol	applications in the food and pharmaceutical industries, sweetener for diabetics, ingredients of chewing gums	<i>Candida azyma</i>	0.3 g/g	[106]
Polyhydroxyalkanoates (PHA)	bioplastics, packaging materials	<i>Pandoraea</i> sp.	1.56 g/L	[107]
Propionic acid	chemical intermediate used in the synthesis of vitamin E, cellulose fibers, artificial fruit flavors, fragrances, and perfumes	<i>Propionibacterium acidipropionici</i>	0.7 g/g	[108]
Pyruvic acid	used to synthesize other valuable products in pharmaceutical, cosmetic, food, and chemical industries, ingredient in food supplements for athletes	<i>Yarrowia lipolytica</i> SKO6	0.63 g/g	[85]
Succinic acid	building block chemicals, precursor in specific polyesters production and a component of some alkyd resins	<i>Yarrowia lipolytica</i> PGC01003	0.4 g/g	[40]

Table 2.8 Global overview of the state of production facilities of different chemicals [76, 109]

Product	Production facilities			Company	Price (\$/t)	Global Biobased Capacity (kta)
	EU	North America	South America			
Ethanol	M	M	M	Many	815	80,800
Sorbitol		M		ADM, Roquette, Cargill, Ingredion	650	1,800
Lysine		M		BBCA, Evonik, Draths, Ajinomoto		1,100
Furfural	D	M		Central Romana Corporation	1,000-1,450	300-700
n-butanol	R	D	M	Cathay Industrial Biotech, Jiangsu Lianhai Biological Technology, Laihe Rockley Bio-Chemicals, Lianyungang Lianhua Chemicals, Shi Jinyan, Songyuan Ji'an Biochemical, Tongliao Zhongke Tianyuan Starch Chemical Co	1,890	590
Epichlorohydrin		M		Solvay, Spolchemie, Yang Nong Jiang Su		540
Lactic acid	M	M	M	Chongqing Bofei-Biochemical Products, Corbion Purac, Galactic, Henan Jindan, HISun, Wuhan Sanjiang Space Gude Biotech	1,450	472
Ethylene			M	Braskem	1,300-2,000	200
Xylitol	M	R		DuPont Danisco, Roquette	3,900	190
Ethylene glycol	R		M	Global Biochem, Greencol Taiwan Corporation, India Glycols, Novepha	1,300-1,500	175
Acetone	R	D	M	Cathay Industrial Biotech, Jiangsu Lianhai Biological Technology, Laihe Rockley Bio-Chemicals, Lianyungang Lianhua Chemicals, Shi Jinyan, Songyuan Ji'an Biochemical, Tongliao Zhongke Tianyuan Starch Chemical Co	1,400	174
Propylene glycol		M		ADM, Global Biochem, Novepha, Oleon		120
Itaconic acid		R		Alpha Chemika, Jinan Huaming Biochemistry, Qingdao Kehai Biochemistry Co, Zhejiang Guoguang Biochemistry	1,900	90
1,3 propanediol	R	M		DuPont Tate & Lyle BioProducts, Zhangjiagang Glory Biomaterial	1,760	77

Table 2.8 Global overview of the state of production facilities of different chemicals [76, 109] (cont.)

Product	Production facilities			Company	Price (\$/t)	Global Biobased Capacity (kta)
	EU	North America	South America			
Ethyl acetate	M	D	M	Dhampur Alco-Chem, Jubilant Lifescience, Laxmi Organic Industries, Sekab , Somalya, Songyuan Ji'an Biochemical		36
Succinic acid	M	M		Myriant, Reverdia, Succinity, BioAmber	2,940	34
1,4 butanediol	R	D		BASF, Genomatica		30
Acetic acid	M	D	M	Jubilant Lifescience, Sekab , Songyuan Ji'an Biochemical, Wacker, Godovari Biorefineries Ltd, Zeachem	617	25
Isosorbide	D	R	D	Jinan Hongbaifeng Industry & Trade, Roquette		20
PHAs	R		R	Bio-on, Kaneka Crop, MetaboliX	6,500	17
Iso-butanol	R	M		Butamax, Gevo	1,721	6-9
1,2 butanediol			M	Global Biochem	3,000	3
Levulinic acid	D	R	D	Segetis, Zibo Shuangyu Chemical	6,500	3
P-xylylene		R		Gevo, Virent	1,415	1.5
Acrylic acid	R	R		ADM, Arkema, BASF, OPX Bio	2,688	0.3
3-HPA		R		Cargill/Novozymes, OPX Bio, Perstorp	1,100	0.04
5-HMF	R			AVA Biochem	2,655	0.02
Isoprene	R	R	R	Amyris, DuPont, Glycos Biotechnologies	2,000	0.02
Iso-butene	R			Global Bioenergies, Lanxess	1,850	0.01
Adipic acid		R		BioAmber, DSM, Rennovia, Verdezyne	2,150	0.001

Notes: kta: kilotonnes per annum; R: research/pilot; D: demonstration M: manufacturing

2.1.3 Propionic acid (PA)

Propionic acid is a C-3 carboxylic acid with the formula of $\text{CH}_3\text{CH}_2\text{COOH}$. It is on the list of the top thirty potential chemicals that can be transformed into high-value chemicals, according to the National Renewable Energy Laboratory (NREL) [28]. Table 2.9 lists the PA properties. PA and its derivatives could be converted into valuable chemicals and biomaterials [28]. The application of its derivatives is illustrated in Figure 2.5. Further, PA is versatile – it is used as a food preservative as well as an ingredient in pharmaceutical products, perfumes, herbicides, paints, and polymers [14, 110, 111]. The world market demand of propionic acid was approximately 470,000 tonnes in 2020 [112] with the CAGR of up to 10% by 2027 [113]. The four top PA manufacturers are BASF, Dow, Eastman Chemical Company, and Perstorp [114]. The largest producer of propionic acid is BASF company, accounting for about 31% of the total market share [110]. In addition, the price of PA is 3 USD per kg [115] which is more expensive than the price of crude glycerol (see Table 2.4).

Table 2.9 Properties of propionic acid [116]

Property Name	Property Value
Molecular Formula	$\text{C}_3\text{H}_6\text{O}_2$
Molecular Weight	74.08 g/mol
Melting Point	-24 to -23°C
Boiling Point	141°C
Density	0.993 g/mL at 25°C

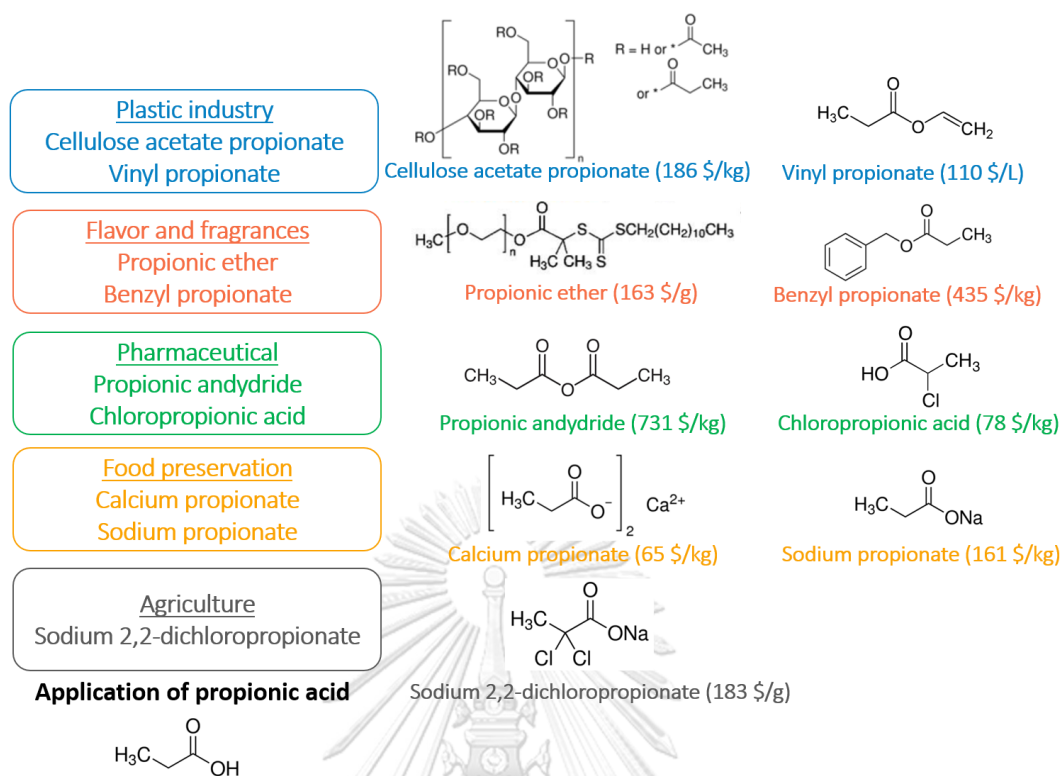


Figure 2.5 Chemical structures and prices of propionic acid derivatives [27]

Currently, the existing technology of PA synthesis employs petroleum-based feedstock. In this technology, ethylene, CO, and steam are converted into PA at 285 °C and 230 bara via the carboxylation process [110, 114]. The reaction takes place in a high-pressure tubular reactor where $\text{Ni}(\text{CO})_4$ is used as a catalyst. Although petroleum-based technology provides a higher conversion of glycerol and a higher selectivity of PA, this technology depends on non-renewable feedstock which is not sustainable in the long term. Thus, to align with the attempt to replace the petroleum-based feedstock, PA should be produced alternatively via fermentation of glycerol using various types of bacteria [10, 117, 118].

Glycerol has been considered as a suitable raw material given its high availability and its cost advantage [27]. In addition, as provided in Table 2.10, the major advantages of using glycerol for the production of bio-based PA are the highest product yield and the highest product quality when compared to other types of renewable sources [117-120].

Table 2.10 Propionic acid from different carbon sources and microbial strains

Strain	Substrate	Substrate concentration (g/L)	Propionic acid concentration (g/L)	Productivity (g/L/h)	Yield (g/g)	Ref.
<i>P. freudenreichii</i>	Glucose	20	6.40	0.07	0.16	[117]
<i>P. freudenreichii</i>	Glycerol	20	9.00	0.18	0.47	[117]
<i>P. acidipropionici</i>	Glucose	20	8.70	0.24	0.22	[117]
<i>P. acidipropionici</i>	Glycerol	20	12.0	0.42	0.64	[117]
<i>P. jensenii</i>	Glycerol	300	33.2	0.15	0.11	[120]
<i>P. acidipropionici</i>	Glycerol	50	28.5	0.19	0.57	[119]
<i>P. acidipropionici</i>	Sorbitol	40	20.4	0.39	0.55	[118]
<i>P. acidipropionici</i>	Xylose	40	18.4	0.25	0.48	[118]

The fermentation of glycerol for PA production is influenced by several factors, including microbial types, pH, temperature, and concentrations of carbon and nitrogen sources [33]. Among all types of bacteria, *Propionibacterium* [29] exhibited the highest efficacy for the production of PA which had been shown promising for industrial applications [110]. In addition, as provided in Table 2.10, *Propionibacterium* could digest other carbon sources, such as glucose, sorbitol, and xylose for the production of PA [121]. Thus, the flexibility of utilized feedstocks is also another advantage gained in the fermentation process using *Propionibacterium*.

2.1.4 Succinic acid (SA)

Succinic acid is a substance that has a wide range of applications. The major applications of succinic acid are surfactants, detergents, and foaming agents. Second, use is as an anti-corrosion agent for metals. Next, it is used in food industries as a pH modifier, flavoring agent, and microbial growth inhibitor. Besides, it is applied in antibiotics, amino acids, and vitamins [31, 122]. It serves as a precursor in the synthesis of high-value chemicals as shown in Figure 2.6, such as 1,4-butanediol, tetrahydrofuran, and succinonitrile [123]. Owing to its broad range of applications, the global succinic acid market is growing rapidly. The demand for SA is expected to

increase, from 50,276 tonnes in 2017 to 97,099 tonnes by 2024 [86]. In addition, the price of SA is 3 USD per kg [124], which is relatively high compared to other glycerol-derivative products [125]. Table 2.11 lists the properties of SA.

Table 2.11 Properties of succinic acid [116]

Property Name	Property Value
Molecular Formula	$C_4H_6O_4$
Molecular Weight	118.09 g/mol
Melting Point	185°C
Boiling Point	235°C
Density	1.19 g/mL at 25°C

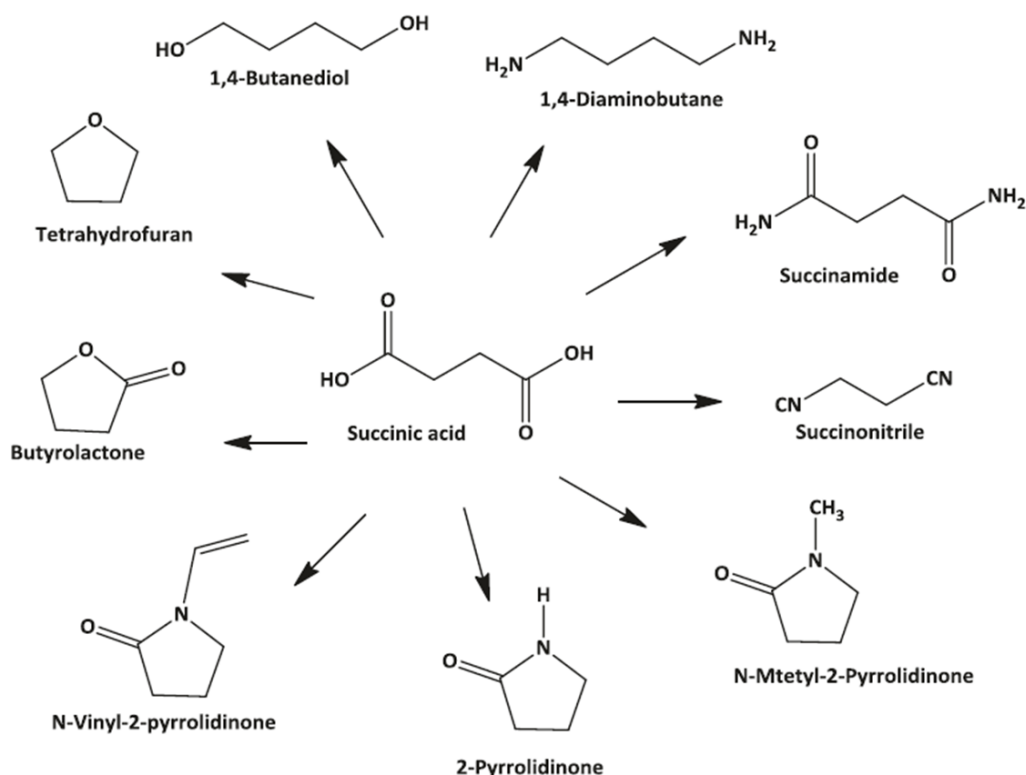


Figure 2.6 Some chemicals produced from succinic acid [14]

Nowadays, petroleum is the primary source of SA production through the hydrogenation of maleic anhydride [31]. Synthesis from non-renewable fossil fuels with butane is the starting material to produce maleic anhydride via direct oxidation and then converted it to succinic acid [57]. As evidenced in 2021, the petroleum-based SA held a market share of more than 50% [126]. The cost of maleic anhydride is important to the overall cost of succinic acid from this path [14]. Moreover, due to the price fluctuations of petroleum-based SA as well as the environmental impacts caused by the utilization of petroleum, an attempt has been made to replace petroleum-based technology with bio-based technologies in SA synthesis [123].

According to bio-based technologies, bacterial fermentation provides various advantages over the petroleum pathway, including milder operating conditions, a greener approach, and lower GHG emissions [46]. In addition, SA microbiological production requires the addition of CO₂ to the culture broth, contributing to the direct consumption of CO₂ [23]. The strains typically employed to produce SA were *Actinobacillus succinogenes*, *Anaerobiospirillum succiniciproducens*, *Mannheimia succiniciproducens*, and *Escherichia coli* (*E. coli*) [31]. These microorganisms can metabolize a wide range of sugars derived from agricultural or industrial wastes, such as crude glycerol, wheat, and waste bread as shown in Table 2.12. At present, SA is commercially produced using sugar as a raw material. The bio-based SA manufacturers are BASF, Myriant, and Succinity. However, glycerol is very competitive when compared with other carbon sources such as glucose, xylose, and fructose. Owing to the high degree of reduction per carbon of glycerol, it can be used as a substrate instead of a sugar platform [81].

The commercialization of bio-based SA appears to be restricted by its higher production costs; hence, the technological advancements that can reduce the overall production cost are key to the success of the bio-based SA commercialization [46].

Table 2.12 Succinic acid from different carbon sources and microbial strains

Strain	Substrate	Succinic acid concentration (g/L)	Productivity (g/L/h)	Yield (g/g)	Ref.
<i>A. succinogenes</i>	glycerol	18	0.24	0.84	[6]
<i>A. succinogenes</i>	wheat	15.9	0.31	0.47	[127]
<i>A. succinogenes</i>	waste bread	47.3	1.12	1.16	[128]
<i>A. succinogenes</i>	sugarcane bagasse	22.5	1.01	0.43	[129]
<i>A. succinogenes</i>	cassava roots	93.34	1.87	0.77	[130]
<i>A. succinogenes</i>	xylose	27.4	0.45	0.70	[131]
<i>B. succiniciproducens</i>	xylose	25.97	0.55	0.76	[131]
<i>M. succiniciproducens</i>	wood hydrolysate	11.73	1.17	0.56	[132]
<i>Y. lipolytica</i>	glycerol	160.2	0.40	0.40	[40]
<i>E. coli</i>	glucose	97.5	1.21	0.96	[133]

2.1.5 Dihydroxyacetone (DHA)

Dihydroxyacetone (DHA) is one of the most significant value-added chemicals from glycerol. Its main usage is as an ingredient in tanning products [22, 134]. In the United States, the tanning market grew 27% from USD 135 million to USD 171 million from 2011 to 2016 [53]. For many years, it has been utilized in the cosmetic, food, and pharmaceutical industries [53, 72]. It also serves as a key component in the synthesis of chemicals such as lactic acid, a biodegradable polymer. Moreover, it can be used as a nutritional supplement in the development of the visual system and the prevention of heart disease [54].

The global DHA market value was worth 169.6 million USD in 2022 and has been projected to increase to 224.7 million USD by 2028 [51]. Europe is the largest market with over 60% of the market share, followed by China which contributes about 28% of the market share [135]. In addition, the price of DHA is 25 USD per kg [52], which is relatively high compared to other glycerol-derivative products [125]. Table 2.13 lists the properties of DHA.

Table 2.13 Properties of dihydroxyacetone [116]

Property Name	Property Value
Molecular Formula	$C_3H_6O_3$
Molecular Weight	90.08 g/mol
Melting Point	75-80°C
Boiling Point	107.25°C
Density	1.52 g/mL at 20°C

DHA can be produced from glycerol both chemical route by oxidation and biotechnological route, but oxidation results in low selectivity values. This involves significant investment in DHA separation and purification, which is a significant part of the total cost of the process [72]. Moreover, this route involves costly catalysts, for example, Au/C Au-Pd/C, Pt/C, or Pt-Bi/C. The production of DHA is expensive from chemical synthesis and the process requires more safety. Therefore, DHA synthesis is more economically appropriate through microbial processes [22].

Commercial synthesis of DHA is preferred via the biological route as compared to the chemical route due to the nature of their microorganisms and the mild process environment [55, 56]. The industrial strains for producing DHA from glycerol are *Acetobacter* species, *Yeast* species, and *Gluconobacter* species [55]. Among these, *Gluconobacter* strains have been used extensively in the recent studies of DHA production as shown in Table 2.14 [55, 136-138].

Although the biological route can give excellent DHA selectivity, they have some limitations. The main challenge of DHA production is the inhibitory effect on bacterial growth due to the high concentrations of glycerol [57, 58], leading to the low DHA production capacity.

Table 2.14 Dihydroxyacetone produced from different carbon sources and microbial strains

Carbon source	Strain	DHA concentration (g/L)	DHA productivity (g/L/h)	Yield (g/g)	Ref.
Crude glycerol	<i>Acetobacter sp.</i>	48.3	0.50	0.48	[136]
Crude glycerol	<i>B. licheniformis</i>	39.2	0.41	0.39	[136]
Crude glycerol	<i>G. oxydans</i>	69.0	0.72	0.69	[136]
Crude glycerol	<i>G. frateurii</i>	23.8	0.44	0.79	[137]
Refined glycerol	<i>G. thailandicus</i>	58.0	0.81	0.97	[138]
Crude glycerol	<i>G. thailandicus</i>	40.8	0.55	0.68	[138]
Treated crude glycerol	<i>G. thailandicus</i>	55.8	0.78	0.93	[138]
Crude glycerol + Glucose	<i>G. oxydans</i>	39.0	1.65	0.98	[55]
Crude glycerol + Sorbitol	<i>G. oxydans</i>	36.0	1.50	0.90	[55]

2.2 Literature reviews

Researchers have paid attention to the utilization of glycerol for the synthesis of diverse chemicals. For example, Posada et al. [10] evaluated the stand-alone processes for production of nine selected chemicals from glycerol by chemical routes (syn-gas, acrolein, and 1,2-propanediol) and biochemical routes (ethanol, 1,3-propanediol, D-lactic acid, succinic acid, propionic acid, and poly-3-hydroxybutyrate). The results revealed that the designed processes were profitable given the cheapness and the high availability of glycerol. They also concluded that the purification step in each production highly influenced the process feasibility, which can be implied that proper selection and design of the purification technology could be key to feasible commercialization.

The followings are examples of research for the production of value-added chemicals from glycerol that can indicate production efficiency as well as guidelines for developing production from both upstream and downstream processes.

2.2.1 Propionic acid (PA)

The alternatives to the bio-based PA production have been extensively investigated. The advantage of using glycerol as a carbon source could decrease the number of purification steps and improve the quality of the final product because less acetic acid is produced during the glycerol consumption [33, 119]. The most commonly used bacteria for the propionic acid producer is *Propionibacteria* [29]. According to Gonzalez-Garcia et al. [110], *Propionibacteria* is the best and most suitable propionate producer for industrial production. Propionic acid has been studied through strains such as *P. shermanii* and *P. jensenii*, but this does not compete with *P. acidipropionici*. *Propionibacterium* is an excellent natural propionic acid producer.

In 2000, Himmi et al. [117] compared two strains of bacteria, *P. acidipropionici* and *P. freudenreichii ssp. Shermanii*, and found that *P. acidipropionici* was higher effective. Furthermore, the effects of carbon sources (glucose, glycerol) have been compared. This research showed that the acetic acid concentration from glycerol consumption is twice as low (2 g/L) compared to glucose (4 g/L). This represents the production of glycerol as an advantage over the use of glucose.

In 2015, Zhang et al. [108] compared the production of propionic acid from glycerol and glucose using *P. acidipropionici*. It was found that the production from glycerol gave better yields and less co-products, which had a positive effect on the separation process. The yield and productivity of glycerol and glucose were 0.7 g/g, 0.12 g/L/h, and 0.35 g/g, 0.2 g/L/h, respectively.

In 2016, Liu et al. [120] used *P. jensenii* for the propionic acid production. However, this strain still needs to be improved due to its low yield and intense concentration of glycerol used (300 g/L). In addition to upstream studies, downstream technologies play a significant role in the production of carboxylic acids. According to Morales et al. [31] indicated that 60–70% of the total cost of production is obtained through the purification process.

According to the study of Keshav and Wasewar [39], appropriate selection in the forward and the backward steps was justified based on the extraction efficiency

of propionic acid. For example, if the temperature-swing regeneration technique was selected as the backward step, the appropriate pair of extractant and diluent was TOA and MIBK. If the utilization of TMA was selected, the appropriate pair of extractant and diluent was TOA and 2-octanol. Although the appropriate selection had been provided, other factors (e.g., the process economics, the energy consumption, and the CO₂ emission) should be accounted for in the appropriate selection also. In fact, these factors are especially important when the reactive extraction is considered for upscaling to a commercial level. To facilitate the selection that accounts for these factors, a process simulator should be employed.

2.2.2 Succinic acid (SA)

Tan et al. [139] demonstrated succinic acid production when using various biomass derivatives. The economic viability depends on three indicators: the price of biomass per tonnes, the availability of biomass, and the yield. In this work, fifteen biomass sources were compared, one of which was glycerol as shown in Table 2.15.

Table 2.15 Biomass ranking in terms of feasibility on a commercial scale [139]

Ranking	Biomass	Scores for cost (per 40)	Scores for yield (per 40)	Scores for availability (per 20)	Total scores (per 100)
1	Corn straw	39.1	24.4	20.0	83.4
2	Glycerol	30.3	40.0	11.8	82.1
3	Cotton straw	39.2	37.0	2.1	78.3
3	Wheat straw	38.1	22.3	18.0	78.3
5	Rice straw	39.7	18.9	15.8	74.4
6	Waste bread	38.6	34.9	0.0	73.5
7	Sugarcane bagasse	40.0	26.8	1.5	68.2
8	Corn core	39.7	26.8	1.7	68.1
9	Wheat	27.5	24.4	13.9	65.7
10	Sugarcane molasses	34.4	28.9	1.1	64.4
11	Wood (oak) hydrolysate	27.8	26.5	0.0	64.3
12	Soybean meal	15.2	1.9.2	3.0	37.4
13	Rapeseed meal	24.8	3.6	0.6	29.0
14	Whey	0.0	24.1	0.0	24.1
15	Sake lees	NA	17.7	NA	17.7

Glycerol has the potential to be comparable to other commercial succinic acid feedstocks for succinic acid fermentation because glycerol has a global availability of approximately 600 million tonnes per year of crude glycerol from the biodiesel manufacture. It also has a conversion of up to 1.33 g of succinic acid per 1 g of glycerol. However, the cost of raw glycerol is 0.22 USD per kg, which is still higher than some biomass, such as corn straw, wheat straw, etc.

To decrease the production cost of the bio-based SA, two regimes should be focused on including the advancements in the upstream (e.g., SA productivity) and downstream (e.g., SA separation and purification) technologies.

The advancement in upstream technology improved yield and selectivity of SA. The strains typically employed to produce SA were *Actinobacillus succinogenes*, *Anaerobiospirillum succiniciproducens*, *Mannheimia succiniciproducens*, and *Escherichia coli* (*E. coli*) [31]. However, their low production rates, caused by the redox imbalance during cell growth hindered the application of these microorganisms in the production of SA from glycerol. To increase the rate, the addition of external electron acceptors was found effective as evidenced in *A. succinogenes* according to Carvalho et al. [23].

Carvalho et al. [23] reported that the use of dimethyl sulfoxide (DMSO) as an electron acceptor at concentrations ranging from 1 to 4 Vol% significantly increased the production of succinic acid and glycerol consumption. In fed-batch fermentation, the yield was 0.87 g SA/g glycerol, and the production rate was 2.31 g SA/L·h, which was the highest record in literature for *A. succinogenes* using glycerol as a carbon source. This impressive result could offer a new perspective on glycerol valorization via fermentation with *A. succinogenes* for bio-based SA production. Furthermore, DMSO is a non-toxic commercial organic solvent that its usage has been increased for pharmaceutical and electronics manufacturing purposes [47]. Additionally, DMSO is inexpensive as it is a by-product of kraft paper manufacturing [48]. The price of DMSO is about 0.267 USD per kg [49]. Therefore, the addition of DMSO in SA production could be cost-effective and environmentally friendly.

In 2016, Gao et al. [40] applied *Yarrowia lipolytica* to study the succinic acid production from glycerol. This strain has great tolerance to environmental stress. It

was demonstrated the robust production of succinic acid by yeast *Y. lipolytica* from crude glycerol without pretreatment. The fed-batch system and the *Y. lipolytica* strain PGC01003 showed the productivity of succinic acid at 0.4 g/L/h, and also obtained the highest succinic acid titer of 160.2 g/L.

In 2020, Kuenz et al. [140] tested the use of pure glycerol and crude glycerol as a carbon source for the production of succinic acid. When pure glycerol was applied, the yield was 1.3 g/g and the productivity was 0.34 g/L/h, while using pure glycerol, the yield was 0.9 g/g and the productivity was 0.33 g/L/h. This study showed that pure glycerol and crude glycerol can be effectively used as a carbon source to generate succinic acid.

In addition to the upstream process, the separation and purification of SA obtained from the fermentation broth also need careful investigation. A variety of technologies were proposed for the recovery of bio-based SA, including electrodialysis, ion exchange, extraction, direct crystallization, and membrane separation [123, 141]. Technological performances of some of the downstream processes were evaluated through process simulation as exemplified in the work of Morales et al. [31].

Morales et al. [31] studied the downstream technologies including reactive extraction, electrodialysis, and ion exchange reactions. The processes were assessed with sustainable assessments, including environmental impact, economic and hazard. The work concluded that using *E. coli* in the fermentation paired with the reactive extraction for the purification was the most competitive technology that provided sustainable benefits, particularly for the environment.

Cok et al. [50] evaluated the separation and purification processes in SA production e.g., direct crystallization, electrodialysis and ammonium sulfate (by-product) production. It was found that electrodialysis required a large amount of electricity, which was consistent with Morales et al. [31]. The overall results indicated that direct crystallization was the environmentally beneficial approach for bio-based SA – the reduction of greenhouse gas emissions by 48% and 40% was obtained when compared to the electrodialysis and the ammonium sulfate production, respectively.

2.2.3 Dihydroxyacetone (DHA)

The main challenge of DHA production is the inhibitory effect on bacterial growth due to the high concentrations of glycerol [57, 58], leading to the low DHA production capacity. To improve the bacterial growth rate, recent studies attempted to add secondary carbon sources such as sugars. According to Lu et al. [55] and Liebminger's work [59], the growth efficiency of *Gluconobacter* strains was greatly enhanced by growing the strains in a medium, containing glucose and sorbitol as the secondary carbon sources. By considering these works, it can be inferred that the addition of secondary carbon sources can be beneficial for cost reduction. To prove this inference, process simulation is needed.

Liu et al. [142] studied the effect of impurities contained in crude glycerol on cell growth rate and DHA production. They observed that the high concentration of sodium ion in crude glycerol could affect the DHA production [143]. According to Jittjang et al. [138], crude glycerol that was treated with an ion exchange resin (capable of 74% removal efficiency relative to the sodium salt input) could yield the DHA content comparable to that produced from refined glycerol. The results from this work suggested that the removal of the sodium content in crude glycerol could enhance the DHA production.

According to de la Morena et al. [72], increasing glycerol concentrations had an important inhibitory effect on the product. It can be stated that the oxygen transfer rate (OTR) depends on the concentration of biomass. Also, in terms of production conditions, pH is necessary to maintain production and should be higher than 4 to ensure glycerol consumption. It was found that the consumption of glycerol decreased when the pH dropped below 4.

In 2010, Hu et al. [58] used *Gluconobacter oxydans* to produce DHA using total glycerol at concentrations of 182.5 g/L and pH 5.0. The result was 161.9 g/L of DHA at glycerol conversion rate of 88.7%. This work shows the effect of glycerol feeding strategies on DHA production, in line with de la Morena's work. The initial biomass concentration determines the final content of bacteria produced in the broth, which is considered to have a direct influence on the rate of DHA production.

2.2.4 Sustainability assessment

The sustainability assessment is crucial for the development of sustainable processes. In this regard, recent works available in the literature provided performance assessments of chemical processes in terms of economic, energy, exergy, and environmental impact [144-146]. Such an assessment contributed to the identification of hotspots, by which further process enhancement could be undertaken.

Mongkhonsiri et al. [124] evaluated the performance of a biorefinery-integrated kraft pulping network in terms of energy consumption, and economic and environmental impacts. The hotspots that consumed an excessive amount of energy were identified. The innovative scenarios were suggested to achieve the enhanced sustainable process. Thus, it was confirmed that the integration of biorefinery networks in an existing pulping process could improve the sustainability of the pulping process – the process performances in terms of economic, energy utilization and environmental impacts were improved.

Charoensuppanimit et al. [147] designed the process that converted ethanol into diethyl ether (DEE) through analysis of energy consumption, economic, and CO₂ emissions. This analysis facilitated the identification of hotspots, which resulted in a process improvement that was more energy efficient and caused less environmental impact. For example, the acetaldehyde removal from DEE using adsorption was more economically attractive and more energy efficient when compared to the conventional method using extractive distillation.

Zhou et al. [148] applied the life-cycle analysis in achieving sustainable development goals for DHA production from glycerol. By applying the life-cycle analysis, the hotspots were identified – the production and transportation process of purified glycerol has the most significant contribution to non-renewable energy and greenhouse gas emissions, accounting for 28-38%, and 57-63%, respectively.

Morales et al. [30] designed the process for lactic acid production from glycerol through analysis of environmental and economic aspects. The analysis revealed that the novel cascade process from using biocatalytic DHA production

from glycerol followed by chemocatalytic LA production was shown to have substantially lower operating costs and less harm to the environment compared to the traditional technology. Thus, both environmental and economic assessments were proven capable of facilitating the decision-making for raw materials and technology selection that caused less environmental impacts.

Sadhukhan [124] evaluated the environmental performance of the sewage sludge application in energy generation and agricultural processes using Life Cycle Assessments (LCA). The results of the evaluation showed that the anaerobic digestion of sewage sludge contributed to a significant reduction in atmospheric emissions and considerable saving of fossil resources. Biogas produced by anaerobic digestion of sewage sludge can reduce global warming potential by 0.079 kg of CO₂ equivalence per MJ of biogas production. Thus, the LCA was proven capable of facilitating the decision-making for raw materials and technology selection that caused less environmental impacts.

Marchesan et al. [146] designed the process for lactic acid production from sugarcane via fermentation and compared their designed cases using techno-economic analysis. The analysis revealed that the novel process configuration demonstrated economic potential and decreased fuel demand when compared to the conventional process. Also, by applying the energy analysis, the hotspots were identified – the downstream processes were the most contributor in energy demand.

As seen from the previous examples, the hotspot identification was undertaken based on a typical evaluation of economic, energy consumption and environmental impacts. Another performance index that could directly point out inefficient unit operations namely exergy was found useful by many researchers [149-151].

Meramo Hurtado et al. [151] evaluated the production of levulinic acid from banana empty fruit bunches through exergy analysis. The processes could be divided into three main categories: pretreatment, acid-dehydration, and separation. According to the exergy analysis, the pretreatment stage presented the lowest exergy efficiency (66%). These results indicate that the pretreatment stage in biological processes is still a technology that needs to be improved in order to achieve higher efficiency.

Additionally, acid-dehydration has shown the greatest potential for waste recycling to optimize process performance since this unit provided the highest exergy of waste.

Im-orb et al. [149] investigated the synthesis of bio-methanol from oil palm waste through a gasification pathway. In terms of exergy analysis, the gasifier had the highest exergy destruction, which implies that the gasifier was an important unit for enhancing overall process efficiency. The analysis of the variation of the exergy efficiency under various gasification conditions revealed that the exergy efficiency of the system decreased with increasing the gasification temperature. In addition, bio-methanol was reduced due to the concentration of hydrogen in syngas decreasing when the gasification temperature increased.



CHAPTER 3

METHODOLOGY

This chapter provides the details of research procedures. The research procedures were divided into two parts including process simulation and process evaluation as follows.

3.1 Process simulation

In this section, Aspen Plus[®] V.11 was used to simulate the entire process. The UNIFAC model was employed to describe the phase-equilibrium behaviors of the systems, according to Eric Carlson's recommendation [152]. The process simulation of value-added chemicals was divided into three main parts including sustainable process design of propionic acid production from glycerol: a comparative study of bio-based and petroleum-based technologies (Chapter 4), succinic acid production from glycerol by *Actinobacillus succinogenes*: techno-economic, environmental, and exergy analyses (Chapter 5), and sustainability assessment of dihydroxyacetone (DHA) production from glycerol: A comparative study between biological and catalytic oxidation routes (Chapter 6).

In this study, an overview of the superstructure of biochemical production from glycerol is illustrated in Figure 3.1. The process was designed on the basis of laboratory information (residence time, temperature, pH controller, feed concentration to the fermenter, etc.). It was assumed that reported laboratory scale data will be applicable to an industrial process. The operating conditions were fixed at the same values as appeared in the fermentation experiment. Details are provided in Appendixes B to D. In the downstream processes as well, conditions were adjusted to be consistent with the experimental results. Therefore, the simulation could give a correct mass balance (which corresponded with the operating conditions) that reflected what happened in the experiment.

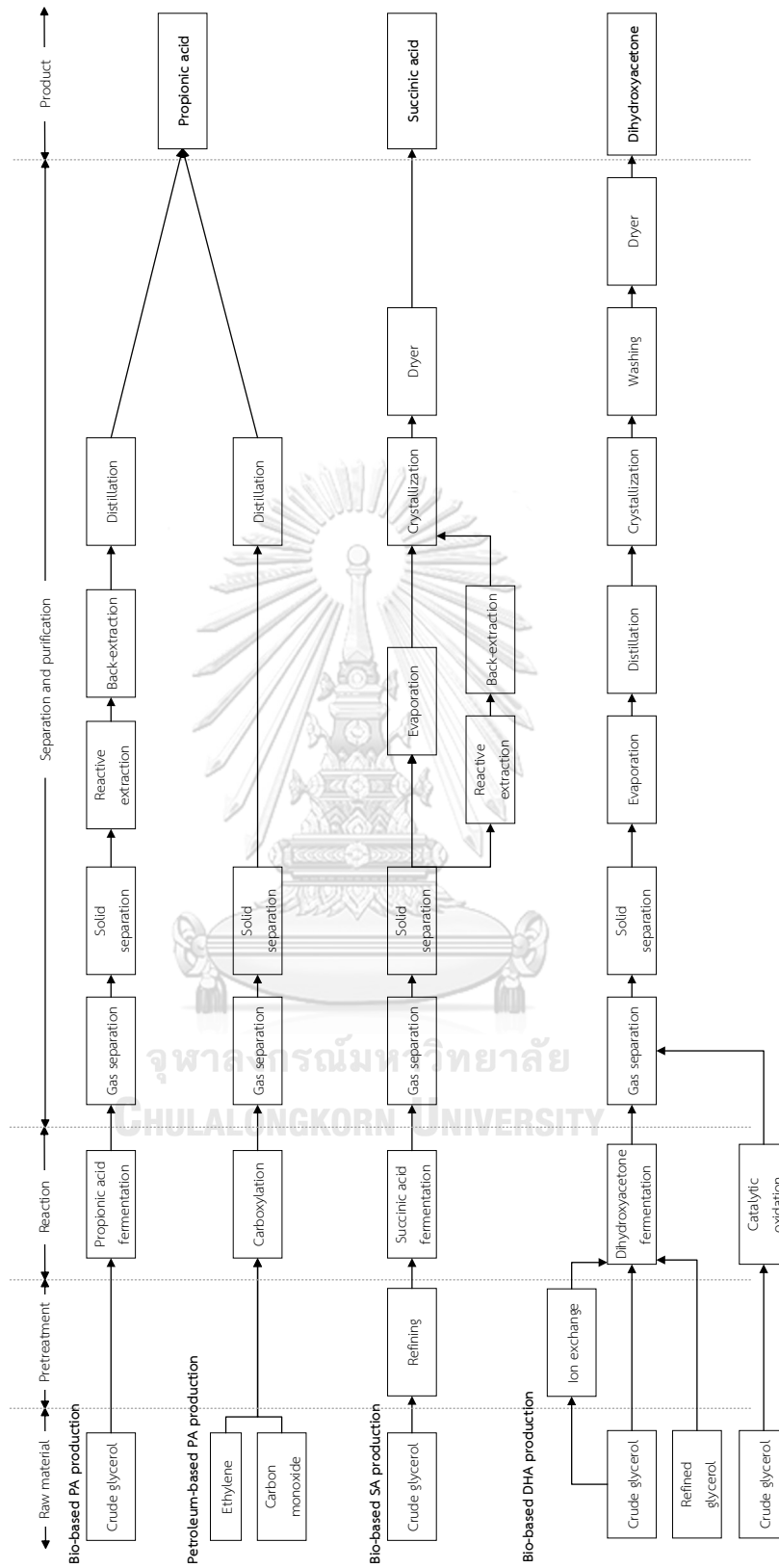


Figure 3.1 Superstructure for the production of value-added chemicals from glycerol including propionic acid, succinic acid, and dihydroxyacetone

Initially, the operating unit must be selected in accordance with the available data and indicate operating conditions such as temperature, pressure, and conversion. Please note that stoichiometric reactor (RStoic) block was used for the fermentation tanks. Since the reaction pathway occurred in the fermenter could not be identified exactly due to the complexity involved in a biological process, earlier studies circumvented such complexity by converting the experimental results into stoichiometric coefficients [153]. Hence, the stoichiometric coefficients were employed to describe the fermentation process.

In separation and purification steps according to Figure 3.1, the fermenter effluent was sent to the flash drum and the tubular cross-flow filter to separate gas and microorganism, respectively. For the recovery of biochemicals different technologies have been proposed such as electrodialysis, ion exchange, reactive extraction, and precipitation. For the PA recovery, the technologies based on reactive extraction were investigated. Please note that reactive extraction is a multifunctional reactor having reaction and extraction in a single unit. However, Aspen Plus does not have a unit operation that could perform the reactive extraction directly. Therefore, the reactive extraction was designed by a cascade model containing the reactor and the decanter (Figure 3.2) according to Nieder-Heitmann [154].

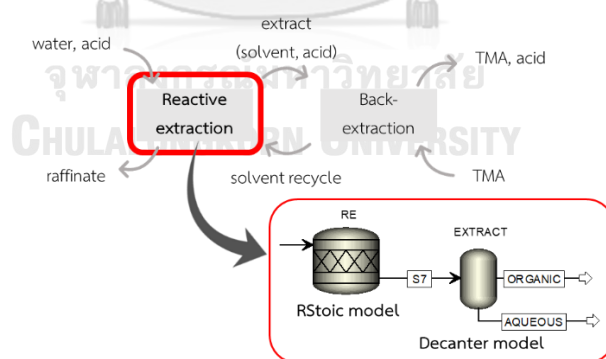


Figure 3.2 Simulation of the reactive extraction unit in Aspen Plus

For SA and DHA recovery, the main unit of production of SA and DHA was crystallization. The crystallizer model was used based on solubility data. The purpose was to crystallize SA and DHA from the aqueous slurry, because in the industry these chemicals are sold in solid form. The simulation data of the crystallizer model is shown in Figure 3.3.

Figure 3.3 Aspen simulation of the crystallizer model

In the distillation column simulation, please note that a flash model was used to determine the bubble point pressure. After that, a shortcut distillation model (DSTWU) was used to determine the basic information (e.g., feed stage location, reflux ratio, and distillate rate), and then used the resulting data in the RadFrac model. The simulation data of the RadFrac model is shown in Figure 3.4. To achieve the purity required by industry, design specification may be necessary. Detailed information on the streams and equipment was calculated by employed simulator and then forwarded to the next step for analysis. The detailed descriptions of process simulations involved in the production of value-added chemicals are described in Chapters 4 to 6.

Figure 3.4 Aspen simulation of RadFrac model

3.2 Process evaluation

In this work, several performance indexes were used in the process evaluation to acquire a broader perspective on the sustainability of the technology, including glycerol and carbon utilization, process economics, energy utilization, exergy analysis, and environmental impacts. Ultimately, these indexes were used to assess the process performances comparing to the petroleum-based production and were useful in decision-making regarding the feasibility of bio-based production.

3.2.1 Glycerol and carbon utilization efficiencies

The glycerol utilization was calculated as the quotient between the desired substance present in the product stream and glycerol feed amount as expressed in Equation (1), whereas the carbon utilization [122] was calculated as the quotient between carbon content in the product stream and carbon content in the glycerol stream as expressed in Equation (2).

$$\text{Glycerol utilization} = \frac{\text{Desired substance present in the product stream (kg/h)}}{\text{Glycerol feed amount (kg/h)}} \quad (1)$$

$$\text{Carbon utilization} = \frac{\text{Carbon content in the product stream (kg/h)}}{\text{Carbon content in the glycerol stream (kg/h)}} \quad (2)$$

3.2.2 Economic performance

Economic analysis is necessary for the process design because it can determine whether the process is economically feasible. In the economic analysis, Aspen Economic Analyzer was used to quantify the three economic indicators including discounted present value (DPV), discounted payback period (DPP), and discounted cash flow rate of return (DCFROR). To perform equipment sizing and cost estimation for the major equipment, we first matched the equipment type with each unit operation in the flowsheet. Then Aspen Plus Process Economic Analyzer evaluated the size of the equipment. After that, we clicked on the button "Project evaluation" to perform calculations. An example of selecting the type of equipment is illustrated in Figure 3.5.

Please note that the economic assessment of each simulated process was estimated based on 15 years of the project lifetime. A brief of the investment parameters considered in this work is presented in Table 3.1. The prices of utilities and feedstocks involved in the production scenarios are given in Tables 3.2 and 3.3. For simplification, the price of microorganism was assumed at 0.03 USD per kg based on previous studies [124, 155].

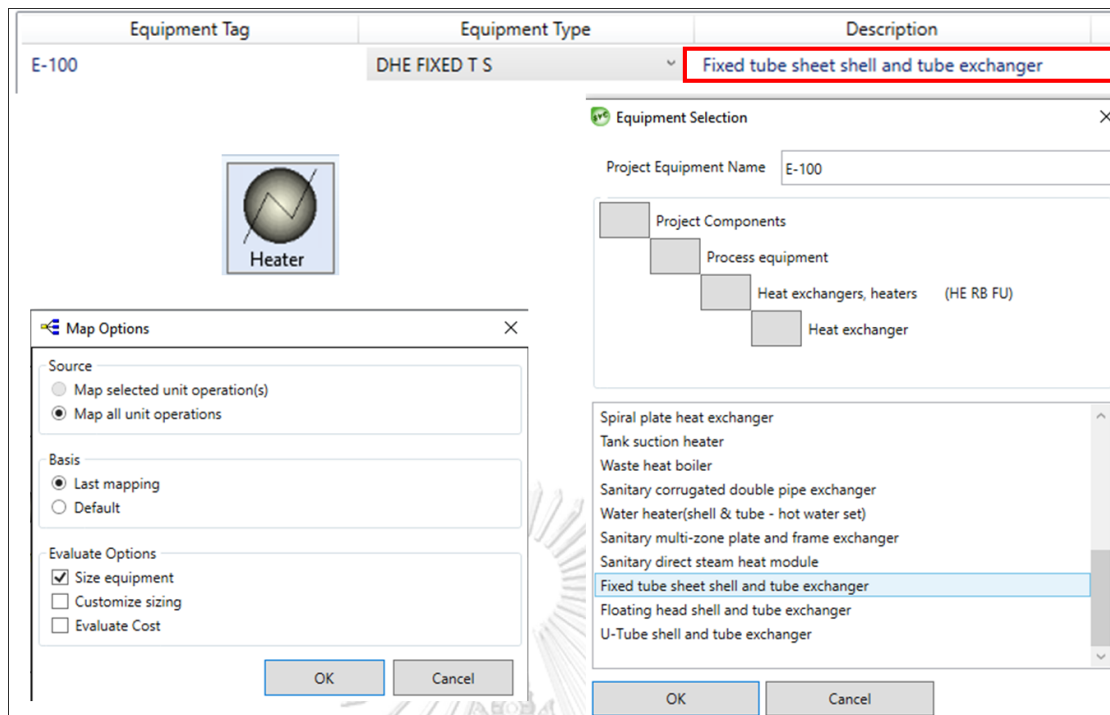


Figure 3.5 The “Equipment Selection” window to modify the equipment type

Table 3.1 General investment parameters for economic analysis

Parameter	Value
Plant life	15 years
Tax rate	20% (based on Thailand) [156]
Interest rate	0.5% (based on Thailand) [157]
Working capital cost	5% of fixed capital investment
Salvage value	20% of initial capital cost
Depreciation method	straight line
Plant life	15 years

Table 3.2 Summary of the prices of utilities

Utility	Price	Unit	Reference
Electricity	0.107	\$/kWh	[158]
Process water	0.177	\$/tonne	[159]
Cooling tower water	0.378	\$/GJ	[159]
Low pressure steam	4.54	\$/GJ	[159]
Medium pressure steam	4.77	\$/GJ	[159]
High pressure steam	5.66	\$/GJ	[159]
Refrigerant	4.77	\$/GJ	[159]

Table 3.3 Summary of raw material and product prices

Chemicals	Price (\$/kg)	Reference
2-octanol	0.7	[160]
Acetone	0.67	[161]
Ammonia	0.42	[124]
Benzyl alcohol	0.6	[160]
Calcium hydroxide	0.08	[160]
Carbon dioxide	0.035	[162]
Carbon monoxide	0.39	[162]
Crude glycerol	0.14	[163]
Dihydroxyacetone	25	[52]
Dimethyl sulfoxide (DMSO)	0.267	[49]
Dimethylformamide (DMF)	0.79	[160]
Ethylene	1.01	[164]
Glucose	0.35	[165]
Hydrochloric Acid	0.15	[146]
Magnesium carbonate	0.5	[160]
Methanol	0.55	[166]
Methyl isobutyl ketone (MIBK)	1	[163]
Microorganism	0.03	[124]
Nickel propionate (NP)	1	[163]
Nitrogen	0.09	[160]
Oxygen	0.03	[162]
Phosphoric acid	1.22	[167]
Propionic acid	3	[115]
Refined glycerol	0.895	[163]
Sodium hydroxide	0.4	[124]
Sorbitol	0.54	[168]
Succinic acid	3	[124]
Trimethylamine (TMA)	0.65	[163]
Trioctylamine (TOA)	1	[163]
Non-Hazardous waste disposal*	0.032	[169]
Wastewater disposal*	7.77E-05	[170]
Solid waste disposal*	0.037	[169]

*Waste treatment costs are served as a penalty for emission of pollution.

3.2.3 Energy utilization

The energy utilization was quantified using the specific energy consumption (SEC) expressed in Equation (3) [171, 172]. According to this expression, the smaller the SEC was, the higher the performance of energy utilization became. Heating, cooling, and electrical power are the three main components of energy utilization. The total amount of utilized energy can be found by defining the type of utility in each unit operation in Aspen Plus. An example of selecting the type of utility is illustrated in Figure 3.6.

$$SEC = \frac{\text{Total amount of utilized energy (kW)}}{\text{Total rate of product production (kg/h)}} \quad (3)$$

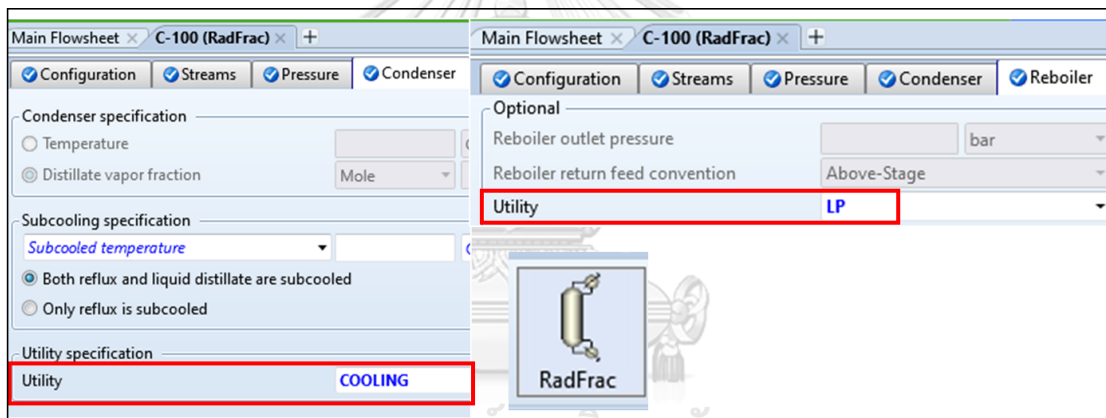


Figure 3.6 Utilities related to equipment

3.2.4 Exergy analysis

According to Table 5.6, the total energy consumption was the major problem with the bio-based SA production. Therefore, if inefficient units can be identified and developed, the bio-based production would be more promising and could compete with the petroleum-based production. The exergy is the maximum theoretical work of the process based on the second law of thermodynamics. The exergy analysis is beneficial to indicate its most inefficient component. According to Wiranarongkorn et al. [173], the exergy balance equation of each component could be performed as expressed in Equation (4).

$$\dot{E}x_{in}^{\dot{Q}} + \dot{E}x_{in}^{\dot{W}} + \sum \dot{m}_{in} ex_{in} = \dot{E}x_{out}^{\dot{Q}} + \dot{E}x_{out}^{\dot{W}} + \sum \dot{m}_{out} ex_{out} + \dot{E}x_d \quad (4)$$

where \dot{m}_{in} and \dot{m}_{out} are the mass flow rate of the inlet and outlet stream, respectively, ex_{in} and ex_{out} are the specific exergy of the inlet and outlet streams, respectively, $\dot{E}x^{\dot{Q}}$ and $\dot{E}x^{\dot{W}}$ are the exergy rate related to heat transfer (Equation (5)) and mechanical work or electrical work (Equation (6)), respectively, and $\dot{E}x_d$ represents the exergy destruction rate related to irreversibility.

$$\dot{E}x^{\dot{Q}} = \dot{Q} \left(1 - \frac{T_0}{T} \right) \quad (5)$$

where \dot{Q} is the heat transfer rate at the inlet or outlet of the component or system, T_0 is the reference temperature (25°C), and T is the absolute temperature boundary.

$$\dot{E}x^{\dot{W}} = \dot{W} \quad (6)$$

where \dot{W} is the work transfer rate of mechanical work at the inlet or outlet of the component.

According to Equation (4), the specific exergy (ex) was obtained from the physical exergy and chemical exergy, as seen in Equation (7).

$$ex_i = ex_{ph,i} + ex_{ch,i} \quad (7)$$

where $ex_{ph,i}$ is the physical exergy, $ex_{ch,i}$ is the chemical exergy. The physical exergy and chemical exergy could be determined from Equation (8) and Equation (9), respectively.

$$ex_{ph,i} = h_i - h_0 - T_0(s_i - s_0) \quad (8)$$

where h_i and h_0 are the specific enthalpy of the stream i at the operating and reference conditions (25°C, 1 atm), respectively, and s_i and s_0 are the specific entropy of the stream i at the operating and reference conditions (25°C, 1 atm), respectively.

$$ex_{ch,i} = \sum y_j ex_{ch,j}^0 + RT_0 \sum y_j \ln y_j \quad (9)$$

where y_j is the mole fraction of component j , $ex_{ch,j}^0$ is the standard specific chemical exergy of component j , and R represents the gas constant in kJ/kmol K. In this study, the standard specific chemical exergy of components is expressed in Table C15 in Appendix C.

To identify the significant losses within the process, the exergy efficiency (ψ) and the irreversibility (y_D) were computed using Equation (10) and Equation (11), respectively.

$$\psi = \frac{Exergy_{out}}{Exergy_{in}} \quad (10)$$

$$y_D = \frac{\dot{Ex}_{d,k}}{\sum \dot{Ex}_{d,k}} \quad (11)$$

Please note that Aspen Plus can calculate only physical exergy of stream, but chemical exergy can also be added to the analysis without too much effort. In “Property sets” folder, search through the options for the three exergy-related options name “EXERGYFL”, “EXERGYML”, and “EXERGYMS”, as shown in Figure 3.7. Preferred units can be selected in the “Units” column next to the “Physical properties” column. Mass exergy (EXERGYMS) will calculate the exergy value per unit mass of the process stream. Molar exergy (EXERGYML) will calculate the exergy value per unit mole of the process stream. Exergy flow rate (EXERGYFL) will calculate exergy per unit time that the process stream is carrying.

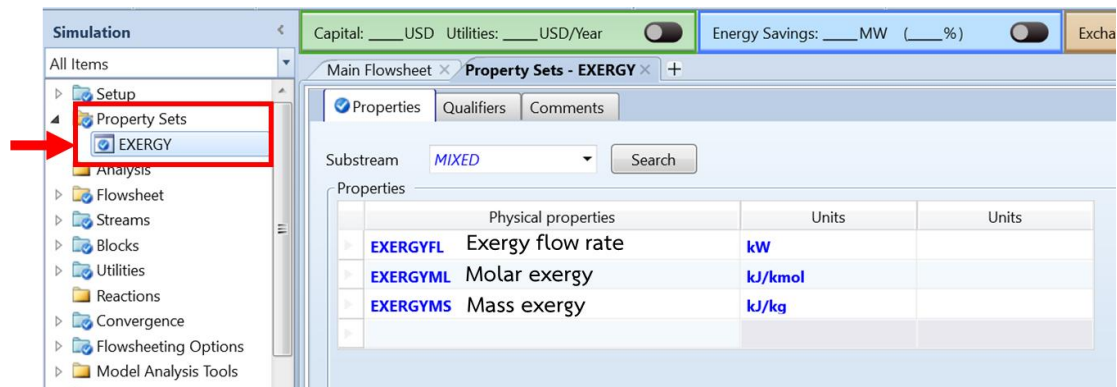


Figure 3.7 Exergy calculation in the “Property Sets” folder

Next, select the “Setup” | “Unit Sets” | “Report Options” | “Stream” menu, clicked on the “Property Sets” button. Move the desired exergy property sets from “Available property sets” to “Selected property sets”, as shown in Figure 3.8.

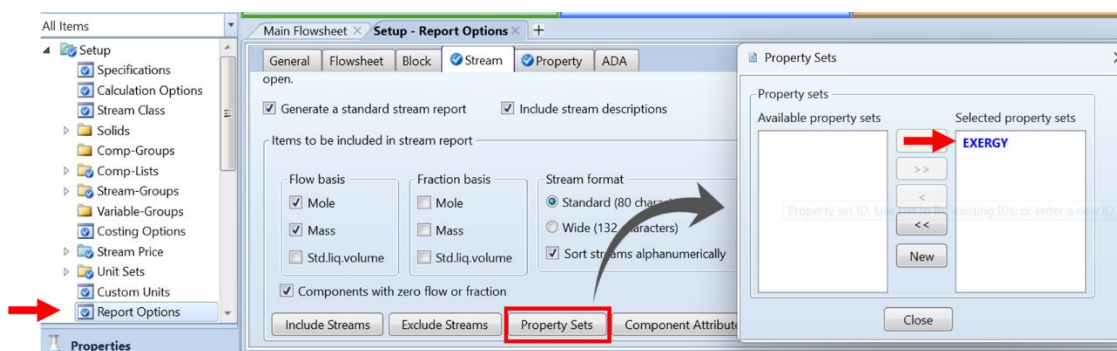


Figure 3.8 Select property sets in the “Report Options” menu

3.2.5 Environmental impacts

To compare the environmental impacts of all simulated processes, the Life Cycle Assessment (LCA) approach was adopted. The LCA is a standardized method that is extensively accepted and used to assess the potential environmental impacts of a product system throughout its life cycle [122]. The four main stages of an LCA study are as follows: goal and scope definition, life cycle inventory, impact assessment, and interpretation as shown in Figure 3.9.

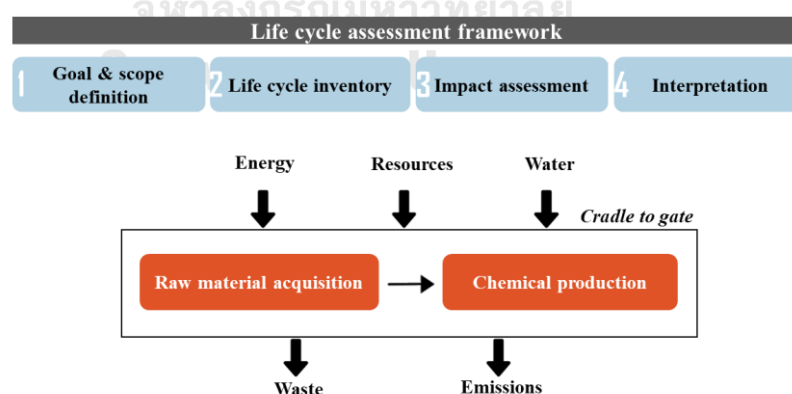


Figure 3.9 Life cycle assessment of chemical production

Herein, the goal of the LCA study was to compare the environmental impacts of chemical production from biological and chemical routes. The functional unit was one kilogram of value-added chemicals produced. The system boundary was cradle-

to-gate, as indicated in Figure 3.9. It involved two sections, namely, the acquisition of raw materials, and the production of value-added chemicals.

For the environmental impact assessment of propionic acid and succinic acid production scenarios, the global warming potential was quantified using the CO₂ equivalent emission. The emissions of other pollutants, such as ethylene, CO, and N₂ were also converted to the CO₂ equivalence (CO_{2-eq}) expressed in Equation (12).

$$CO_{2-eq} = \text{Characterization factor} \times \text{Inventory value} \quad (12)$$

where, the characterization factor was the potential to cause the CO₂ equivalent emissions which was collected from the previous research works [174, 175] and OpenLCA software [176].

For the environmental impact assessment of dihydroxyacetone production scenarios, the main categories of impacts considered can be divided into six categories, including global warming, terrestrial ecotoxicity, human non-carcinogenic toxicity, land use, fossil resource scarcity, and water consumption. The LCA was undertaken via SimaPro V. 9.3.0.3 based on Ecoinvent 3.8 and USLCI inventory databases. An example of entering life cycle inventory data in SimaPro is illustrated in Figure 3.10.

Documentation		Input/output	Parameters	System description				
Products								
Outputs to technosphere: Products and co-products		Amount	Unit	Quantity	Allocation %	Waste type	Category	Comment
DHA treated		1	kg	Mass	100 %	not defined	Chemic...Transformation	
Add line								
Outputs to technosphere: Avoided products		Amount	Unit	Distribution	SD2 or 2SD	Min	Max	Comment
Add line								
Inputs								
Inputs from nature		Subcompartment	Amount	Unit	Distribution	SD2 or 2SD	Min	Max
Water, cooling, unspecified natural origin, TH			2.93019527	m3	Undefined			
Add line								
Inputs from technosphere: materials/fuels		Amount	Unit	Distribution	SD2 or 2SD	Min	Max	Comment
Glycerin, at biodiesel plant/kg/RNA		1.319300641	kg	Undefined				
Tap water [RER] market group for Cut-off, S		20.83766617	kg	Undefined				
Hydrochloric acid, at plant /kg/RNA		0.017548966	kg	Undefined				
Ammonia, anhydrous, liquid [SAS] ammonia production, steam reforming, liquid Cut-off, S		0.00075831	kg	Undefined				
Sodium hydroxide, without water, in 50% solution state [GLO] market for Cut-off, S		0.019251439	kg	Undefined				
Methanol [GLO] market for Cut-off, S		0.217859094	kg	Undefined				
Acetone, liquid [GLO] market for Cut-off, S		0.43003022	kg	Undefined				
Cationic resin [GLO] market for Cut-off, S		0.131617248	kg	Undefined				
Anionic resin [GLO] market for Cut-off, S		0.144385791	kg	Undefined				
Add line								
Inputs from technosphere: electricity/heat		Amount	Unit	Distribution	SD2 or 2SD	Min		
Electricity, medium voltage [TH] market for Cut-off, S		0.060047256	kWh	Undefined				
Heat, central or small-scale, biomethane [GLO] market group for heat, central or small-scale, biomethane Cut-off, S		112.7955288	MJ	Undefined				
Outputs to technosphere: Waste treatment		Amount	Unit	Distribution	SD2 or 2SD	Min	Max	Comment
Spent cation exchange resin from potable water production [GLO] market for Cut-off, S		0.131617248	kg	Undefined				
Spent anion exchange resin from potable water production [GLO] market for Cut-off, S		0.144385791	kg	Undefined				
Add line								

Figure 3.10 The life cycle inventory data in SimaPro

CHAPTER 4

SUSTAINABLE PROCESS DESIGN OF PROPIONIC ACID PRODUCTION FROM GLYCEROL: A COMPARATIVE STUDY OF BIO-BASED AND PETROLEUM-BASED TECHNOLOGIES

Regarding the simulation study, the process economic of the bio-based PA production could be improved by enhancing the performance of the PA recovery process. This could be undertaken by selecting the appropriate diluent and the extractant as well as the suitable technique in the backward step in the reactive extraction. Thus, this chapter aims to 1) demonstrate that proper design of the acid-recovery process can significantly enhance the overall process performances in terms of glycerol utilization, economic, energy consumption and CO₂ equivalent emissions of every design project, and 2) provide insight of the bio-based production such that its advantages in terms of CO₂ equivalent emissions and disadvantages in terms of economic compared to the petroleum-based production could be pointed out.

4.1 Process description of propionic acid production

In this study, PA production at 10,000 tonnes per year was considered, representing 2.13% of global PA demand in 2020 [112]. The synthesized product was industrial-grade propionic acid with the product purity of 99.5 wt% according to the propionic acid supplier data [177]. UNIFAC model was employed to describe phase-equilibrium behaviors of the systems, according to the Eric Carlson's recommendation [152]. In this study, the major advantages of UNIFAC model included 1) UNIFAC was a group-contribution method capable of describing phase-equilibrium behaviors based on molecular structures – this model was typically applied when the equilibrium data were limited or unavailable, and 2) UNIFAC was developed based on the local-composition theory which was suitable for non-ideal systems. In this study, there were 4 investigated scenarios. Scenarios I to III were the bio-based production of PA whereas Scenario IV was the petroleum-based

production, which was provided for comparative purposes. For clarity, the key attributes in each scenario are summarized in Table 4.1.

Table 4.1 Key attributes in Scenarios I to IV for propionic acid production

Scenario	Production type	Reactive extraction		
		Forward step		Backward step
		Extractant	Diluent	
I	Bio-based	TOA	MIBK	Temperature-swing regeneration
II	Bio-based	TOA	MIBK	Utilization of TMA
III	Bio-based	TOA	2-Octanol	Utilization of TMA
IV	Petroleum-based	-	-	-

According to Table 4.1, the difference between Scenarios I and II was the selected technology in the backward step of the reactive extraction. In Scenario I, the temperature-swing-regeneration technique was employed in the backward step. This technique utilized thermal energy to cleave the bond of PA-TOA complex, which was presented in the organic phase. Then, water (which was not a foreign component and was not costly) was added to extract PA back to the aqueous phase. For illustrative purposes, Figure 4.1 provides the change in PA feed composition (from the left-hand side to the right-hand side of the azeotrope point) after the temperature swing regeneration was applied. In other words, the temperature-swing-regeneration technique was used to change the concentration of PA such that PA could be purified using distillation – the high purity PA could be obtained as the bottom product. However, the addition of water may put burden on the PA purification since the large amount of the added water must be removed.

In Scenario II, the addition of water was not required due to the utilization of TMA in the backward step. In this technique, TMA directly substituted TOA – the resultant PA-TMA complex was completely miscible in the aqueous phase. Although the addition of TMA was required, the separation of TMA from the aqueous solution was undertaken easily given the high volatility of TMA. Since the addition of water

was not required in this technique, an advantage should be attained in the PA purification as well as the lower environmental impact caused by the wastewater.

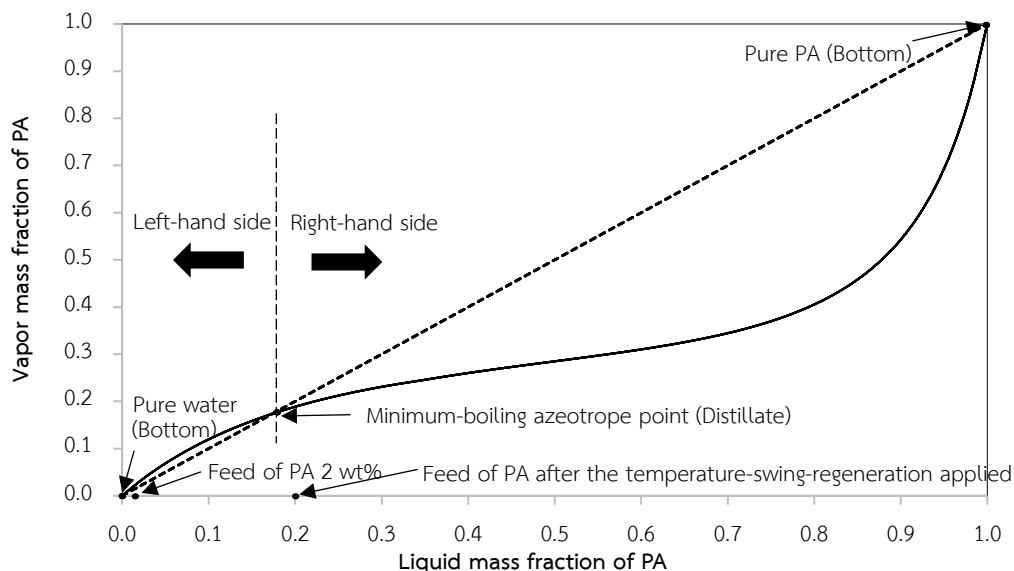


Figure 4.1 The shift of PA feed composition after the temperature-swing-regeneration applied

The utilization of TMA in Scenario II could display better performances in terms of glycerol utilization, energy utilization, economics and CO₂ equivalent emissions when compared to the temperature-swing-regeneration technique in Scenario I. The performance of Scenario II could be enhanced further by changing the diluent to 2-octanol (Scenario III). Lastly, the bio-based production was compared with the carbonylation of ethylene (Scenario IV).

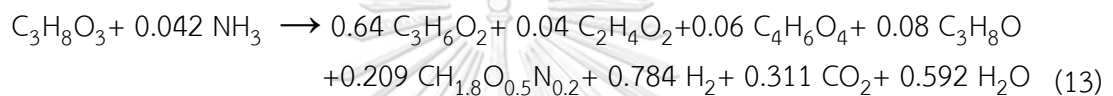
4.1.1 Scenario I (extractant: TOA, diluent: MIBK and back-extraction: temperature-swing regeneration)

For illustrative purposes, Figure 4.2 provides the general block flow diagram of bio-based process. The comprehensive process flow diagram is given in Figure B1 in Appendix B. Details of the processing blocks are given as follows.

Zone I given in Figure 4.2 highlighted the glycerol fermentation. Crude glycerol and other compounds were fed to the mixer. The mixer effluent was sent to a sterilizer operating at 121°C to prevent death of *Propionibacterium* [178]. After the

sterilization, the outlet stream was passed through two heat exchangers to reduce the temperature and sent to a fermenter.

Since the reaction pathway occurred in the fermenter could not be identified exactly due to the complexity involved in a biological process, earlier studies [153] circumvented such complexity by converting the experimental results into stoichiometric coefficients. Hence, the stoichiometric coefficients as expressed in Equation (13) were employed to describe the fermentation process in R-100, whose operating temperature was maintained at 32°C and 1 bar. Then, the fermenter effluent was sent to the knock-out drum to remove gas.



The product stream was passed through a tubular filter to remove a solid impurity. This solid representing microorganism ($\text{CH}_{1.8}\text{O}_{0.5}\text{N}_{0.2}$) that did not exist in the Aspen Plus database was treated as a CISOLID. The properties of microorganism were obtained based on the data from National Renewable Energy Laboratory (NREL) [179].

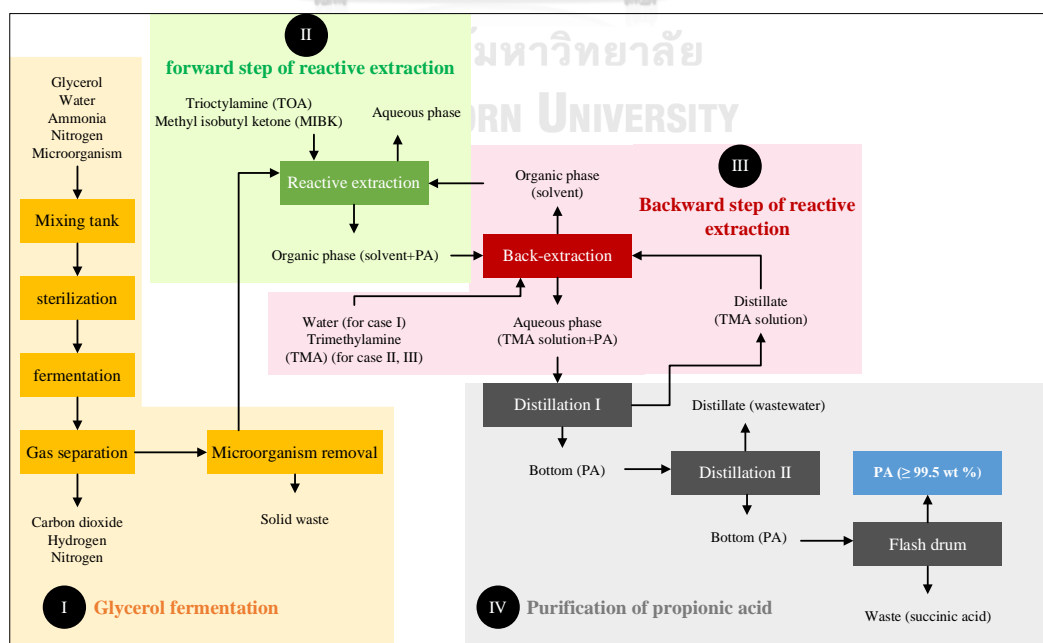


Figure 4.2 General block flow diagram of bio-based PA production

Zone II given in Figure 4.2 highlighted the forward step of the reactive extraction (also see Figure B1 in Appendix B for the detailed process description). The forward step in the reactive extraction was modeled using a reactor (R-101) and a separator (S-101) connected in series according to Jurado and coworkers [180]. Trioctylamine (TOA as the extractant) and methyl isobutyl ketone (MIBK as the diluent) were selected based on the best combination that maximized the extraction efficacy of 85% according to (Keshav) [181]. TOA and MIBK were mixed in M-101 before entering the extractive reactor (R-101).

In R-101, three sequential steps had been proposed for the chemical binding process between TOA (amine (R_3N)) and propionic acid (carboxylic acid (HA)). The binding process included the dissociation of carboxylic acid as expressed in Equation (14), the transfer of proton to the amine as expressed in Equation (15), and the recombination of acid-amine complex as expressed in Equation (16) [38].

Dissociation of carboxylic acid



Proton transfer to amine



Recombination of acid-amine complex



The overall reaction



Zone III in Figure 4.2 provides the backward step of reactive extraction. Stream 19 was increased from 32°C to 90°C before entering the R-102 where the cleavage of PA-TOA complex occurred. Water was added to R-102 to extract PA back to the aqueous phase. The R-102 and the decanter (S-102) were simulated based on the experimental results from Keshav & Wasewar [39]. After the bond cleavage, the organic phase consisting of TOA and MIBK was recovered and recycled whereas PA that had stronger affinity to water dissolved back to the aqueous phase. Please note that after the back extraction, the feed composition of PA was shifted to the right-

hand side of the azeotrope point as demonstrated in Figure 4.1. Thus, the aqueous phase was sent to the distillation column (C-100) to obtain high purity PA. Details of the operating conditions of C-100 were shown in Table B5 in Appendix B.

Zone IV in Figure 4.2 provides the purification of propionic acid. The bottom stream from C-100 was sent to the distillation column (C-102) to separate the remaining water. The bottom stream of C-102 comprised the heavy extractant and the organic acids. This stream was delivered to the evaporator (D-105) whose operating pressure was 1 bar. After the evaporation, propionic acid at the purity of 99.5 wt% was attained.

4.1.2 Scenario II (extractant: TOA, diluent: MIBK, back-extraction: utilization of TMA)

The process flowsheet for Scenario II is depicted in Figure B2 in Appendix B. Since the fermentation and the forward-step of reactive extraction blocks were identical to those in Scenario I, this section provided details regarding the backward step of reactive extraction, e.g., the utilization of TMA.

The organic phase from S-101 and TMA were fed to the R-102 where the reaction between TMA and PA-TOA complex occurred [39]. The reactor effluent was sent to the decanter (S-102) to recover the organic phase (for recycling) and the aqueous phase containing the PA-TMA complex for further PA purification. The stream containing PA-TMA complex was passed through the pump (P-100) prior to the column (RD-100). The reactive distillation column (RD-100) was utilized to simultaneously remove water and thermally decompose the PA-TMA complex as expressed in Equation (18).



In the top products of RD-100, TMA and water were attained. Since the relative volatility of TMA and water were 35, which was significantly different, TMA could be recovered easily using a one-stage evaporator D-102.

After the back-extraction process, water was removed via the top product of C-100 whereas PA and succinic acid were obtained at the column bottom. Since the

relative volatility of PA and succinic acid were 310, which was significantly different, utilization of a one-stage condenser (D-104) was sufficient. Finally, PA with the product purity of 99.5 wt% was attained. The comprehensive stream table of process simulation is given in Table B8 in Appendix B.

4.1.3 Scenario III (extractant: TOA, diluent: 2-octanol, back-extraction: utilization of TMA)

According to Keshav & Wasewar [39], when the utilization of TMA was selected as the back-extraction technique, the appropriate pair of extractant and diluent was TOA and 2-octanol. To illustrate this, the degree of extraction (E), the distribution coefficient (K_D), and the extraction equilibrium constant (K_E) obtained from Keshav & Wasewar [39] were used to select the most appropriate compounds in the forward-step of reactive extraction. As seen in Table 4.2, the pair of TOA and 2-octanol exhibited the highest performance as indicated. Furthermore, the price of 2-octanol was slightly cheaper than that of MIBK and the production of 2-octanol was more environmentally friendly [182].

Table 4.2 Summary of optimum diluent [181]

Extractant	Diluent	E (%)	K_D^*	K_E^{**} (m ³ /kmol)
tri-n-octylamine (TOA)	MIBK	85.0	5.67	16.5
tri-n-octylamine (TOA)	1-decanol	92.4	12.1	37.7
tri-n-octylamine (TOA)	Oleyl alcohol	85.1	5.72	16.4
tri-n-octylamine (TOA)	2-octanol	93.3	13.9	44.5

* Distribution coefficient (K_D) = $[\text{acid}]_{\text{org}}/[\text{acid}]_{\text{aq}}$

** Extraction equilibrium constant (K_E) = $[\text{complex}]_{\text{org}}/[\text{extractant}]_{\text{org}}[\text{acid}]_{\text{aq}}$

Accordingly, 2-octanol was selected to investigate if the change of diluent could improve the performances of PA production leading to the analysis in Scenario III. Regarding the process flowsheet, each processing block was relatively the same as that in Scenario II – the only difference between Scenarios II and III was the utilized diluent, i.e., MIBK VS 2-octanol.

4.1.4 Scenario IV (propionic acid production from the petroleum-based feedstock)

The process flowsheet in Scenario IV followed the BASF design [183]. Since the process was operated at a high temperature of 285°C and a high pressure of 230 atm, the Peng-Robison model was used in describing the physical properties according to Eric Carlson's guideline [152]. The flowsheet of petroleum-based propionic acid production is shown in Figure 4.3. The four reactants, including ethylene, CO, steam, and nickel propionate were fed to the reactor (R-100) where the reactions given in Table 4.3 occurred.

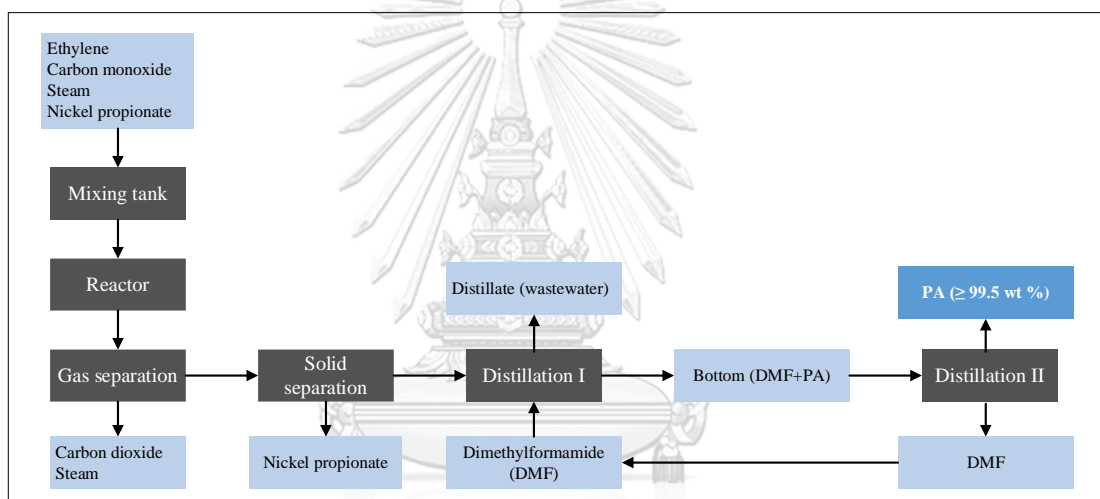


Figure 4.3 General block flow diagram of petroleum-based PA production

A portion of the reactor effluent was recycled to the reactor for temperature control [183], whereas the remaining in Stream 8 was passed through the pressure reducing valve (V-100) to 2 atm before entering the catalyst separation. Stream 9 containing $\text{Ni}(\text{CO})_4$ and PA was treated using N_2 and O_2 at 80°C and 2 atm to remove nickel carbonyl from a product stream [184]. The solid impurity was removed from the stream using S-100 via stream 14. The aqueous mixture containing PA in stream 16 was delivered to the extractive distillation column C-100 using dimethylformamide as the entrainer. Finally, PA with the purity of 99.5 wt% was obtained as the top product from C-101.

Table 4.3 Summary of reactions involved in petroleum-based production of propionic acid

Reaction	Chemical Reaction	Key reactant	Conversion (%)
Catalyst formation	$\text{Ni}(\text{C}_3\text{H}_5\text{O}_2)_2 + 5\text{CO} + \text{H}_2\text{O} \rightarrow \text{Ni}(\text{CO})_4 + 2\text{HC}_3\text{H}_5\text{O}_2 + \text{CO}_2$	Nickel propionate	42.4
Carbonylation	$\text{C}_2\text{H}_4 + \text{CO} + \text{H}_2\text{O} \rightarrow \text{C}_3\text{H}_6\text{O}_2$	Ethylene	93.0
Water-gas shift reaction	$\text{H}_2\text{O} + \text{CO} \rightarrow \text{CO}_2 + \text{H}_2$	Carbon monoxide	5.87
Ethane formation	$\text{H}_2 + \text{C}_2\text{H}_4 \rightarrow \text{C}_2\text{H}_6$	Ethylene	3.66
Diethyl ketone formation	$\text{H}_2 + 2\text{C}_2\text{H}_4 + \text{CO} \rightarrow \text{C}_5\text{H}_{10}\text{O}$	Ethylene	1.40
Ethanol formation	$\text{H}_2\text{O} + \text{C}_2\text{H}_4 \rightarrow \text{C}_2\text{H}_6\text{O}$	Ethylene	0.036
Ethyl propionate formation	$\text{C}_2\text{H}_6\text{O} + \text{C}_3\text{H}_6\text{O}_2 \rightarrow \text{C}_5\text{H}_{10}\text{O}_2 + \text{H}_2\text{O}$	Ethanol	100

4.2 Process evaluation

4.2.1 Representation of selected thermodynamic model

Since the bio-based processes were low-pressure operation that involved the coexistence of polar and non-polar compounds, the local composition models, such as NRTL, UNIQUAC and UNIFAC should be employed. Given the absence of binary interaction parameters between the amine and the involved compounds in the NRTL model, the group-contribution model, viz. UNIFAC was utilized to circumvent the problem. To ensure accuracy of the UNIFAC model, the VLE data that were available in NIST TDE were tested via the model representation depicted in Figure 4.4. As seen from the figure, the UNIFAC model was capable of representing the equilibrium behavior of PA and water with appreciable accuracy.

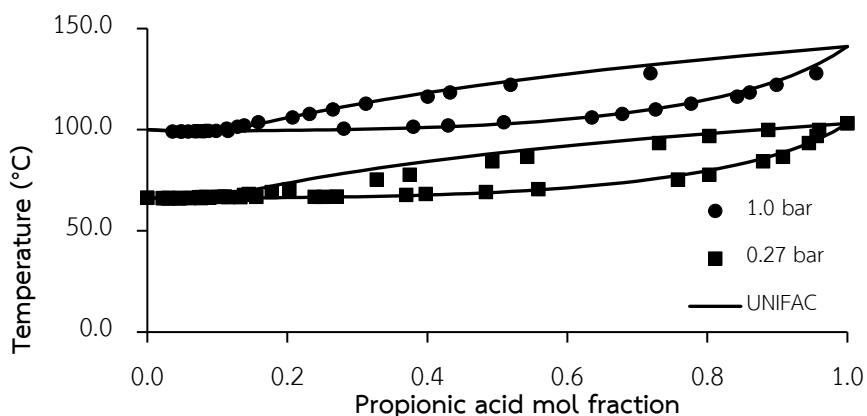


Figure 4.4 Representation of propionic acid/water vapor-liquid equilibrium system using UNIFAC model

4.2.2 Glycerol utilization

The production capacity of propionic acid and its corresponding amount of required glycerol in each scenario are summarized in Table 4.4. According to Equation 1, the glycerol utilization was determined for each scenario as: 0.35 for Scenario I, 0.36 for Scenario II and 0.38 for Scenario III.

Table 4.4 Summary of glycerol utilization for propionic acid production scenarios

Scenario	Propionic acid production	Glycerol feed rate	Glycerol utilization
	[tonnes/y]	[tonnes/y]	
I	1.00E+04	2.82E+04	0.35
II	1.00E+04	2.76E+04	0.36
III	1.00E+04	2.60E+04	0.38

Scenario	Propionic acid from reactor effluent	Propionic acid after back-extraction	% Recovery
	[tonnes/h]	[tonnes/h]	
I	1.39	1.17	84.3
II	1.36	1.15	84.4
III	1.28	1.15	89.6

As seen from the determined results, Scenario III displayed the highest glycerol utilization when compared to other scenarios. This was contributed to the highest recovery of propionic acid offered by the appropriate choices of 1) the

appropriate pairing of extractant and diluent, e.g., TOA and 2-octanol and 2) the appropriate choice of back-extraction technique, e.g., the utilization of TMA. To highlight this, the percentage recoveries of PA are also provided in Table 4.4 for comparative purposes. According to Table 4.4, the significant increase of PA recovery was observed in Scenario III. Thus, in terms of the glycerol utilization, the optimal design was obtained when TOA and 2-octanol as well as the utilization of TMA were selected in the reactive extraction for the efficient recovery of propionic acid.

4.2.3 Energy utilization

According to Table 4.5, the SEC of each scenario was determined as 98.4 kWh/kg, 83.3 kWh/kg, 80.6 kWh/kg, and 5.09 kWh/kg for Scenarios I to IV, respectively. The significant reduction of the SEC value was observed when Scenarios II and III were compared with Scenario I, indicating the improvement of the energy-utilization performance. As seen in Table 4.5, the substantial amount of thermal energy was consumed in Scenario I. This was contributed by the removal of water and MIBK recovery as required by the temperature-swing-regeneration technique. Thus, the utilization of TMA as the back-extraction technique was more attractive given the better performance in terms of extraction efficacy [39] and the energy utilization.

Table 4.5 Summary of energy utilization for propionic acid production scenarios

Type of duty	Unit	Scenario I	Scenario II	Scenario III	Scenario IV
Total heating duty	kW	5.64E+04	4.76E+04	4.61E+04	2.77E+03
Total cooling duty	kW	5.57E+04	4.73E+04	4.58E+04	3.05E+03
Total electric power	kW	57.68	56.44	54.38	0.241
Total power requirement	kW	1.12E+05	9.50E+04	9.20E+04	5.81E+03
PA production	kg/h	1.14E+03	1.14E+03	1.14E+03	1.14E+03
SEC	kWh/kg	98.4	83.3	80.6	5.09

However, if the SEC value of Scenario III was compared with that of Scenario IV, the petroleum-based production still outperformed the bio-based production. In Scenario III, the complexity of separation-and-purification scheme in the bio-based

production demanded a large amount of energy given the dilute amount of PA present in the fermentation broth. To resolve this issue; thus, the bacterium used in the production of PA should be reengineered to provide a higher yield and the higher selectivity of propionic acid that eventually increased the acid content in the broth.

However, the comparisons of process performances between Scenarios II and III using either of these indexes were not clear-cut given their slight differences. Thus, the economic performance which is highlighted in the following section was used to justify which scenario was more superior.

4.2.4 Economic performance

The economic indicators obtained in each scenario are provided in Table 4.6. As seen from Scenarios I to III, the bio-based processes were feasible given the positive numbers of DPV. Fermentation tanks for bio-based PA production were batch. The size of each fermenter was 1,000 m³, which was comparable to the fermenter used by DuPont [185]. With a production capacity of 10,000 tonnes per year and a fermentation period of 62.5 hours, a total of 7 fermentation tanks were required. For this reason, the fermenters were the most expensive equipment which was about 80-84% of the total equipment cost.

In scenario I, the total equipment cost as well as the total operating cost appeared the highest when compared to other scenarios. The highest costs contribute largely from the selection of temperature-swing-regeneration technique. To elaborate this, a large amount of water was required in this technique to achieve the MIBK recovery at 32°C and part of the cost was due to the water separation.

Please note that the addition of TMA (Scenarios II and III) did not introduce the burden previously observed in Scenario I. To illustrate this, PA-TMA complex could dissolve in the aqueous phase at appreciable amount without the addition of water. Furthermore, TMA was highly volatile. Thus, it could be concluded that the choice of back-extraction technique highly influenced the feasibility of the bio-based production.

As seen in Table 4.6, Scenario III was more attractive than Scenario II given the higher DPV of 118 million USD, the higher % DCFROR of 18.2% and the shorter DPP of 7.12 years. The better economic results obtained in Scenario III were contributed from the higher recovery of PA as provided in Table 4.4. In addition, in terms of the recovery of diluent, 2-octanol was separated from water more easily than MIBK. To illustrate this, the solubilities of 2-octanol and MIBK in water were 1,120 mg/L and 19,000 mg/L at 25°C [116]. Given the better separation from water, the fresh-feed amount of 2-octanol was lower when compared to MIBK since a larger amount of 2-octanol was recycled; 0.861 tonnes/h VS 0.342 tonnes/h. This led to the cost saving of about 5.45 million USD/y as reported in Table 4.7.

Table 4.6 Summary of economic performance for propionic acid production scenarios

Economic information	Unit	Scenario	Scenario	Scenario	Scenario
		I	II	III	IV
Total Capital Cost	\$	3.89E+07	3.68E+07	3.69E+07	1.13E+07
Total Operating Cost	\$/y	2.65E+07	2.53E+07	2.08E+07	1.22E+07
Total Equipment Cost	\$	9.10E+06	8.74E+06	8.77E+06	1.02E+06
Total Operating Labor Cost	\$/y	1.08E+06	1.08E+06	1.08E+06	9.20E+05
Total Maintenance Cost	\$/y	8.56E+05	8.33E+05	8.35E+05	9.31E+04
Total Utilities Cost	\$/y	9.05E+06	7.68E+06	7.45E+06	5.45E+05
Total Products Sales	\$/y	2.71E+07	2.71E+07	2.72E+07	2.74E+07
Total Raw Materials Cost	\$/y	1.23E+07	1.26E+07	8.66E+06	9.03E+06
Main Material Cost					
Glycerol	\$/y	3.81E+06	3.72E+06	3.51E+06	-
Methyl isobutyl ketone (MIBK)	\$/y	8.36E+06	7.55E+06	-	-
Trioctylamine (TOA)	\$/y	9.96E+05	9.74E+05	9.23E+05	-
Trimethylamine (TMA)	\$/y	-	1.22E+06	2.66E+06	-
2-Octanol	\$/y	-	-	2.10E+06	-
Carbon monoxide	\$/y	-	-	-	4.89E+06
Ethylene	\$/y	-	-	-	4.61E+06
Economic indicator					
DPV	\$	3.24E+07	5.18E+07	1.18E+08	2.62E+08
DCFROR	%	5.65	8.81	18.2	85.6
DPP	y	12.6	10.8	7.12	2.32

Table 4.7 Comparison of hotspots for propionic acid production scenarios

Hotspot	Unit	Scenario I	Scenario II	Scenario III	Scenario IV
The most expensive equipment	\$	7.35E+06 (R-100)	7.35E+06 (R-100)	7.35E+06 (R-100)	4.29E+05 (C-101)
Contribution in the total equipment cost	%	80.8	84.2	83.9	41.9
Diluent fresh feed rate	tonnes/h	0.95 (MIBK)	0.861 (MIBK)	0.342 (2-Octanol)	-
Diluent cost	\$/y	8.36E+06	7.55E+06	2.10E+06	-

According to Table 4.8, the ratio of total capital investment to propionic acid production rate of each scenario was determined as 4.29 USD/kg, 4.06 USD/kg, 4.07 USD/kg, and 1.25 USD/kg for Scenarios I to IV, respectively. The reduction of this value was observed when Scenarios II and III were compared with Scenario I, confirming the improvement of the back-extraction technique by the utilization of TMA.

Table 4.8 Summary of total capital investment for propionic acid production scenarios

Information	Unit	Scenario I	Scenario II	Scenario III	Scenario IV
Fixed capital investment	\$/y	4.09E+07	3.86E+07	3.88E+07	1.19E+07
Working capital	\$/y	2.04E+06	1.93E+06	1.94E+06	5.93E+05
Total capital investment	\$/y	4.29E+07	4.06E+07	4.07E+07	1.25E+07
PA production	kg/y	1.00E+07	1.00E+07	1.00E+07	1.00E+07
Total capital investment/PA production	\$/kg	4.29	4.06	4.07	1.25

However, in terms of economics, the bio-based production in Scenario III could not compete with the petroleum-based production in Scenario IV. Given the less complexity and the much simple chemical reactions involved in the petroleum-based production, Scenario IV yielded the lowest capital cost, operating cost and raw material cost as reported in Table 4.6. However, since the utilization of ethylene and CO was not sustainable, its CO₂ equivalent emissions should be taken into consideration.

4.2.5 CO₂ equivalent emissions

Figures 4.5 and 4.6 show the feedstocks, utilities, as well as the emissions from the processing blocks of PA production. The CO₂ emissions in each scenario were categorized based on the origins of CO₂: raw material acquisition, transportation, reaction, as well as recovery and purification as illustrated in Table 4.9.

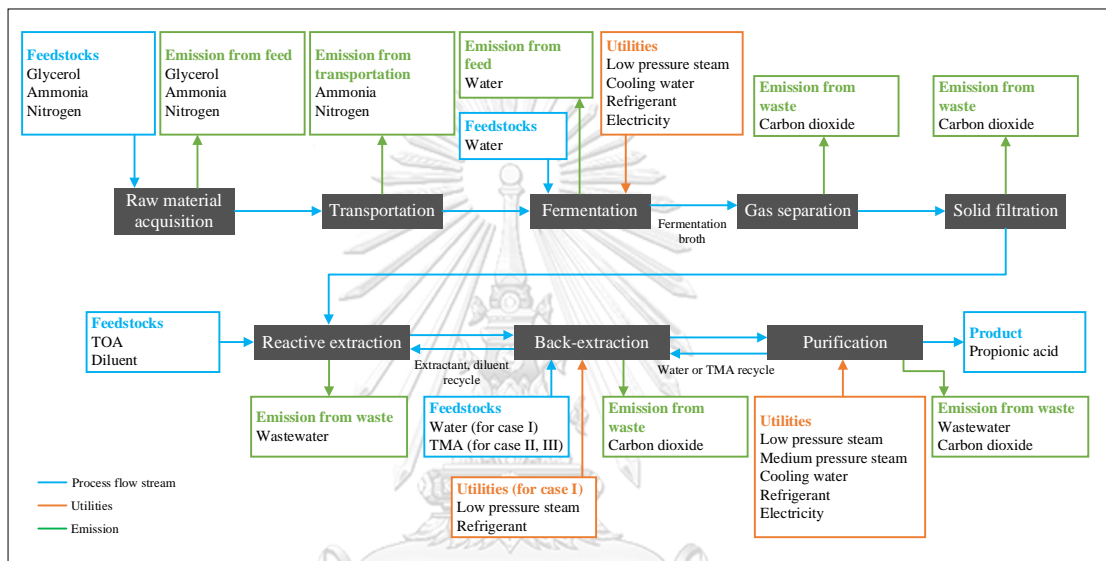


Figure 4.5 Diagram with relevant parameters of glycerol-based process

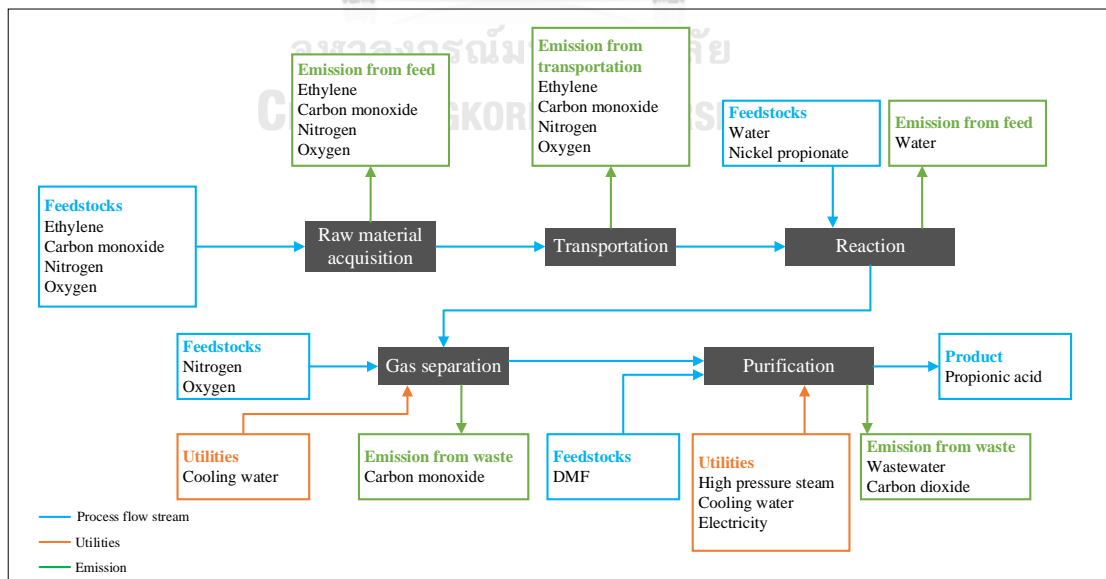


Figure 4.6 Diagram with relevant parameters of petroleum-based process

According to Table 4.9, the greatest CO₂ equivalent emissions were observed in Scenario IV followed by Scenarios I, II and III. In Scenario IV, about 82% of the total emissions originated from the reaction block which was contributed from the estimated CO₂ equivalence (CO_{2-eq}) caused by the utilization of petroleum-based feedstocks, e.g., CO and ethylene (see Table B4 in Appendix B). Furthermore, about 7.16 kg CO_{2-eq}/kg product was discharged to the environment in Scenario IV compared to the 4.75 to 5.39 kg CO_{2-eq}/kg product range in the bio-based scenarios from the cradle-to-gate analysis.

Table 4.9 Summary of emissions of CO₂ equivalence (cradle to gate) for propionic acid production

CO ₂ origin	Unit	Scenario I	Scenario II	Scenario III	Scenario IV
Raw material	kg CO _{2-eq} /h	2.06E+03	2.01E+03	1.90E+03	6.73E+03
Transportation	kg CO _{2-eq} /h	5.08E+01	5.07E+01	5.06E+01	1.39E+02
Reaction	kg CO _{2-eq} /h	2.82E+03	2.75E+03	2.60E+03	1.89E+01
Recovery and purification	kg CO _{2-eq} /h	1.22E+03	8.27E+02	8.74E+02	1.30E+03
Total	kg CO _{2-eq} /h	6.15E+03	5.65E+03	5.43E+03	8.16E+03
PA production	kg/h	1.14E+03	1.14E+03	1.14E+03	1.14E+03
CO_{2-eq} emissions	kg CO _{2-eq} /kg PA	5.39	4.95	4.75	7.16

In addition, significant reduction of the total CO₂ emissions was observed in the bio-based production. To elaborate this, if Scenario III (the best bio-based production scenario) was compared with Scenario IV, the total CO₂ emissions was significantly reduced by 34%. Accordingly, although the petroleum-based production was superior to the bio-based production in both economic and energy-utilization perspectives, the petroleum-based production caused more harm to the environment as evidence by the estimated CO₂ emissions.

4.3 Process sensitivity

In this work, the price variability was set at $\pm 50\%$ for each material. For the bio-based production, only Scenario III was selected for the sensitivity analysis given its most promising economic performance compared to other bio-based scenarios. According to Table 4.6, the main feeding materials for the bio-based PA production included glycerol, TOA, TMA, and 2-octanol. As seen from the cost per year of these materials, the cost of TOA was significantly lower compared to other materials. Thus, glycerol, TMA and 2-octanol were included in the sensitivity analysis. Propionic acid was also included in the analysis given the main product in this study.

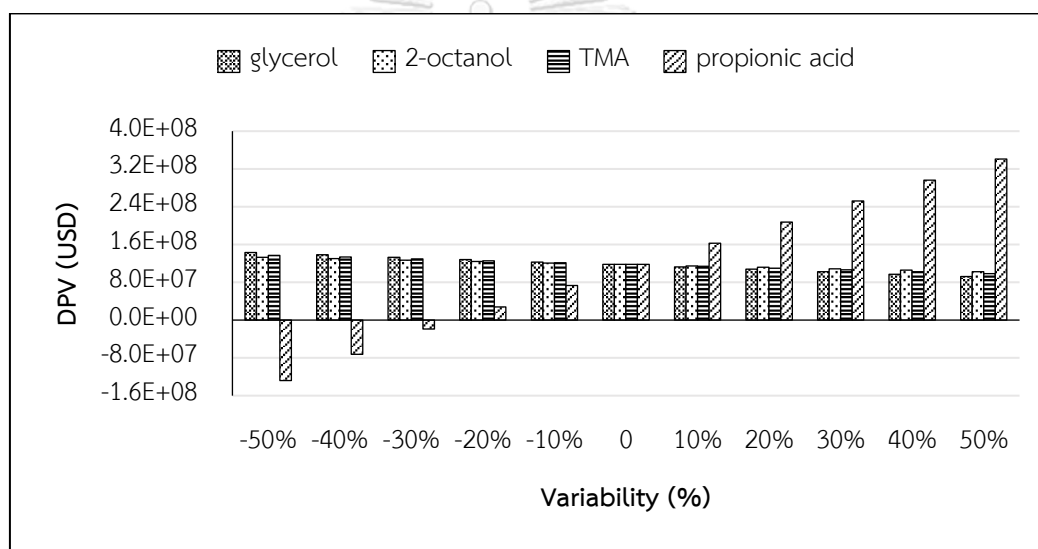


Figure 4.7 Effect of the price of Scenario III on DPV for propionic acid production

The results obtained from the sensitivity analysis are illustrated in Figure 4.7. According to the figure, the process DPV appeared highly influenced by the price of propionic acid. If the price of PA was reduced by 30%, the DPV became negative. Regarding the feeding materials, the DPV appeared sensitive to the price of glycerol. However, it was not as sensitive when compared to the price variability of propionic acid. Therefore, if the price of propionic acid was lower than 2.1 USD/kg, the bio-based production of propionic acid became infeasible.

CHAPTER 5

SUCCINIC ACID PRODUCTION FROM GLYCEROL BY *ACTINOBACILLUS SUCCINOGENES*: TECHNO-ECONOMIC, ENVIRONMENTAL, AND EXERGY ANALYSES

This chapter investigates the enhanced succinic acid productivity via the addition of dimethyl sulfoxide along with the selection of the purification technologies justified by the performance indexes (e.g., economic, energy consumption, and GHG emissions). In addition, the exergy analysis, which had never been undertaken for bio-based succinic acid production would be provided. This would be useful for further improvement plans since inefficient unit operations would be identified. Therefore, this chapter aims to analyze the DMSO-assisted bio-based SA production from glycerol via process simulation to evaluate process performances in terms of economic performance, energy consumption, exergy analysis, and greenhouse gas (GHG) emissions.

5.1 Process description of succinic acid production

In this techno-economic study, glycerol was fermented with *Actinobacillus succinogenes* for an SA production capacity of 10,000 tonnes per year (required about 12,851 tonnes/year of glycerol which was sufficient based on the surplus amount of glycerol at 57,159 tonnes/year of Pathum Vegetable Oil Company, a major biodiesel producer in Thailand) [186] with a purity of 99.5 wt% industrial grade [187]. The rigorous process simulation for the production of SA was performed using Aspen Plus[®] V.11. According to the guideline of Carlson [152], the UNIFAC model was used in the simulation based on the operating conditions and the existence of polar and non-polar compounds in the simulated systems.

The different process routes investigated are listed in Table 5.1. According to the table, the difference between Scenario I and Scenario II was the downstream technique for the removal of water (water was the major problem with the purification of SA production). However, the fermentation of glycerol consumed a

substantial amount of time. To mitigate this, the additive, DMSO served as an electron acceptor could be utilized to enhance the SA productivity in the fermentation process as highlighted in Scenario III and IV.

Table 5.1 Key attributes in Scenarios I to IV of glycerol-based production

Scenario	Fermentation description	Downstream processing
I	pH controlled by MgCO ₃ , 75 h, 37°C*	Direct crystallization
II	pH controlled by MgCO ₃ , 75 h, 37°C*	Reactive extraction
III	DMSO 1.8% Vol, pH controlled by NaOH, 30 h, 37°C**	Direct crystallization
IV	DMSO 1.8% Vol, pH controlled by NaOH, 30 h, 37°C**	Reactive extraction

* The experimental data was obtained from Vlysidis et al. [6]

** The experimental data was obtained from Carvalho et al. [23]

5.1.1 Scenario I: SA purification using direct crystallization (no addition of DMSO)

The comprehensive process flow diagram for Scenario I is depicted in Figure C1 in Appendix C. For illustrative purposes, the general block flow diagram of bio-based SA production is shown in Figure 5.1. The SA production was divided into three sections. In each section, the various equipment involved was identified and designed. Major detailed descriptions of each section are as follows.

Zone I in Figure 5.1 provides details about crude glycerol pretreatment. Crude glycerol from the biodiesel industry contains about 83% glycerol [188]. Common impurities in crude glycerol include water, ash, methanol, and matter organic non glycerol (MONG). These impurities should be eliminated to achieve higher glycerol consumption in the fermentation stage. For the ash removal in crude glycerol, the Ssplit filter model (S-100) was applied. After that, the glycerol stream was treated via an evaporator (D-100) at 0.1 atm to remove methanol and water according to Chang [189]. Finally, Stream 8 containing glycerol and MONG was passed through the pump (P-100) before the separator (S-101) to increase the pressure at 1 atm. The separator was used to separate MONG.

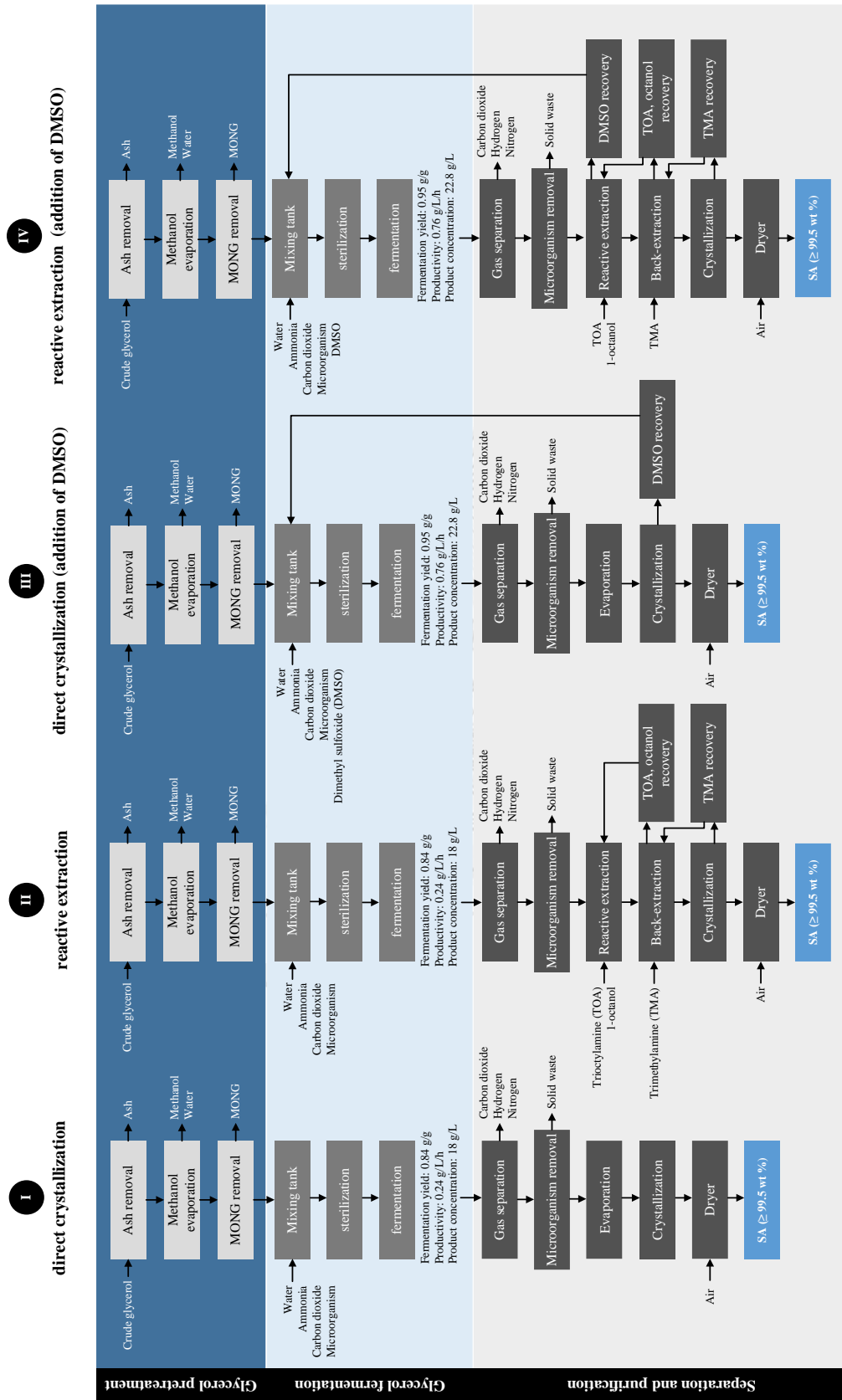


Figure 5.1 General block flow diagram of bio-based SA production

Zone II in Figure 5.1 provides details about glycerol fermentation. Before entering the fermenter (R-100), the relevant feedstocks must be sterilized (E-101) at 121°C to avoid possible contamination [123]. Due to the complexity involved in biological processes, the previous research works [30, 153] circumvented such complexity by converting the experimental results to stoichiometric coefficients to simplify the fermentation process. SA fermentation from glycerol has yield, concentration, and productivity of 0.84 g SA/g glycerol, 18 g/L, and 0.24 g/L/h, respectively. Details of the reaction of R-100 are available in Table C5 in Appendix C.

Zone III in Figure 5.1 provides details about separation and purification. The fermentation broth (Stream 20) was sent to the flash drum (D-101) and the tubular cross-flow filter (S-102) to separate off-gas and solid impurities, respectively. After that, Stream 24 was passed through the heater (E-104) before the evaporator (D-102). In the evaporation process, the dissolved product stream was concentrated by the evaporator (D-102) at 101.2°C. After that, CR-100 was used to separate SA into solid form for further SA purification. The solid was separated using S-103. Finally, SA with a product purity of 99.5 wt% was attained after drying (in DR-100) with hot air. The full stream table of rigorous process simulation is given in Table C6 (in Appendix C).

5.1.2 Scenario II: SA purification using reactive extraction (no addition of DMSO)

The process flow diagram is given in Figure C2 in Appendix C. The fermentation process was the same as that in Scenario I. The difference in production started after the S-102. The reactive extraction was designed by a cascade model containing the reactor (R-101) and the decanter (S-103) according to Nieder-Heitmann [154]. Please note that reactive extraction is a multifunctional reactor having reaction and extraction in a single unit. However, Aspen Plus does not have a unit operation that could perform the reactive extraction directly. Trioctylamine (TOA) and 1-octanol were used as the extractant and the diluent, respectively due to the best combination for succinic acid extraction with 96% extraction efficiency [190].

Regarding the reactive extraction, Stream 25 containing SA and water was sent to R-101. At this stage, the reactive extraction was performed by the formation of a complex compound between SA and TOA (SA-TOA complex) which could dissolve in the 1-octanol-rich phase. After the reactive extraction, Stream 30 (1-octanol-rich phase containing SA-TOA complex) was passed to the back-extraction system, consisting of the reactor (R-102) and the decanter (S-104). Trimethylamine (TMA) was added in this step to substitute the TOA by which the SA-TMA complex was formed. The organic phase consisting of TOA and 1-octanol was recovered (Stream 36) and returned to the reactive extraction, whereas Stream 34 containing SA-TMA complex was sent to the crystallization (CR-100). CR-100 was operated at 20°C to obtain a solid form of SA via the separator (S-105). The crystallizer effluent was sent to the evaporator (D-102) to recover the TMA for recycling. Product (Stream 41) was passed to the dryer (DR-100) and obtained product in Stream 49 with a purity of 99.5 wt%.

5.1.3 Scenario III: SA purification using direct crystallization (addition of DMSO)

In this techno-economic study, dimethylsulfoxide (DMSO) was used as an electron acceptor in the glycerol fermentation by *Actinobacillus succinogenes*. According to Carvalho et al. [23], it was stated that the use of an electron acceptor such as DMSO helped increase the glycerol consumption rate and succinic acid production. The detailed descriptions of unit operations involved are schematized in Table C9 (in Appendix C).

Zone III in Figure 5.1 provides the separation and purification of SA. The addition of DMSO required additional equipment to recover DMSO for recycling. The crystallizer effluent (Stream 30) was passed through the pump (P-101) before the distillation column (C-100). The column was used to separate water and DMSO. DMSO was passed through the valve (V-101) and the cooler (E-108) to reduce the pressure and the temperature to 1 atm and 37°C, respectively. This process was able to recover approximately 90% of DMSO, resulting in an actual DMSO feed rate of 112

kg/h. A full stream table is provided in Table C10 in Appendix C. After the drying process, SA at the purity of 99.5 wt% was attained.

5.1.4 Scenario IV: SA purification using reactive extraction (addition of DMSO)

For complete comparisons among all scenarios, Scenario IV consisting of the addition of DMSO in the fermentation plus the utilization of reactive extraction in the purification was also provided.

5.2 Process evaluation

In this techno-economic study, the simulated processes were evaluated with five performance indexes, including glycerol and carbon utilization, economic performance, energy utilization, exergy analysis, and GHG emissions. Ultimately, these indicators were useful in decision-making regarding the feasibility of bio-based succinic acid production.

5.2.1 Glycerol and carbon utilization

According to Table 5.2, the glycerol utilization of each scenario is determined as 0.59, 0.50, 0.76, and 0.71 for Scenarios I to IV, respectively. Likewise, the carbon utilization of Scenarios I to IV is determined as 0.62, 0.52, 0.79, and 0.73, respectively (see Table 5.3). Scenario III is more attractive than Scenario I, given the highest glycerol and carbon utilization. This was due to the addition of DMSO which could improve the SA yield while the fermentation time was reduced to 30 h. However, Scenario I was the most efficient in terms of SA recovery as seen in Table 5.2. This indicated that the addition of DMSO reduced the SA separation efficiency – SA was carried over with DMSO in Stream 31. It was also observed in the downstream processing (e.g., SA separation and purification) that the direct crystallization had better SA recovery performance and glycerol utilization than the reactive extraction as seen from the 87% SA recovery compared to 73% SA recovery.

Table 5.2 Summary of glycerol utilization for bio-based production scenarios

Scenario	Salable Succinic acid [tonnes/y]	Glycerol feed rate [tonnes/y]	Glycerol utilization
I	1.00E+04	1.68E+04	0.59
II	1.00E+04	2.00E+04	0.50
III	1.00E+04	1.32E+04	0.76
IV	1.00E+04	1.42E+04	0.71

Scenario	Succinic acid from reactor effluent [tonnes/y]	Salable Succinic acid (after purification) [tonnes/y]	% Recovery
I	1.15E+04	1.00E+04	87.0
II	1.37E+04	1.00E+04	73.2
III	1.29E+04	1.00E+04	77.7
IV	1.36E+04	1.00E+04	73.5

Table 5.3 Summary of carbon utilization for bio-based production scenarios

Scenario	Carbon content in product [tonnes/y]	Carbon content in glycerol [tonnes/y]	Carbon utilization
I	4.06E+03	6.58E+03	0.62
II	4.06E+03	7.82E+03	0.52
III	4.06E+03	5.17E+03	0.79
IV	4.06E+03	5.54E+03	0.73

5.2.2 Economic performance

In terms of economic performance, the results obtained from Aspen Economic Analyzer are shown in Table 5.4. The results of the three indicators in the table showed that Scenario III gave the highest DPV of 190 million USD, the highest % DCFROR of 33.3%, and the shortest DPP of 4.48 years when all four scenarios were compared. Although DMSO recovery added complexity to Scenarios III and IV, it lightly affected the process economics since DMSO could be separated from water using the single distillation column (C-100) – the distillation column costs only 4.3% of the total equipment cost. To emphasize this, the hotspots for each scenario are illustrated in Table 5.5.

Total equipment cost is highest in Scenario II. Thus, it could be concluded that the choice of downstream technique significantly influenced the feasibility of bio-based SA production. However, if comparing the operating cost in Scenarios II and IV with the work of Morales et al. [31] using glucose derived from wood, the operating cost per succinic acid produced in Scenarios II and IV was reduced by 11% (2.32 VS 2.6 USD/kg SA). This indicated that although TOA and 1-octanol were used in the same downstream technique, the glycerol-based carbon source was preferable to using glucose. As a result, the expensive procedures necessary for the lignocellulosic pretreatment could be avoided when using glycerol as the starting material, which was consistent with Tan et al. [139]. Furthermore, glycerol has a greater reduction state of carbon than glucose, which leads to better product yields [191].

Table 5.4 Summary of economic performance for bio-based production scenarios

Economic information	Unit	Scenario	Scenario	Scenario	Scenario
		I	II	III	IV
Total Capital Cost	\$	4.37E+07	4.95E+07	2.80E+07	3.24E+07
Total Operating Cost	\$/y	2.19E+07	2.32E+07	1.63E+07	2.33E+07
Total Equipment Cost	\$	1.13E+07	1.25E+07	5.46E+06	5.99E+06
Total Operating Labor Cost	\$/y	9.20E+05	1.08E+06	1.08E+06	1.77E+06
Total Maintenance Cost	\$/y	1.12E+06	1.19E+06	5.09E+05	5.29E+05
Total Utility Cost	\$/y	1.40E+07	1.01E+07	1.04E+07	1.21E+07
Total Product Sales	\$/y	2.70E+07	2.71E+07	2.70E+07	2.72E+07
Total Raw Material Cost	\$/y	3.02E+06	7.74E+06	2.09E+06	6.51E+06
Main material cost					
Glycerol	\$/y	2.27E+06	2.70E+06	1.79E+06	1.91E+06
Trimethylamine (TMA)	\$/y	-	2.95E+06	-	3.01E+06
2-Octanol	\$/y	-	1.19E+06	-	1.14E+06
Dimethyl sulfoxide (DMSO)	\$/y	-	-	1.23E+05	2.62E+05
Economic indicator					
DPV	\$	9.89E+07	7.36E+07	1.90E+08	8.89E+07
DCFROR	%	13.9	10.0	33.3	15.2
DPP	Y	8.45	10.1	4.48	8.16

Table 5.5 Comparison of the most expensive equipment in each scenario

Hotspot	Unit	Scenario I	Scenario II	Scenario III	Scenario IV
The most expensive equipment	\$	1.02E+07 (R-100)	1.10E+07 (R-100)	4.16E+06 (R-100)	4.16E+06 (R-100)
Contribution to the total equipment cost	%	90.3	87.9	76.1	69.5

In addition to the influence of the separation technique, it was revealed in Table 5.5 that the highest equipment cost was observed at the fermentation tank which accounted for 76% to 90% of the total cost in each scenario. As observed from the table, Scenarios III and IV had the lowest cost of the fermenter as a result of the addition of DMSO that accelerated the fermentation process as discussed previously.

5.2.3 Energy utilization

Heating, cooling, and electrical power are the three main components of energy utilization as provided in Table 5.6. The SECs of Scenarios I to IV were determined as 134.4, 115.3, 100.3, and 113.7 kWh/kg product, respectively. Even if no foreign substances (TOA, 1-octanol, and TMA) were added in Scenario I, the separation process in Scenario I consumed a substantial amount of energy due to the heat required for the water removal in the evaporator (E-104) – accounted for 31.9% of the total energy consumption as shown in Figure 5.2. In other words, although the reactive extraction in Scenarios II and IV required the addition of foreign substances, the energy utilization was lower when compared to the direct crystallization in Scenario I.

Table 5.6 Summary of energy utilization for bio-based production scenarios

Type of duty	Unit	Scenario I	Scenario II	Scenario III	Scenario IV
Total heating duty	kW	1.01E+05	6.53E+04	7.35E+04	8.18E+04
Total cooling duty	kW	5.23E+04	6.62E+04	4.10E+04	4.78E+04
Total electric power	kW	7.43E+01	8.35E+01	3.09E+01	3.26E+01
Total energy requirement	kW	1.53E+05	1.32E+05	1.14E+05	1.30E+05
SA production	kg/h	1.14E+03	1.14E+03	1.14E+03	1.14E+03
SEC	kWh/kg	134.4	115.3	100.3	113.7

However, a significant reduction of the SEC value was observed when Scenario III was compared with Scenario I. Even with the DMSO recovery unit, Scenario III yielded less SEC value (about a 25% reduction) than Scenario I. The addition of DMSO could reduce the fermentation time resulting in less number of fermenters which influenced the power consumed by the agitation calculated from CheCalc [192]. It was found that the power used for the fermenter was reduced by 58% when DMSO was added in Scenario III. Furthermore, the addition of DMSO also reduced the heat duty in the sterilization as a result of the less feed to achieve the same 10,000 tonnes per year of SA.

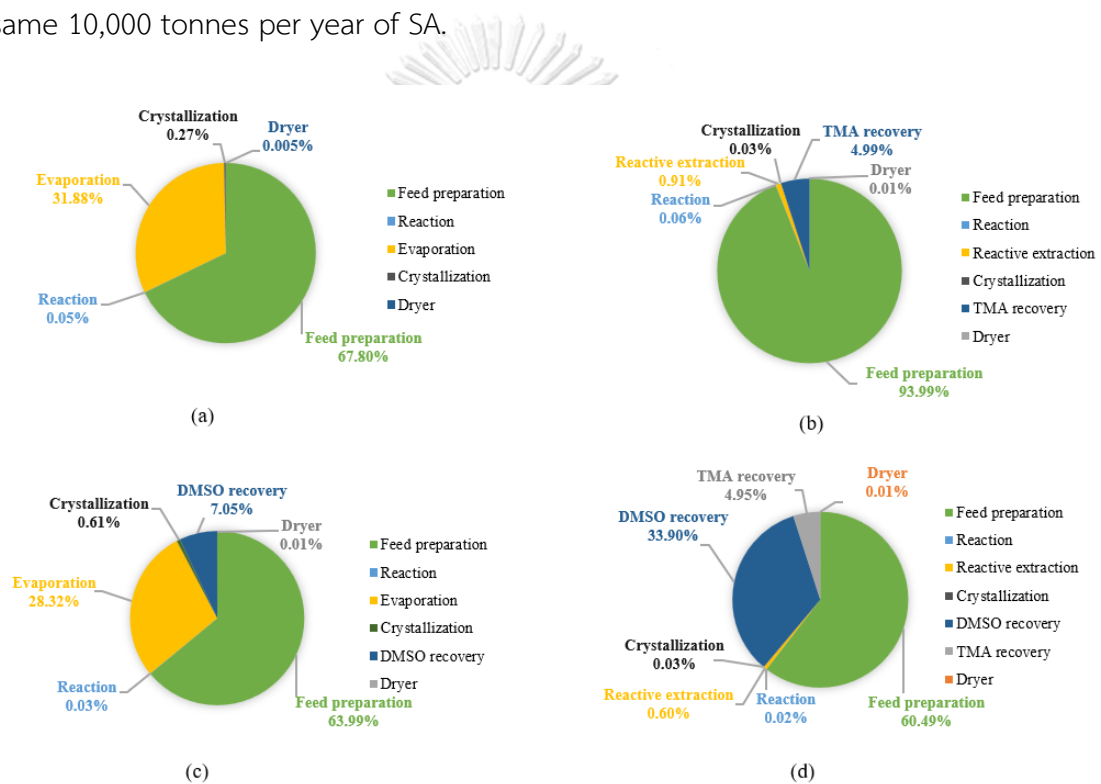


Figure 5.2 Effect of the utility duty of the bio-based succinic acid production: (a) Scenario I, (b) Scenario II, (c) Scenario III, and (d) Scenario IV

5.2.4 Exergy analysis

The exergy analysis was carried out in Scenario III to identify inefficient energy units and to highlight the importance of the energy which could be utilized further for the heat integration design. Table 5.7 depicts the contribution of units to exergy destruction ($\dot{E}_{x,D}$), exergy efficiency (ψ), and irreversibility (y_D).

As shown in Table 5.7, column C-100 had the highest exergy destruction rate of 3,326 kW and the lowest exergy efficiency of 47.05% due to the amount of high-pressure steam required in the reboiler. The heater (E-101) after the sterilization stage contributed the second highest exergy destruction rate of 1,761 kW. When the exergy destruction rates of all the units were compared, they revealed that the C-100 had the highest irreversibility ratio of 44.56%. In order to achieve the most efficient design in terms of energy, a heat integration design could be undertaken to reduce the exergy losses.

Table 5.7 Summary of exergy analysis for Scenario III

Stage	Exergy inlet (kW)	Exergy outlet (kW)	\dot{E}_{x_d} (kW)	y_D (%)	Ψ (%)
S-100	6.75E+03	6.75E+03	2.87E+00	0.04	99.96
V-100	6.68E+03	6.68E+03	2.99E-02	0.00	100.00
E-100	6.72E+03	6.70E+03	1.13E+01	0.15	99.83
D-100	6.70E+03	6.70E+03	5.50E-01	0.01	99.99
P-100	6.65E+03	6.65E+03	5.13E-02	0.00	100.00
S-101	6.65E+03	6.65E+03	4.97E-02	0.00	100.00
M-100	1.56E+04	1.54E+04	1.71E+02	2.29	98.91
E-101	2.43E+04	2.26E+04	1.76E+03	23.60	92.76
E-102	2.26E+04	2.18E+04	7.90E+02	10.58	96.50
E-103	1.58E+04	1.56E+04	2.74E+02	3.68	98.27
R-100	1.61E+04	1.55E+04	5.59E+02	7.49	96.52
D-101	1.61E+04	1.61E+04	3.54E+01	0.47	99.78
S-102	1.56E+04	1.56E+04	2.05E+01	0.28	99.87
E-104	2.15E+04	2.12E+04	3.62E+02	4.85	98.32
D-102	2.12E+04	2.12E+04	3.25E+00	0.04	99.98
E-105	1.30E+04	1.29E+04	8.21E+01	1.10	99.37
CR-100	1.29E+04	1.29E+04	5.06E+00	0.07	99.96
S-103	1.30E+04	1.29E+04	1.56E+01	0.21	99.88
P-101	7.98E+03	7.98E+03	5.17E-01	0.01	99.99
C-100	6.28E+03	2.96E+03	3.33E+03	44.56	47.05
V-101	7.89E+03	7.89E+03	4.27E+00	0.06	99.95
E-108	7.89E+03	7.86E+03	3.37E+01	0.45	99.57
E-109	3.10E+00	1.94E+00	1.16E+00	0.02	62.68
DR-100	4.98E+03	4.97E+03	3.73E+00	0.05	99.92
sum	2.83E+05	2.75E+05	7.46E+03	100	

Please note that although the exergy analysis suggested that heat integration should be undertaken, heat integration was not performed in this work due to two practical reasons. First, the condenser and reboiler in C-100 were used primarily to control the distillate and bottom product purities. The temperature control in C-100 would be more difficult if the heat integration was applied to the condenser and the reboiler in C-100. Second, the temperature in Stream 16 was too high to cool streams that required cooling.

5.2.5 Greenhouse gas emissions

The GHG emissions were calculated based on the emission factor from OpenLCA software. The results are shown in Table 5.8. According to Table 5.8, the GHG emissions boundary of the SA production was divided into four categories according to the cradle-to-gate: raw materials acquisition, transportation, upstream processing, and downstream processing.

Table 5.8 Summary of emission of CO₂ equivalence (cradle to gate) for bio-based production scenarios

CO ₂ origin	Unit	Scenario	Scenario	Scenario	Scenario
		I	II	III	IV
Raw material	kg CO ₂ -eq/h	1.60E+03	1.90E+03	9.16E+02	9.80E+02
Transportation	kg CO ₂ -eq/h	5.26E+01	5.34E+01	4.91E+01	4.92E+01
Upstream processing	kg CO ₂ -eq/h	1.80E+03	2.14E+03	8.99E+02	3.46E+02
Downstream processing	kg CO ₂ -eq/h	1.23E+03	1.65E+03	1.05E+03	2.15E+03
Total	kg CO ₂ -eq/h	4.68E+03	5.74E+03	2.92E+03	3.53E+03
SA production	kg/h	1.14E+03	1.14E+03	1.14E+03	1.14E+03
CO₂-eq emissions	kg CO ₂ -eq/kg SA	4.10	5.03	2.56	3.09

The greatest GHG emissions were observed in Scenario II followed by Scenarios I, Scenario IV and III with 5.03, 4.10, 3.09, and 2.56 kg CO₂-eq/kg product, respectively. In all four categories, the transportation sector had the least impact on GHG emissions. The raw materials acquisition showed that glycerol was the hotspot, followed by pH controller and ammonia, respectively. According to Table C1 in Appendix C, ammonia from the steam reforming had a higher characterization factor

than glycerol from the palm oil production. However, glycerol was used as the main feedstock to produce succinic acid. Therefore, it had a significant impact on GHG.

The results also demonstrated that steam and cooling water used in the downstream processing were the biggest contributors to GHG emissions (see Table C4 in Appendix C). When comparing the GHG emissions in every scenario, Scenario III yielded the lowest GHG emissions given 1) the lower emission from transportation due to the better glycerol efficiency (less required raw material to produce 10,000 tonnes/y SA, 2) the lower energy consumption in the upstream and downstream processes as indicated from the less power used in agitation from the less number of fermenters and the lowest SEC value.

According to the simulated processes, scenario III was suitable for further development to an industrial scale from the perspective of economic performance, energy utilization, GHG emissions and exergy analysis. Thus, this scenario was compared with the petroleum-based process to highlight the benefit of adopting bio-based production.

5.3 Comparison between bio-based and petroleum-based SA production

In this section, the three bio-based productions were compared with petroleum-based production in terms of operating cost, SEC, and GHG emissions. Data regarding the impact categories for petroleum-based production were obtained from the previous studies by Morales et al. [31] for the operating cost and the GHG emissions data and Pinazo et al. [193] for the energy consumption data.

Table 5.9 Comparison between glycerol-based and petroleum-based SA production

Indicator	Unit	Scenario	Scenario	Scenario	Scenario	Petroleum
		I	II	III	IV	
Operating cost	\$/kg	2.19	2.32	1.63	2.33	1.92*
Energy aspect (SEC)	kWh/kg	134.4	115.3	100.3	113.7	15.3**
Environmental aspect (CO _{2-eq} emissions)	kg CO _{2-eq} /kg	4.10	5.03	2.56	3.09	3.46*

* The data was obtained from Morales et al. [31]

** The data was obtained from Pinazo et al. [193]

According to the results shown in Table 5.9, the bio-based production in each scenario consumed more energy than the petroleum-based production. However, in terms of the GHG emission and operating cost, the bio-based production in Scenario III was superior to the petroleum-based production. To highlight this, the operating cost of 1.63 was attained in Scenario III which was about 15% lower when compared to the petroleum-based production. A significant reduction in the total GHG emissions was also observed, 2.56 VS 3.46, which was about a 26% reduction. This is due to the production of succinic acid from maleic anhydride through hydrogenation followed by hydration involves an expensive catalyst like palladium. Furthermore, the recycling and purification of water in the hydration tank increase the consumption of electricity by 20% [193]. This observation also emphasized that the addition of DMSO was environmentally beneficial as seen from the significant decrease in the SEC value and the GHG emissions in Scenario III compared to Scenario I.

5.4 Process sensitivity

In this study, the sensitivity analysis was conducted to investigate and understand the influence of the uncertainties associated with the feedstock costs, the product sales price, the utility cost, and the plant capacity on the economic indicators.

5.4.1 Effect of feedstock and product prices on DPV

In sensitivity analysis, only Scenario III was considered due to the most promising production based on previous assessments. According to Table 5.4, the main raw material in Scenario III consisted of glycerol and the make-up DMSO. Therefore, the variations in the costs of glycerol, DMSO, utilities and the selling price of SA were investigated. The prices of all these parameters varied between -50% and 50% of their nominal values.

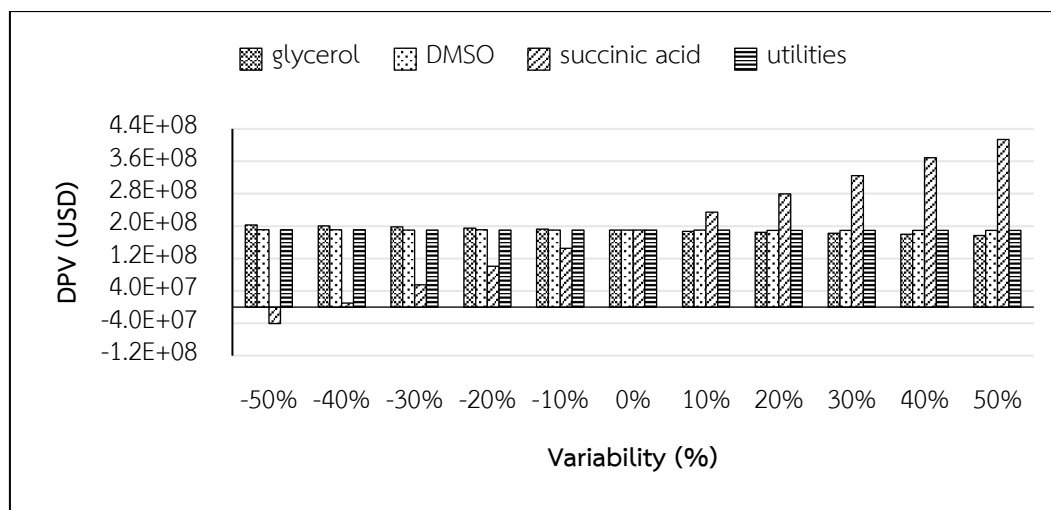


Figure 5.3 Effect of the price of Scenario III on DPV for succinic acid production

The results obtained for each case of price sensitivity on the process DPV are provided in Figure 5.3. According to the figure, the price of succinic acid had a significant effect on the DPV, as evidenced by the negative DPV when the price fell below 50% (1.5 USD/kg). Meanwhile, the price effect of the two feedstocks, glycerol and DMSO, was relatively negligible in comparison to the SA sales price.

5.4.2 Effect of SA production capacity on economic indicators

The results of the sensitivity analysis with three production capacities are summarized in Table 5.10. All production capacities were analyzed for techno-economic study by the same investment parameters. Please also note that the SA yields (or glycerol conversion) in this work were assumed to be the same values from the experiments of Vlysidis et al. [2] and Carvalho et al. [23]. In practice, however, extrapolation from the experimental data may not be undertaken straightforwardly given that large reactor sizes (e.g., 250, 500 and 1,000 m³ as seen in this work) could affect the SA production such as agitation and poor heat transfer problems. In fact, these problems could be minimized with a proper design during the process scale-up. For example, implementation of similarity law of sizing geometry and utilization of standard aspect ratios of tank and agitator could help minimize such problems. Thus, to assert that the fermentation size used in this work was practical, a commercial fermenter tank with a maximum capacity of 1,000 m³ was implemented

according to DuPont company [185]. The design of the fermentation tank was undertaken using the operation of 6–8 batch fermenters to enable continuous production of SA from the reactor in Table 5.10. Details of the fermentation reactor design are available in the supplementary material.

Table 5.10 The economic indicators with a different succinic acid capacity of Scenario III

Information	Unit	Capacity [tonnes/y]		
		5,000	10,000	30,000
Fermenter				
Number of required fermenters	tank	6	6	8
Reactor size	m ³	250	500	1,000
Economic indicator				
DPV	\$	7.20E+07	1.90E+08	6.68E+08
DCFROR	%	19.1	33.3	59.3
DPP	Y	6.76	4.48	3.06

According to Table 5.10, all production capacity numbers are feasible given the positive DPV. Based on the SA sales price adopted in this work, the results suggested that the bio-based production of SA in Scenario III was attractive since it began to be profitable at 5,000 tonnes/y of SA production (required 6,616 tonnes/y of glycerol) with the pay-out period of about 6.76 years, which was half of the assumed plant life. If the glycerol availability was more than 6,616 tonnes/y, there would be room for the production of other chemicals. In other words, the glycerol conversion complex (e.g. production of various chemicals from glycerol) would be less vulnerable since the revenue did not depend only on the SA sales volume.

CHAPTER 6

SUSTAINABILITY ASSESSMENT OF DIHYDROXYACETONE (DHA) PRODUCTION FROM GLYCEROL: A COMPARATIVE STUDY BETWEEN BIOLOGICAL AND CATALYTIC OXIDATION ROUTES

Previously, a variety of naturally occurring microorganisms have been proven capable of consuming crude glycerol, making microbial conversion more effective than other approaches. This novel study for the first time simulates glycerol-based DHA production via microbial fermentation. Regarding the simulation study focused herein, the process of glycerol-based DHA production could be improved by enhancing the performance of the upstream processing. This could be undertaken by selecting an appropriate carbon source, controlling the impurity contained in crude glycerol, and choosing suitable techniques in the upstream processing. Therefore, this chapter aims to develop the more efficient production of DHA from crude glycerol using process simulation to evaluate process performances in terms of energy utilization, economic, and environmental performance.

6.1 Process description of dihydroxyacetone production

For illustrative purposes, Figure 6.1 depicts an overview of the applied framework, including data collection, process simulation, process evaluation, and process improvement by heat integration. In this study, the DHA production at 2,000 tonnes per year was considered [53]. According to DHA supplier data, the synthesized product was industrial-grade DHA with a product purity of 99 wt% [52]. Aspen Plus V.11 was employed. According to Eric Carlson's guideline [152], the UNIFAC model was used to describe phase-equilibrium. In order to evaluate the techno-economic feasibility of the DHA production, the efficiency of glycerol and carbon utilization, energy consumption, economic performance, and environmental impacts were evaluated. A hotspot in the promising scenario was identified and the subsequent debottlenecking was conducted using heat integration. Finally, scenarios with the heat integration were re-evaluated.

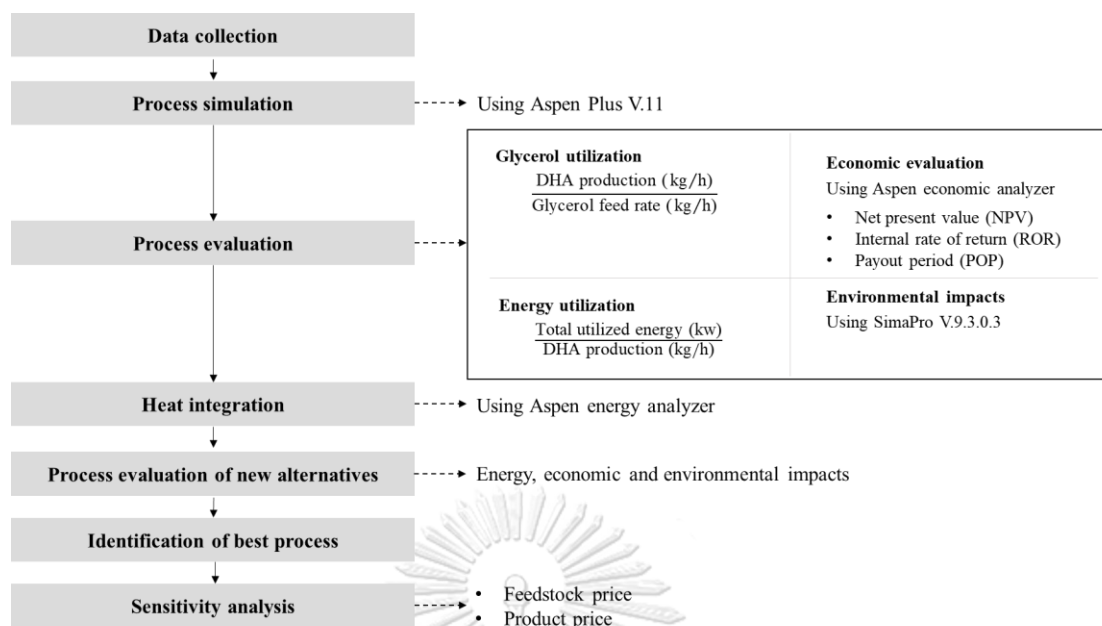


Figure 6.1 Overview of the framework in the design of DHA production

In this section, the process was designed on the basis of laboratory information. In this study, there were six investigated scenarios. Scenarios I to V were the microbial fermentation to produce DHA whereas Scenario VI was the catalytic oxidation. For clarity, the key attributes in each scenario are summarized in Table 6.1.

Table 6.1 Overview of Scenarios I to VI for DHA production

Scenario	Production type	Carbon source	Strain	Process description
I	Conventional production	Refined glycerol	<i>G. thailandicus</i>	Refined glycerol 60 g/L, 72 h, 30°C*
II	Fermentation	Crude glycerol	<i>G. thailandicus</i>	Crude glycerol 60 g/L, 72 h, 30°C*
III	Fermentation	Treated crude glycerol	<i>G. thailandicus</i>	Treated crude glycerol 60 g/L by ion exchange, 72 h, 30°C*
IV	Fermentation	Crude glycerol + Glucose	<i>G. oxydans</i>	Crude glycerol 40 g/L, glucose 20 g/L, 24 h, 30°C**
V	Fermentation	Crude glycerol + Sorbitol	<i>G. oxydans</i>	Crude glycerol 60 g/L, sorbitol 80 g/L, 24 h, 30°C**
VI	Catalytic oxidation	Catalyst = 2Au/CuO, glycerol conversion = 100% , DHA selectivity = 70.6% , 5 h of reaction, temperature = 50°C, pressure = 10 atm		

* The experimental data was obtained from Jittjang et al. [138]

**The experimental data was obtained from Lu et al. [55]

According to Table 6.1, the difference between Scenarios I to III was the types of glycerol, e.g., refined glycerol, crude glycerol, and treated crude glycerol. DHA is commercially produced using bacteria of the genus *Gluconobacter* and generally produced using refined glycerol [53, 194]. Herein, Scenario I represents commercial production. Typically, the fermentation of glycerol consumed a substantial amount of time. To mitigate this, glucose and sorbitol were served as the secondary carbon sources that could be utilized to enhance the DHA productivity in the biological route as highlighted in Scenario IV and V.

6.1.1 Biological route

The comprehensive process flow diagram for Scenarios I to V is depicted in Figure D1-D3 in Appendix D. Note that the difference between Figure D1 and D2 was the ion-exchange units (S-100 and S-101), by which the sodium content was removed from crude glycerol to obtain treated crude glycerol in Scenario III. For illustrative purposes, the general block flow diagram of bio-based DHA production is shown in Figure 6.2. The DHA production was divided into seven major steps as shown in Figure 6.3 – the fermentation, the gas and solid separation, the water separation, the crystallization, the methanol recovery, the washing, and the drying. Major detailed descriptions of each section are as follows.

Crude glycerol used in this work was estimated from a palm oil-based biodiesel plant in Thailand operated by Patum Vegetable Oil (composition: 83.3 wt% glycerol, 11.2 wt% water, 4.8 wt% sodium salts, 0.62 wt% other organics) [188]. According to Figure 6.3, crude glycerol and other compounds were fed to the mixer. Before entering the fermenter (R-100), the relevant feedstocks must be sterilized (E-101) at 121°C to avoid possible contamination [123]. After the sterilization, the outlet stream was passed through two heat exchangers to reduce the temperature from 121°C to 30°C. After the reduction of temperature, the stream was sent to a fermenter where the conversion of glycerol occurs at 30°C and 1 bar.

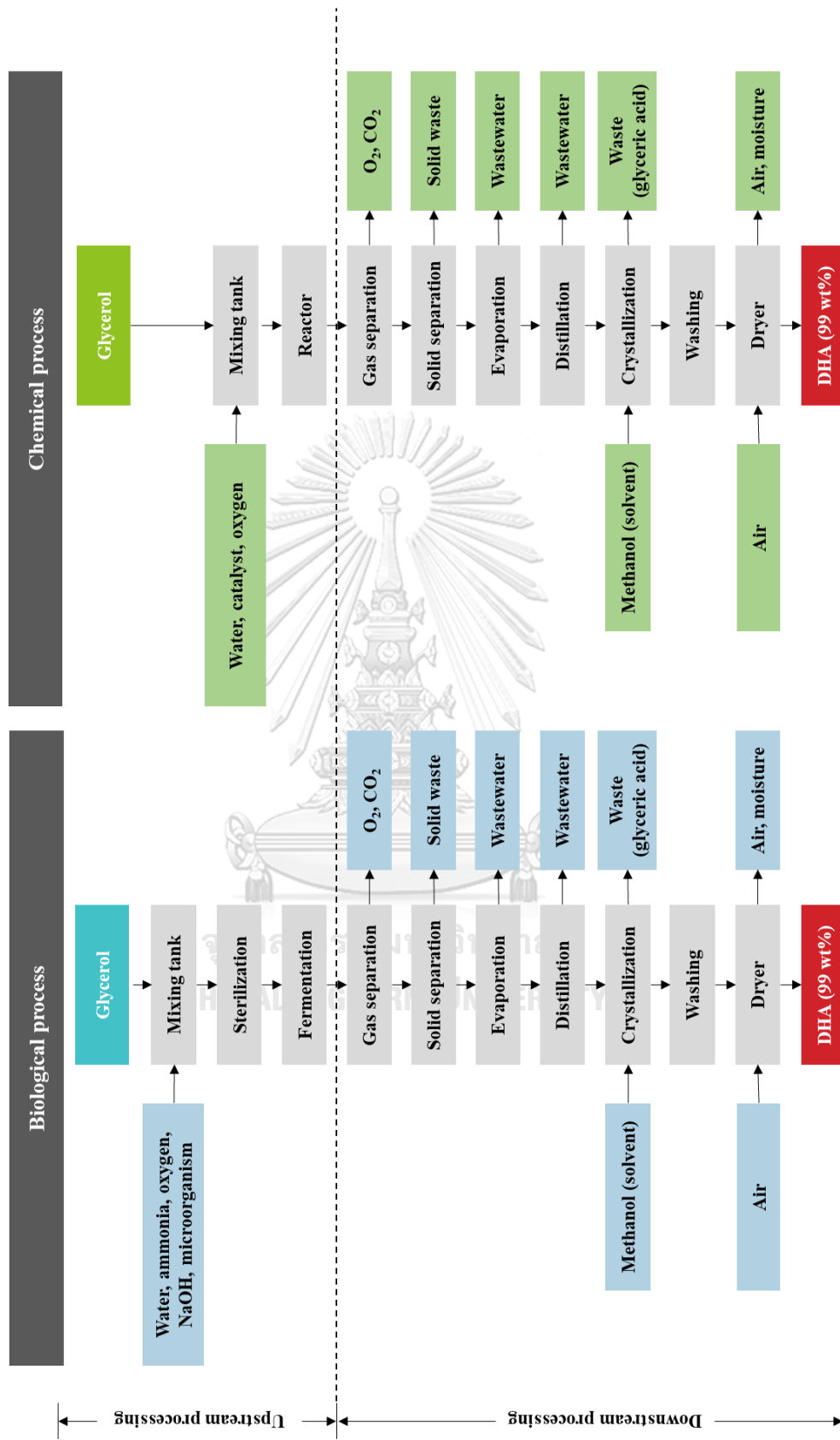


Figure 6.2 General block flow diagram of DHA production

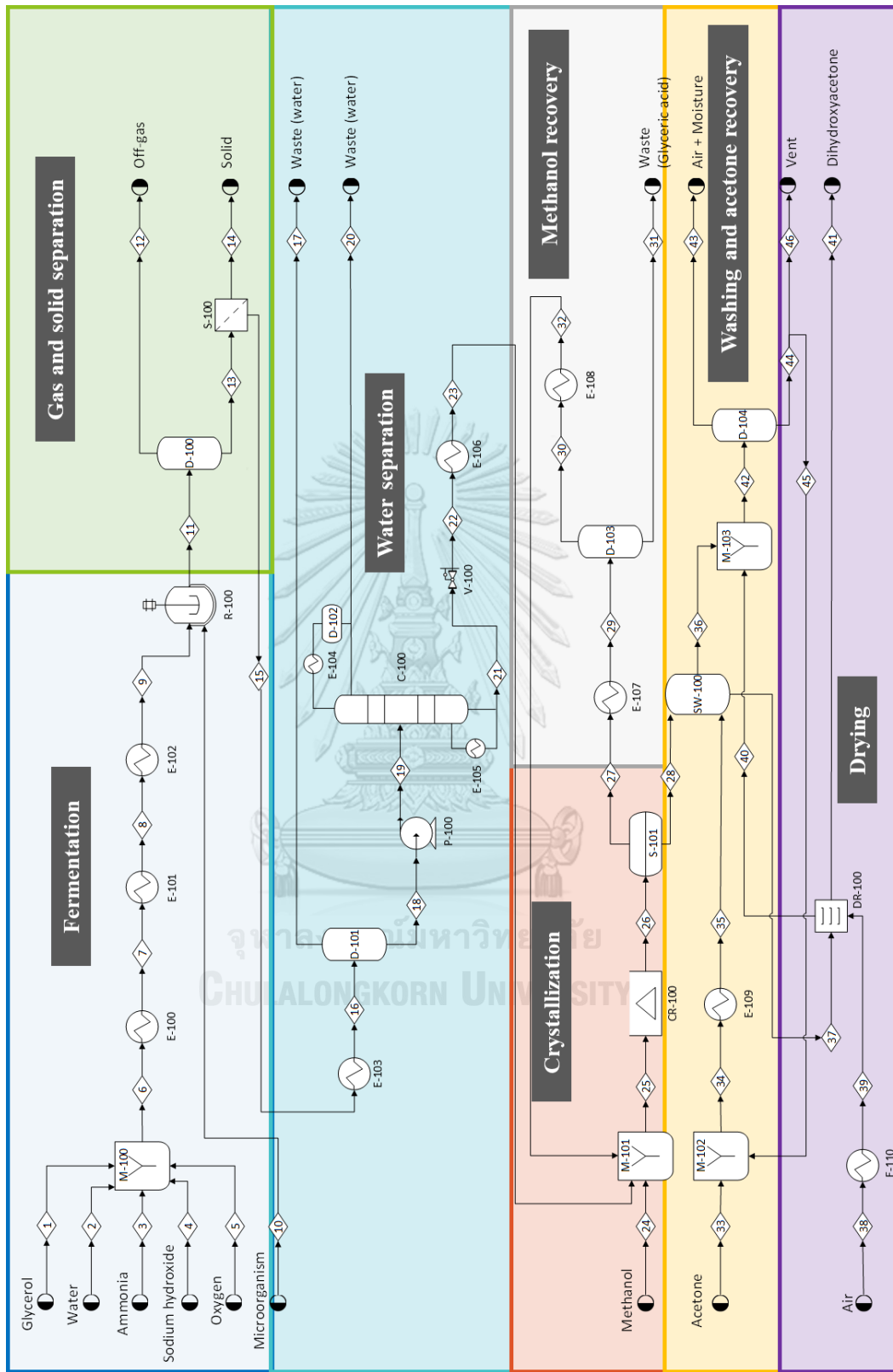


Figure 6.3 Process flow diagram of DHA production

Because of the complexity of biological routes, the previous research works [30, 153] simplified the fermentation process by converting the experimental results to stoichiometric coefficients. Details of the reaction of R-100 are available in Table D7 in Appendix D. The fermenter effluent (Stream 11) was passed to the flash drum (D-100) to separate off-gas and the tubular crossflow filter (S-100) to separate solid contaminants. This solid, which represented a microorganism ($\text{CH}_{1.8}\text{O}_{0.5}\text{N}_{0.2}$), was handled as a CISOLID in Aspen Plus. The properties of microorganisms were determined using the data from National Renewable Energy Laboratory (NREL) [179].

The next stage was to remove the water component from the product stream, which can be divided into two main steps. The first step was the evaporator (D-101) to evaporate some of the water before entering the distillation column (C-100) in the second step. In the evaporation process, the dissolved product stream was concentrated by the evaporator at 101.85°C . Residual water was removed using the distillation column (C-100) (see Table D7 in Appendix D for the detailed unit description). As provided in Figure 6.3, the pressure in Stream 21 was reduced from 2.5 atm to 1 atm and the temperature from 249°C to 5°C before entering the crystallizer (CR-100).

Crystallization was the key unit operation for producing high-quality DHA. The difficulty in DHA crystallization was due to its high solubility in aqueous solutions [195]. To deal with this issue, a solvent was employed. In this study, methanol was used as the solvent for the crystallization of DHA because methanol exhibited the best performance according to Martínez-Gallegos et al. [196]. Solubility was the most significant factor when considering a solvent – DHA solubility in methanol was 78.96 g/L at 5°C [196].

After crystallization, the solid was separated using S-101. The DHA after the solid separation, was further washed (SWASH solid model in Aspen Plus) with acetone. The acetone to DHA mass ratio in the input and output of the washer was set to 2 [197]. Finally, DHA with a product purity of 99 wt% was attained after drying (in DR-100) with hot air. The hot air to DHA mass ratio in the dryer was set to 1 [197]. The full stream table of rigorous process simulation is given in Table D8 (in Appendix D).

6.1.2 Chemical route (catalytic oxidation)

The process flowsheet for Scenario VI is depicted in Figure D4 in Appendix D. The downstream processing was the same as that in Scenarios I to V whereas the difference was at the upstream processing. Crude glycerol from the biodiesel industry contains approximately 83 wt% glycerol [188]. Common impurities in crude glycerol include water, ash, methanol, and matter organic non-glycerol (MONG). These impurities should be eliminated to achieve higher DHA productivity in the chemical route since the impurities affected the product yield [138, 198].

The Ssplit filter model (S-100) was used to remove ash from crude glycerol. Then, the glycerol stream (Stream 5) was treated using an evaporator (D-100) at 0.1 atm to remove methanol and water based on the work of Chang [189]. Finally, Stream 7 containing glycerol and MONG was passed via the pump (P-100) to increase the pressure by 1 atm. Finally, MONG was separated using the separator (S-101).

Table 6.2 Summary of reactions involved in catalytic oxidation

Reaction	Chemical Reaction	Key reactant	Conversion (%)
DHA formation	$C_3H_8O_3 + 0.5O_2 \rightarrow C_3H_6O_3 + H_2O$	Glycerol	100
Glycolic acid formation	$C_3H_6O_3 + 1.5O_2 \rightarrow C_2H_4O_3 + CO_2 + H_2O$	DHA	29.4
Oxalic acid formation	$C_2H_4O_3 + O_2 \rightarrow C_2H_2O_4 + H_2O$	Glycolic acid	95.2
CO ₂ formation	$C_2H_2O_4 + 0.5O_2 \rightarrow 2CO_2 + H_2O$	Oxalic acid	99.3

In the chemical route, the four reactants including glycerol, water, catalyst, and oxygen were fed to the reactor (R-100), whose operating temperature and pressure were maintained at 50°C and 10 atm for the reactions listed in Table 6.2. Then, the fermenter effluent was sent to the knock-out drum (D-101) to remove gas. The product stream was passed through a tubular filter to remove a solid impurity. After this, the downstream process was the same as that in biological route, consisting of the water separation, the crystallization, the methanol recovery, the washing, the acetone recovery, and the drying to obtain DHA at a purity of 99 wt%.

6.2 Process evaluation

6.2.1 Glycerol and carbon utilization efficiencies

According to Table 6.3, the glycerol utilization of each scenario was determined as 0.79, 0.45, 0.63, 0.64, 0.59, and 0.37 for Scenarios I to VI, respectively. Likewise, the carbon utilization of Scenarios I to VI was determined as 0.82, 0.47, 0.66, 0.67, 0.62, and 0.38, respectively (see Table 6.4). Superficially, Scenario I could be more attractive than other scenarios, given the highest glycerol and carbon utilizations. This was due to the high purity of glycerol which could boost the DHA yield. Moreover, the major impurity in crude glycerol obtained from biodiesel is sodium chloride (NaCl) which negatively affects the DHA yield [138], as observed in Scenario II. To emphasize this, the DHA percentage recoveries are also presented in Table 6.3. According to Table 6.3, a relatively high DHA recovery was also observed in Scenario I due to the purity of the glycerol as well as the advantage of less impurities (glyceric acid, CO₂) from fermenter effluent as compared to Scenarios IV to V which the secondary carbon source was added.

Table 6.3 Summary of glycerol utilization for DHA production scenarios

Scenario	DHA production [tonnes/y]	Glycerol feed rate [tonnes/y]	Glycerol utilization
I	2.00E+03	2.53E+03	0.79
II	2.00E+03	4.41E+03	0.45
III	2.00E+03	3.17E+03	0.63
IV	2.00E+03	3.12E+03	0.64
V	2.00E+03	3.37E+03	0.59
VI	2.00E+03	5.40E+03	0.37

Scenario	DHA from reactor effluent [tonnes/y]	DHA production [tonnes/y]	% Recovery
I	2.45E+03	2.00E+03	81.7
II	2.50E+03	2.00E+03	80.1
III	2.45E+03	2.00E+03	81.5
IV	2.54E+03	2.00E+03	78.8
V	2.52E+03	2.00E+03	79.3
VI	3.65E+03	2.00E+03	54.7

Table 6.4 Summary of carbon utilization for DHA production scenarios

Scenario	Carbon content in product [tonnes/y]	Carbon content in glycerol [tonnes/y]	Carbon utilization
I	8.13E+02	9.89E+02	0.82
II	8.13E+02	1.72E+03	0.47
III	8.13E+02	1.24E+03	0.66
IV	8.13E+02	1.22E+03	0.67
V	8.13E+02	1.32E+03	0.62
VI	8.13E+02	2.11E+03	0.38

When comparing the DHA production from the biological route in Scenarios I to V with the chemical route in Scenario VI, the results indicated that Scenario VI had the lowest DHA recovery. This was due to the DHA yield of chemical route lower than that of the biological route. In addition, the large amount of water was required to dilute glycerol because the required glycerol concentration was only 0.1 molar for the catalytic oxidation route [199]. Since a substantial amount of water must be removed in the purification process, the loss of DHA dissolved in water was inevitable in the DHA production via the catalytic oxidation route.

6.2.2 Energy utilization efficiency

According to Table 6.5, the SEC of each scenario was determined as 47.2 kWh/kg, 68.1 kWh/kg, 49.5 kWh/kg, 86.0 kWh/kg, 80.4 kWh/kg, and 211.7 kWh/kg for Scenarios I to VI, respectively. When Scenarios I to V were compared with Scenario VI, a significant reduction in the SEC value was observed. This could point out the superior energy efficiency of the biological route compared to the chemical route.

Furthermore, as observed from Table 6.5, the amount of feed water in each scenario played a crucial role in the overall energy efficiency of the system – the larger the water feed amount, the higher the SEC values became. To illustrate this, the energy consumption in each scenario was contributed to 1) the sterilization step – steam was required to increase the temperature to 121°C; cooling water was used to reduce the temperature to 30°C before entering the fermentation tank, and 2) the water removal step – the utilities were used in the evaporation and the distillation

for water removal. In other words, the larger the amount of water present in the system, the more energy would be required in the sterilization and the water removal steps. Also, the SEC value in Scenario VI was the highest among other scenarios. This again stressed that for DHA production, the biological route was superior when compared to the catalytic oxidation route.

Table 6.5 Summary of energy utilization for DHA production scenarios

Type of duty	Unit	Scenario	Scenario	Scenario	Scenario	Scenario	Scenario
		I	II	III	IV	V	VI
Total heating duty	kW	6.78E+03	9.88E+03	7.15E+03	1.27E+04	1.18E+04	4.75E+04
Total cooling duty	kW	3.97E+03	5.63E+03	4.14E+03	6.92E+03	6.51E+03	7.07E+02
Total electric power	kW	1.18E+01	1.53E+01	1.37E+01	8.21E+00	7.87E+00	1.31E+02
Total power requirement	kW	1.08E+04	1.55E+04	1.13E+04	1.96E+04	1.83E+04	4.83E+04
PA production	kg/h	2.28E+02	2.28E+02	2.28E+02	2.28E+02	2.28E+02	2.28E+02
SEC	kWh/kg	47.2	68.1	49.5	86.0	80.4	211.7

Although Scenario I could be preferred given the highest glycerol utilization and the lowest energy consumption, the price of refined glycerol that were more expensive than crude glycerol should be considered also, i.e., refined glycerol was about 8 times more expensive than crude glycerol. Thus, the economic performance which is highlighted in the following section was also evaluated.

6.2.3 Economic performance

As seen from all scenarios in Table 6.6, the glycerol-based processes were feasible given the positive numbers of DPV. In scenario II, the total equipment cost appeared the highest when compared to other scenarios. The highest costs were contributed largely from the selection of crude glycerol as a carbon source. This was due to the large amount of water required in this technique to achieve the DHA production at 2,000 tonnes per year, and part of the production cost was due to the water separation.

Table 6.6 Summary of economic performance for DHA production scenarios

Economic information	Unit	Scenario	Scenario	Scenario	Scenario	Scenario	Scenario
		I	II	III	IV	V	VI
Total Capital Cost	\$	2.41E+07	2.52E+07	2.41E+07	1.98E+07	1.95E+07	2.12E+07
Total Operating Cost	\$/y	7.21E+06	6.18E+06	5.46E+06	6.27E+06	6.20E+06	1.20E+07
Total Equipment Cost	\$	3.10E+06	3.48E+06	3.03E+06	2.33E+06	2.28E+06	2.75E+06
Total Operating Labor Cost	\$/y	1.24E+06	1.24E+06	1.24E+06	1.24E+06	1.24E+06	1.24E+06
Total Maintenance Cost	\$/y	3.05E+05	3.46E+05	2.92E+05	2.19E+05	2.14E+05	2.54E+05
Total Utilities Cost	\$/y	1.16E+06	1.62E+06	1.21E+06	1.99E+06	1.87E+06	6.46E+06
Total Products Sales	\$/y	4.56E+07	4.56E+07	4.56E+07	4.56E+07	4.56E+07	4.56E+07
Total Raw Materials Cost	\$/y	2.89E+06	1.42E+06	1.24E+06	1.31E+06	1.38E+06	2.13E+06
Economic indicator							
DPV	\$	6.38E+08	6.24E+08	6.44E+08	6.44E+08	6.45E+08	5.58E+08
DCFROR	%	113.23	112.3	118.2	142.2	144.05	107.81
DPP	y	2.06	2.06	2.03	1.79	1.78	2.11

According to Table 6.6, the results of the three indicators in the table showed that Scenario V gave the highest DPV of 645 million USD, the highest % DCFROR of 144.05%, and the shortest DPP of 1.78 years when all six scenarios were compared. These results showed that the use of sorbitol as the secondary carbon source to accelerate microbial growth could increase profitability. This was because the fermentation time played an important role in equipment costs – when the fermentation time was reduced, the equipment cost was also reduced due to the smaller size of the fermenter.

In general, Aspen Plus is a steady-state simulator. However, to make ASPEN reflect the batch operation of the fermenters, we simulated them as if we had a staggered batch operation. Herein, the size of each fermenter is shown in Table 6.7. With a production capacity of 2,000 tonnes per year and the fermentation time of 72 hours in Scenarios I to III and 24 hours in Scenarios IV to V, multiple fermentation tanks were required. For this reason, the fermenters were the most expensive equipment which was about 55-71% of the total equipment cost (as indicated in Table 6.7).

Table 6.7 Comparison of hotspot in each scenario for DHA production

Information	Unit	Scenario	Scenario	Scenario	Scenario	Scenario	Scenario
		I	II	III	IV	V	VI
Number of required fermenters	tank	10	10	8	5	5	4
Reactor size	m ³	70	90	90	100	95	180
The most expensive equipment	\$	2.13E+06 (R-100)	2.48E+06 (R-100)	1.98E+06 (R-100)	1.32E+06 (R-100)	1.28E+06 (R-100)	1.50E+06 (R-100)
Contribution in the total equipment cost	%	68.7	71.2	65.4	56.7	56.1	54.6

Regarding the types of secondary carbon sources, Scenario V gave better economic results than Scenario IV. Although the total raw material cost in Scenario V was higher (sorbitol 0.54 USD per kg VS glucose 0.35 USD per kg), a large amount of water must be added in scenario IV to reach a glucose concentration of 20 g/L [55]. The water component is a key factor in the separation process, resulting in low capital and utilities costs. Thus, Scenario V had better overall economic indicators than Scenario IV.

When the raw material costs in Scenario I was compared to Scenario II, it was found that the total raw material cost in Scenario I was approximately twice relative to that of Scenario II. Although Scenario I gave the best glycerol and energy efficiency outcomes as shown in Tables 6.3 and 6.5, the results of the economics evaluation were not different from Scenario II since the price of refined glycerol at 99.7 wt% was 0.895 USD per kg whereas the price of crude glycerol was 0.135 USD per kg [163]. Furthermore, it was found that scenario VI was the least profitable, corresponding with glycerol and energy efficiency. This highlighted that the production process for DHA was more economically viable if produced via the biological route.

6.2.4 Environmental impacts

The relevant parameters in each processing block of DHA production required for LCA are depicted in Figure 6.4. As a result of the glycerol refining process, the environmental impacts of refined glycerol should be higher than crude glycerol.

However, refined glycerol was not available in the SimaPro database. To increase the accuracy of evaluating refined glycerol, the life cycle inventory of glycerol refining were used according to Cespi's work [200].

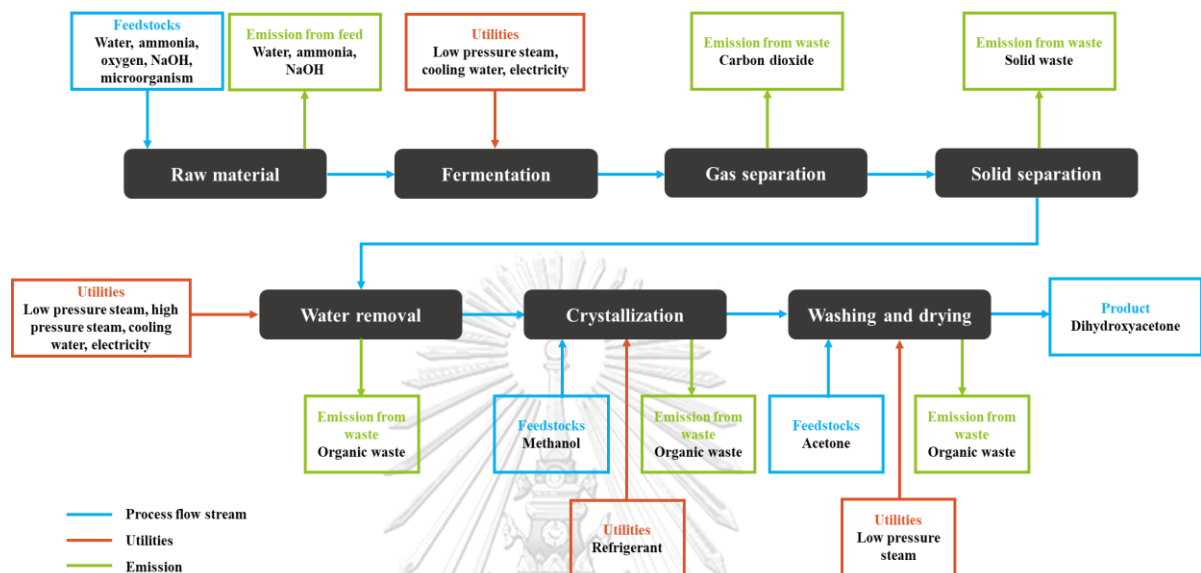


Figure 6.4 Diagram with relevant parameters of the glycerol-based DHA production

According to Table 6.8, it was found that terrestrial ecotoxicity was the most important factor causing the highest environmental impact, followed by land use and global warming. Scenario I was the most environmentally friendly compared to other scenarios because 1) glycerol was required less than other scenarios to produce the same amount of DHA at 2,000 tons per year, and 2) it used lower amounts of heating and cooling duties. When all input and output substances were considered, it was discovered that heating was the leading cause of environmental impacts in several aspects as seen in Tables D1-D6 in Appendix D. As a result, Scenarios II to VI which needed a huge amount of heat (see Table 6.5) had a significant influence on the environment, particularly scenario VI, which had the highest total energy requirement.

Table 6.8 Summary of environmental impacts (Cradle to gate)

Impact category	Unit	Scenario	Scenario	Scenario	Scenario	Scenario	Scenario
		I	II	III	IV	V	VI
Global warming	kg CO ₂ eq	4.782	4.961	5.055	5.227	5.102	15.99
Terrestrial ecotoxicity	kg 1,4-DCB	7.303	7.919	7.968	9.372	8.902	424.0
Human non-carcinogenic toxicity	kg 1,4-DCB	1.925	2.298	2.634	2.729	2.585	73.15
Land use	m ² a crop eq	4.877	7.079	5.097	5.125	5.488	11.18
Fossil resource scarcity	kg oil eq	2.166	1.626	1.679	1.687	1.659	4.226
Water consumption	m ³	2.903	4.009	3.046	4.608	4.392	1.383

In addition, the catalytic oxidation caused more harm to the environment. To elaborate this, if the global warming aspect of Scenario VI was compared with Scenarios I to V, the total amount of CO₂ emissions would be significantly larger by about three times. This result emphasized that the biological route was superior to the chemical route in both economic and environmental perspectives.

From the evaluation of simulated processes in terms of glycerol utilization, energy utilization, and environmental impacts, it was found that Scenario I preferred to produce DHA. However, economic analysis revealed that Scenario V was the most profitable. The problem with using crude glycerol as a substrate was due to its high energy requirement. Therefore, if energy consumption in the system could be reduced or an alternative to enhance energy efficiency could be found, the production of DHA from crude glycerol could be more promising than from refined glycerol due to its price advantage. To further enhance the potential of DHA production from crude glycerol, the heat exchanger network design was implemented in this work, as described in detail in the following section.

6.3 Heat integration

The process that produced DHA from glycerol consumed a substantial amount of energy. Excessive energy was released into the atmosphere resulting in environmental impact and increasing production costs. Therefore, heat exchanger network design was important for the design of the DHA production process from

glycerol. Starting from the pinch analysis, the composite curve was generated as illustrated in Figure 6.5 (example of Scenario V). These indicated that some of the energy in the process streams could be exchanged internally.

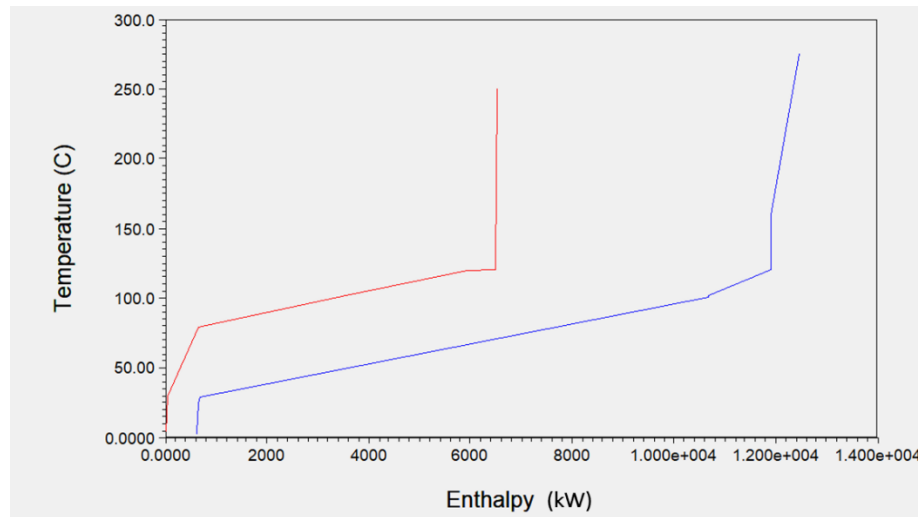


Figure 6.5 The composite curve of Scenario V

In this work, the Aspen Energy Analyzer V.11 program was used to design the heat exchanger network (HEN). After the HEN was completed, the processes with HEN were re-evaluated in terms of energy utilization efficiency, economic performance, and environmental impacts. The results after HEN are shown in Tables 6.9-6.11. According to the analysis of the energy utilization of each unit operation in Scenarios I to V showed similar hot spots – the same two units with high energy consumptions were that 1) sterilization required a large amount of cooling water in the E-101 to cool down before entering the fermenter, and 2) water evaporation required a large amount of steam in the E-103. Therefore, the heating from the E-101 unit could be exchanged with the cooling from the E-103 unit as shown in Figure 6.6. As a result of heat exchange, the overall energy efficiency could be increased by 52-58%. However, Scenario VI cannot implement the heat exchanger network design because there are no units capable of exchanging enough excess heat in the system.

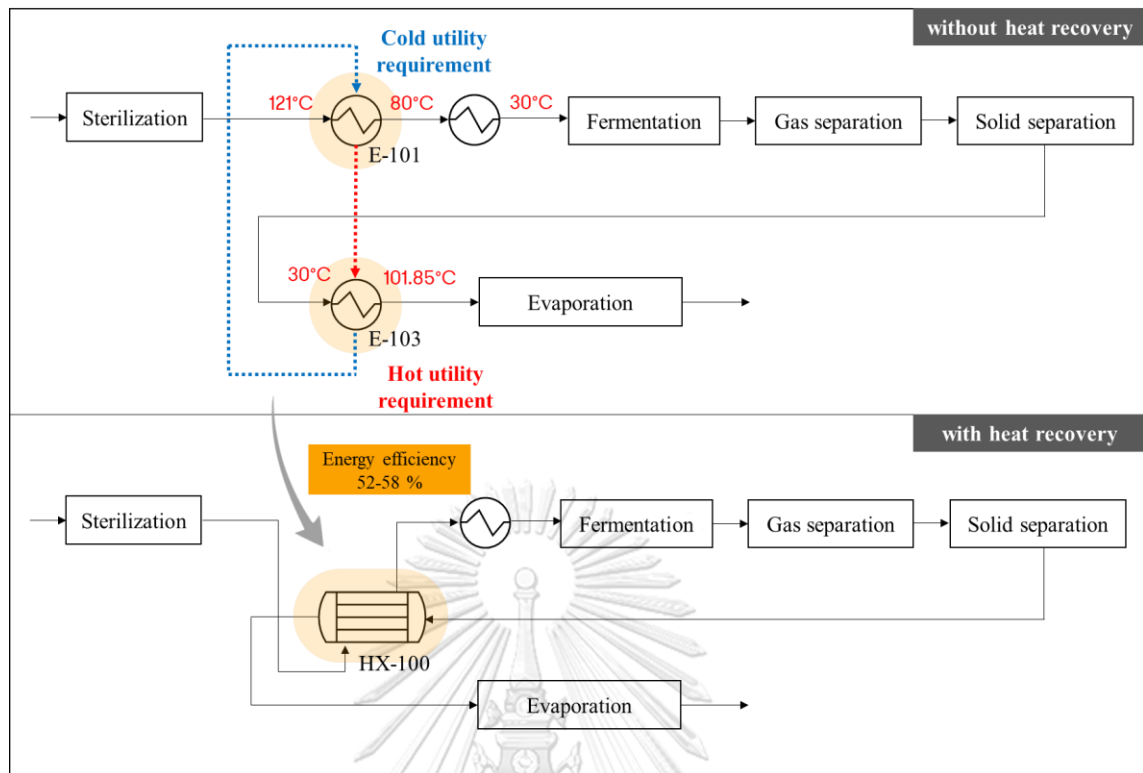


Figure 6.6 Heat integration of DHA production via the fermentation process

Table 6.9 Summary of energy utilization after HEN

Type of duty	Unit	Scenario	Scenario	Scenario	Scenario	Scenario
		I	II	III	IV	V
Total heating duty	kW	4.00E+03	5.66E+03	4.17E+03	7.01E+03	6.56E+03
Total cooling duty	kW	1.18E+03	1.41E+03	1.16E+03	1.25E+03	1.25E+03
Total electric power	kW	1.18E+01	1.53E+01	1.37E+01	8.21E+00	7.87E+00
Total power requirement	kW	5.19E+03	7.09E+03	5.34E+03	8.27E+03	7.82E+03
PA production	kg/h	2.28E+02	2.28E+02	2.28E+02	2.28E+02	2.28E+02
SEC	kWh/kg	22.7	31.1	23.4	36.3	34.3

Table 6.10 Summary of economic performance after HEN

Economic information	Unit	Scenario	Scenario	Scenario	Scenario	Scenario
		I	II	III	IV	V
Total Capital Cost	\$	2.39E+07	2.50E+07	2.38E+07	1.97E+07	1.95E+07
Total Operating Cost	\$/y	6.81E+06	5.55E+06	5.03E+06	5.40E+06	5.40E+06
Total Equipment Cost	\$	3.10E+06	3.47E+06	3.03E+06	2.29E+06	2.27E+06
Total Operating Labor Cost	\$/y	1.24E+06	1.24E+06	1.24E+06	1.24E+06	1.24E+06
Total Maintenance Cost	\$/y	3.05E+05	3.46E+05	2.93E+05	2.19E+05	2.14E+05
Total Utilities Cost	\$/y	7.87E+05	1.03E+06	8.05E+05	1.19E+06	1.13E+06
Total Products Sales	\$/y	4.56E+07	4.56E+07	4.56E+07	4.56E+07	4.56E+07
Total Raw Materials Cost	\$/y	2.89E+06	1.42E+06	1.24E+06	1.31E+06	1.38E+06
Economic indicator						
DPV	\$	6.47E+08	6.30E+08	6.56E+08	6.55E+08	6.56E+08
DCFROR	%	115.4	115.1	121.9	145.4	148.4
DPP	y	2.04	2.04	1.99	1.78	1.75

Table 6.11 Summary of environmental impacts after HEN

Impact category	Unit	Scenario	Scenario	Scenario	Scenario	Scenario
		I	II	III	IV	V
Global warming	kg CO ₂ eq	4.104	3.935	4.403	3.848	3.822
Terrestrial ecotoxicity	kg 1,4-DCB	5.592	5.332	6.144	5.894	5.673
Human non-carcinogenic toxicity	kg 1,4-DCB	1.424	1.539	2.100	1.709	1.638
Land use	m ² a crop eq	4.823	6.997	5.039	5.015	5.386
Fossil resource scarcity	kg oil eq	2.008	1.387	1.522	1.365	1.361
Water consumption	m ³	2.803	3.288	2.768	2.314	2.190

The overall assessments of all scenarios are shown in Figure 6.7. From the figure, it was found that Scenario VI had the greatest impact on the environment, especially terrestrial ecotoxicity caused by copper oxide used as a catalyst. Furthermore, it was found that Scenario V was more environmentally friendly than other scenarios when considering the global warming aspect. As a result of reduced

energy consumption, less carbon dioxide was discharged into the atmosphere. The production cost was also reduced, which was observed from the DPV, DCFROR, and DPP effects of Scenario V as shown in Table 6.10. From the evaluation of several factors, it could be concluded that Scenario V was the best process for producing DHA from crude glycerol.

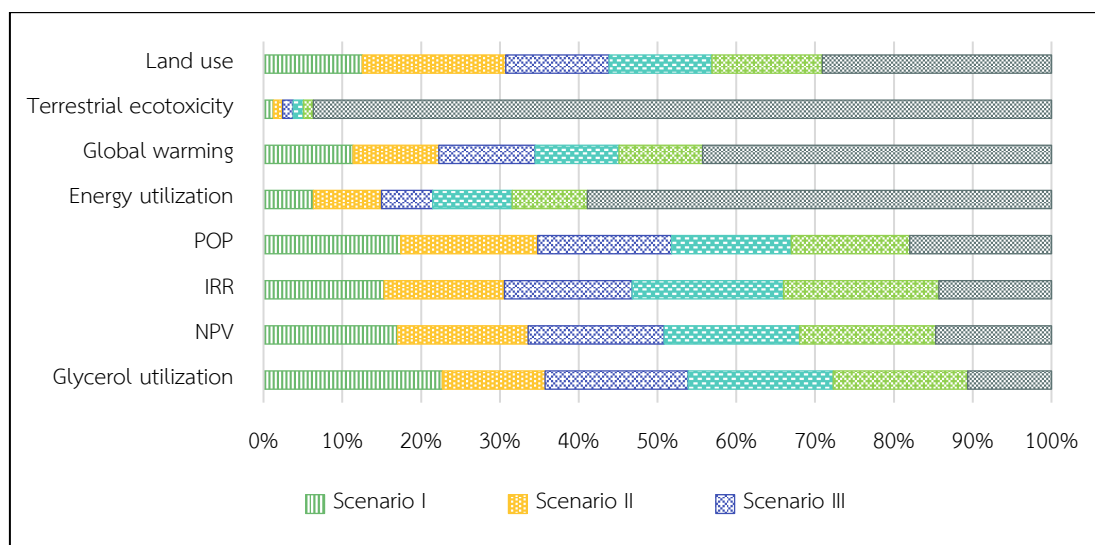


Figure 6.7 Summary of all assessments of DHA production

6.4 Process sensitivity

In this work, the price variability was set at $\pm 50\%$ for each material. Only Scenario V was chosen for the sensitivity analysis due to its more promising economic performance when compared to other scenarios. Glycerol, sorbitol, and acetone were the main feedstocks for the manufacture of DHA based on biotechnology. Given that DHA was the main product in this study, its sale price was also included in the analysis.

Figure 6.8 depicts the results obtained for each case of price sensitivity on DPV. According to the results, it was found that all of the price variabilities were feasible given the positive DPV. In addition, the process feasibility was most sensitive to the variability of DHA price. On the other hand, the impact on the price of feedstock was minor.

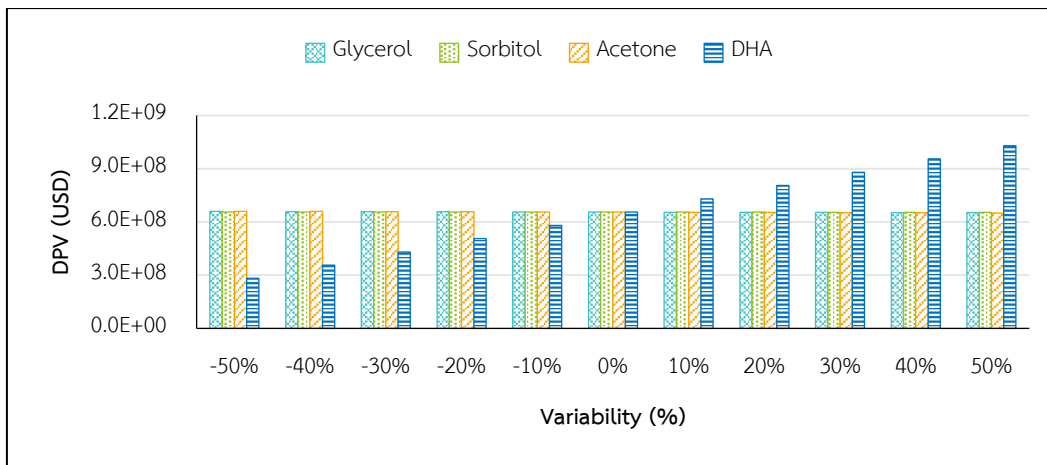


Figure 6.8 Effect of the price of Scenario V on DPV

Regarding the environmental impact, the geographical location as well as the production of raw materials influenced the environmental impact also. Please note that only the variability of locations that glycerol was obtained was examined because glycerol was served as the primary raw material in this work. According to Figure 6.9, it was observed that when using glycerol derived from Brazilian soybean oil, it had an impact on several environmental aspects, especially terrestrial ecotoxicity, global warming, and land use. Additionally, the environmental impact could be decreased in this design process if glycerol derived from French waste cooking oil was selected.

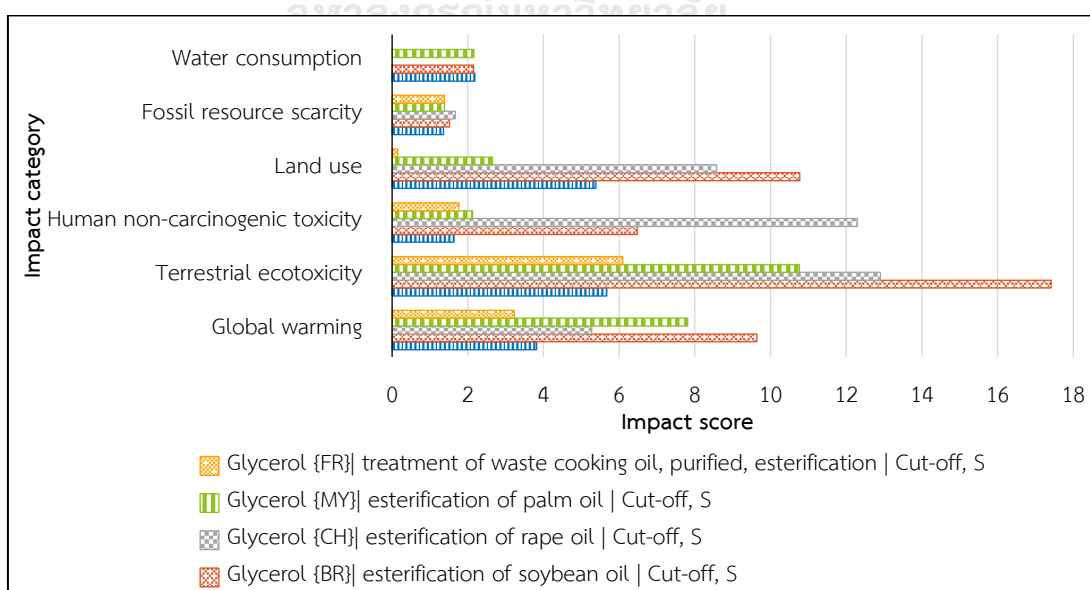


Figure 6.9 Effect of the origins of glycerol on environmental impacts

CHAPTER 7

CONCLUSIONS AND RECOMMENDATIONS

7.1 Conclusions

7.1.1 Propionic acid production

The bio-based propionic acid production was thoroughly investigated. Since the propionic acid content present in the fermentation broth was typically dilute, the acid recovery using conventional techniques, such as distillation and liquid-liquid extraction were not effective. To enhance the recovery, the reactive extraction was implemented in this study. According to this work, it was found that the appropriate selection of 1) diluent and extractant pair and 2) the back-extraction technique in reactive extraction greatly improved the overall process performances.

Scenario III provided the best economic performance, i.e., 118 million USD of the DPV, 18.2 of the % DCFROR, and 7.12 years of the DPP. This scenario also outperformed other bio-based scenarios in terms of glycerol utilization, energy utilization, as well as CO₂ equivalent emissions. Although the addition of a foreign component was required in Scenario III, the utilization of TMA helped reduce the burden of water removal which eventually enhanced the process economic substantially. In addition, the useful sensitivity analysis was performed to point out which compound that involved in the bio-based production influenced the process profitability. According to the results, it was found that the process feasibility was most sensitive to the price variability of propionic acid.

Regarding the current study, the bio-based production could not compete with the petroleum-based production from the perspectives of economic and energy utilization. However, the CO₂ equivalent emissions caused by the petroleum-based production caused more harm to the environment than the bio-based production since the estimated CO₂ equivalence was significantly higher. The main culprit for such high emissions was the utilization of non-renewable feedstocks, e.g., CO and ethylene. Although the bio-based production was not as attractive as the petroleum-

based production in terms of the profitability, the best production scenario III appeared promising given the implementation of glycerol valorization, especially if the price of the product continued to increase.

7.1.2 Succinic acid production

Processing technologies in both upstream and downstream in the bio-based SA production from glycerol were evaluated in terms of economic, energy, exergy, and GHG emissions analyses. From a techno-economic study, direct crystallization was proven the most promising technique for removing SA from the fermentation broth. According to this work, the results indicated that adding DMSO to the fermenter with direct crystallization as the SA purification method (Scenario III) was the most cost-effective and environmentally friendly. The best economic performance was attained in Scenario III with 190 million USD of DPV, 33.3% of DCFROR, and 4.48 years of DPP. Furthermore, this scenario yielded about a 26% reduction in GHG emissions when compared to the petroleum-based SA production from maleic anhydride.

Future work should focus on the reduction of energy consumed in bio-based production as pointed out by the high SEC values in Table 5.6. The major bottleneck encountered in bio-based production was the downstream processing technology used in SA purification. If a technique that was more energy efficient was developed, bio-based production would be more attractive and could eventually replace petroleum-based production.

7.1.3 Dihydroxyacetone production

The bio-based DHA production was thoroughly investigated. Since the DHA yield was usually less if crude glycerol was used as the only carbon source, this study used the addition of a secondary carbon source to increase the efficiency of DHA production. From this work, it was found that 1) the addition of sorbitol as the secondary carbon source was the most cost-effective and environmentally friendly, 2) the HEN greatly improved overall process efficiency, and 3) the microbial

fermentation was superior to the catalytic oxidation for DHA production from crude glycerol.

Scenario V had the highest economic performance, with the DPV of 656 million USD, the % DCFROR of 148.4%, and the DPP of 1.75 years. Even though the addition of a foreign component, e.g., sorbitol was needed in Scenario V, the reduction in fermentation time helped reduce the number of fermenters which eventually enhanced the process economics. Moreover, important findings from this investigation also revealed that the amount of water had a major effect on both energy utilization and CO₂ emissions into the atmosphere. In addition, apart from the safety measures and regulations that encouraged the utilization of the biological route, the results available in this work confirmed that DHA production via the biological route was superior in terms of the raw material utilization, the economic performance, and the environmental impacts than the catalytic oxidation route.

Finally, the biodiesel manufacturer could gain benefits from the production of high-value-added chemicals from crude glycerol such as DHA. According to this study, DHA produced from crude glycerol had a high potential for commercial production as observed from the process performances evaluated herein.

7.2 Recommendations for future works

The following recommendations are provided for further studies on the development of production of value-added chemicals from glycerol.

7.2.1 The development of techniques that can be more energy efficient should be emphasized in process design to address bottlenecks due to the high energy consumption of biological processes.

7.2.2 Since the variability of geographic locations as well as raw material acquisition processes affect environmental assessments, these aspects should be considered in environmental assessments.

7.2.3 For better process improvement, the other factors that can affect biological production should be investigated such as microbial species, and carbon source concentration.

7.2.4 Future work should compare which chemicals are the best to produce from glycerol under the same operating conditions to ensure that the comparisons are equitable. This work is difficult to compare because it employs different variables and unit operations, such as the types of glycerol, the refining of crude glycerol, etc.



REFERENCES

- [1] Singh, D., D. Sharma, S.L. Soni, S. Sharma, and D. Kumari, *Chemical compositions, properties, and standards for different generation biodiesels: A review*. Fuel, 2019. **253**: p. 60-71.
- [2] Vlysidis, A., M. Binns, C. Webb, and C. Theodoropoulos, *A techno-economic analysis of biodiesel biorefineries: assessment of integrated designs for the co-production of fuels and chemicals*. Energy, 2011. **36**(8): p. 4671-4683.
- [3] USDA. *Biofuels Annual*. 2023 [cited 2023 May 10]; 05-10]. Available from: https://apps.fas.usda.gov/newgainapi/api/Report/DownloadReportByFileName?fileName=Biofuels%20Annual_Bangkok_Thailand_TH2023-0034.pdf.
- [4] Holmgren, J., C. Gosling, T. Marker, P. Kokayeff, G. Faraci, and C. Perego. *Green diesel production from vegetable oil*. in *2007 Spring AIChE Conference*. 2007.
- [5] Severo, I.A., S.F. Siqueira, M.C. Depra, M.M. Maroneze, L.Q. Zepka, and E. Jacob-Lopes, *Biodiesel facilities: What can we address to make biorefineries commercially competitive?* Renewable Sustainable Energy Reviews, 2019. **112**: p. 686-705.
- [6] Vlysidis, A., M. Binns, C. Webb, and C. Theodoropoulos, *Glycerol utilisation for the production of chemicals: conversion to succinic acid, a combined experimental and computational study*. Biochemical Engineering Journal, 2011. **58**: p. 1-11.
- [7] OECD/FAO. *OECD-FAO Agricultural Outlook 2021–2030*. 2021 [cited 2021 July 15]; 07-15]. Available from: <http://www.fao.org/3/cb5332en/Biofuels.pdf>.
- [8] Nupuang, S., P. Oosterveer, and A.P.J. Mol, *Implementing a palm oil-based biodiesel policy: The case of Thailand*. Energy Science & Engineering, 2018. **6**(6): p. 643-657.
- [9] Gebremariam, S.N. and J.M. Marchetti, *Biodiesel production technologies: review*. AIMS Energy, 2017. **5**(3): p. 425-457.
- [10] Posada, J.A., L.E. Rincon, and C.A. Cardona, *Design and analysis of biorefineries based on raw glycerol: addressing the glycerol problem*. Bioresource

- technology, 2012. **111**: p. 282-293.
- [11] Research and Markets. *Global Glycerol Industry (2020 to 2027)*. 2021 [cited 2023 June 20]; 06-20]. Available from: <https://www.businesswire.com/news/home/20210115005399/en/Global-Glycerol-Industry-2020-to-2027---Market-Trends-and-Drivers---ResearchAndMarkets.com>.
- [12] Kaur, J., A.K. Sarma, M.K. Jha, and P. Gera, *Valorisation of crude glycerol to value-added products: Perspectives of process technology, economics and environmental issues*. Biotechnology Reports, 2020. **27**: p. 1-23.
- [13] Monteiro, M.R., C.L. Kugelmeier, R.S. Pinheiro, M.O. Batalha, and A. da Silva César, *Glycerol from biodiesel production: Technological paths for sustainability*. Renewable and Sustainable Energy Reviews, 2018. **88**: p. 109-122.
- [14] Mota, C.J.A., B.P. Pinto, and A.L. de Lima, *Glycerol*. 2017, Cham, Switzerland: Springer. 116.
- [15] Chaminand, J., L. aurent Djakovitch, P. Gallezot, P. Marion, C. Pinel, and C. Rosier, *Glycerol hydrogenolysis on heterogeneous catalysts*. Green chemistry, 2004. **6**(8): p. 359-361.
- [16] Dasari, M.A., P.-P. Kiatsimkul, W.R. Sutterlin, and G.J. Suppes, *Low-pressure hydrogenolysis of glycerol to propylene glycol*. Applied Catalysis A: General, 2005. **281**(1-2): p. 225-231.
- [17] Maris, E.P. and R.J. Davis, *Hydrogenolysis of glycerol over carbon-supported Ru and Pt catalysts*. Journal of Catalysis, 2007. **249**(2): p. 328-337.
- [18] Meher, L.C., R. Gopinath, S. Naik, and A.K. Dalai, *Catalytic hydrogenolysis of glycerol to propylene glycol over mixed oxides derived from a hydrotalcite-type precursor*. Industrial & engineering chemistry research, 2009. **48**(4): p. 1840-1846.
- [19] Bienholz, A., H. Hofmann, and P. Claus, *Selective hydrogenolysis of glycerol over copper catalysts both in liquid and vapour phase: Correlation between the copper surface area and the catalyst's activity*. Applied Catalysis A: General, 2011. **391**(1-2): p. 153-157.
- [20] Rode, C., R. Mane, A. Potdar, P. Patil, P. Niphadkar, and P. Joshi, *Copper*

- modified waste fly ash as a promising catalyst for glycerol hydrogenolysis. Catalysis today*, 2012. **190**(1): p. 31-37.
- [21] Shozi, M.L., V.D. Dasireddy, S. Singh, P. Mohlala, D.J. Morgan, and H.B. Friedrich, *Hydrogenolysis of glycerol to monoalcohols over supported Mo and W catalysts. ACS Sustainable Chemistry & Engineering*, 2016. **4**(10): p. 5752-5760.
- [22] Sivasankaran, C., P.K. Ramanujam, B. Balasubramanian, and J. Mani, *Recent progress on transforming crude glycerol into high value chemicals: a critical review. Biofuels*, 2019. **10**(3): p. 309-314.
- [23] Carvalho, M., M. Matos, C. Roca, and M.A. Reis, *Succinic acid production from glycerol by Actinobacillus succinogenes using dimethylsulfoxide as electron acceptor. New biotechnology*, 2014. **31**(1): p. 133-139.
- [24] Samudrala, S.P., *Glycerol Transformation to Value-Added 1, 3-Propanediol Production: A Paradigm for a Sustainable Biorefinery Process*, in *Glycerine Production and Transformation-An Innovative Platform for Sustainable Biorefinery and Energy*. 2019, IntechOpen. p. 64-86.
- [25] Mazumdar, S., M.D. Blankschien, J.M. Clomburg, and R. Gonzalez, *Efficient synthesis of L-lactic acid from glycerol by metabolically engineered Escherichia coli. Microbial cell factories*, 2013. **12**(1): p. 1-11.
- [26] Posada, J.A. and C.A. Cardona, *Propionic Acid Production from Raw Glycerol Using Commercial and Engineered Strains. Industrial & Engineering Chemistry Research*, 2012. **51**(5): p. 2354-2361.
- [27] Ranaei, V., Z. Pilevar, A. Mousavi Khaneghah, and H. Hosseini, *Propionic acid: Method of production, current state and perspectives. Food Technology and Biotechnology*, 2020. **58**(2): p. 115-127.
- [28] Werpy, T. and G. Petersen, *Top value added chemicals from biomass: volume I--results of screening for potential candidates from sugars and synthesis gas*. 2004: National Renewable Energy Lab., Golden, CO (US).
- [29] Es, I., A.M. Khaneghah, S.M.B. Hashemi, and M. Koubaa, *Current advances in biological production of propionic acid. Biotechnol Lett*, 2017. **39**(5): p. 635-645.
- [30] Morales, M., P.Y. Dapsens, I. Giovinazzo, J. Witte, C. Mondelli, S. Papadokonstantakis, K. Hungerbühler, and J. Pérez-Ramírez, *Environmental and*

- economic assessment of lactic acid production from glycerol using cascade bio- and chemocatalysis*. Energy & Environmental Science, 2015. **8**(2): p. 558-567.
- [31] Morales, M., M. Ataman, S. Badr, S. Linster, I. Kourlimpinis, S. Papadokonstantakis, V. Hatzimanikatis, and K. Hungerbühler, *Sustainability assessment of succinic acid production technologies from biomass using metabolic engineering*. Energy & Environmental Science, 2016. **9**(9): p. 2794-2805.
- [32] Berg, L. and A.-I. Yeh, *Dehydration of propionic acid by extractive distillation*, U.S. Patent and Trademark Office, Editor. 1987: US.
- [33] Ahmadi, N., K. Khosravi-Darani, and A.M. Mortazavian, *An overview of biotechnological production of propionic acid: From upstream to downstream processes*. Electronic Journal of Biotechnology, 2017. **28**: p. 67-75.
- [34] Karp, E.M., R.M. Cywar, L.P. Manker, P.O. Saboe, C.T. Nimlos, D. Salvachúa, X. Wang, B.A. Black, M.L. Reed, W.E. Michener, N.A. Rorrer, and G.T. Beckham, *Post-Fermentation Recovery of Biobased Carboxylic Acids*. ACS Sustainable Chemistry & Engineering, 2018. **6**(11): p. 15273-15283.
- [35] Keshav, A., K.L. Wasewar, and S. Chand, *Extraction of propionic acid using different extractants (tri-n-butylphosphate, tri-n-octylamine, and Aliquat 336)*. Industrial engineering chemistry research, 2008. **47**(16): p. 6192-6196.
- [36] Datta, D., S. Kumar, and H. Uslu, *Status of the Reactive Extraction as a Method of Separation*. Journal of Chemistry, 2015. **2015**: p. 1-16.
- [37] Eda, S., *Recovery and Regeneration of Carboxylic Acids from Aqueous Solutions Using Process Intensification*. 2017, RMIT University: Melbourne, Australia.
- [38] Hong, Y.K., W.H. Hong, and D.H. Han, *Application of reactive extraction to recovery of carboxylic acids*. Biotechnology and Bioprocess Engineering, 2001. **6**(6): p. 386-394.
- [39] Keshav, A. and K.L. Wasewar, *Back extraction of propionic acid from loaded organic phase*. Chemical Engineering Science, 2010. **65**(9): p. 2751-2757.
- [40] Gao, C., X. Yang, H. Wang, C.P. Rivero, C. Li, Z. Cui, Q. Qi, and C.S.K. Lin, *Robust succinic acid production from crude glycerol using engineered Yarrowia*

- lipolytica*. *Biotechnol Biofuels*, 2016. **9**(1): p. 1-11.
- [41] Almena, A. and M. Martin, *Technoeconomic analysis of the production of epichlorohydrin from glycerol*. *Industrial & Engineering Chemistry Research*, 2016. **55**(12): p. 3226-3238.
- [42] BioSpace. *Succinic Acid Market Trends 2022-2030: Product Launches and Research for Advanced Succinic Acid*. 2022 [cited 2022 September 10]; 09-10]. Available from: <https://www.biospace.com/article/succinic-acid-market-trends-2022-2030-product-launches-and-research-for-advanced-succinic-acid/#:~:text=According%20to%20the%20current%20analysis,at%20a%20CAGR%20of%2018.01%25.>
- [43] Nghiem, N., S. Kleff, and S. Schwegmann, *Succinic Acid: Technology Development and Commercialization*. *Fermentation*, 2017. **3**(2).
- [44] Quispe, C.A.G., C.J.R. Coronado, and J.A. Carvalho Jr, *Glycerol: Production, consumption, prices, characterization and new trends in combustion*. *Renewable and Sustainable Energy Reviews*, 2013. **27**: p. 475-493.
- [45] Hejna, A., P. Kosmela, K. Formela, Ł. Piszczyk, and J.T. Haponiuk, *Potential applications of crude glycerol in polymer technology—Current state and perspectives*. *Renewable and Sustainable Energy Reviews*, 2016. **66**: p. 449-475.
- [46] Gadkari, S., D. Kumar, Z.-h. Qin, C.S.K. Lin, and V. Kumar, *Life cycle analysis of fermentative production of succinic acid from bread waste*. *Waste Management*, 2021. **126**: p. 861-871.
- [47] Gaylord Chemical *Dimethyl Sulfoxide (health and safety information)*. 2014.
- [48] ACS. *Dimethyl sulfoxide*. 2021 [cited 2022 July 30]; 07-30]. Available from: <https://www.acs.org/content/acs/en/molecule-of-the-week/archive/d/dimethyl-sulfoxide.html>.
- [49] ECHEMI. *Chemical prices*. 2022 [cited 2022 May 30]; 05-30]. Available from: <https://www.echemi.com/productsinformation/pd20150901217-dimethyl-sulfoxide.html>.
- [50] Cok, B., I. Tsiropoulos, A.L. Roes, and M.K. Patel, *Succinic acid production derived from carbohydrates: An energy and greenhouse gas assessment of a*

- platform chemical toward a bio-based economy*. Biofuels, Bioproducts Biorefining, 2014. **8**(1): p. 16-29.
- [51] Newsnet. *Dihydroxyacetone Market*. 2023 [cited 2023 May 20]; 05-20]. Available from: [https://www.newsnetmedia.com/story/48388803/Dihydroxyacetone-\(DHA\)-Market](https://www.newsnetmedia.com/story/48388803/Dihydroxyacetone-(DHA)-Market).
- [52] Made-in-china. *Chemical prices*. 2023 [cited 2023 May 10]; 05-10]. Available from: www.made-in-china.com.
- [53] Ciriminna, R., A. Fidalgo, L.M. Ilharco, and M. Pagliaro, *Dihydroxyacetone: an updated insight into an important bioproduct*. ChemistryOpen, 2018. **7**(3): p. 233-236.
- [54] Pradima, J., M.R. Kulkarni, and Archana, *Review on enzymatic synthesis of value added products of glycerol, a by-product derived from biodiesel production*. Resource-Efficient Technologies, 2017. **3**(4): p. 394-405.
- [55] Lu, L., L. Wei, K. Zhu, D. Wei, and Q. Hua, *Combining metabolic engineering and adaptive evolution to enhance the production of dihydroxyacetone from glycerol by Gluconobacter oxydans in a low-cost way*. Bioresource Technology, 2012. **117**: p. 317-324.
- [56] San Kong, P., M.K. Aroua, and W.M.A.W. Daud, *Conversion of crude and pure glycerol into derivatives: A feasibility evaluation*. Renewable and Sustainable Energy Reviews, 2016. **63**: p. 533-555.
- [57] Wendisch, V.F., S.N. Lindner, and T.M. Meiswinkel, *Use of glycerol in biotechnological applications*. 2011: InTech. 39.
- [58] Hu, Z.-C., Z.-Q. Liu, Y.-G. Zheng, and Y.-C. Shen, *Production of 1, 3-dihydroxyacetone from glycerol by Gluconobacter oxydans ZJB09112*. Microbiol Biotechnol, 2010. **20**(2): p. 340-345.
- [59] Liebminger, S., R. Hofbauer, M. Siebenhofer, G.S. Nyanhongo, and G.M. Guebitz, *Microbial conversion of crude glycerol to dihydroxyacetone*. Waste and Biomass Valorization, 2014. **5**: p. 781-787.
- [60] Permpool, N. and S.H. Gheewala, *Environmental and energy assessment of alternative fuels for diesel in Thailand*. Journal of Cleaner Production, 2017.

- 142:** p. 1176-1182.
- [61] OECD/FAO. *OECD-FAO Agricultural Outlook 2021–2030*. 2021 [cited 2021 July 15]; Available from: <https://www.fao.org/3/cb5332en/Biofuels.pdf>.
- [62] Rabaçal, M., A.F. Ferreira, C.A. Silva, and M. Costa, *Biorefineries: targeting energy, high value products and waste valorisation*. Vol. 57. 2017: Springer.
- [63] OECD/FAO. *OECD-FAO Agricultural Outlook”, OECD Agriculture statistics (database)*. 2022; Available from: <https://www.oecd-ilibrary.org/sites/cdc97c88-en/index.html?itemId=/content/component/cdc97c88-en>.
- [64] Win, S.S. and T.A. Trabold, *Sustainable Waste-to-Energy Technologies: Transesterification*, in *Sustainable Food Waste-To-energy Systems*. 2018, Elsevier. p. 89-109.
- [65] Karmakar, B. and G. Halder, *Progress and future of biodiesel synthesis: Advancements in oil extraction and conversion technologies*. Energy conversion and management, 2019. **182:** p. 307-339.
- [66] Luo, X., X. Ge, S. Cui, and Y. Li, *Value-added processing of crude glycerol into chemicals and polymers*. Bioresour Technol, 2016. **215:** p. 144-154.
- [67] Chatzifragkou, A. and S. Papanikolaou, *Effect of impurities in biodiesel-derived waste glycerol on the performance and feasibility of biotechnological processes*. Applied microbiology and biotechnology, 2012. **95:** p. 13-27.
- [68] Wan Isahak, W.N.R., Z.A. Che Ramli, M. Ismail, J. Mohd Jahim, and M.A. Yarmo, *Recovery and Purification of Crude Glycerol from Vegetable Oil Transesterification*. Separation & Purification Reviews, 2014. **44(3):** p. 250-267.
- [69] Rodrigues, A., J.C. Bordado, and R.G.d. Santos, *Upgrading the Glycerol from Biodiesel Production as a Source of Energy Carriers and Chemicals—A Technological Review for Three Chemical Pathways*. Energies, 2017. **10(11)**.
- [70] Ardi, M.S., M.K. Aroua, and N.A. Hashim, *Progress, prospect and challenges in glycerol purification process: A review*. Renewable and Sustainable Energy Reviews, 2015. **42:** p. 1164-1173.
- [71] de Caro, P., M. Bandres, M. Urrutigoity, C. Cecutti, and S. Thiebaud-Roux, *Recent Progress in Synthesis of Glycerol Carbonate and Evaluation of Its Plasticizing Properties*. Front Chem, 2019. **7:** p. 308.

- [72] de la Morena, S., M.G. Acedos, V.E. Santos, and F. Garcia-Ochoa, *Dihydroxyacetone production from glycerol using Gluconobacter oxydans: Study of medium composition and operational conditions in shaken flasks*. Biotechnol Prog, 2019. **35**(4): p. 1-9.
- [73] Samudrala, S.P., S. Kandasamy, and S. Bhattacharya, *Turning biodiesel waste glycerol into 1, 3-Propanediol: catalytic performance of sulphuric acid-activated montmorillonite supported platinum catalysts in glycerol hydrogenolysis*. Scientific reports, 2018. **8**(1): p. 1-12.
- [74] Balaraju, M., V. Rekha, P.S. Prasad, R. Prasad, and N. Lingaiah, *Selective hydrogenolysis of glycerol to 1, 2 propanediol over Cu-ZnO catalysts*. Catalysis Letters, 2008. **126**(1-2): p. 119-124.
- [75] Reportlinker. *Global Bio-Based Chemicals Market Forecast 2019–2027*. [cited 2020 April 28]; Available from: <https://www.reportlinker.com/p05001382/Global-Bio-Based-Chemicals-Market-Forecast.html>.
- [76] de Jong, E., A. Higson, P. Walsh, and M. Wellisch, *Bio-based chemicals*. IEA Bioenergy, 2020.
- [77] Sánchez, G., B. Dlugogorski, E. Kennedy, and M. Stockenhuber, *Zeolite-supported iron catalysts for allyl alcohol synthesis from glycerol*. Applied Catalysis A: General, 2016. **509**: p. 130-142.
- [78] El Roz, A., P. Fongarland, F. Dumeignil, and M. Capron, *Glycerol to Glyceraldehyde Oxidation Reaction Over Pt-Based Catalysts Under Base-Free Conditions*. Front Chem, 2019. **7**: p. 156.
- [79] Wang, S., K. Yin, Y. Zhang, and H. Liu, *Glycerol Hydrogenolysis to Propylene Glycol and Ethylene Glycol on Zirconia Supported Noble Metal Catalysts*. ACS Catalysis, 2013. **3**(9): p. 2112-2121.
- [80] Kim, T., S. Cho, H. Woo, S.-M. Lee, J. Lee, Y. Um, and J.-H. Seo, *High production of 2,3-butanediol from glycerol without 1,3-propanediol formation by Raoultella ornithinolytica B6*. Appl Microbiol Biotechnol, 2017. **101**(7): p. 2821-2830.
- [81] Yazdani, S.S. and R. Gonzalez, *Anaerobic fermentation of glycerol: a path to economic viability for the biofuels industry*. Current opinion in biotechnology,

2007. **18**(3): p. 213-219.
- [82] Tabah, B., A. Varvak, I.N. Pulidindi, E. Foran, E. Banin, and A. Gedanken, *Production of 1, 3-propanediol from glycerol via fermentation by Saccharomyces cerevisiae*. Green Chemistry, 2016. **18**(17): p. 4657-4666.
- [83] Zhu, H., X. Yi, Y. Liu, H. Hu, T.K. Wood, and X. Zhang, *Production of acetol from glycerol using engineered Escherichia coli*. Bioresour Technol, 2013. **149**: p. 238-243.
- [84] Mohamad, M.H., R. Awang, and W.M. Yunus, *A review of acetol: application and production*. American Journal of Applied Sciences, 2011. **8**(11): p. 1135.
- [85] Cybulski, K., L. Tomaszewska-Hetman, M. Rakicka, P. Juszczak, and A. Rywinska, *Production of pyruvic acid from glycerol by Yarrowia lipolytica*. Folia Microbiol (Praha), 2019. **64**(6): p. 809-820.
- [86] Research informatic. *Succinic acid market size*. 2022 [cited 2022 July 12]; 07-12]. Available from: <https://www.researchinformatic.com/reports/succinic-acid-market-45>.
- [87] Bio-based News. *METabolic EXplorer and SK CHEMICALS Co. Ltd., Signature of an exclusive agreement to manufacture and sell PDO*. 2014 [cited 2021 June 11]; Available from: <https://news.bio-based.eu/metabolic-explorer-sk-chemicals-co-ltd-signature-exclusive-agreement-manufacture-sell-pdo/>.
- [88] Jiangsu Libert. *Zhangjiagang Glory Biomaterial*. 2018 [cited 2021 June 11]; Available from: <http://www.cnlbt.com/en/operation/customerDetail.aspx?ID=234>.
- [89] Raddadi, N., S. De Giorgi, and F. Fava, *Recent Achievements in the Production of Biobased 1, 3-Propanediol*, in *Microbial Factories*. 2015, Springer: New Delhi, India. p. 121-134.
- [90] Mordor Intelligence. *1,3-PROPANEDIOL (PDO) MARKET - GROWTH, TRENDS, COVID-19 IMPACT, AND FORECASTS (2021 - 2026)*. 2021 [cited 2021 June 11]; Available from: <https://www.mordorintelligence.com/industry-reports/1-3-propanediol-pdo-market>.
- [91] Herliati, R. Yunus, U. Rashid, Z.Z. Abidin, and I.S. Ahamad, *Synthesis of 1,3-Dichloropropanol from Glycerol Using Muriatic Acid as Chlorinating Agent*. Asian

- Journal of Chemistry, 2014. **26**(10): p. 2907-2912.
- [92] Arundhathi, R., T. Mizugaki, T. Mitsudome, K. Jitsukawa, and K. Kaneda, *Highly selective hydrogenolysis of glycerol to 1,3-propanediol over a boehmite-supported platinum/tungsten catalyst*. ChemSusChem, 2013. **6**(8): p. 1345-1347.
- [93] Wang, M., H. Yang, Y. Xie, X. Wu, C. Chen, W. Ma, Q. Dong, and Z. Hou, *Catalytic transformation of glycerol to 1-propanol by combining zirconium phosphate and supported Ru catalysts*. RSC Advances, 2016. **6**(35): p. 29769-29778.
- [94] Chiu, C.W., M.A. Dasari, G.J. Suppes, and W.R. Sutterlin, *Dehydration of glycerol to acetol via catalytic reactive distillation*. AIChE Journal, 2006. **52**(10): p. 3543-3548.
- [95] Tsukuda, E., S. Sato, R. Takahashi, and T. Sodesawa, *Production of acrolein from glycerol over silica-supported heteropoly acids*. Catalysis Communications, 2007. **8**(9): p. 1349-1353.
- [96] Imbault, A.L., J. Gong, and R. Farnood, *Photocatalytic production of dihydroxyacetone from glycerol on TiO₂ in acetonitrile*. RSC Advances, 2020. **10**(9): p. 4956-4968.
- [97] Zhang, J., M. Sun, and Y. Han, *Selective oxidation of glycerol to formic acid in highly concentrated aqueous solutions with molecular oxygen using V-substituted phosphomolybdic acids*. RSC Adv., 2014. **4**(67): p. 35463-35466.
- [98] Rittiron, P., C. Niamnuy, W. Donphai, M. Chareonpanich, and A. Seubsai, *Production of Glycerol Carbonate from Glycerol over Templated-Sodium-Aluminate Catalysts Prepared Using a Spray-Drying Method*. ACS Omega, 2019. **4**(5): p. 9001-9009.
- [99] Rahman, M.M., *H₂ production from aqueous-phase reforming of glycerol over Cu-Ni bimetallic catalysts supported on carbon nanotubes*. International Journal of Hydrogen Energy, 2015. **40**(43): p. 14833-14844.
- [100] Mohamed, M., T.S. Ting, N. Amin, T. Abdullah, and R. Mat. *Conversion of glycerol to methanol in the presence of zeolite based catalysts*. in *2011 IEEE Conference on Clean Energy and Technology (CET)*. 2011. IEEE.
- [101] Sajid, M., M. Ayoub, Y. Uemura, S. Yusup, M. Saleem, B. Abdullah, and A.U. Khan, *Comparative study of glycerol conversion to polyglycerol via conventional and*

- microwave irradiation reactor*. *Materials Today: Proceedings*, 2019. **16**: p. 2101-2107.
- [102] Mufrodi, Z., R. Rochmadi, S. Sutijan, and A. Budiman, *Synthesis acetylation of glycerol using batch reactor and continuous reactive distillation column*. *Engineering Journal*, 2014. **18**(2): p. 29-40.
- [103] Lin, D.S., H.W. Yen, W.C. Kao, C.L. Cheng, W.M. Chen, C.C. Huang, and J.S. Chang, *Bio-butanol production from glycerol with Clostridium pasteurianum CH4: the effects of butyrate addition and in situ butanol removal via membrane distillation*. *Biotechnol Biofuels*, 2015. **8**: p. 168.
- [104] Rymowicz, W., A. Rywińska, and M. Marcinkiewicz, *High-yield production of erythritol from raw glycerol in fed-batch cultures of Yarrowia lipolytica*. *Biotechnology Letters*, 2009. **31**(3): p. 377-380.
- [105] Wong, M.S., M. Li, R.W. Black, T.Q. Le, S. Puthli, P. Campbell, and D. Monticello, *Microaerobic conversion of glycerol to ethanol in Escherichia coli*. *Appl. Environ. Microbiol.*, 2014. **80**(10): p. 3276-3282.
- [106] Yoshikawa, J., H. Habe, T. Morita, T. Fukuoka, T. Imura, H. Iwabuchi, S. Uemura, T. Tamura, and D. Kitamoto, *Production of mannitol from raw glycerol by Candida azyma*. *Journal of bioscience bioengineering*, 2014. **117**(6): p. 725-729.
- [107] de Paula, F.C., S. Kakazu, C.B.C. de Paula, J.G.C. Gomez, and J. Contiero, *Polyhydroxyalkanoate production from crude glycerol by newly isolated Pandoraea sp.* *Journal of King Saud University - Science*, 2017. **29**(2): p. 166-173.
- [108] Zhang, A., J. Sun, Z. Wang, S.T. Yang, and H. Zhou, *Effects of carbon dioxide on cell growth and propionic acid production from glycerol and glucose by Propionibacterium acidipropionici*. *Bioresour Technol*, 2015. **175**: p. 374-381.
- [109] Taylor, R., L. Nattrass, G. Alberts, P. Robson, C. Chudziak, A. Bauen, I. Libelli, G. Lotti, M. Prussi, and R. Nistri, *From the sugar platform to biofuels and biochemicals: final report for the European Commission Directorate-General Energy*. 2015, E4tech/Re-CORD/Wageningen UR.
- [110] Gonzalez-Garcia, R., T. McCubbin, L. Navone, C. Stowers, L. Nielsen, and E. Marcellin, *Microbial Propionic Acid Production*. *Fermentation*, 2017. **3**(2): p. 1-20.

- [111] Liu, L., Y. Zhu, J. Li, M. Wang, P. Lee, G. Du, and J. Chen, *Microbial production of propionic acid from propionibacteria: current state, challenges and perspectives*. Crit Rev Biotechnol, 2012. **32**(4): p. 374-381.
- [112] Grand View Research. *Propionic Acid Market Size Worth \$1.53 Billion By 2020*. 2021 [cited 2021 June 14]; 06-14]. Available from: <https://www.grandviewresearch.com/press-release/global-propionic-acid-market>.
- [113] Research and Markets. *Propionic Acid - Global Market Trajectory & Analytics*. 2021 [cited 2021 June 14]; 06-14]. Available from: <https://www.researchandmarkets.com/reports/5030547/propionic-acid-global-market-trajectory-and>.
- [114] Yang, H., Z. Wang, M. Lin, and S.T. Yang, *Propionic acid production from soy molasses by Propionibacterium acidipropionici: Fermentation kinetics and economic analysis*. Bioresource Technology, 2018. **250**: p. 1-9.
- [115] ChemicalBook. *Propionic acid*. 2022 [cited 2022 March 10]; 03-10]. Available from: https://www.chemicalbook.com/ProductDetail_EN_1631045.htm.
- [116] PubChem. *Chemical and Physical Properties*. 2020 December 20]; 12-20]. Available from: <https://pubchem.ncbi.nlm.nih.gov/>.
- [117] Himmi, E.H., A. Bories, A. Boussaid, and L. Hassani, *Propionic acid fermentation of glycerol and glucose by Propionibacterium acidipropionici and Propionibacterium freudenreichii ssp. shermanii*. Applied Microbiology Biotechnology, 2000. **53**(4): p. 435-440.
- [118] Suwannakham, S., *Metabolic engineering for enhanced propionic acid fermentation by Propionibacterium acidipropionici*. 2005, The Ohio State University: Ohio, US.
- [119] Zhu, Y., J. Li, M. Tan, L. Liu, L. Jiang, J. Sun, P. Lee, G. Du, and J. Chen, *Optimization and scale-up of propionic acid production by propionic acid-tolerant Propionibacterium acidipropionici with glycerol as the carbon source*. Bioresource technology, 2010. **101**(22): p. 8902-8906.
- [120] Liu, L., N. Guan, G. Zhu, J. Li, H.D. Shin, G. Du, and J. Chen, *Pathway engineering of Propionibacterium jensenii for improved production of propionic acid*. Scientific reports, 2016. **6**: p. 1-9.

- [121] Panda, S.K., L. Sahu, S.K. Behera, and R.C. Ray, *Research and Production of Organic Acids and Industrial Potential*. Bioprocessing for Biomolecules Production, 2019: p. 195-209.
- [122] Sadhukhan, J., K.S. Ng, and E.M. Hernandez, *Biorefineries and Chemical Processes: Design, Integration and Sustainability Analysis*. 2014, UK: Wiley. 676.
- [123] González-García, S., L. Argiz, P. Míguez, and B. Gullón, *Exploring the production of bio-succinic acid from apple pomace using an environmental approach*. Chemical Engineering Journal, 2018. **350**: p. 982-991.
- [124] Mongkhonsiri, G., A. Anantpinijwatna, P. Charoensuppanimit, A. Arpornwichanop, R. Gani, and S. Assabumrungrat, *Novel biorefinery-Integrated-Kraft-pulping network for sustainable development*. Chemical Engineering Processing-Process Intensification, 2021. **163**: p. 108373.
- [125] Lari, G.M., G. Pastore, M. Haus, Y. Ding, S. Papadokonstantakis, C. Mondelli, and J. Pérez-Ramírez, *Environmental and economical perspectives of a glycerol biorefinery*. Energy & Environmental Science, 2018. **11**(5): p. 1012-1029.
- [126] Grand View Research. *Succinic Acid Market Size*. 2022 [cited 2022 July 15]; 07-15]. Available from: <https://www.grandviewresearch.com/industry-analysis/succinic-acid-market>.
- [127] Du, C., S.K.C. Lin, A. Koutinas, R. Wang, and C. Webb, *Succinic acid production from wheat using a biorefining strategy*. Applied microbiology and biotechnology, 2007. **76**: p. 1263-1270.
- [128] Leung, C.C.J., A.S.Y. Cheung, A.Y.-Z. Zhang, K.F. Lam, and C.S.K. Lin, *Utilisation of waste bread for fermentative succinic acid production*. Biochemical engineering journal, 2012. **65**: p. 10-15.
- [129] Borges, E.R. and N.P. Jr, *Succinic acid production from sugarcane bagasse hemicellulose hydrolysate by Actinobacillus succinogenes*. Journal of Industrial Microbiology and Biotechnology, 2011. **38**(8): p. 1001-1011.
- [130] Thuy, N.T.H., A. Kongkaew, A. Flood, and A. Boontawan, *Fermentation and crystallization of succinic acid from Actinobacillus succinogenes ATCC55618 using fresh cassava root as the main substrate*. Bioresource technology, 2017. **233**: p. 342-352.

- [131] Pateraki, C., H. Almqvist, D. Ladakis, G. Lidén, A.A. Koutinas, and A. Vlysidis, *Modelling succinic acid fermentation using a xylose based substrate*. Biochemical Engineering Journal, 2016. **114**: p. 26-41.
- [132] Kim, D.Y., S.C. Yim, P.C. Lee, W.G. Lee, S.Y. Lee, and H.N. Chang, *Batch and continuous fermentation of succinic acid from wood hydrolysate by Mannheimia succiniciproducens MBEL55E*. Enzyme and Microbial Technology, 2004. **35**(6-7): p. 648-653.
- [133] Vemuri, G., M. Eiteman, and E. Altman, *Succinate production in dual-phase Escherichia coli fermentations depends on the time of transition from aerobic to anaerobic conditions*. Journal of Industrial Microbiology and Biotechnology, 2002. **28**: p. 325-332.
- [134] Almeida, J.R., L.C. Fávaro, and B.F. Quirino, *Biodiesel biorefinery: opportunities and challenges for microbial production of fuels and chemicals from glycerol waste*. Biotechnology for biofuels, 2012. **5**(1): p. 48.
- [135] Global Information. *Global Dihydroxyacetone (DHA) Market Insights and Forecast to 2027*. 2021 [cited 2023 April 12]; 04-12]. Available from: <https://www.giiresearch.com/report/qyr1038080-global-dihydroxyacetone-dha-market-insights.html>.
- [136] Sudarshan, B. and K. Sanjay, *Optimization of fermentation conditions for production of 1, 3-dihydroxyacetone from glycerol obtained as a byproduct during biodiesel production*. Microbiology Research Journal International, 2018. **25**(3): p. 1-9.
- [137] Poljungreed, I. and S. Boonyarattanakalin, *Low-cost biotransformation of glycerol to 1, 3-dihydroxyacetone through Gluconobacter frateurii in medium with inorganic salts only*. Letters in applied microbiology, 2018. **67**(1): p. 39-46.
- [138] Jittjang, S., I. Jiratthiticheep, P. Kajonpradabkul, T. Tiatongjitman, W. Siriwatwechakul, and S. Boonyarattanakalin, *Effect of NaCl removal from biodiesel-derived crude glycerol by ion exchange to enhance dihydroxyacetone production by Gluconobacter thailandicus in minimal medium*. Journal of Chemical Technology & Biotechnology, 2020. **95**(1): p. 281-

288.

- [139] Tan, J.P., J. Md. Jahim, T.Y. Wu, S. Harun, B.H. Kim, and A.W. Mohammad, *Insight into Biomass as a Renewable Carbon Source for the Production of Succinic Acid and the Factors Affecting the Metabolic Flux toward Higher Succinate Yield*. *Industrial & Engineering Chemistry Research*, 2014. **53**(42): p. 16123-16134.
- [140] Kuenz, A., L. Hoffmann, K. Goy, S. Bromann, and U. Prüße, *High-Level Production of Succinic Acid from Crude Glycerol by a Wild Type Organism*. *Catalysts*, 2020. **10**(5).
- [141] Dickson, R., E. Mancini, N. Garg, J.M. Woodley, K.V. Gernaey, M. Pinelo, J. Liu, and S.S. Mansouri, *Sustainable bio-succinic acid production: superstructure optimization, techno-economic, and lifecycle assessment*. *Energy Environmental Science*, 2021. **14**(6): p. 3542-3558.
- [142] Liu, Y.P., Y. Sun, C. Tan, H. Li, X.J. Zheng, K.Q. Jin, and G. Wang, *Efficient production of dihydroxyacetone from biodiesel-derived crude glycerol by newly isolated *Gluconobacter frateurii**. *Bioresour Technol*, 2013. **142**: p. 384-389.
- [143] Nanda, M., Z. Yuan, W. Qin, M. Poirier, and X. Chunbao, *Purification of crude glycerol using acidification: effects of acid types and product characterization*. *Austin Journal of Chemical Engineering*, 2014. **1**(1): p. 1-7.
- [144] Junsittiwate, R., T.R. Srinophakun, and S. Sukpancharoen, *Techno-economic, environmental, and heat integration of palm empty fruit bunch upgrading for power generation*. *Energy for Sustainable Development*, 2022. **66**: p. 140-150.
- [145] De Meester, S., R.A. Alvarenga, and J. Dewulf, *Sustainability assessment of renewables-based products: methods and case studies*. 2015: John Wiley & Sons. 388.
- [146] Marchesan, A.N., J.F. Leal Silva, R. Maciel Filho, and M.R. Wolf Maciel, *Techno-Economic Analysis of Alternative Designs for Low-pH Lactic Acid Production*. *ACS Sustainable Chemistry Engineering*, 2021. **9**(36): p. 12120-12131.
- [147] Charoensuppanimit, P., B. Chaiapha, S. Assabumrungrat, and B. Jongsomjit, *Incorporation of diethyl ether production to existing bioethanol process: Techno-economic analysis*. *Journal of Cleaner Production*, 2021. **327**: p. 129438.
- [148] Zhou, X., Q. Sun, H. Yan, C. Yang, and N. Yan, *Integrating Time, Region, and*

- Society Dimensions into a Multi-Dimensional Life-Cycle Analysis for Sustainable Dihydroxyacetone Production*. ACS Sustainable Chemistry & Engineering, 2023. **11**(29): p. 10795-10811.
- [149] Im-orb, K., A.N. Phan, and A. Arpornwichanop, *Bio-methanol production from oil palm residues: A thermodynamic analysis*. Energy Conversion and Management, 2020. **226**: p. 113493.
- [150] Meramo-Hurtado, S., K. Moreno-Sader, and Á.D. González-Delgado, *Computer-aided simulation and exergy analysis of TiO₂ nanoparticles production via green chemistry*. PeerJ, 2019. **7**: p. 1-19.
- [151] Meramo Hurtado, S.I., P. Puello, and A. Cabarcas, *Technical evaluation of a levulinic acid plant based on biomass transformation under techno-economic and exergy analyses*. ACS omega, 2021. **6**(8): p. 5627-5641.
- [152] Carlson, E.C., *Don't gamble with physical properties for simulations*. Chemical engineering progress, 1996. **92**(10): p. 35-46.
- [153] Gargalo, C.L., P. Cheali, J.A. Posada, and G. Sin, *Economic Risk Assessment of Early Stage Designs for Glycerol Valorization in Biorefinery Concepts*. Industrial & Engineering Chemistry Research, 2016. **55**(24): p. 6801-6814.
- [154] Nieder-Heitmann, M., *Techno-economic and life cycle analyses for comparison of biorefinery scenarios for the production of succinic acid, itaconic acid and polyhydroxybutyrate (PHB) from sugarcane lignocelluloses*. 2019, Stellenbosch University: Stellenbosch, South Africa.
- [155] Lee, H., *Development of lactic and succinic acid biorefinery configurations for integration into a thermomechanical pulp mill*. 2015, École Polytechnique de Montréal.
- [156] Trading Economics. *Thailand Corporate Tax Rate*. 2021 [cited 2022 April 1]; 04-01]. Available from: <https://tradingeconomics.com/thailand/corporate-tax-rate>.
- [157] Trading Economics. *Thailand Interest Rate*. 2022 [cited 2022 April 1]; 04-01]. Available from: <https://tradingeconomics.com/thailand/interest-rate>.
- [158] GlobalPetrolPrices. *Thailand electricity prices*. 2022 [cited 2022 May 6]; 05-06]. Available from: https://www.globalpetrolprices.com/Thailand/electricity_prices/.
- [159] Turton, R., J.A. Shaeiwitz, D. Bhattacharyya, and W.B. Whiting, *Analysis, synthesis*

- and design of chemical processes*. 2018, London: Pearson. 1549.
- [160] Alibaba. *Chemical prices*. 2022 [cited 2022 March 10]; 03-10]. Available from: <https://www.alibaba.com/>.
- [161] ChemAnalyst. *Propionic Acid Price Trend and Forecast*. 2022 [cited 2022 May 10]; Available from: <https://www.chemanalyst.com/Pricing-data/propionic-acid-1184>.
- [162] Nakyai, T. and D. Saebea, *Exergoeconomic comparison of syngas production from biomass, coal, and natural gas for dimethyl ether synthesis in single-step and two-step processes*. *Journal of Cleaner Production*, 2019. **241**: p. 118334.
- [163] Guidechem. *Chemical prices*. 2022 [cited 2022 May 6]; 05-06]. Available from: <https://www.guidechem.com/product/>.
- [164] Statista. *Price of ethylene worldwide from 2017 to 2021*. 2022 [cited 2022 May 6]; 05-06]. Available from: <https://www.statista.com/statistics/1170573/price-ethylene-forecast-globally/>.
- [165] Selina Wamucii. *Thailand Glucose Prices*. 2023 [cited 2023 September 22]; 09-22]. Available from: <https://www.selinawamucii.com/insights/prices/thailand/glucose/>.
- [166] Mancini, E., R. Dickson, S. Fabbri, I.A. Udugama, H.I. Ullah, S. Vishwanath, K.V. Gernaey, J. Luo, M. Pinelo, and S.S. Mansouri, *Economic and environmental analysis of bio-succinic acid production: From established processes to a new continuous fermentation approach with in-situ electrolytic extraction*. *Chemical Engineering Research Design*, 2022. **179**: p. 401-414.
- [167] Procurement Resource. *Phosphoric Acid Price Trend and Forecast*. 2023 [cited 2023 May 10]; 05-10]. Available from: <https://www.procurementresource.com/resource-center/phosphoric-acid-price-trends>.
- [168] IndexBox. *Thailand - Sorbitol - Market Analysis, Forecast, Size, Trends And Insights*. 2023 [cited 2023 September 22]; 09-22]. Available from: <https://www.indexbox.io/blog/thailand-sorbitol-price-in-july-2023/>.
- [169] Khwanjaisakun, N., S. Amornraksa, L. Simasatitkul, P. Charoensuppanimit, and S. Assabumrungrat, *Techno-economic analysis of vanillin production from Kraft*

- lignin: Feasibility study of lignin valorization*. Bioresource Technology, 2020. **299**: p. 122559.
- [170] Sakdasri, W., R. Sawangkeaw, and S. Ngamprasertsith, *Techno-economic analysis of biodiesel production from palm oil with supercritical methanol at a low molar ratio*. Energy, 2018. **152**: p. 144-153.
- [171] Charoensuppanimit, P., K. Kitsahawong, P. Kim-Lohsoontorn, and S. Assabumrungrat, *Incorporation of hydrogen by-product from NaOCH₃ production for methanol synthesis via CO₂ hydrogenation: Process analysis and economic evaluation*. Journal of Cleaner Production, 2019. **212**: p. 893-909.
- [172] Palamutcu, S., *Energy footprints in the textile industry*, in *Handbook of Life Cycle Assessment (LCA) of Textiles and Clothing*, S.S. Muthu, Editor. 2015, Woodhead Publishing. p. 31-61.
- [173] Wiranarongkorn, K., K. Im-orb, J. Panpranot, F. Maréchal, and A. Arpornwichanop, *Exergy and exergoeconomic analyses of sustainable furfural production via reactive distillation*. Energy, 2021. **226**: p. 120339.
- [174] Choodonwai, A. and S. Khuntong, *Carbon and Water Footprint Analysis of Super Absorbent Polymer*. 2018, Kasetsart University: Thailand.
- [175] TGO. *Emission Factor*. 2021 [cited 2021 January 27]; 01-27]. Available from: <http://thaicarbonlabel.tgo.or.th/>.
- [176] OpenLCA, *OpenLCA*. 2020.
- [177] Dow. *Propionic Acid, Industrial Grade*. 2021 [cited 2021 June 20]; 06-20]. Available from: <https://www.dow.com/en-us/pdp.propionic-acid-industrial-grade.377582z.html>.
- [178] Dishisha, T., M.T. Alvarez, and R. Hatti-Kaul, *Batch- and continuous propionic acid production from glycerol using free and immobilized cells of Propionibacterium acidipropionici*. Bioresour Technol, 2012. **118**: p. 553-562.
- [179] Wooley, R.J. and V. Putsche, *Development of an ASPEN PLUS physical property database for biofuels components*. 1996: National Renewable Energy Lab., Golden, CO (US).
- [180] Jurado, M.G., V. Plesu, J.B. Ruiz, A.B. Ruiz, A. Tuluc, and J.L. Llacuna, *Simulation of a hybrid reactive extraction unit. Biodiesel synthesis*. Chemical Engineering

- Transactions, 2013. **35**: p. 205-210.
- [181] Keshav, A., *Intensification of recovery of carboxylic acid by reactive extraction*, in *Faculty of engineering*. 2009, Indian Institute of Technology Roorkee: Uttarakhand, India.
- [182] Byrne, F.P., S. Jin, G. Paggiola, T.H. Petchey, J.H. Clark, T.J. Farmer, A.J. Hunt, C.R. McElroy, and J. Sherwood, *Tools and techniques for solvent selection: green solvent selection guides*. Sustainable chemical processes, 2016. **4**(1): p. 1-24.
- [183] Hohenschutz, H., D. Franz, H. Buelow, and G. Dinkhauser, *Production of propionic acid*, in *Ludwigshafen, Germany*, U.S. Patent and Trademark Office, Editor. 1974: US.
- [184] Hohenschutz, H., P. Hornberger, and H. Buelow, *Removing nickel carbonyl from crude propionic acid*, in *Ludwigshafen, Germany*, U.S. Patent and Trademark Office, Editor. 1973: US.
- [185] Petrides, D. and R. Da Gama, *Production of 1, 3 Propanediol (PDO) via Fermentation—Process Modeling and Techno-Economic Assessment (TEA) Using SuperPro Designer*. Inc.: Scotch Plains, NJ, USA, 2020.
- [186] Tunpaiboon, N. *Industry Outlook 2021-2023: Biodiesel*. 2021 [cited 2021 August 31]; 08-31]. Available from: <https://www.krungsri.com/en/research/industry/industry-outlook/Energy-Utilities/Biodiesel/IO/io-biodiesel-21>.
- [187] Moussa, H.I., A. Elkamel, and S.B. Young, *Assessing energy performance of bio-based succinic acid production using LCA*. Journal of cleaner production, 2016. **139**: p. 761-769.
- [188] Kanchanasuta, S., V. Champreda, N. Pisutpaisal, and C. Singhakant, *Optimization of bio-succinic fermentation process from crude glycerol by Actinobacillus succinogenes*. Environmental Engineering Research, 2021. **26**(4): p. 1-8.
- [189] Chang, W.M., *Glycerol (medical grade) preparation method using a by-product of a bio-diesel process*, in *HDLS Patent & Trademark Services*. 2010: US.
- [190] Hong, Y.K. and W.H. Hong, *Equilibrium studies on reactive extraction of succinic acid from aqueous solutions with tertiary amines*. Bioprocess Engineering, 2000. **22**(6): p. 477-481.

- [191] Ferone, M., F. Raganati, G. Olivieri, and A. Marzocchella, *Bioreactors for succinic acid production processes*. *Critical reviews in biotechnology*, 2019. **39**(4): p. 571-586.
- [192] CheCalc. *Agitator Power*. 2022 [cited 2022 May 6]; 05-06]. Available from: <https://checalc.com/solved/agitator.html>.
- [193] Pinazo, J.M., M.E. Domine, V. Parvulescu, and F. Petru, *Sustainability metrics for succinic acid production: A comparison between biomass-based and petrochemical routes*. *Catalysis Today*, 2015. **239**: p. 17-24.
- [194] Ripoll, M., E. Jackson, J.A. Trelles, and L. Betancor, *Dihydroxyacetone production via heterogeneous biotransformations of crude glycerol*. *Journal of Biotechnology*, 2021. **340**: p. 102-109.
- [195] Zhu, Y., D. Youssef, C. Porte, A. Rannou, M. Delplancke-Ogletree, and B.L.M. Lung-Somarriba, *Study of the solubility and the metastable zone of 1, 3-dihydroxyacetone for the drowning-out process*. *Journal of crystal growth*, 2003. **257**(3-4): p. 370-377.
- [196] Martínez-Gallegos, J.F., A. Burgos-Cara, F. Caparrós-Salvador, G. Luzón-González, and M. Fernández-Serrano, *Dihydroxyacetone crystallization: Process, environmental, health and safety criteria application for solvent selection*. *Chemical Engineering Science*, 2015. **134**: p. 36-43.
- [197] Lari, G.M., C. Mondelli, S. Papadokonstantakis, M. Morales, K. Hungerbühler, and J. Pérez-Ramírez, *Environmental and economic assessment of glycerol oxidation to dihydroxyacetone over technical iron zeolite catalysts*. *Reaction Chemistry & Engineering*, 2016. **1**(1): p. 106-118.
- [198] Kumar, L.R., S.K. Yellapu, R.D. Tyagi, and X. Zhang, *A review on variation in crude glycerol composition, bio-valorization of crude and purified glycerol as carbon source for lipid production*. *Bioresour Technol*, 2019. **293**: p. 122155.
- [199] Liu, S.-S., K.-Q. Sun, and B.-Q. Xu, *Specific selectivity of Au-catalyzed oxidation of glycerol and other C3-polyols in water without the presence of a base*. *ACS Catalysis*, 2014. **4**(7): p. 2226-2230.
- [200] Cespi, D., F. Passarini, G. Mastragostino, I. Vassura, S. Larocca, A. Iaconi, A. Chierigato, J.-L. Dubois, and F. Cavani, *Glycerol as feedstock in the synthesis of*

- chemicals: a life cycle analysis for acrolein production*. Green Chemistry, 2015. **17**(1): p. 343-355.
- [201] Gargalo, C.L., P. Cheali, J.A. Posada, K.V. Gernaey, and G. Sin, *Economic risk assessment of early stage designs for glycerol valorization in biorefinery concepts*. Industrial Engineering Chemistry Research, 2016. **55**(24): p. 6801-6814.
- [202] Cornils, B., W.A. Herrmann, M. Beller, and R. Paciello, *Applied homogeneous catalysis with organometallic compounds: a comprehensive handbook in four volumes*. Vol. 4. 2017: John Wiley & Sons.
- [203] Ding, Y., *Toward A Glycerol Based (Bio) refinery: Process Design, Simulation and Assessment of Chemocatalytic Production Paths*. 2017, PhD Thesis, University of Technology.
- [204] Stephen, H., *Solubilities of inorganic and organic compounds*. Ternary Multicomponent Systems, 1964. **2**: p. 100-101.
- [205] Kurzrock, T., S. Schallinger, and D. Weuster-Botz, *Integrated separation process for isolation and purification of biosuccinic acid*. Biotechnology progress, 2011. **27**(6): p. 1623-1628.
- [206] Volk, A. *Calculate density and viscosity of glycerol/water mixtures*. 2018 [cited 2022 May 6]; 05-06]. Available from: http://www.met.reading.ac.uk/~sws04cdw/viscosity_calc.html.
- [207] Chemeo. *Gibbs free energy*. 2022 [cited 2022 July 12]; 07-12]. Available from: <https://www.chemeo.com/>.
- [208] Exergoecology. *Exergy calculator*. 2022 [cited 2022 July 12]; 07-12]. Available from: <https://www.exergoecology.com/excalc/exergy-calculator>.
- [209] Fallahi, A., S. Farzad, S.S. Mohtasebi, M. Mandegari, J.F. Görgens, V.K. Gupta, S.S. Lam, M. Tabatabaei, and M. Aghbashlo, *Sustainability assessment of sugarcane residues valorization to biobutadiene by exergy and exergoeconomic evaluation*. Renewable Sustainable Energy Reviews, 2021. **147**: p. 111214.
- [210] Aghbashlo, M., M. Tabatabaei, H. Rastegari, and H.S. Ghaziaskar, *Optimization of continuous glycerol esterification with acetic acid based on exergoeconomic and exergoenvironmental approaches*. Sustainable Production Consumption,

2019. **17**: p. 62-73.

- [211] Kumar, S., N. Katiyar, S. Kumar, and S. Yadav, *Exergy analysis of oxidative steam reforming of methanol for hydrogen production: modeling study*. International Journal of Chemical Reactor Engineering, 2013. **11**(1): p. 489-500.



APPENDIX A

GROSS PROFIT MARGIN ANALYSIS

Assumption

- Capital costs, utilities and operating costs were not considered.
- By-products were classified as non-valuable products.
- The amount of glycerol (feedstock) was 1 kg.

Since glycerol can be converted to various value-added chemicals. The chemicals selected were determined by the price of substance and conversion to calculate a suitable product to be produced from glycerol. Initially, the gross profit margin was calculated for each alternative according to Equation (1). Gross profit margin is obtained by subtracting the raw materials costs from revenue products. The results of gross profit calculations are shown in Table A1, where the top three substances were selected to be considered – propionic acid, succinic acid, and dihydroxyacetone.

$$\text{Gross profit margin} = \text{revenue} - \text{cost} \quad (1)$$

Example Gross profit margin for 1,2-propanediol production (conversion = 71%)

Reaction	Glycerol + Hydrogen \rightarrow 1,2-propanediol + Water			
MW (g/mol)	92	2	76	18
Mole	1	1	0.71	0.71
Mass (g)	92	2	53.96	12.78
Feed (kg)	1	$= \frac{1}{92} \times 2$ = 0.022	$= \frac{1}{92} \times 53.96$ = 0.587	$= \frac{1}{92} \times 12.78$ = 0.139

$$\begin{aligned} \text{Gross profit margin} &= (0.587 \text{ kg})(1.66 \text{ USD/kg}) - (1 \text{ kg})(0.14 \text{ USD/kg}) \\ &\quad - (0.022 \text{ kg})(3.19 \text{ USD/kg}) \\ &= 0.76 \text{ USD} \end{aligned}$$

Table A1 Gross profit margin analysis results of value-added chemicals from glycerol

Chemicals	Process	Gross profit margin (USD)
Dihydroxyacetone	Fermentation	4.70
Succinic acid	Fermentation	1.92
Propionic acid	Fermentation	1.32
Polyhydroxyalkanoate	Fermentation	1.13
Lactic acid	Fermentation	1.13
1,3-propanediol	Fermentation	1.10
Triacetin	Esterification	1.08
2,3-butanediol	Fermentation	1.03
Erythritol	Fermentation	0.94
Acrolein	Dehydration	0.92
Citric acid	Fermentation	0.80
1,2-propanediol	Hydrogenolysis	0.76
Ethylene glycol	Hydrogenolysis	0.75
Polyglycerol	Etherification	0.69
Polyhydroxybutyrate	Fermentation	0.60
Butanol	Fermentation	0.49
3-Hydroxypropionic acid	Fermentation	0.46
Ethanol	Fermentation	0.22
Hydrogen	Steam reforming	-0.28
Epichlorohydrin	Chlorination	-4.25

APPENDIX B
SUPPLEMENTARY INFORMATION OF CHAPTER 4

Table B1 Summary of CO₂ equivalence in scenario I

	Raw material	Transportation	Reaction	Recovery & Purification	sum
Analyze the contributions to the environmental impact (kg _{CO2eq} /h)					
Glycerol	1.89E+03	-	-	-	1.89E+03
NH ₃	1.61E+02	2.58E+01	-	-	1.87E+02
N ₂	1.01E+01	2.50E+01	-	-	3.51E+01
Water	-	-	2.04E+01	2.72E+00	2.31E+01
Steam	-	-	8.09E+02	2.10E+02	1.02E+03
Cooling water	-	-	6.47E+02	1.49E+02	7.96E+02
Refrigerant	-	-	1.31E+03	4.82E+02	1.79E+03
Electricity	-	-	3.41E+01	7.17E-01	3.48E+01
Wastewater	-	-	-	1.36E+02	1.36E+02
CO ₂	-	-	-	2.37E+02	2.37E+02
sum	2.06E+03	5.08E+01	2.82E+03	1.22E+03	6.15E+03

Table B2 Summary of CO₂ equivalence in scenario II

	Raw material	Transportation	Reaction	Recovery & Purification	sum
Analyze the contributions to the environmental impact (kg _{CO2eq} /h)					
Glycerol	1.85E+03	-	-	-	1.85E+03
NH ₃	1.57E+02	2.57E+01	-	-	1.83E+02
N ₂	9.90E+00	2.50E+01	-	-	3.49E+01
Water	-	-	2.00E+01	-	2.00E+01
Steam	-	-	7.90E+02	6.94E+01	8.60E+02
Cooling water	-	-	6.32E+02	3.76E+01	6.69E+02
Refrigerant	-	-	1.28E+03	3.68E+02	1.65E+03
Electricity	-	-	3.36E+01	4.74E-01	3.41E+01
Wastewater	-	-	-	1.18E+02	1.18E+02
CO ₂	-	-	-	2.34E+02	2.34E+02
sum	2.01E+03	5.07E+01	2.75E+03	8.27E+02	5.65E+03

Table B3 Summary of CO₂ equivalence in scenario III

	Raw material	Transportation	Reaction	Recovery & Purification	sum
Analyze the contributions to the environmental impact (kg _{CO2eq} /h)					
Glycerol	1.74E+03	-	-	-	1.74E+03
NH ₃	1.48E+02	2.56E+01	-	-	1.74E+02
N ₂	9.34E+00	2.49E+01	-	-	3.43E+01
Water	-	-	1.88E+01	-	1.88E+01
Steam	-	-	7.46E+02	8.77E+01	8.34E+02
Cooling water	-	-	5.96E+02	5.08E+01	6.47E+02
Refrigerant	-	-	1.21E+03	4.04E+02	1.61E+03
Electricity	-	-	3.23E+01	5.01E-01	3.28E+01
Wastewater	-	-	-	1.10E+02	1.10E+02
CO ₂	-	-	-	2.21E+02	2.21E+02
sum	1.90E+03	5.06E+01	2.60E+03	8.74E+02	5.43E+03

Table B4 Summary of CO₂ equivalence in scenario IV

	Raw material	Transportation	Reaction	Recovery & Purification	sum
Analyze the contributions to the environmental impact (kg _{CO2eq} /h)					
Ethylene	9.10E+02	3.53E+01	-	-	9.45E+02
CO	5.81E+03	5.50E+01	-	-	5.87E+03
N ₂	3.68E+00	2.45E+01	-	-	2.81E+01
O ₂	3.15E+00	2.43E+01	-	-	2.74E+01
Water	-	-	1.89E-01	-	1.89E-01
Wastewater	-	-	-	4.07E-01	4.07E-01
CO ₂	-	-	-	1.20E+03	1.20E+03
Steam	-	-	-	5.00E+01	5.00E+01
Cooling water	-	-	-	4.88E+01	4.88E+01
Electricity	-	-	-	1.45E-01	1.45E-01
sum	6.73E+03	1.39E+02	1.89E-01	1.30E+03	8.16E+03

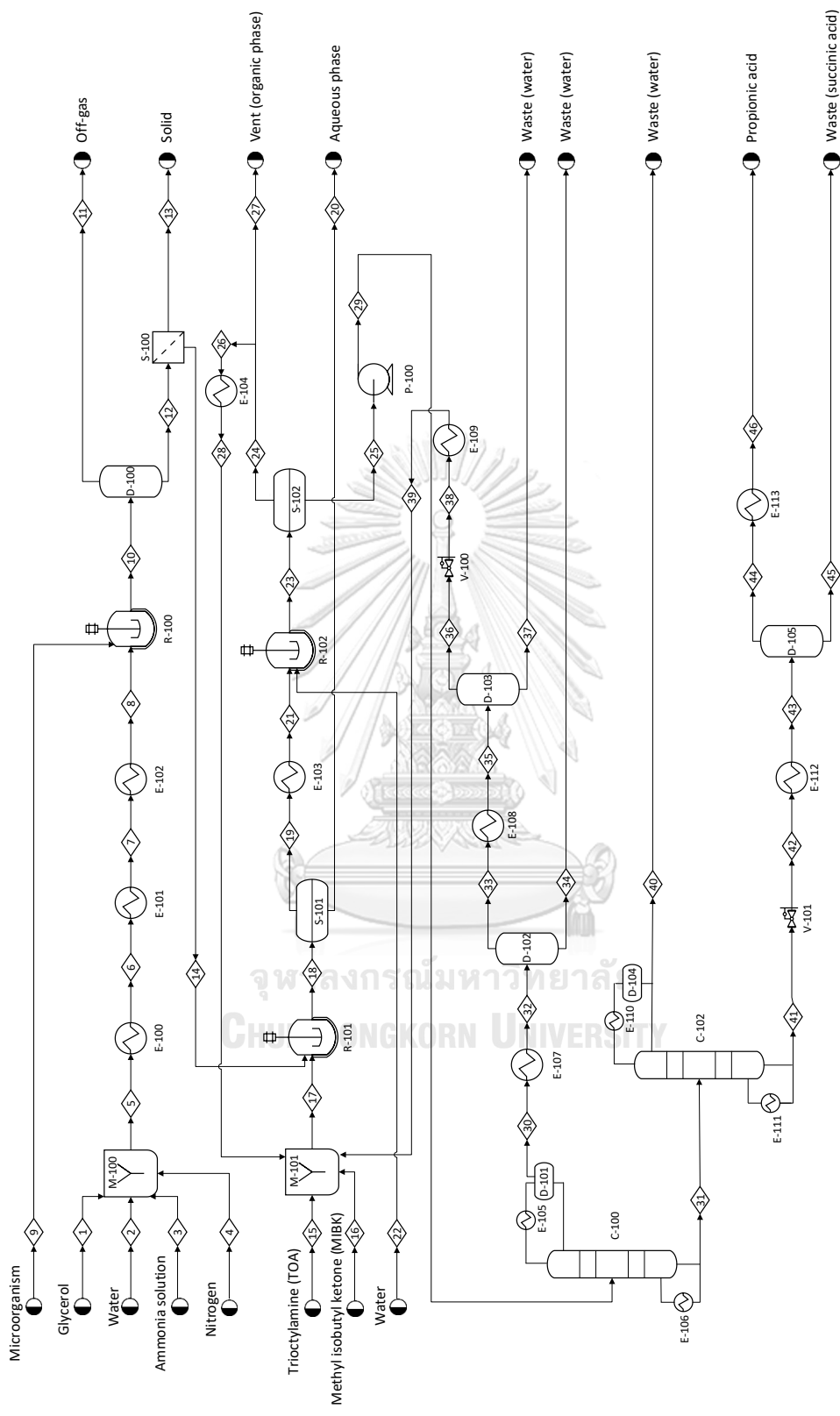


Figure B1 Process flow diagram of scenario I (extractant: TOA, diluent: MIBK and back-extraction: temperature-swing regeneration)

Table B5 Description of unit operation in Scenario I (extractant: TOA, diluent: MIBK, back-extraction: temperature-swing)

Unit	Process Description	Equipment type	Model	Operating Conditions	Design comment
M-100	Liquid mixing tank	Agitated tank-enclosed	Mixer	Pressure drop: 0 atm	
E-100	Sterilization	Fixed tube sheet heat exchanger	Heater	Outlet temperature: 121°C Pressure drop: 0 atm	- Conditions based on the work of Dishisha et al. [178]
E-101	Feedstock cooler	Fixed tube sheet heat exchanger	Heater	Outlet temperature: 100°C Pressure drop: 0 atm	- The cost of equipment, installation and utilities are calculated to determine the optimal temperature.
E-102	Feedstock cooler	Fixed tube sheet heat exchanger	Heater	Outlet temperature: 32°C Pressure drop: 0 atm	- The cost of equipment, installation and utilities are calculated to determine the optimal temperature.
R-100	Fermentation	Agitated tank-enclosed and jacketed	RStoic	Temperature: 32°C Pressure drop: 0 atm Reaction: GLY + 0.042 NH ₃ → 0.640 PA + 0.040 AA + 0.060 SA + 0.080 Propanol + 0.209 MICROOR + 0.784 H ₂ + 0.311 CO ₂ + 0.592 H ₂ O (100% conversion of glycerol)	- The reactor operates isothermally ($\Delta T > 15\%$ of T_{inlet}). - Reaction based on the work of Dishisha et al. [178] and Gargalo et al. [201]
D-100	Gas separation	Vertical process vessel	Flash2	Pressure drop: 0 atm Duty: 0	
S-100	Microorganism removal	Tubular cross-flow filter	CFilter	Pressure drop: 0 atm Solids to solid outlet: 1 Liquid load of solids outlet: 0.3	- Conditions based on the work of Nieder-Heitmann [154]
M-101	Liquid mixing tank	Agitated tank-enclosed	Mixer	Pressure drop: 0 atm	
R-101	Reactive extraction	Agitated tank-enclosed	RStoic	Temperature: 32°C	- Conditions based on the work of Keshav

Unit	Process Description	Equipment type	Model	Operating Conditions	Design comment
		and jacketed		Pressure drop: 0 atm Reaction: PA + TOA \rightarrow PA-TOA (73.49% conversion of PA)	[181] - Iterative calculation is performed until the results match with the experimental data.
S-101	Reactive extraction	Vertical process vessel	Sep	Split fraction: H ₂ O = 0.981 NH ₃ = 0.626 N ₂ = 0.655 PA = 0.508 SA = 0.895 AA = 0.751 Propanol = 0.457 CO ₂ = 0.432 H ₂ = 0.704 TOA = 6.23E-11 MIBK = 0.024 PA-TOA = 3.67E-11	- The decanter model is used in the simulation. - Recovery data is performed based on the work of Keshav [181]
E-103	Organic phase heater	Fixed tube sheet heat exchanger	Heater	Outlet temperature: 90°C Pressure drop: 0 atm	- Temperature based on the work of Keshav & Wasewar [39]
R-102	Back-extraction	Agitated tank-enclosed and jacketed	RStoic	Temperature: 90°C Pressure drop: 0 atm Reaction: PA-TOA \rightarrow PA + TOA (100% conversion of PA-TOA)	- Temperature based on the work of Keshav & Wasewar [39] - Assumption: 100% conversion
E-104	Organic phase cooler	Fixed tube sheet heat	Heater	Outlet temperature: 32°C	

Unit	Process Description	Equipment type	Model	Operating Conditions	Design comment
S-102	Back-extraction	Vertical process vessel	Sep	Pressure drop: 0 atm $H_2O = 0.995$ $NH_3 = 0.883$ $N_2 = 0.898$ $PA = 0.880$ $SA = 0.972$ $AA = 0.932$ $Propanol = 0.815$ $CO_2 = 0.800$ $H_2 = 0.9113$ $TOA = 6.02E-09$ $MIBK = 0.029$	<ul style="list-style-type: none"> The decanter model is used in the simulation. Recovery data is performed based on the work of Keshav & Wasewar [39]
P-100	Pump	Centrifugal pump	Pump	Outlet pressure: 2.5 atm	
C-100	Water separation	Distillation column (Partial condenser)	RadFrac	1 st stage pressure: 2 atm pressure drop: 0.5 atm Number of stages: 17 Feed stage: 9 Condenser: Partial-vapor Reboiler: Kettle Distillate rate: 10,355.7 kg/h Molar reflux ratio: 0.561	<ul style="list-style-type: none"> Flash model was used to determine the bubble point pressure. The shortcut distillation model (DSTWU) was used for preliminary specifications. The optimum distillate rate and molar reflux ratio were obtained from the design spec.
E-107	Distillate cooler	Fixed tube sheet heat exchanger	Heater	Outlet temperature: 115°C Pressure drop: 0 atm	Temperature was obtained from the design spec to find the optimum MIBK removal.
D-102	MIBK separation	Vertical process vessel	Flash2	Pressure drop: 0 atm	

Unit		Process Description		Equipment type		Model		Operating Conditions		Design comment	
E-108	MIBK cooler	U-tube exchanger	Heater					Duty: 0 Outlet temperature: 105°C Pressure drop: 0 atm	Temperature was obtained from the design spec to find the optimum MIBK removal.		
D-103	MIBK separation	Vertical process vessel	Flash2					Pressure drop: 0 atm Duty: 0			
V-100	Valve	Pressure reducing valve	Valve					Outlet pressure: 1 atm			
E-109	MIBK cooler	U-tube exchanger	Heater					Outlet temperature: 32°C Pressure drop: 0 atm			
C-102	Water separation	Distillation column (Total condenser)	RadFrac					1 st stage pressure: 2 atm pressure drop: 0.5 atm Number of stages: 16 Feed stage: 9 Condenser: Total Reboiler: Kettle Distillate rate: 55.87 kg/h Molar reflux ratio: 9.93	<ul style="list-style-type: none"> - Flash model was used to determine the bubble point pressure. - The shortcut distillation model (DSTWU) was used for preliminary specifications. The optimum distillate rate and molar reflux ratio were obtained from the design spec.		
V-101	Valve	Pressure reducing valve	Valve					Outlet pressure: 1 atm			
E-112	Bottom product heater	U-tube exchanger	Heater					Outlet temperature: 171°C Pressure drop: 0 atm	Temperature was obtained from the design spec.		
D-105	Succinic acid separation	Vertical process vessel	Flash2					Pressure drop: 0 atm Duty: 0			
E-113	Product cooler	U-tube exchanger	Heater					Outlet temperature: 50°C Pressure drop: 0 atm			

Table B6 Stream table of process in Scenario I (extractant: TOA, diluent: MIBK, back-extraction: temperature-swing)

Stream	1	2	3	4	5	6	7	8	9	10
Temperature (°C)	32.0	32.0	32.0	32.0	32.2	121.0	90.0	32.0	32.0	32.0
Pressure (atm)	1.0	1.0	1.0	1.0	1.0	1.0	1.0	1.0	1.0	1.0
Mass vapor fraction	0.000	0.000	0.244	1.000	0.000	0.952	0.001	0.000	0.000	0.005
Total flow (kg/h)	3.22E+03	6.19E+04	7.46E+01	4.02E+01	6.52E+04	6.52E+04	6.52E+04	6.52E+04	9.46E+00	6.52E+04
Component Mass Fractions										
Glycerol	0.840	0.000	0.000	0.000	0.041	0.041	0.041	0.041	0.000	0.000
H ₂ O	0.120	1.000	0.720	0.000	0.956	0.956	0.956	0.956	0.000	0.960
NH ₃	0.000	0.000	0.280	0.000	0.000	0.000	0.000	0.000	0.000	0.000
N ₂	0.000	0.000	0.000	1.000	0.001	0.001	0.001	0.001	0.000	0.001
Propionic acid	0.000	0.000	0.000	0.000	0.000	0.000	0.000	0.000	0.000	0.021
Succinic acid	0.000	0.000	0.000	0.000	0.000	0.000	0.000	0.000	0.000	0.003
Acetic acid	0.000	0.000	0.000	0.000	0.000	0.000	0.000	0.000	0.000	0.001
Propanol	0.000	0.000	0.000	0.000	0.000	0.000	0.000	0.000	0.000	0.002
CO ₂	0.000	0.000	0.000	0.000	0.000	0.000	0.000	0.000	0.000	0.006
H ₂	0.000	0.000	0.000	0.000	0.000	0.000	0.000	0.000	0.000	0.001
TOA	0.000	0.000	0.000	0.000	0.000	0.000	0.000	0.000	0.000	0.000
MIBK	0.000	0.000	0.000	0.000	0.000	0.000	0.000	0.000	0.000	0.000
TMA	0.000	0.000	0.000	0.000	0.000	0.000	0.000	0.000	0.000	0.000
PA-TOA	0.000	0.000	0.000	0.000	0.000	0.000	0.000	0.000	0.000	0.000
PA-TMA	0.000	0.000	0.000	0.000	0.000	0.000	0.000	0.000	0.000	0.000
Tripalmitin	0.020	0.000	0.000	0.000	0.001	0.001	0.001	0.001	0.000	0.001
NaCl	0.020	0.000	0.000	0.000	0.001	0.001	0.001	0.001	0.000	0.001
Microorganism	0.000	0.000	0.000	0.000	0.000	0.000	0.000	0.000	1.000	0.002

Table B6 Stream table of process in Scenario I (extractant: TOA, diluent: MIBK, back-extraction: temperature-swing) (cont.)

Stream	41	42	43	44	45	46
Temperature (°C)	173.3	141.5	171.0	171.0	171.0	50.0
Pressure (atm)	2.5	1	1	1	1	1
Mass vapor fraction	0.000	0.139	0.978	1.000	0.000	0.000
Total flow (kg/h)	1.17E+03	1.17E+03	1.17E+03	1.14E+03	2.54E+01	1.14E+03
Component Mass Fractions						
Glycerol	0.000	0.0000	0.0000	0.0000	0.0000	0.0000
H ₂ O	0.000	0.0000	0.0000	0.0000	0.0000	0.0000
NH ₃	0.000	0.0000	0.0000	0.0000	0.0000	0.0000
N ₂	0.000	0.0000	0.0000	0.0000	0.0000	0.0000
Propionic acid	0.980	0.9800	0.9800	0.9951	0.2985	0.9951
Succinic acid	0.018	0.0183	0.0183	0.0031	0.7012	0.0031
Acetic acid	0.002	0.0017	0.0017	0.0017	0.0004	0.0017
Propanol	0.000	0.0000	0.0000	0.0000	0.0000	0.0000
CO ₂	0.000	0.0000	0.0000	0.0000	0.0000	0.0000
H ₂	0.000	0.0000	0.0000	0.0000	0.0000	0.0000
TOA	0.000	0.0000	0.0000	0.0000	0.0000	0.0000
MIBK	0.000	0.0000	0.0000	0.0000	0.0000	0.0000
TMA	0.000	0.0000	0.0000	0.0000	0.0000	0.0000
PA-TOA	0.000	0.0000	0.0000	0.0000	0.0000	0.0000
PA-TMA	0.000	0.0000	0.0000	0.0000	0.0000	0.0000
Tripalmitin	0.000	0.0000	0.0000	0.0000	0.0000	0.0000
NaCl	0.000	0.0000	0.0000	0.0000	0.0000	0.0000
Microorganism	0.000	0.0000	0.0000	0.0000	0.0000	0.0000

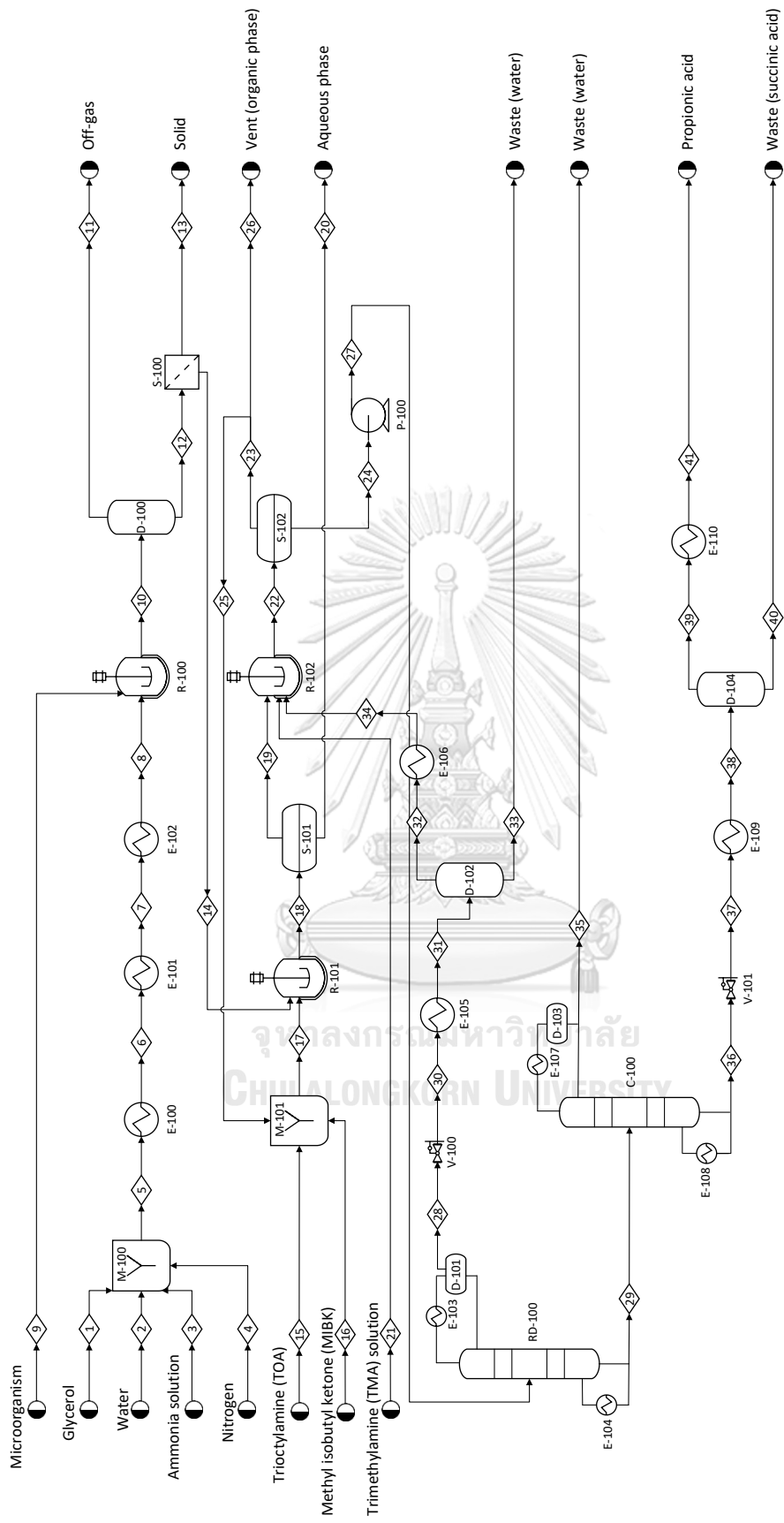


Figure B2 Process flow diagram of scenario II (extractant: TOA, diluent: MIBK and back-extraction: utilization of TMA)

Table B7 Description of unit operation in Scenario II (extractant: TOA, diluent: MIBK, back-extraction: utilization of TMA)

Unit	Process Description	Equipment type	Unit Model	Operating Conditions	Design comment
M-100	Liquid mixing tank	Agitated tank-enclosed	Mixer	Pressure drop: 0 atm	
E-100	Sterilization	Fixed tube sheet heat exchanger	Heater	Outlet temperature: 121°C Pressure drop: 0 atm	- Conditions based on the work of Dishisha et al. [178]
E-101	Feedstock cooler	Fixed tube sheet heat exchanger	Heater	Outlet temperature: 90°C Pressure drop: 0 atm	- The cost of equipment, installation and utilities are calculated to determine the optimal temperature.
E-102	Feedstock cooler	Fixed tube sheet heat exchanger	Heater	Outlet temperature: 32°C Pressure drop: 0 atm	- The cost of equipment, installation and utilities are calculated to determine the optimal temperature.
R-100	Fermentation	Agitated tank-enclosed and jacketed	RStoic	Temperature: 32°C Pressure drop: 0 atm Reaction: GLY + 0.042 NH ₃ → 0.640 PA + 0.040 AA + 0.060 SA + 0.080 Propanol + 0.209 MICROOR + 0.784 H ₂ + 0.311 CO ₂ + 0.592 H ₂ O (100% conversion of glycerol)	- The reactor operates isothermally ($\Delta T > 15\%$ of T_{inlet}). - Reaction based on the work of Dishisha et al. [178] and Gargalo et al. [201]
D-100	Gas separation	Vertical process vessel	Flash2	Pressure drop: 0 atm Duty: 0	
S-100	Microorganism removal	Tubular cross-flow filter	CFilter	Pressure drop: 0 atm Solids to solid outlet: 1 Liquid load of solids outlet: 0.3	- Conditions based on the work of Nieder-Heitmann [154]
M-101	Liquid mixing tank	Agitated tank-enclosed	Mixer	Pressure drop: 0 atm	
R-101	Reactive extraction	Agitated tank-enclosed and	RStoic	Temperature: 32°C	- Conditions based on the work of Keshav

Unit	Process Description	Equipment type	Unit Model	Operating Conditions	Design comment
S-101	Reactive extraction	jacketed Vertical process vessel	Sep	Pressure drop: 0 atm Reaction: PA + TOA → PA-TOA (70.91% conversion of PA) Split fraction: H ₂ O = 0.981 NH ₃ = 0.626 N ₂ = 0.655 PA = 0.508 SA = 0.895 AA = 0.751 Propanol = 0.457 CO ₂ = 0.432 H ₂ = 0.704 TOA = 6.23E-11 MIBK = 0.024 PA-TOA = 3.67E-11	[181] - Iterative calculation is performed until the results match with the experimental data. - The decanter model is used in the simulation. - Recovery data is performed based on the work of Keshav [181]
R-102	Back-extraction	Agitated tank-enclosed and jacketed	RStoic	Temperature: 32°C Pressure drop: 0 atm Reaction: PA-TOA + TMA → PA-TMA + TOA (100% conversion of PA-TOA)	- Temperature based on the work of Keshav & Wasewar [39] - Assumption: 100% conversion
S-102	Back-extraction	Vertical process vessel	Sep	Split fraction: H ₂ O = 0.971 NH ₃ = 0.820	- The decanter model is used in the simulation. - Recovery data is performed based on the

Unit	Process Description	Equipment type	Unit Model	Operating Conditions	Design comment
P-100	Pump	Centrifugal pump	Pump	N ₂ = 0.839 PA = 0.891 SA = 0.979 AA = 0.926 Propanol = 0.907 CO ₂ = 0.765 H ₂ = 0.840 TOA = 9.73E-11 MIBK = 0.002 TMA = 0.918 PA-TMA = 0.994 Outlet pressure: 2.5 atm	work of Keshav & Wasewar [39]
RD-100	Water separation	Distillation column (Partial condenser)	RadFrac	1 st stage pressure: 2 atm pressure drop: 0.5 atm Number of stages: 17 Feed stage: 9 Condenser: Partial-vapor Reboiler: Kettle Distillate rate: 4,535.9 kg/h Molar reflux ratio: 0.601 Reaction: PA-TMA → PA + TMA (100% conversion of PA-TMA)	<ul style="list-style-type: none"> - Flash model was used to determine the bubble point pressure. - The shortcut distillation model (DSTWU) was used for preliminary specifications. - The optimum distillate rate and molar reflux ratio were obtained from the design spec. - Assumption: 100% conversion
V-100	Valve	Pressure reducing valve	Valve	Outlet pressure: 1 atm	
E-105	Distillate cooler	U-tube exchanger	Heater	Outlet temperature: 85.74°C	Temperature was obtained from the design

Unit		Process Description		Equipment type		Unit Model		Operating Conditions		Design comment
D-102	Trimethylamine separation	Vertical process vessel	Flash2	Pressure drop: 0 atm				spec.		
E-106	Trimethylamine cooler	Fixed tube sheet heat exchanger	Heater	Outlet temperature: 32°C Pressure drop: 0 atm						
C-100	Water separation	Distillation column (Total condenser)	RadFrac	1 st stage pressure: 2 atm pressure drop: 0.5 atm Number of stages: 19 Feed stage: 10 Condenser: Total Reboiler: Kettle Distillate rate: 684.5 kg/h Molar reflux ratio: 0.807 Reaction: PA-TMA → PA + TMA (100% conversion of PA-TMA)					<ul style="list-style-type: none"> - Flash model was used to determine the bubble point pressure. - The shortcut distillation model (DSTWU) was used for preliminary specifications. - The optimum distillate rate and molar reflux ratio were obtained from the design spec. Assumption: 100% conversion 	
V-101	Valve	Pressure reducing valve	Valve	Outlet pressure: 1 atm						
E-109	Bottom product heater	U-tube exchanger	Heater	Outlet temperature: 170.3°C Pressure drop: 0 atm				Temperature was obtained from the design spec.		
D-104	Succinic acid separation	Vertical process vessel	Flash2	Pressure drop: 0 atm Duty: 0						
E-110	Product cooler	U-tube exchanger	Heater	Outlet temperature: 50°C Pressure drop: 0 atm						

Table B8 Stream table of process in Scenario II (extractant: TOA, diluent: MIBK, back-extraction: utilization of TMA)

Stream	1	2	3	4	5	6	7	8	9	10
Temperature (°C)	32.0	32.0	32.0	32.0	32.2	121.0	90.0	32.0	32.0	32.0
Pressure (atm)	1.0	1.0	1.0	1.0	1.0	1.0	1.0	1.0	1.0	1.0
Mass vapor fraction	0.000	0.000	0.244	1.000	0.000	0.952	0.001	0.000	0.000	0.005
Total flow (kg/h)	3.14E+03	6.05E+04	7.29E+01	3.93E+01	6.37E+04	6.37E+04	6.37E+04	6.37E+04	9.24E+00	6.37E+04
Component Mass Fractions										
Glycerol	0.840	0.000	0.000	0.000	0.041	0.041	0.041	0.041	0.000	0.000
H ₂ O	0.120	1.000	0.720	0.000	0.956	0.956	0.956	0.956	0.000	0.960
NH ₃	0.000	0.000	0.280	0.000	0.000	0.000	0.000	0.000	0.000	0.000
N ₂	0.000	0.000	0.000	1.000	0.001	0.001	0.001	0.001	0.000	0.001
Propionic acid	0.000	0.000	0.000	0.000	0.000	0.000	0.000	0.000	0.000	0.021
Succinic acid	0.000	0.000	0.000	0.000	0.000	0.000	0.000	0.000	0.000	0.003
Acetic acid	0.000	0.000	0.000	0.000	0.000	0.000	0.000	0.000	0.000	0.001
Propanol	0.000	0.000	0.000	0.000	0.000	0.000	0.000	0.000	0.000	0.002
CO ₂	0.000	0.000	0.000	0.000	0.000	0.000	0.000	0.000	0.000	0.006
H ₂	0.000	0.000	0.000	0.000	0.000	0.000	0.000	0.000	0.000	0.001
TOA	0.000	0.000	0.000	0.000	0.000	0.000	0.000	0.000	0.000	0.000
MIBK	0.000	0.000	0.000	0.000	0.000	0.000	0.000	0.000	0.000	0.000
TMA	0.000	0.000	0.000	0.000	0.000	0.000	0.000	0.000	0.000	0.000
PA-TOA	0.000	0.000	0.000	0.000	0.000	0.000	0.000	0.000	0.000	0.000
PA-TMA	0.000	0.000	0.000	0.000	0.000	0.000	0.000	0.000	0.000	0.000
Tripalmitin	0.020	0.000	0.000	0.000	0.001	0.001	0.001	0.001	0.000	0.001
NaCl	0.020	0.000	0.000	0.000	0.001	0.001	0.001	0.001	0.000	0.001
Microorganism	0.000	0.000	0.000	0.000	0.000	0.000	0.000	0.000	1.000	0.002

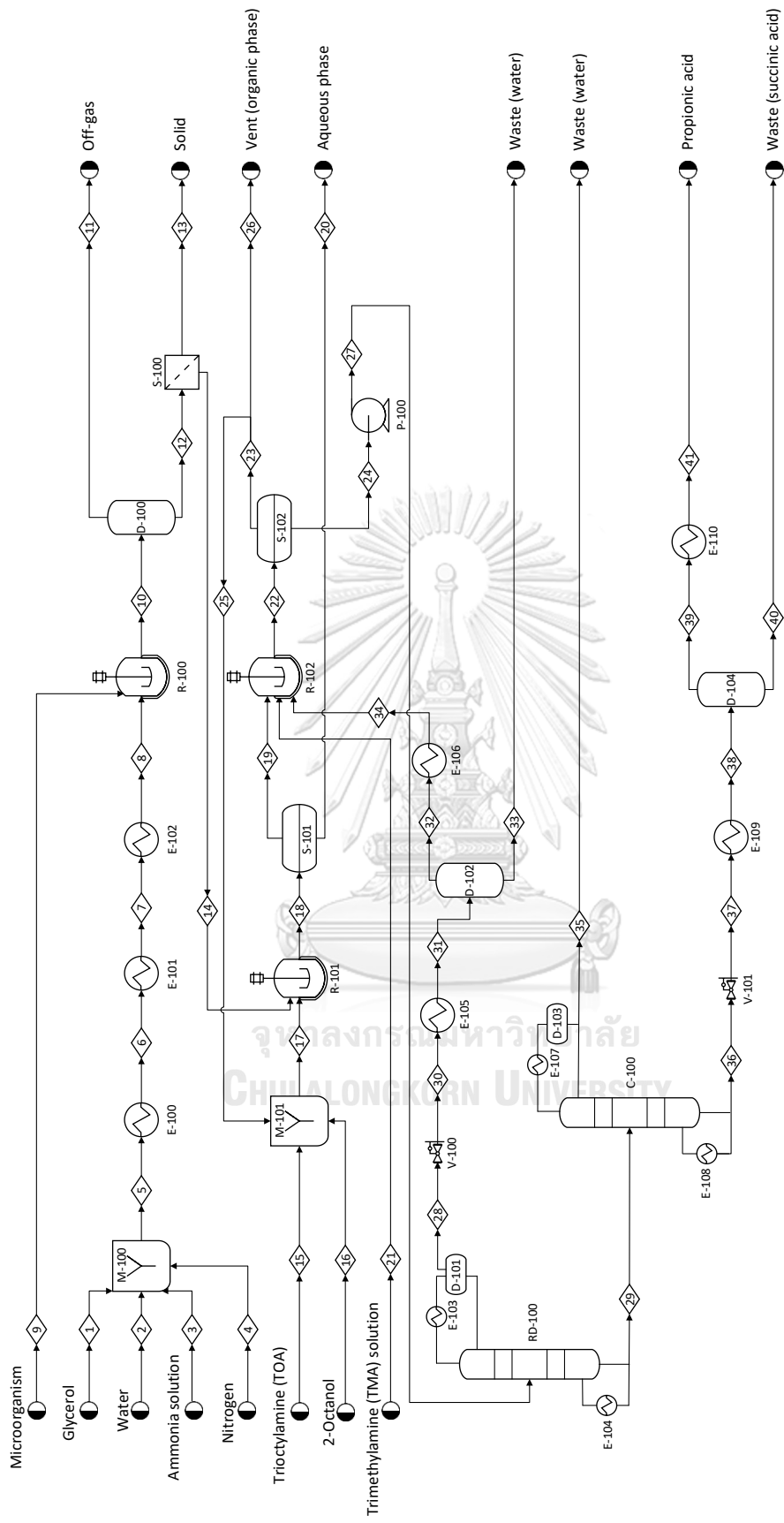


Figure B3 Process flow diagram of scenario III (extractant: TOA, diluent: 2-octanol and back-extraction: utilization of TMA)

Table B9 Description of unit operation in Scenario III (extractant: TOA, diluent: 2-octanol, back-extraction: utilization of TMA)

Unit		Process Description		Equipment type		Model		Operating Conditions		Design comment
M-100	Liquid mixing tank	Agitated tank-enclosed	Mixer	Pressure drop: 0 atm						- Conditions based on the work of Dishisha et al. [178]
E-100	Sterilization	Fixed tube sheet heat exchanger	Heater	Outlet temperature: 121°C Pressure drop: 0 atm						- The cost of equipment, installation and utilities are calculated to determine the optimal temperature.
E-101	Feedstock cooler	Fixed tube sheet heat exchanger	Heater	Outlet temperature: 90°C Pressure drop: 0 atm						- The cost of equipment, installation and utilities are calculated to determine the optimal temperature.
E-102	Feedstock cooler	Fixed tube sheet heat exchanger	Heater	Outlet temperature: 32°C Pressure drop: 0 atm						- The cost of equipment, installation and utilities are calculated to determine the optimal temperature.
R-100	Fermentation	Agitated tank-enclosed and jacketed	RStoic	Temperature: 32°C Pressure drop: 0 atm Reaction: GLY + 0.042 NH ₃ → 0.640 PA + 0.040 AA + 0.060 SA + 0.080 Propanol + 0.209 MICROOR + 0.784 H ₂ + 0.311 CO ₂ + 0.592 H ₂ O (100% conversion of glycerol)						- The reactor operates isothermally ($\Delta T > 15\%$ of T_{inlet}). - Reaction based on the work of Dishisha et al. [178] and Gargalo et al. [201]
D-100	Gas separation	Vertical process vessel	Flash2	Pressure drop: 0 atm Duty: 0						
S-100	Microorganism removal	Tubular cross-flow filter	CFFilter	Pressure drop: 0 atm Solids to solid outlet: 1 Liquid load of solids outlet: 0.3						- Conditions based on the work of Nieder-Heitmann [154]
M-101	Liquid mixing tank	Agitated tank-enclosed	Mixer	Pressure drop: 0 atm						
R-101	Reactive extraction	Agitated tank-enclosed and jacketed	RStoic	Temperature: 32°C Pressure drop: 0 atm Reaction:						- Conditions based on the work of Keshav [181] - Iterative calculation is performed until the results match with the experimental data.

Unit	Process Description	Equipment type	Model	Operating Conditions	Design comment
S-101	Reactive extraction	Vertical process vessel	Sep	PA + TOA \rightarrow PA-TOA (87.10% conversion of PA) Split fraction: H ₂ O = 0.969 NH ₃ = 0.574 N ₂ = 0.598 PA = 0.514 SA = 0.893 AA = 0.740 Propanol = 0.356 CO ₂ = 0.383 H ₂ = 0.656 TOA = 2.54E-10 OCTANOL = 0.004 PA-TOA = 1.78E-10	<ul style="list-style-type: none"> - The decanter model is used in the simulation. - Recovery data is performed based on the work of Keshav [181]
R-102	Back-extraction	Agitated tank-enclosed and jacketed	RStoic	Temperature: 32°C Pressure drop: 0 atm Reaction: PA-TOA + TMA \rightarrow PA-TMA + TOA (100% conversion of PA-TOA)	<ul style="list-style-type: none"> - Temperature based on the work of Keshav & Wasewar [39] - Assumption: 100% conversion
S-102	Back-extraction	Vertical process vessel	Sep	Split fraction: H ₂ O = 0.956 NH ₃ = 0.828 N ₂ = 0.844 PA = 0.851 SA = 0.962 AA = 0.906	<ul style="list-style-type: none"> - The decanter model is used in the simulation. - Recovery data is performed based on the work of Keshav & Wasewar [39]

Unit	Process Description	Equipment type	Model	Operating Conditions	Design comment
P-100	Pump	Centrifugal pump	Pump	Propanol = 0.806 CO ₂ = 0.763 H ₂ = 0.851 TOA = 3.96E-05 OCTANOL = 3.22E-04 TMA = 0.837 PA-TMA = 0.960 Outlet pressure: 2.5 atm	
RD-100	Water separation	Distillation column (Partial condenser)	RadFrac	1 st stage pressure: 2 atm pressure drop: 0.5 atm Number of stages: 17 Feed stage: 9 Condenser: Partial-vapor Reboiler: Kettle Distillate rate: 5,276.1 kg/h Molar reflux ratio: 0.608 Reaction: PA-TMA → PA + TMA (100% conversion of PA-TMA)	<ul style="list-style-type: none"> - Flash model was used to determine the bubble point pressure. - The shortcut distillation model (DSTWU) was used for preliminary specifications. - The optimum distillate rate and molar reflux ratio were obtained from the design spec.
V-100	Valve	Pressure reducing valve	Valve	Outlet pressure: 1 atm	
E-105	Distillate cooler	Fixed tube sheet heat exchanger	Heater	Outlet temperature: 88°C Pressure drop: 0 atm	<ul style="list-style-type: none"> - Temperature was obtained from the design spec.
D-102	Trimethylamine separation	Vertical process vessel	Flash2	Pressure drop: 0 atm Duty: 0	
E-106	Trimethylamine cooler	Fixed tube sheet heat exchanger	Heater	Outlet temperature: 32°C Pressure drop: 0 atm	

Unit	Process Description	Equipment type	Model	Operating Conditions	Design comment
C-100	Water separation	Distillation column (Total condenser)	RadFrac	1 st stage pressure: 2 atm pressure drop: 0.5 atm Number of stages: 19 Feed stage: 10 Condenser: Total Reboiler: Kettle Distillate rate: 746.5 kg/h Molar reflux ratio: 0.786 Reaction: PA-TMA → PA + TMA (100% conversion of PA-TMA)	<ul style="list-style-type: none"> - Flash model was used to determine the bubble point pressure. - The shortcut distillation model (DSTWU) was used for preliminary specifications. - The optimum distillate rate and molar reflux ratio were obtained from the design spec. Assumption: 100% conversion
V-101	Valve	Pressure reducing valve	Valve	Outlet pressure: 1 atm	
E-109	Bottom product heater	U-tube exchanger	Heater	Outlet temperature: 164.8°C Pressure drop: 0 atm	Temperature was obtained from the design spec.
D-104	Succinic acid separation	Vertical process vessel	Flash2	Pressure drop: 0 atm Duty: 0	
E-110	Product cooler	U-tube exchanger	Heater	Outlet temperature: 50°C Pressure drop: 0 atm	

Table B10 Stream table of process in Scenario III (extractant: TOA, diluent: 2-octanol, back-extraction: utilization of TMA)

Stream	1	2	3	4	5	6	7	8	9	10
Temperature (°C)	32.0	32.0	32.0	32.0	32.2	121.0	90.0	32.0	32.0	32.0
Pressure (atm)	1.0	1.0	1.0	1.0	1.0	1.0	1.0	1.0	1.0	1.0
Mass vapor fraction	0.000	0.000	0.244	1.000	0.000	0.952	0.001	0.000	0.000	0.005
Total flow (kg/h)	2.97E+03	5.71E+04	6.88E+01	3.71E+01	6.02E+04	6.02E+04	6.02E+04	6.02E+04	8.72E+00	6.02E+04
Component Mass Fractions										
Glycerol	0.840	0.000	0.000	0.000	0.041	0.041	0.041	0.041	0.000	0.000
H ₂ O	0.120	1.000	0.720	0.000	0.956	0.956	0.956	0.956	0.000	0.960
NH ₃	0.000	0.000	0.280	0.000	0.000	0.000	0.000	0.000	0.000	0.000
N ₂	0.000	0.000	0.000	1.000	0.001	0.001	0.001	0.001	0.000	0.001
Propionic acid	0.000	0.000	0.000	0.000	0.000	0.000	0.000	0.000	0.000	0.021
Succinic acid	0.000	0.000	0.000	0.000	0.000	0.000	0.000	0.000	0.000	0.003
Acetic acid	0.000	0.000	0.000	0.000	0.000	0.000	0.000	0.000	0.000	0.001
Propanol	0.000	0.000	0.000	0.000	0.000	0.000	0.000	0.000	0.000	0.002
CO ₂	0.000	0.000	0.000	0.000	0.000	0.000	0.000	0.000	0.000	0.006
H ₂	0.000	0.000	0.000	0.000	0.000	0.000	0.000	0.000	0.000	0.001
TOA	0.000	0.000	0.000	0.000	0.000	0.000	0.000	0.000	0.000	0.000
Octanol	0.000	0.000	0.000	0.000	0.000	0.000	0.000	0.000	0.000	0.000
TMA	0.000	0.000	0.000	0.000	0.000	0.000	0.000	0.000	0.000	0.000
PA-TOA	0.000	0.000	0.000	0.000	0.000	0.000	0.000	0.000	0.000	0.000
PA-TMA	0.000	0.000	0.000	0.000	0.000	0.000	0.000	0.000	0.000	0.000
Tripalmitin	0.020	0.000	0.000	0.000	0.001	0.001	0.001	0.001	0.000	0.001
NaCl	0.020	0.000	0.000	0.000	0.001	0.001	0.001	0.001	0.000	0.001
Microorganism	0.000	0.000	0.000	0.000	0.000	0.000	0.000	0.000	1.000	0.002

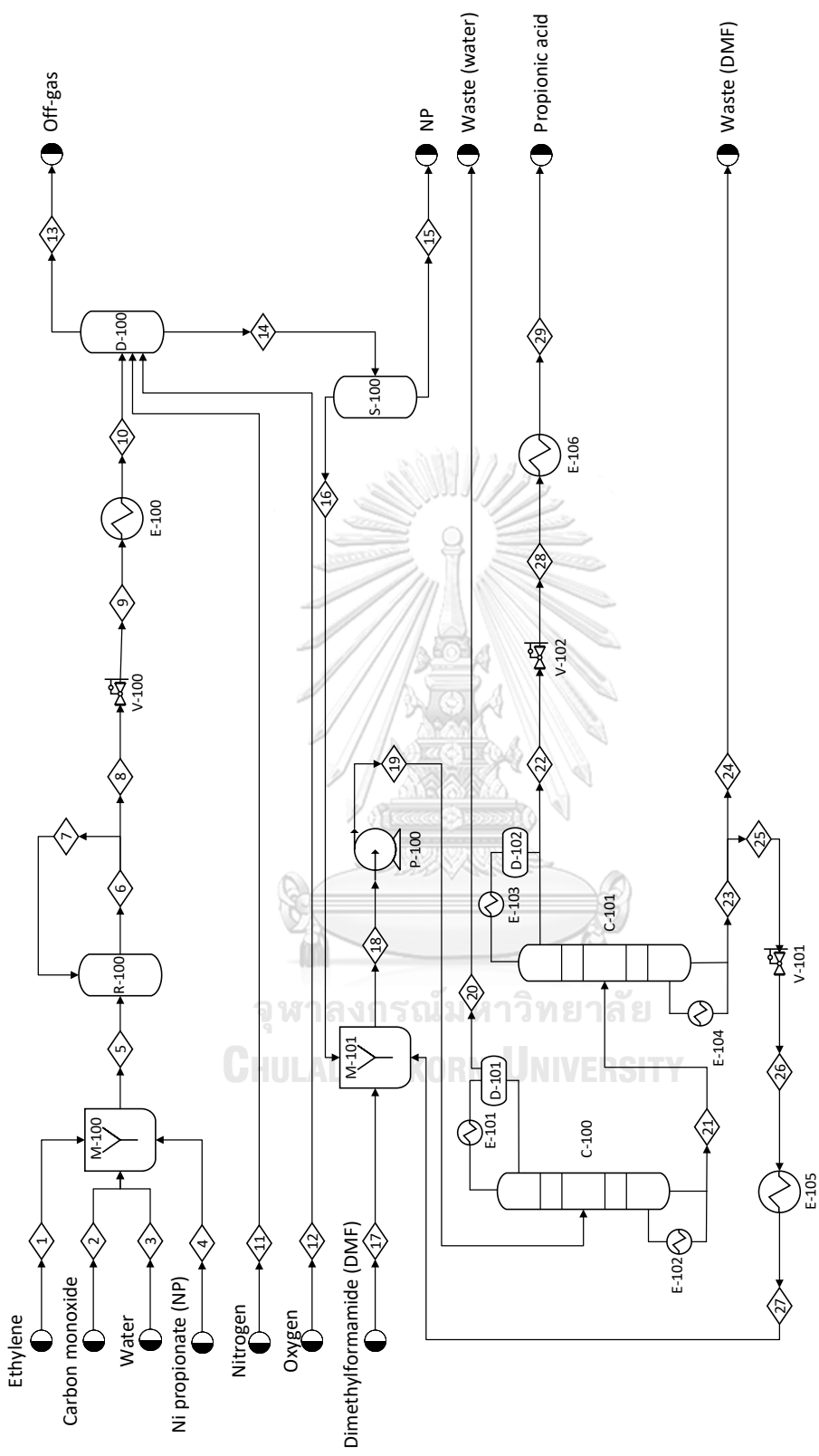


Figure B4 Process flow diagram of scenario IV (propionic acid production using the petroleum-based feedstock)

Table B11 Description of unit operation in Scenario IV (production of PA using petroleum-based feedstock)

Unit	Process Description	Equipment type	Model	Operating Conditions	Design comment
M-100	Gas mixing	Vertical process vessel	Mixer	Pressure drop: 0 atm Temperature: 285°C Pressure drop: 0 atm Reaction: NP + 5CO + H ₂ O → NC + 2PA + CO ₂ (42.36% conversion of NP) Ethylene + CO + H ₂ O → PA (92.95% conversion of ethylene) Ethylene + H ₂ → Ethane (3.66% conversion of ethylene) 2Ethylene + H ₂ + CO → Ketone (1.40% conversion of ethylene) H ₂ O + CO → CO ₂ + H ₂ (5.87% conversion of H ₂ O) H ₂ O + Ethylene → Ethanol (0.036% conversion of ethylene) Ethanol + PA → Ester + H ₂ O (100% conversion of ethanol)	- The reactor operates isothermally ($\Delta T > 15\%$ of T_{inlet}). - Reactions based on the work of Cornils et al. [202] and Hohenschutz et al. [183] - Conversion of water-gas shift reaction was obtained from the design spec.
R-100	Carbonylation	Agitated tank-enclosed and jacketed	RStoic		
V-100	Valve	Pressure reducing valve	Valve	Outlet pressure: 2 atm	
E-100	Cooler	U-tube exchanger	Heater	Outlet temperature: 80°C Pressure drop: 0 atm	- Conditions based on the work of Hohenschutz et al. [184]
D-100	Catalyst separation	Vertical process vessel	Flash2	Pressure drop: 0 atm Duty: 0	
S-100	Solid separation	Vertical process vessel	Sep	Split fraction: 100% NP removal	- Assumption: 100% removal
M-101	Liquid mixing tank	Agitated tank-enclosed	Mixer	Pressure drop: 0 atm	
P-100	Pump	Centrifugal pump	Pump	Outlet pressure: 2.5 atm	

Unit	Process Description	Equipment type	Model	Operating Conditions	Design comment
C-100	Water separation	Distillation column (Partial condenser)	RadFrac	<p>1st stage pressure: 2 atm pressure drop: 0.5 atm Number of stages: 16 Feed stage: 8 Condenser: Partial-vapor Reboiler: Kettle Distillate rate: 216.89 kg/h Molar reflux ratio: 1.84</p>	<ul style="list-style-type: none"> - Flash model was used to determine the bubble point pressure. - The shortcut distillation model (DSTWU) was used for preliminary specifications. - The optimum distillate rate and molar reflux ratio were obtained from the design spec.
C-101	Dimethylformamide separation	Distillation column (Total condenser)	RadFrac	<p>1st stage pressure: 2 atm pressure drop: 0.5 atm Number of stages: 49 Feed stage: 27 Condenser: Total Reboiler: Kettle Distillate rate: 1,140.8 kg/h Molar reflux ratio: 13.90</p>	<ul style="list-style-type: none"> - Flash model was used to determine the bubble point pressure. - The shortcut distillation model (DSTWU) was used for preliminary specifications. - The optimum distillate rate and molar reflux ratio were obtained from the design spec.
V-101	Valve	Pressure reducing valve	Valve	Outlet pressure: 2 atm	
E-105	Dimethylformamide cooler	U-tube exchanger	Heater	Outlet temperature: 50°C Pressure drop: 0 atm	- Conditions based on the work of Berg & Yeh [32]
V-102	Valve	Pressure reducing valve	Valve	Outlet pressure: 1 atm	
E-106	Product cooler	U-tube exchanger	Heater	Outlet temperature: 50°C Pressure drop: 0 atm	

Table B12 Stream table of process in Scenario IV (production of PA using petroleum-based feedstock) (cont.)

Stream	11	12	13	14	15	16	17	18	19	20
Temperature (°C)	80	80	80	80	80	80	50	55	55	121
Pressure (atm)	2	2	2	2	2	2	2	2	3	2
Mass vapor fraction	1.0000	1.0000	1.0000	0.0000	0.0000	0.0000	0.0000	0.0000	0.0000	1.0000
Total flow (kg/h)	1.46E+01	5.00E+00	1.20E+03	1.36E+03	4.11E+00	1.35E+03	4.46E+01	5.18E+03	5.18E+03	2.17E+02
Component Mass Fractions										
Ethylene	0.0000	0.0000	0.0041	0.0000	0.0000	0.0000	0.0000	0.0000	0.0000	0.0001
CO	0.0000	0.0000	0.0597	0.0000	0.0000	0.0000	0.0000	0.0000	0.0000	0.0001
H ₂ O	0.0000	0.0000	0.3308	0.1536	0.0000	0.1541	0.0000	0.0402	0.0402	0.9581
H ₂	0.0000	0.0000	0.0366	0.0000	0.0000	0.0000	0.0000	0.0000	0.0000	0.0000
CO ₂	0.0000	0.0000	0.3473	0.0013	0.0000	0.0013	0.0000	0.0003	0.0003	0.0082
N ₂	1.0000	0.0000	0.0635	0.0000	0.0000	0.0000	0.0000	0.0000	0.0000	0.0001
NP	0.0000	0.0000	0.0000	0.0030	1.0000	0.0000	0.0000	0.0000	0.0000	0.0000
NC	0.0000	0.0000	0.0042	0.0001	0.0000	0.0001	0.0000	0.0000	0.0000	0.0009
Propionic acid	0.0000	0.0000	0.1266	0.8383	0.0000	0.8409	0.0000	0.2232	0.2232	0.0041
Ethane	0.0000	0.0000	0.0170	0.0001	0.0000	0.0001	0.0000	0.0000	0.0000	0.0004
Ethanol	0.0000	0.0000	0.0001	0.0000	0.0000	0.0000	0.0000	0.0000	0.0000	0.0003
Ester	0.0000	0.0000	0.0002	0.0001	0.0000	0.0001	0.0000	0.0000	0.0000	0.0005
Ketone	0.0000	0.0000	0.0056	0.0033	0.0000	0.0033	0.0000	0.0009	0.0009	0.0204
O ₂	0.0000	1.0000	0.0042	0.0000	0.0000	0.0000	0.0000	0.0000	0.0000	0.0000
DMF	0.0000	0.0000	0.0000	0.0000	0.0000	0.0000	1.0000	0.7353	0.7353	0.0068

Table B12 Stream table of process in Scenario IV (production of PA using petroleum-based feedstock) (cont.)

Stream	21	22	23	24	25	26	27	28	29
Temperature (°C)	184	165	189	189	189	179	50	140	50
Pressure (atm)	3	2	3	3	3	2	2	1	1
Mass vapor fraction	0.0000	0.0000	0.0000	0.0000	0.0000	0.0483	0.0000	0.3567	0.0000
Total flow (kg/h)	4.96E+03	1.14E+03	3.82E+03	3.82E+01	3.78E+03	3.78E+03	3.78E+03	1.14E+03	1.14E+03
Component Mass Fractions									
Ethylene	0.0000	0.0000	0.0000	0.0000	0.0000	0.0000	0.0000	0.0000	0.0000
CO	0.0000	0.0000	0.0000	0.0000	0.0000	0.0000	0.0000	0.0000	0.0000
H ₂ O	0.0001	0.0004	0.0000	0.0000	0.0000	0.0000	0.0000	0.0004	0.0004
H ₂	0.0000	0.0000	0.0000	0.0000	0.0000	0.0000	0.0000	0.0000	0.0000
CO ₂	0.0000	0.0000	0.0000	0.0000	0.0000	0.0000	0.0000	0.0000	0.0000
N ₂	0.0000	0.0000	0.0000	0.0000	0.0000	0.0000	0.0000	0.0000	0.0000
NP	0.0000	0.0000	0.0000	0.0000	0.0000	0.0000	0.0000	0.0000	0.0000
NC	0.0000	0.0000	0.0000	0.0000	0.0000	0.0000	0.0000	0.0000	0.0000
Propionic acid	0.2328	0.9951	0.0053	0.0053	0.0053	0.0053	0.0053	0.9951	0.9951
Ethane	0.0000	0.0000	0.0000	0.0000	0.0000	0.0000	0.0000	0.0000	0.0000
Ethanol	0.0000	0.0000	0.0000	0.0000	0.0000	0.0000	0.0000	0.0000	0.0000
Ester	0.0000	0.0000	0.0000	0.0000	0.0000	0.0000	0.0000	0.0000	0.0000
Ketone	0.0000	0.0001	0.0000	0.0000	0.0000	0.0000	0.0000	0.0001	0.0001
O ₂	0.0000	0.0000	0.0000	0.0000	0.0000	0.0000	0.0000	0.0000	0.0000
DMF	0.7671	0.0044	0.9947	0.9947	0.9947	0.9947	0.9947	0.0044	0.0044

APPENDIX C
SUPPLEMENTARY INFORMATION OF CHAPTER 5

Table C1 Summary of CO₂ equivalence in scenario I

	Raw material	Transportation	Upstream processing	Downstream processing	sum
Analyze the contributions to the environmental impact (kg _{CO2eq} /h)					
glycerol	1.13E+03	-	-	-	1.13E+03
NH ₃	3.06E+01	2.45E+01	-	-	5.51E+01
MgCO ₃	4.40E+02	2.82E+01	-	-	4.68E+02
CO ₂	-	-	-4.28E+01	8.60E+01	4.32E+01
water	-	-	2.40E+01	-	2.40E+01
steam	-	-	9.41E+02	8.84E+02	1.82E+03
cooling water	-	-	8.31E+02	-	8.31E+02
refrigerant	-	-	-	1.23E+02	1.23E+02
electricity	-	-	4.48E+01	-	4.48E+01
wastewater	-	-	3.42E-01	1.36E+02	1.37E+02
sum	1.60E+03	5.26E+01	1.80E+03	1.23E+03	4.68E+03

Table C2 Summary of CO₂ equivalence in scenario II

	Raw material	Transportation	Upstream processing	Downstream processing	sum
Analyze the contributions to the environmental impact (kg _{CO2eq} /h)					
glycerol	1.34E+03	-	-	-	1.34E+03
NH ₃	3.64E+01	2.45E+01	-	-	6.09E+01
MgCO ₃	5.23E+02	2.89E+01	-	-	5.52E+02
CO ₂	-	-	-5.09E+01	1.02E+02	5.14E+01
water	-	-	2.85E+01	-	2.85E+01
steam	-	-	1.12E+03	6.07E+01	1.18E+03
cooling water	-	-	9.89E+02	-	9.89E+02
refrigerant	-	-	-	1.33E+03	1.33E+03
electricity	-	-	5.04E+01	-	5.04E+01
wastewater	-	-	4.06E-01	1.63E+02	1.64E+02
sum	1.90E+03	5.34E+01	2.14E+03	1.65E+03	5.74E+03

Table C3 Summary of CO₂ equivalence in scenario III

	Raw material	Transportation	Upstream processing	Downstream processing	sum
Analyze the contributions to the environmental impact (kg _{CO2eq} /h)					
glycerol	8.87E+02	-	-	-	8.87E+02
NH ₃	2.81E+01	2.44E+01	-	-	5.25E+01
NaOH	7.56E-01	2.47E+01	-	-	2.55E+01
CO ₂	-	-	-3.85E+02	2.73E+01	-3.58E+02
water	-	-	1.69E+01	-	1.69E+01
steam	-	-	6.62E+02	6.65E+02	1.33E+03
cooling water	-	-	5.86E+02	5.90E+01	6.45E+02
refrigerant	-	-	-	2.07E+02	2.07E+02
electricity	-	-	1.82E+01	4.74E-01	1.86E+01
wastewater	-	-	2.69E-01	9.54E+01	9.57E+01
sum	9.16E+02	4.91E+01	8.99E+02	1.05E+03	2.92E+03

Table C4 Summary of CO₂ equivalence in scenario IV

	Raw material	Transportation	Upstream processing	Downstream processing	sum
Analyze the contributions to the environmental impact (kg _{CO2eq} /h)					
glycerol	9.50E+02	-	-	-	9.50E+02
NH ₃	3.01E+01	2.45E+01	-	-	5.45E+01
NaOH	0.00E+00	2.48E+01	-	-	2.48E+01
CO ₂	-	-	-4.12E+02	2.92E+01	-3.83E+02
water	-	-	1.80E+01	-	1.80E+01
steam	-	-	7.09E+02	7.70E+02	1.48E+03
cooling water	-	-	1.09E+01	7.47E+01	8.56E+01
refrigerant	-	-	-	1.18E+03	1.18E+03
electricity	-	-	1.91E+01	5.58E-01	1.97E+01
wastewater	-	-	2.88E-01	1.02E+02	1.02E+02
sum	9.80E+02	4.92E+01	3.46E+02	2.15E+03	3.53E+03

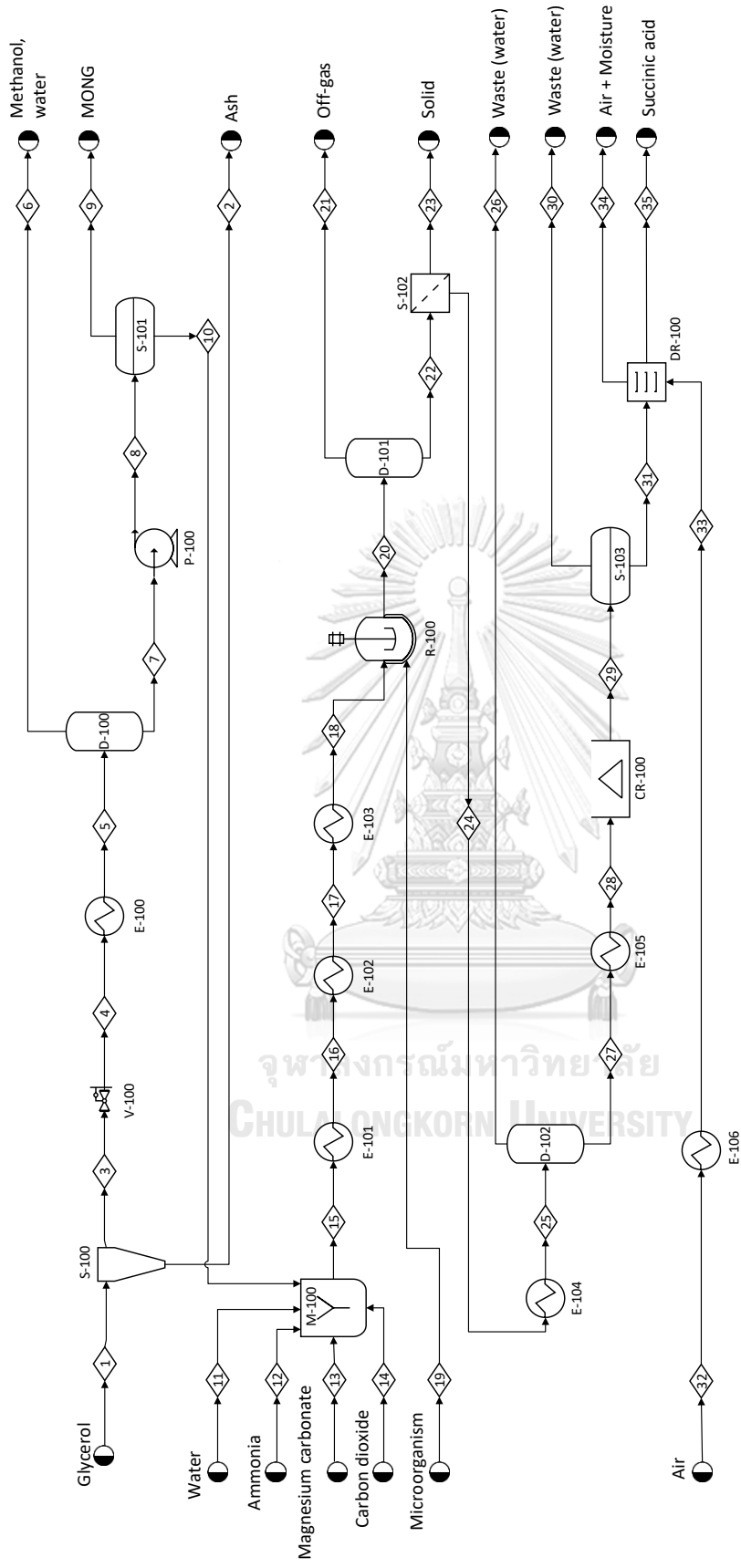


Figure C1 Process flow diagram of scenario I (SA purification using direct crystallization (no addition of DMSO))

Table C5 Description of unit operation in Scenario I (SA purification using direct crystallization (no addition of DMSO))

Unit	Process Description	Equipment type	Model	Operating Conditions	Design comment
S-100	Ash removal	Splitter	SSplit	Split fraction MIXED stream: 0.99 CSOLID stream: 0.01	Conditions based on the work of Ding [203]
V-100	Valve	Pressure reducing valve	Valve	Outlet pressure: 0.1 atm	Pressure based on the patent of Chang [189]
E-100	Methanol and water separation	U-tube exchanger	Heater	Outlet temperature: 95°C Pressure drop: 0 atm	Temperature based on the patent of Chang [189]
D-100	Gas separation	Vertical process vessel	Flash2	Pressure drop: 0 atm Duty: 0	
P-100	Pump	Centrifugal pump	Pump	Outlet pressure: 1 atm	
S-101	MONG removal	Vertical process vessel	Sep	MONG 99% separation	Removal data is performed based on the work of Ding [203]
M-100	Liquid mixing tank	Agitated tank-enclosed	Mixer	Pressure drop: 0 atm	
E-101	Sterilization	Fixed tube sheet heat exchanger	Heater	Outlet temperature: 121°C Pressure drop: 0 atm	- Conditions based on the work of Vlysidis et al. [6]
E-102	Feedstock cooler	Fixed tube sheet heat exchanger	Heater	Outlet temperature: 90°C Pressure drop: 0 atm	- The cost of equipment, installation and utilities are calculated to determine the optimal temperature.
E-103	Feedstock cooler	Fixed tube sheet heat exchanger	Heater	Outlet temperature: 37°C Pressure drop: 0 atm	- The cost of equipment, installation and utilities are calculated to determine the optimal temperature.
R-100	Fermentation	Agitated tank-enclosed and jacketed	RStoic	Temperature: 37°C Pressure drop: 0 atm Reaction: GLY + 0.048 NH ₃ + 0.056 CO ₂ → 0.653 SA + 0.077 AA + 0.050 FA + 0.240 MICROOR + 0.126 H ₂ O + 1.567 H ₂ (100 % conversion of glycerol)	- The reactor operates isothermally ($\Delta T > 15\%$ of T_{inlet}). - Reaction based on the work of Vlysidis et al. [6] and Gargalo et al. [153] - Fermentation yield: 0.84 g/g Productivity: 0.24 g/L/h Product concentration: 18 g/L
D-101	Gas separation	Vertical process vessel	Flash2	Pressure drop: 0 atm Duty: 0	

Unit	Process Description	Equipment type	Model	Operating Conditions	Design comment
S-102	Microorganism removal	Tubular cross-flow filter	CFFilter	Pressure drop: 0 atm Solids to solid outlet: 1 Liquid load of solids outlet: 0.3	- Conditions based on the work of Nieder-Heitmann [154]
E-104	Evaporation	Fixed tube sheet heat exchanger	Heater	Outlet temperature: 101.2°C Pressure drop: 0 atm	- Temperature was obtained from the design spec.
D-102	Evaporation	Vertical process vessel	Flash2	Pressure drop: 0 atm Duty: 0	
E-105	Crystallization	U-tube exchanger	Heater	Outlet temperature: 20°C Pressure drop: 0 atm	- Temperature based on the work of Nieder-Heitmann [154]
CR-100	Crystallization	Oslo growth type crystallizer	Crystallizer	Temperature: 20°C Pressure: 1 atm SA → SACRYS (Succinic acid crystal, Solid) Solubility is concentration data with 45.52 gm/L at 11.85°C.	- Conditions based on the work of Nieder-Heitmann [154] - Solubility was obtained on the work of Stephen [204]
S-103	Crystal separation	Vertical process vessel	Sep	SACRYS 100 % separation	
E-106	Air heater	U-tube exchanger	Heater	Outlet temperature: 130°C Pressure drop: 0 atm	- Temperature based on the work of Nieder-Heitmann [154]
DR-100	Dryer	Atmospheric tray batch dryer	Dryer	Operation mode: continuous Dryer type: shortcut Pressure drop: 0 atm Heat duty: 0 Moisture specification basis: WET, H ₂ O 0.5 wt%	- Conditions based on the work of Nieder-Heitmann [154] - Moisture content based on the work of Moussa et al. [187]

Table C6 Stream table of process in Scenario I (SA purification using direct crystallization (no addition of DMSO)) (cont.)

Stream	24	25	26	27	28	29	30	31	32	33	34	35
Temperature (°C)	37.0	101.2	101.2	101.2	20.0	20.0	20.0	20.0	25.0	130.0	25.0	25.0
Pressure (atm)	1.0	1.0	1.0	1.0	1.0	1.0	1.0	1.0	1.0	1.0	1.0	1.0
Mass vapor fraction	0.000	0.933	1.000	0.000	0.000	0.000	0.000	0.000	1.000	1.000	0.406	0.000
Total flow (kg/h)	7.41E+04	7.41E+04	6.92E+04	4.95E+03	4.95E+03	4.95E+03	3.43E+03	1.52E+03	2.51E+02	2.51E+02	6.26E+02	1.14E+03
Component Mass Fractions												
Glycerol	0.000	0.000	0.000	0.000	0.000	0.000	0.000	0.000	0.000	0.000	0.000	0.000
H ₂ O	0.981	0.981	0.998	0.735	0.735	0.735	0.953	0.240	0.000	0.000	0.571	0.005
NH ₃	0.000	0.000	0.000	0.000	0.000	0.000	0.000	0.000	0.000	0.000	0.000	0.000
CO ₂	0.000	0.000	0.000	0.000	0.000	0.000	0.000	0.000	0.010	0.010	0.004	0.000
Succinic acid	0.018	0.018	0.000	0.264	0.264	0.035	0.045	0.011	0.000	0.000	0.028	0.000
Acetic acid	0.001	0.001	0.001	0.001	0.001	0.001	0.001	0.000	0.000	0.000	0.000	0.000
Formic acid	0.001	0.001	0.001	0.000	0.000	0.000	0.000	0.000	0.000	0.000	0.000	0.000
H ₂	0.000	0.000	0.000	0.000	0.000	0.000	0.000	0.000	0.000	0.000	0.000	0.000
O ₂	0.000	0.000	0.000	0.000	0.000	0.000	0.000	0.000	0.210	0.210	0.084	0.000
N ₂	0.000	0.000	0.000	0.000	0.000	0.000	0.000	0.000	0.780	0.780	0.312	0.000
Methanol	0.000	0.000	0.000	0.000	0.000	0.000	0.000	0.000	0.000	0.000	0.000	0.000
MgCO ₃	0.000	0.000	0.000	0.000	0.000	0.000	0.000	0.000	0.000	0.000	0.000	0.000
MONG	0.000	0.000	0.000	0.000	0.000	0.000	0.000	0.000	0.000	0.000	0.000	0.000
Ash	0.000	0.000	0.000	0.000	0.000	0.000	0.000	0.000	0.000	0.000	0.000	0.000
Microorganism	0.000	0.000	0.000	0.000	0.000	0.000	0.000	0.000	0.000	0.000	0.000	0.000
SACRY5	0.000	0.000	0.000	0.000	0.000	0.230	0.000	0.749	0.000	0.000	0.000	0.995

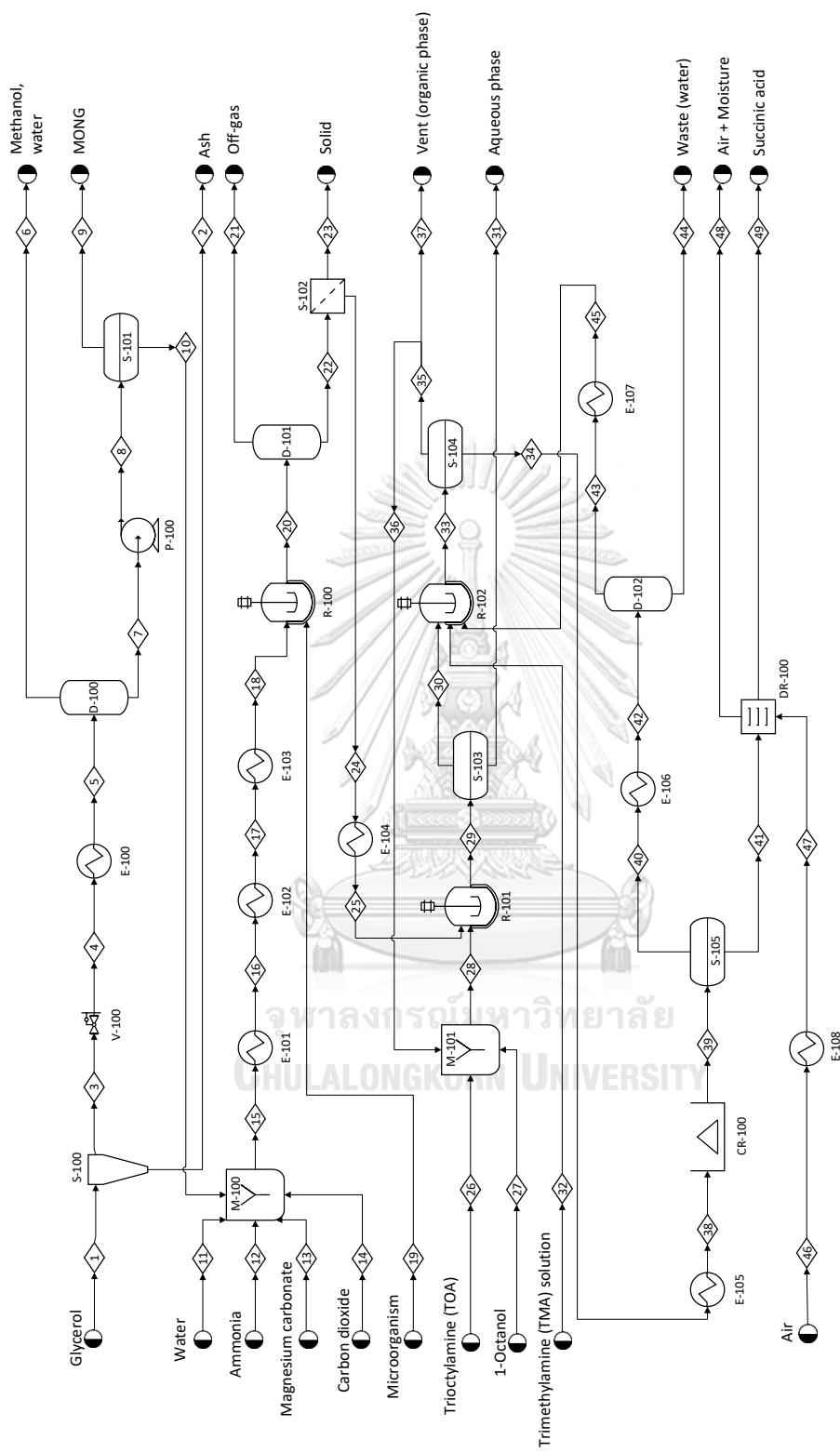


Figure C2 Process flow diagram of scenario II (SA purification using reactive extraction (no addition of DMSO))

Table C7 Description of unit operation in Scenario II (SA purification using reactive extraction (no addition of DMSO))

Unit	Process Description	Equipment type	Model	Operating Conditions	Design comment
S-100	Ash removal	Splitter	SSplit	Split fraction MIXED stream: 0.99 CSOLID stream: 0.01	- Conditions based on the work of Ding [203]
V-100	Valve	Pressure reducing valve	Valve	Outlet pressure: 0.1 atm	- Pressure based on the patent of Chang [189]
E-100	Methanol and water separation	U-tube exchanger	Heater	Outlet temperature: 95°C Pressure drop: 0 atm	- Temperature based on the patent of Chang [189]
D-100	Gas separation	Vertical process vessel	Flash2	Pressure drop: 0 atm Duty: 0	
P-100	Pump	Centrifugal pump	Pump	Outlet pressure: 1 atm	
S-101	MONG removal	Vertical process vessel	Sep	MONG: 99% separation	- Removal data is performed based on the work of Ding [203]
M-100	Liquid mixing tank	Agitated tank-enclosed	Mixer	Pressure drop: 0 atm	
E-101	Sterilization	Fixed tube sheet heat exchanger	Heater	Outlet temperature: 121°C Pressure drop: 0 atm	- Conditions based on the work of Vlysidis et al. [6]
E-102	Feedstock cooler	Fixed tube sheet heat exchanger	Heater	Outlet temperature: 90°C Pressure drop: 0 atm	- The cost of equipment, installation and utilities are calculated to determine the optimal temperature.
E-103	Feedstock cooler	Fixed tube sheet heat exchanger	Heater	Outlet temperature: 37°C Pressure drop: 0 atm	- The cost of equipment, installation and utilities are calculated to determine the optimal temperature.
R-100	Fermentation	Agitated tank-enclosed and jacketed	RSioic	Temperature: 37°C Pressure drop: 0 atm Reaction: GLY + 0.048 NH ₃ + 0.056 CO ₂ → 0.653 SA + 0.077 AA + 0.050 FA + 0.240 MICROORP + 0.126 H ₂ O + 1.567 H ₂ (100 % conversion of glycerol)	- The reactor operates isothermally ($\Delta T > 15\%$ of T_{inlet}). - Reaction based on the work of Vlysidis et al. [6] and Gargalo et al. [153] - Fermentation yield: 0.84 g/g Productivity: 0.24 g/L/h Product concentration: 18 g/L
D-101	Gas separation	Vertical process vessel	Flash2	Pressure drop: 0 atm Duty: 0	

Unit	Process Description	Equipment type	Model	Operating Conditions	Design comment
S-102	Microorganism removal	Tubular cross-flow filter	CFilter	Pressure drop: 0 atm Solids to solid outlet: 1 Liquid load of solids outlet: 0.3	- Conditions based on the work of Nieder-Heitmann [154]
E-104	Fermentation broth cooler	Fixed tube sheet heat exchanger	Heater	Outlet temperature: 25°C Pressure drop: 0 atm	- Temperature based on the work of Hong and Hong [190]
M-101	Liquid mixing tank	Agitated tank-enclosed	Mixer	Pressure drop: 0 atm	
R-101	Reactive extraction	Agitated tank-enclosed and jacketed	RStoic	Temperature: 25°C Pressure drop: 0 atm Reaction: SA + TOA → SA-TOA (95.84 % conversion of SA)	- Conditions based on the work of Hong and Hong [190] - Iterative calculation is performed until the results match with the experimental data.
S-103	Reactive extraction	Vertical process vessel	Decanter	Temperature: 25°C Pressure drop: 0 atm	- The decanter model is used in the simulation based on the work of Nieder-Heitmann [154]
R-102	Back-extraction	Agitated tank-enclosed and jacketed	RStoic	Temperature: 25°C Pressure drop: 0 atm Reaction: SA-TOA + TMA → SA-TMA + TOA (100 % conversion of SA-TOA)	- Temperature based on the work of Kurzrock et al. [205] - Assumption: 100% conversion
S-104	Back-extraction	Vertical process vessel	Decanter	Temperature: 25°C Pressure drop: 0 atm	- The decanter model is used in the simulation based on the work of Nieder-Heitmann [154]
E-105	Crystallization	U-tube exchanger	Heater	Outlet temperature: 20°C Pressure drop: 0 atm	- Temperature based on the work of Nieder-Heitmann [154]
CR-100	Crystallization	Oslo growth type crystallizer	Crystallizer	Temperature: 20°C Pressure: 1 atm SA → SACRYS (Succinic acid crystal: Solid) Solubility is concentration data with 45.52 gm/L at 11.85°C.	- Conditions based on the work of Nieder-Heitmann [154] - Solubility was obtained on the work of Stephen [204]
S-105	Crystal separation	Vertical process vessel	Sep	SACRYS 100 % separation	
E-106	TMA heater	Fixed tube sheet heat	Heater	Outlet temperature: 98.4°C	- Temperature was obtained from the design spec.

Unit	Process Description	Equipment type	Model	Operating Conditions	Design comment
		exchanger		Pressure drop: 0 atm	
D-102	TMA separation	Vertical process vessel	Flash2	Pressure drop: 0 atm Duty: 0	
E-107	TMA cooler	Fixed tube sheet heat exchanger	Heater	Outlet temperature: 25°C Pressure drop: 0 atm	
E-108	Air heater	U-tube exchanger	Heater	Outlet temperature: 130°C Pressure drop: 0 atm	- Temperature based on the work of Nieder-Heitmann [154]
DR-100	Dryer	Atmospheric tray batch dryer	Dryer	Operation mode: continuous Dryer type: shortcut Pressure drop: 0 atm Heat duty: 0 Moisture specification basis: WET, H ₂ O 0.5 wt%	- Conditions based on the work of Nieder-Heitmann [154] - Moisture content based on the work of Moussa et al. [187]

Table C8 Stream table of process in Scenario II (SA purification using reactive extraction (no addition of DMSO)) (cont.)

Stream	31	32	33	34	35	36	37	38	39	40
Temperature (°C)	25.0	25.0	25.0	25.0	25.0	25.0	25.0	20.0	20.0	20.0
Pressure (atm)	1.0	1.0	1.0	1.0	1.0	1.0	1.0	1.0	1.0	1.0
Mass vapor fraction	0.000	0.000	0.000	0.000	0.000	0.000	0.000	0.000	0.000	0.000
Total flow (kg/h)	8.58E+04	5.18E+02	3.03E+04	8.49E+03	2.18E+04	2.16E+04	2.18E+02	8.49E+03	8.49E+03	6.77E+03
Component Mass Fractions										
Glycerol	0.000	0.000	0.000	0.000	0.000	0.000	0.000	0.000	0.000	0.000
H ₂ O	0.996	0.807	0.181	0.639	0.003	0.003	0.003	0.639	0.639	0.721
NH ₃	0.000	0.000	0.000	0.000	0.000	0.000	0.000	0.000	0.000	0.000
CO ₂	0.000	0.000	0.000	0.000	0.000	0.000	0.000	0.000	0.000	0.000
Succinic acid	0.001	0.000	0.050	0.176	0.001	0.001	0.001	0.176	0.042	0.048
Acetic acid	0.001	0.000	0.002	0.006	0.000	0.000	0.000	0.006	0.006	0.007
Formic acid	0.001	0.000	0.000	0.000	0.000	0.000	0.000	0.000	0.000	0.000
H ₂	0.000	0.000	0.000	0.000	0.000	0.000	0.000	0.000	0.000	0.000
O ₂	0.000	0.000	0.000	0.000	0.000	0.000	0.000	0.000	0.000	0.000
N ₂	0.000	0.000	0.000	0.000	0.000	0.000	0.000	0.000	0.000	0.000
TOA	0.000	0.000	0.154	0.000	0.214	0.214	0.214	0.000	0.000	0.000
Octanol	0.001	0.000	0.564	0.013	0.778	0.778	0.778	0.013	0.013	0.016
TMA	0.001	0.193	0.049	0.165	0.004	0.004	0.004	0.165	0.165	0.207
SA-TOA	0.000	0.000	0.000	0.000	0.000	0.000	0.000	0.000	0.000	0.000
SA-TMA	0.000	0.000	0.000	0.000	0.000	0.000	0.000	0.000	0.000	0.000
Methanol	0.000	0.000	0.000	0.000	0.000	0.000	0.000	0.000	0.000	0.000
MgCO ₃	0.000	0.000	0.000	0.000	0.000	0.000	0.000	0.000	0.000	0.000
MONG	0.000	0.000	0.000	0.000	0.000	0.000	0.000	0.000	0.000	0.000
Ash	0.000	0.000	0.000	0.000	0.000	0.000	0.000	0.000	0.000	0.000
Microorganism	0.000	0.000	0.000	0.000	0.000	0.000	0.000	0.000	0.000	0.000
SACRY5	0.000	0.000	0.000	0.000	0.000	0.000	0.000	0.000	0.134	0.000

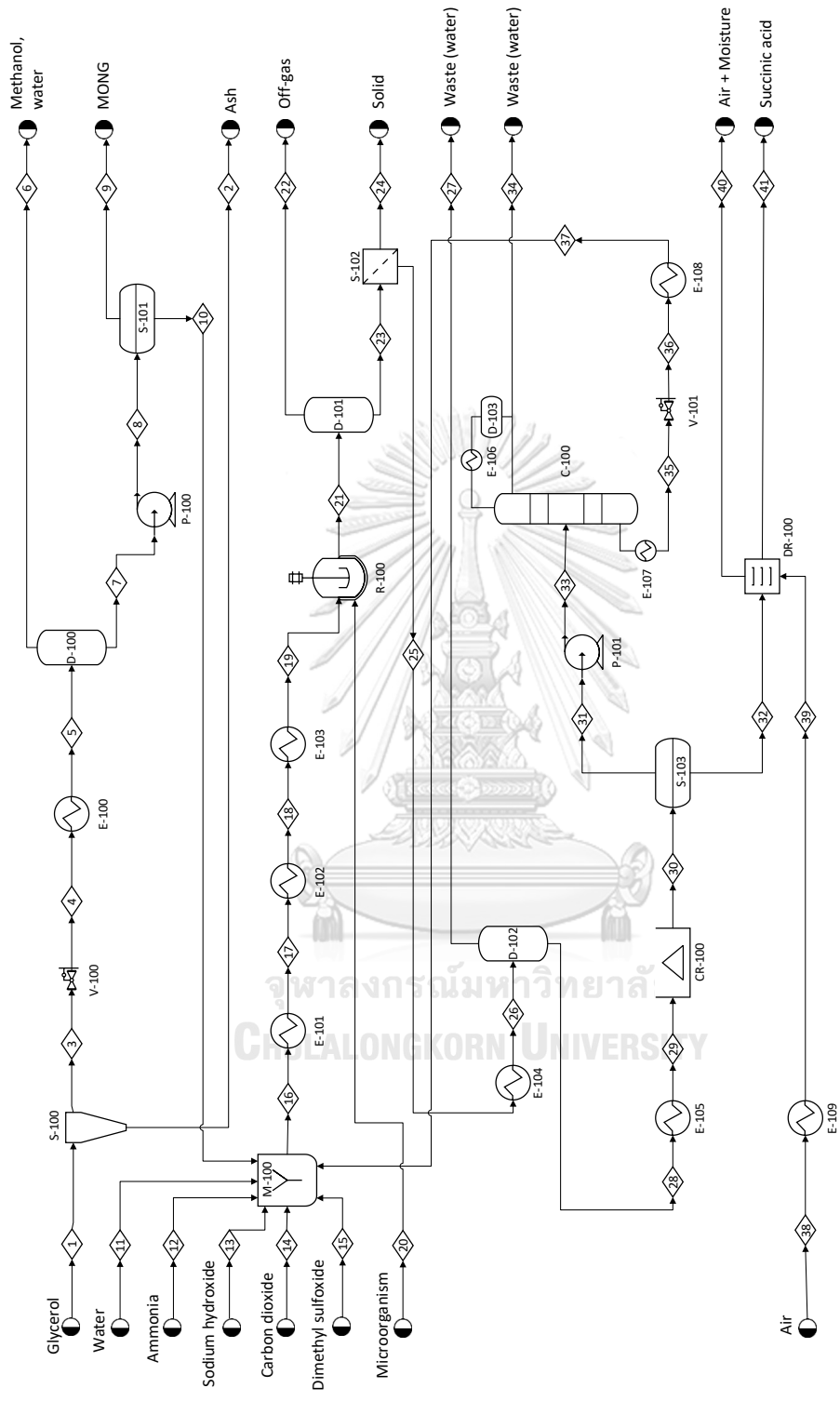


Figure C3 Process flow diagram of scenario III (SA purification using direct crystallization (addition of DMSO))

Table C9 Description of unit operation in Scenario III (SA purification using direct crystallization (addition of DMSO))

Unit	Process Description	Equipment type	Model	Operating Conditions	Design comment
S-100	Ash removal	Splitter	SSplit	Split fraction MIXED stream: 0.99 CISOLID stream: 0.01	Conditions based on the work of Ding [203]
V-100	Valve	Pressure reducing valve	Valve	Outlet pressure: 0.1 atm	Pressure based on the patent of Chang [189]
E-100	Methanol and water separation	U-tube exchanger	Heater	Outlet temperature: 95°C Pressure drop: 0 atm	Temperature based on the patent of Chang [189]
D-100	Gas separation	Vertical process vessel	Flash2	Pressure drop: 0 atm Duty: 0	
P-100	Pump	Centrifugal pump	Pump	Outlet pressure: 1 atm	
S-101	MONG removal	Vertical process vessel	Sep	MONG 99% separation	Removal data is performed based on the work of Ding [203]
M-100	Liquid mixing tank	Agitated tank-enclosed	Mixer	Pressure drop: 0 atm	
E-101	Sterilization	Fixed tube sheet heat exchanger	Heater	Outlet temperature: 121°C Pressure drop: 0 atm	- Conditions based on the work of Viysidis et al. [6]
E-102	Feedstock cooler	Fixed tube sheet heat exchanger	Heater	Outlet temperature: 90°C Pressure drop: 0 atm	- The cost of equipment, installation and utilities are calculated to determine the optimal temperature.
E-103	Feedstock cooler	Fixed tube sheet heat exchanger	Heater	Outlet temperature: 37°C Pressure drop: 0 atm	- The cost of equipment, installation and utilities are calculated to determine the optimal temperature.
R-100	Fermentation	Agitated tank-enclosed and jacketed	RStoic	Temperature: 37°C Pressure drop: 0 atm Reaction: GLY + 0.056 NH ₃ + 0.640 CO ₂ → 0.741 SA + 0.128 AA + 0.142 FA + 0.280 MICROOR + 0.639 H ₂ O +	- The reactor operates isothermally (ΔT > 15% of T _{inlet}). - Reaction based on the work of Carvalho et al. [23] - Fermentation yield: 0.95 g/g

Unit	Process Description	Equipment type	Model	Operating Conditions	Design comment
				0.573 H ₂ (100 % conversion of glycerol)	Productivity: 0.76 g/L/h Product concentration: 22.8 g/L
D-101	Gas separation	Vertical process vessel	Flash2	Pressure drop: 0 atm Duty: 0	
S-102	Microorganism removal	Tubular cross-flow filter	CFilter	Pressure drop: 0 atm Solids to solid outlet: 1 Liquid load of solids outlet: 0.3	- Conditions based on the work of Nieder-Heitmann [154]
E-104	Evaporation	Fixed tube sheet heat exchanger	Heater	Outlet temperature: 101.6°C Pressure drop: 0 atm	- Temperature was obtained from the design spec.
D-102	Evaporation	Vertical process vessel	Flash2	Pressure drop: 0 atm Duty: 0	
E-105	Crystallization	U-tube exchanger	Heater	Outlet temperature: 20°C Pressure drop: 0 atm	- Temperature based on the work of Nieder-Heitmann [154]
CR-100	Crystallization	Oslo growth type crystallizer	Crystallizer	Temperature: 20°C Pressure: 1 atm SA → SACRYS (Succinic acid crystal: Solid) Solubility is concentration data with 45.52 gm/L at 11.85°C.	- Conditions based on the work of Nieder-Heitmann [154] - Solubility was obtained on the work of Stephen [204]
S-103	Crystal separation	Vertical process vessel	Sep	SACRYS 100 % separation	
P-101	Pump	Centrifugal pump	Pump	Outlet pressure: 2.5 atm	
C-100	Water separation	Distillation column (Total condenser)	RadFrac	1 st stage pressure: 2 atm pressure drop: 0.5 atm Number of stages: 22 Feed stage: 10 Condenser: Total Reboiler: Kettle	- Flash model was used to determine the bubble point pressure. - The shortcut distillation model (DSTWU) was used for preliminary specifications. - The optimum distillate rate and molar reflux ratio were obtained from the design spec.

Unit	Process Description	Equipment type	Model	Operating Conditions	Design comment
V-101	Valve	Pressure reducing valve	Valve	Distillate rate: 16,183.9 kg/h Molar reflux ratio: 0.071 Outlet pressure: 1 atm	
E-108	DMSO cooler	U-tube exchanger	Heater	Outlet temperature: 37°C Pressure drop: 0 atm	
E-109	Air heater	U-tube exchanger	Heater	Outlet temperature: 130°C Pressure drop: 0 atm	- Temperature based on the work of Nieder-Heitmann [154]
DR-100	Dryer	Atmospheric tray batch dryer	Dryer	Operation mode: continuous Dryer type: shortcut Pressure drop: 0 atm Heat duty: 0 Moisture specification basis: WET, H ₂ O 0.5 wt%	- Conditions based on the work of Nieder-Heitmann [154] - Moisture content based on the work of Moussa et al. [187]

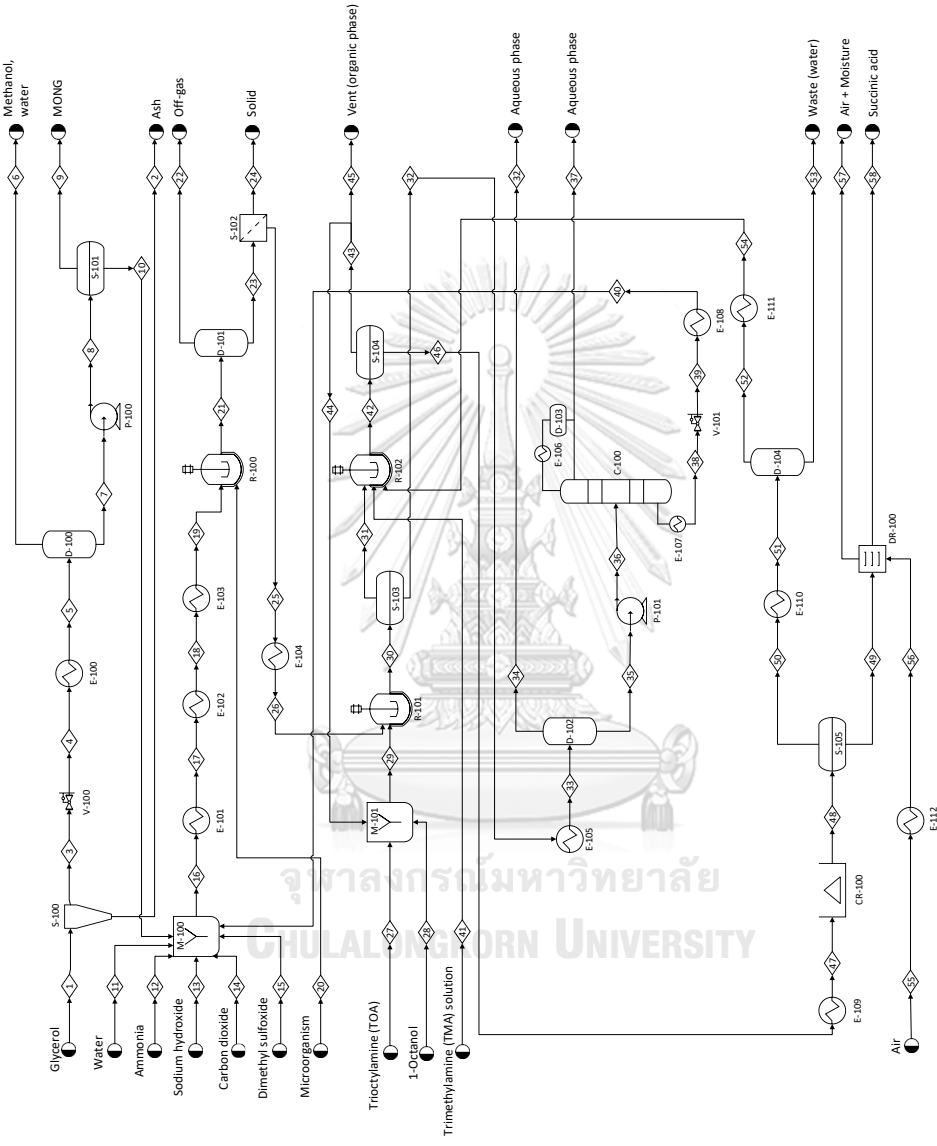


Figure C4 Process flow diagram of scenario IV (SA purification using reactive extraction (addition of DMSO))

Table C11 Description of unit operation in Scenario IV (SA purification using reactive extraction (addition of DMSO))

Unit	Process Description	Equipment type	Model	Operating Conditions	Design comment
S-100	Ash removal	Splitter	SSplit	Split fraction MIXED stream: 0.99 CISOLID stream: 0.01	Conditions based on the work of Ding [203]
V-100	Valve	Pressure reducing valve	Valve	Outlet pressure: 0.1 atm	Pressure based on the patent of Chang [189]
E-100	Methanol and water separation	U-tube exchanger	Heater	Outlet temperature: 95°C Pressure drop: 0 atm	Temperature based on the patent of Chang [189]
D-100	Gas separation	Vertical process vessel	Flash2	Pressure drop: 0 atm Duty: 0	
P-100	Pump	Centrifugal pump	Pump	Outlet pressure: 1 atm	
S-101	MONG removal	Vertical process vessel	Sep	MONG 99% separation	Removal data is performed based on the work of Ding [203]
M-100	Liquid mixing tank	Agitated tank-enclosed	Mixer	Pressure drop: 0 atm	
E-101	Sterilization	Fixed tube sheet heat exchanger	Heater	Outlet temperature: 121°C Pressure drop: 0 atm	- Conditions based on the work of Viysidis et al. [6]
E-102	Feedstock cooler	Fixed tube sheet heat exchanger	Heater	Outlet temperature: 90°C Pressure drop: 0 atm	- The cost of equipment, installation and utilities are calculated to determine the optimal temperature.
E-103	Feedstock cooler	Fixed tube sheet heat exchanger	Heater	Outlet temperature: 37°C Pressure drop: 0 atm	- The cost of equipment, installation and utilities are calculated to determine the optimal temperature.
R-100	Fermentation	Agitated tank-enclosed and jacketed	RStoic	Temperature: 37°C Pressure drop: 0 atm Reaction: GLY + 0.056 NH ₃ + 0.640 CO ₂ → 0.741 SA + 0.128 AA + 0.142 FA + 0.280 MICROOR + 0.639 H ₂ O +	- The reactor operates isothermally (ΔT > 15% of T _{inlet}). - Reaction based on the work of Carvalho et al. [23] - Fermentation yield: 0.95 g/g

Unit		Process Description		Equipment type		Model		Operating Conditions		Design comment	
								0.573 H ₂ (100 % conversion of glycerol)		Productivity: 0.76 g/L/h Product concentration: 22.8 g/L	
D-101	Gas separation	Vertical process vessel	Flash2					Pressure drop: 0 atm Duty: 0			
S-102	Microorganism removal	Tubular cross-flow filter	CFilter					Pressure drop: 0 atm Solids to solid outlet: 1 Liquid load of solids outlet: 0.3		- Conditions based on the work of Nieder-Heitmann [154]	
E-104	Fermentation broth cooler	Fixed tube sheet heat exchanger	Heater					Outlet temperature: 25°C Pressure drop: 0 atm		- Temperature based on the work of Hong and Hong [190]	
M-101	Liquid mixing tank	Agitated tank-enclosed	Mixer					Pressure drop: 0 atm			
R-101	Reactive extraction	Agitated tank-enclosed and jacketed	RStoic					Temperature: 25°C Pressure drop: 0 atm Reaction: SA + TOA → SA-TOA (95.84 % conversion of SA)		- Conditions based on the work of Hong and Hong [190] - Iterative calculation is performed until the results match with the experimental data.	
S-103	Reactive extraction	Vertical process vessel	Decanter					Temperature: 25°C Pressure drop: 0 atm		- The decanter model is used in the simulation based on the work of Nieder-Heitmann [154]	
R-102	Back-extraction	Agitated tank-enclosed and jacketed	RStoic					Temperature: 25°C Pressure drop: 0 atm Reaction: SA-TOA + TMA → SA-TMA + TOA (100 % conversion of SA-TOA)		- Temperature based on the work of Kurzrock et al. [205] - Assumption: 100% conversion	
S-104	Back-extraction	Vertical process vessel	Decanter					Temperature: 25°C Pressure drop: 0 atm		- The decanter model is used in the simulation based on the work of Nieder-Heitmann [154]	
E-105	Evaporation	Fixed tube sheet heat exchanger	Heater					Outlet temperature: 101°C Pressure drop: 0 atm		- Temperature was obtained from the design spec.	

Unit		Process Description		Equipment type		Model		Operating Conditions		Design comment
D-102	Evaporation	Vertical process vessel	Flash2	Pressure drop: 0 atm Duty: 0						
P-101	Pump	Centrifugal pump	Pump	Outlet pressure: 2.5 atm						
C-100	Water separation	Distillation column (Total condenser)	RadFrac	1 st stage pressure: 2 atm pressure drop: 0.5 atm Number of stages: 22 Feed stage: 10 Condenser: Total Reboiler: Kettle Distillate rate: 6,948 kg/h Molar reflux ratio: 0.073						<ul style="list-style-type: none"> - Flash model was used to determine the bubble point pressure. - The shortcut distillation model (DSTWU) was used for preliminary specifications. - The optimum distillate rate and molar reflux ratio were obtained from the design spec.
V-101	Valve	Pressure reducing valve	Valve	Outlet pressure: 1 atm						
E-108	DMSO cooler	U-tube exchanger	Heater	Outlet temperature: 37°C Pressure drop: 0 atm						
E-109	Crystallization	U-tube exchanger	Heater	Outlet temperature: 20°C Pressure drop: 0 atm						<ul style="list-style-type: none"> - Temperature based on the work of Nieder-Heitmann [154]
CR-100	Crystallization	Oslo growth type crystallizer	Crystallizer	Temperature: 20°C Pressure: 1 atm SA → SACRYS (Succinic acid crystal: Solid) Solubility is concentration data with 45.52 gm/L at 11.85°C.						<ul style="list-style-type: none"> - Conditions based on the work of Nieder-Heitmann [154] - Solubility was obtained on the work of Stephen [204]
S-105	Crystal separation	Vertical process vessel	Sep	SACRYS 100 % separation						
E-110	TMA heater	Fixed tube sheet heat exchanger	Heater	Outlet temperature: 98.4°C Pressure drop: 0 atm						<ul style="list-style-type: none"> - Temperature was obtained from the design spec.
D-104	TMA separation	Vertical process vessel	Flash2	Pressure drop: 0 atm Duty: 0						

Unit	Process Description	Equipment type	Model	Operating Conditions	Design comment
E-111	TMA cooler	Fixed tube sheet heat exchanger	Heater	Outlet temperature: 25°C Pressure drop: 0 atm	
E-112	Air heater	U-tube exchanger	Heater	Outlet temperature: 130°C Pressure drop: 0 atm	- Temperature based on the work of Nieder-Heitmann [154]
DR-100	Dryer	Atmospheric tray batch dryer	Dryer	Operation mode: continuous Dryer type: shortcut Pressure drop: 0 atm Heat duty: 0 Moisture specification basis: WET, H ₂ O 0.5 wt%	- Conditions based on the work of Nieder-Heitmann [154] - Moisture content based on the work of Moussa et al. [187]

Table C12 Stream table of process in Scenario IV (SA purification using reactive extraction (addition of DMSO)) (cont.)

Stream	41	42	43	44	45	46	47	48	49	50
Temperature (°C)	25.0	25.0	25.0	25.0	25.0	25.0	20.0	20.0	20.0	20.0
Pressure (atm)	1.0	1.0	1.0	1.0	1.0	1.0	1.0	1.0	1.0	1.0
Mass vapor fraction	0.000	0.000	0.000	0.000	0.000	0.000	0.000	0.000	0.000	0.000
Total flow (kg/h)	5.28E+02	3.01E+04	2.18E+04	2.15E+04	2.18E+02	8.38E+03	8.38E+03	8.38E+03	1.70E+03	6.68E+03
Component Mass Fractions										
Glycerol	0.000	0.000	0.000	0.000	0.000	0.000	0.000	0.000	0.000	0.000
H ₂ O	0.814	0.175	0.003	0.003	0.003	0.621	0.621	0.621	0.306	0.701
NH ₃	0.000	0.000	0.000	0.000	0.000	0.000	0.000	0.000	0.000	0.000
CO ₂	0.000	0.002	0.000	0.000	0.000	0.005	0.005	0.005	0.000	0.007
Succinic acid	0.000	0.050	0.001	0.001	0.001	0.178	0.178	0.042	0.021	0.048
Acetic acid	0.000	0.002	0.000	0.000	0.000	0.008	0.008	0.008	0.004	0.010
Formic acid	0.000	0.000	0.000	0.000	0.000	0.001	0.001	0.001	0.001	0.001
H ₂	0.000	0.000	0.000	0.000	0.000	0.000	0.000	0.000	0.000	0.000
O ₂	0.000	0.000	0.000	0.000	0.000	0.000	0.000	0.000	0.000	0.000
N ₂	0.000	0.000	0.000	0.000	0.000	0.000	0.000	0.000	0.000	0.000
DMSO	0.000	0.002	0.000	0.000	0.000	0.005	0.005	0.005	0.000	0.007
TOA	0.000	0.154	0.213	0.213	0.213	0.000	0.000	0.000	0.000	0.000
Octanol	0.000	0.566	0.778	0.778	0.778	0.014	0.014	0.014	0.000	0.018
TMA	0.186	0.049	0.004	0.004	0.004	0.167	0.167	0.167	0.001	0.209
SA-TOA	0.000	0.000	0.000	0.000	0.000	0.000	0.000	0.000	0.000	0.000
SA-TMA	0.000	0.000	0.000	0.000	0.000	0.000	0.000	0.000	0.000	0.000
Methanol	0.000	0.000	0.000	0.000	0.000	0.000	0.000	0.000	0.000	0.000
NaOH	0.000	0.000	0.000	0.000	0.000	0.000	0.000	0.000	0.000	0.000
MONG	0.000	0.000	0.000	0.000	0.000	0.000	0.000	0.000	0.000	0.000
Ash	0.000	0.000	0.000	0.000	0.000	0.000	0.000	0.000	0.000	0.000
Microorganism	0.000	0.000	0.000	0.000	0.000	0.000	0.000	0.000	0.000	0.000
SACRYL	0.000	0.000	0.000	0.000	0.000	0.000	0.000	0.135	0.668	0.000

Fermenter design

Example of Scenario III, the design of the fermentation tank was undertaken using fermenters of 500 m³. The calculation is exemplified as follows.

Assumption

1. The loading time of 7.5 h and the unloading time of 7.5 h of each batch reactor should be reasonable for the 500 m³ reactor tank. Please note that the loading time is the time that would be required to fill the fermenter.
2. The total mass flowrate feed to the fermenter is 53,215 kg/h (obtained from Scenario III)
3. Residence time (reaction time) is 30 h.

Table C13 Calculation of batch reactor system with the reaction time of 30 h

Every 7.5 h	Unload	Load	7.5	15	22.5	30
7.5	1	6	5	4	3	2
15	2	1	6	5	4	3
22.5	3	2	1	6	5	4
30	4	3	2	1	6	5
37.5	5	4	3	2	1	6
45	6	5	4	3	2	1

According to the table above, at 7.5 h, tank 1 is completely unloaded, tank 6 is completely loaded, tank 5 has been in the fermentation process by 7.5 h, tank 4 by 15 h, tank 3 by 22.5 h, and tank 2 by 30 h. This means that at the next time step (15 h), tank 2 is completely unloaded as displayed in the table.

The calculation of height and diameter was exemplified as follows.

Calculation example

Reactor size	500 m ³
Height to diameter ratio	3
Diameter	$\left(\frac{\text{reactor size} \times 4}{3\pi}\right)^{1/3} = 5.97 \text{ m}$
Height	3 × 5.97 = 17.9 m
Land use for 1 reactor	5.97 × 5.97 = 35.6 m ²
Land use for 6 reactors	35.6 × 6 = approximately 213.6 m ²

In this work, the power requirement for mixing the reactor contents was calculated based on the website from CheCalc [192].

Reactor Geometry

Liquid volume in reactor	403.3 m ³ (obtained from Scenario III)
Agitator	Pitched blade
Agitator diameter to tank diameter ratio	0.4
Scale of agitation	3

Fluid Properties

Density of liquid	989.7 kg/m ³ (obtained from Aspen Plus)
Viscosity of liquid	0.739 cP [206]

Result

Motor Power requirement	5 kW
-------------------------	------

Exergy analysis

Table C14 Summary of Gibbs free energy of components that unknown specific chemical exergy

Chemical	Formula	Specific Gibbs free energy (kJ/mol)
Dimethyl sulfoxide	C ₂ H ₆ O ₅	-251.75
Succinic acid	C ₄ H ₆ O ₄	-548.68
Tripalmitin	C ₅₁ H ₉₈ O ₆	-325.66

According to the table above, the specific Gibbs free energy data was obtained from Chemeo [207]. This values were used in the chemical exergy calculations by Exergoecology [208] as seen in Table C15.

Table C15 Specific chemical exergy of the chemical components in the SA production

Chemical	ex_{chj}^0 (kJ/mol)	References
Acetic acid	1.03E+03	[209]
Ammonia	3.38E+02	[209]
Carbon dioxide	1.99E+01	[209]
Dimethyl sulfoxide	1.89E+03	[208]
Formic acid	1.19E+03	[151]
Glycerol	1.76E+03	[210]
Hydrogen	2.36E+02	[209]
Microorganism	6.17E+02	[209]
Nitrogen	7.20E-01	[209]
Oxygen	3.97E+00	[209]
Sodium chloride	5.33E+00	[208]
Sodium hydroxide	3.85E+01	[208]
Succinic acid	1.81E+03	[208]
Tripalmitin	3.18E+04	[208]
Water	9.00E-01	[209]
Methanol	7.22E+02	[211]

APPENDIX D

SUPPLEMENTARY INFORMATION OF CHAPTER 6

Fermenter design

Example of Scenario I, the design of the fermentation tank was undertaken using fermenters of 70 m³. The calculation of height and diameter was exemplified as follows.

Calculation example

Reactor size	70 m ³
Height to diameter ratio	3
Diameter	$\left(\frac{\text{reactor size} \times 4}{3\pi}\right)^{1/3} = 3.1 \text{ m}$
Height	3 × 3.1 = 9.3 m
Land use for 1 reactor	3.1 × 3.1 = 9.61 m ²
Land use for 10 reactors	9.61 × 10 = approximately 96.1 m ²

In this work, the power requirement for mixing the reactor contents was calculated based on the website from CheCalc [192].

Reactor Geometry

Liquid volume in reactor	44.77 m ³ (obtained from Scenario I)
Agitator	Pitched blade
Agitator diameter to tank diameter ratio	0.4
Scale of agitation	3

Fluid Properties

Density of liquid	989.7 kg/m ³ (obtained from Aspen Plus)
Viscosity of liquid	0.954 cP [206]

Result

Motor Power requirement	1.16 kW
-------------------------	---------

Table D1 Summary of impact assessment in Scenario I

Impact category	Global warming		Terrestrial ecotoxicity		Human non-carcinogenic toxicity		Land use		Fossil resource scarcity		Water consumption	
	kg CO ₂ eq	kg 1,4-DCB	kg 1,4-DCB	kg 1,4-DCB	kg 1,4-DCB	m ² a crop eq	kg oil eq	m ³				
Unit												
Total	4.104	5.592	1.424	4.823	2.008	2.803						
DHA from refined glycerol	0.000	0.000	0.000	0.000	0.000	2.703						
refined glycerol	1.867	1.997	0.344	4.738	0.997	0.062						
Tap water {RER} market group for Cut-off, S	0.007	0.021	0.008	0.000	0.002	0.020						
Ammonia, anhydrous, liquid {SAS} ammonia production, steam reforming, liquid Cut-off, S	0.001	0.001	0.000	0.000	0.000	0.000						
Sodium hydroxide, without water, in 50% solution state {GLO} market for Cut-off, S	0.015	0.065	0.018	0.000	0.004	0.000						
Methanol {GLO} market for Cut-off, S	0.152	0.192	0.048	0.003	0.166	0.001						
Acetone, liquid {GLO} market for Cut-off, S	1.053	0.844	0.256	0.004	0.602	0.013						
Electricity, medium voltage {TH} market for Cut-off, S	0.039	0.021	0.031	0.000	0.011	0.000						
Heat, central or small-scale, biomethane {GLO} market group for heat, central or small-scale, biomethane Cut-off, S	0.972	2.451	0.718	0.078	0.227	0.004						

Table D2 Summary of impact assessment in Scenario II

Impact category	Global warming		Terrestrial ecotoxicity		Human non-carcinogenic toxicity		Land use		Fossil resource scarcity		Water consumption	
	kg CO ₂ eq	kg 1,4-DCB	kg 1,4-DCB	kg 1,4-DCB	kg 1,4-DCB	m ² a crop eq	kg oil eq	m ³				
Unit	kg CO ₂ eq	kg 1,4-DCB	kg 1,4-DCB	kg 1,4-DCB	kg 1,4-DCB	m ² a crop eq	kg oil eq	m ³				
Total	3.935	5.332	1.539	6.997	1.387	3.288						
DHA from crude glycerol	0.000	0.000	0.000	0.000	0.000	0.000	0.000	3.151				
Glycerol, at biodiesel plant/kg/RNA	1.252	0.642	0.133	6.879	0.262	0.087						
Tap water {RER} market group for Cut-off, S	0.010	0.031	0.012	0.000	0.003	0.029						
Ammonia, anhydrous, liquid {SAS} ammonia production, steam reforming, liquid Cut-off, S	0.017	0.020	0.004	0.000	0.006	0.000						
Sodium hydroxide, without water, in 50% solution state {GLO} market for Cut-off, S	0.021	0.094	0.026	0.001	0.005	0.001						
Methanol {GLO} market for Cut-off, S	0.162	0.205	0.051	0.003	0.177	0.001						
Acetone, liquid {GLO} market for Cut-off, S	1.045	0.838	0.255	0.004	0.598	0.013						
Electricity, medium voltage {TH} market for Cut-off, S	0.050	0.028	0.040	0.000	0.014	0.000						
Heat, central or small-scale, biomethane {GLO} market group for heat, central or small-scale, biomethane Cut-off, S	1.377	3.474	1.018	0.110	0.321	0.006						

Table D4 Summary of impact assessment in Scenario IV

Impact category	Global warming		Terrestrial ecotoxicity		Human non-carcinogenic toxicity		Land use		Fossil resource scarcity		Water consumption	
	Unit	kg CO ₂ eq	kg 1,4-DCB	kg 1,4-DCB	kg 1,4-DCB	m ² crop eq	kg oil eq	m ³				
Total		3.848	5.894	1.709	5.015	1.365	2.314					
DHA from glucose + glycerol		0.000	0.000	0.000	0.000	0.000	2.192					
Glycerol, at biodiesel plant/kg/RNA		0.887	0.455	0.094	4.871	0.186	0.062					
Tap water {RER} market group for Cut-off, S		0.012	0.040	0.015	0.000	0.003	0.038					
Ammonia, anhydrous, liquid {SAS} ammonia production, steam reforming, liquid Cut-off, S		0.001	0.001	0.000	0.000	0.000	0.000					
Sodium hydroxide, without water, in 50% solution state {GLO} market for Cut-off, S		0.010	0.045	0.012	0.000	0.003	0.000					
Methanol {GLO} market for Cut-off, S		0.152	0.191	0.047	0.003	0.166	0.001					
Acetone, liquid {GLO} market for Cut-off, S		1.053	0.844	0.257	0.004	0.603	0.013					
Electricity, medium voltage {TH} market for Cut-off, S		0.027	0.015	0.022	0.000	0.008	0.000					
Heat, central or small-scale, biomethane {GLO} market group for heat, central or small-scale, biomethane Cut-off, S		1.706	4.303	1.261	0.136	0.398	0.007					

Table D5 Summary of impact assessment in Scenario V

Impact category	Global warming		Terrestrial ecotoxicity		Human non-carcinogenic toxicity		Land use		Fossil resource scarcity		Water consumption	
	kg CO ₂ eq	kg 1,4-DCB	kg 1,4-DCB	kg 1,4-DCB	kg 1,4-DCB	m ² a crop eq	kg oil eq	m ³				
Unit												
Total	3.822	5.673	1.638	5.386	1.361	2.190						
DHA from sorbitol + glycerol	0.000	0.000	0.000	0.000	0.000	2.067						
Glycerol, at biodiesel plant/kg/RNA	0.956	0.490	0.102	5.251	0.200	0.067						
Tap water {RER} market group for Cut-off, S	0.012	0.037	0.014	0.000	0.003	0.035						
Ammonia, anhydrous, liquid {SAS} ammonia production, steam reforming, liquid Cut-off, S	0.016	0.019	0.004	0.000	0.006	0.000						
Sodium hydroxide, without water, in 50% solution state {GLO} market for Cut-off, S	0.011	0.049	0.013	0.000	0.003	0.000						
Methanol {GLO} market for Cut-off, S	0.154	0.194	0.048	0.003	0.168	0.001						
Acetone, liquid {GLO} market for Cut-off, S	1.051	0.843	0.256	0.004	0.602	0.013						
Electricity, medium voltage {TH} market for Cut-off, S	0.026	0.014	0.021	0.000	0.007	0.000						
Heat, central or small-scale, biomethane {GLO} market group for heat, central or small-scale, biomethane Cut-off, S	1.596	4.027	1.180	0.127	0.372	0.007						

Table D6 Summary of impact assessment in Scenario VI

Impact category	Global warming		Terrestrial ecotoxicity		Human non-carcinogenic toxicity		Land use		Fossil resource scarcity		Water consumption	
	kg CO ₂ eq	kg 1,4-DCB	kg 1,4-DCB	kg 1,4-DCB	kg 1,4-DCB	m ² crop eq	m ² crop eq	kg oil eq	kg oil eq	m ³	m ³	
Unit												
Total	15.99	424.03	73.15	11.18	4.226	1.383						
DHA from catalytic oxidation	0.000	0.000	0.000	0.000	0.000	0.872						
Glycerol, at biodiesel plant/kg/RNA	1.841	0.944	0.196	10.11	0.385	0.129						
Tap water {RER} market group for Cut-off, S	0.095	0.308	0.119	0.003	0.025	0.291						
Methanol {GLO} market for Cut-off, S	0.167	0.211	0.052	0.003	0.182	0.001						
Acetone, liquid {GLO} market for Cut-off, S	1.055	0.846	0.257	0.004	0.604	0.013						
Copper oxide {GLO} market for Cut-off, S	0.858	392.4	63.64	0.134	0.216	0.025						
Electricity, medium voltage {TH} market for Cut-off, S	0.428	0.236	0.344	0.003	0.122	0.002						
Heat, central or small-scale, biomethane {GLO} market group for heat, central or small-scale, biomethane Cut-off, S	11.54	29.12	8.534	0.921	2.691	0.050						

Table D7 Description of unit operation in Scenarios I and II

Unit	Process Description	Equipment type	Model	Operating Conditions	Design comment
M-100	Liquid mixing tank	Agitated tank-enclosed	Mixer	Pressure drop: 0 atm	
E-100	Sterilization	Fixed tube sheet heat exchanger	Heater	Outlet temperature: 121°C Pressure drop: 0 atm	- Conditions based on the work of Jittjant et al. [138]
E-101	Feedstock cooler	Fixed tube sheet heat exchanger	Heater	Outlet temperature: 80°C Pressure drop: 0 atm	- The cost of equipment, installation and utilities are calculated to determine the optimal temperature.
E-102	Feedstock cooler	Fixed tube sheet heat exchanger	Heater	Outlet temperature: 30°C Pressure drop: 0 atm	- The cost of equipment, installation and utilities are calculated to determine the optimal temperature.
R-100	Fermentation	Agitated tank-enclosed and jacketed	RStoic	Temperature: 30°C Pressure drop: 0 atm Reaction: For Scenario I (Refined glycerol) GLY + 0.001 NH ₃ + 0.5111 O ₂ → 0.992 DHA + 0.003 GA + 0.006 MICROOR + 0.01 CO ₂ + 1.012 H ₂ O For Scenario II (Crude glycerol) GLY + 0.016 NH ₃ + 0.876 O ₂ → 0.695 DHA + 0.181 GA + 0.081 MICROOR + 0.289 CO ₂ + 1.322 H ₂ O	- The reactor operates isothermally ($\Delta T > 15\%$ of T_{inlet}). - Reaction based on the work of Jittjant et al. [138] - The stoichiometric coefficients were employed to describe the reaction in fermenter. - Assumed 100 % conversion of glycerol
D-100	Gas separation	Vertical process vessel	Flash2	Pressure drop: 0 atm Duty: 0	
S-100	Microorganism removal	Tubular cross-flow filter	CFilter	Pressure drop: 0 atm Solids to solid outlet: 1 Liquid load of solids outlet: 0.3	- Conditions based on the work of Nieder-Heitmann [154]
E-103	Evaporator	Fixed tube sheet heat exchanger	Heater	Outlet temperature: 101.85°C Pressure drop: 0 atm	- Temperature was obtained from the design spec.
D-101	Evaporator	Vertical process vessel	Flash2	Pressure drop: 0 atm Duty: 0	
P-100	Pump	Centrifugal pump	Pump	Outlet pressure: 2.5 atm	
C-100	Water separation	Distillation column	Radfrac	1 st stage pressure: 2 atm	- Flash model was used to determine the bubble

Unit	Process Description	Equipment type	Model	Operating Conditions	Design comment
		(Total condenser)		pressure drop: 0.5 atm Number of stages: 45 Feed stage: 22 Condenser: Total Reboiler: Kettle For Scenario I (Refined glycerol) Distillate rate: 800.23 kg/h Molar reflux ratio: 0.0195 For Scenario II (Crude glycerol) Distillate rate: 992.6 kg/h Molar reflux ratio: 0.0197	point pressure. - The shortcut distillation model (DSTWU) was used for preliminary specifications. The optimum distillate rate and molar reflux ratio were obtained from the design spec.
V-100	Valve	Pressure reducing valve	Valve	Outlet pressure: 1 atm	
E-106	Crystallization	U-tube exchanger	Heater	Outlet temperature: 5°C Pressure drop: 0 atm	- Temperature based on the work of Martinez-Gallegos et al. [196]
M-101	Liquid mixing tank	Agitated tank-enclosed	Mixer	Pressure drop: 0 atm Temperature: 5°C	
CR-100	Crystallization	Oslo growth type crystallizer	Crystallizer	Pressure: 1 atm DHA → DHACRYS (Dihydroxyacetone crystal: Solid) Solubility is concentration data with 78.96 gm/L at 5°C	- Solubility was obtained on the work of Martinez-Gallegos et al. [196]
S-101	Crystal separation	Vertical process vessel	Sep	DHACRYS 100 % separation	
E-107	Methanol recovery	U-tube exchanger	Heater	For Scenario I (Refined glycerol) Outlet temperature: 99.2°C Pressure drop: 0 atm For Scenario II (Crude glycerol) Outlet temperature: 113.9°C Pressure drop: 0 atm	- Temperature was obtained from the design spec.
D-103	Methanol recovery	Vertical process vessel	Flash2	Pressure drop: 0 atm Duty: 0	
E-108	Methanol cooler	U-tube exchanger	Heater	Outlet temperature: 5°C	

Unit	Process Description	Equipment type	Model	Operating Conditions	Design comment
M-102	Liquid mixing tank	Agitated tank-enclosed	Mixer	Pressure drop: 0 atm	
E-109	Acetone heater	U-tube exchanger	Heater	Pressure drop: 0 atm Outlet temperature: 5°C Pressure drop: 0 atm	
SW-100	Washer	Rotary drum filter	SWash	Liquid to solid mass ratio: 1	- Condition based on the work of Lari et al. [197]
E-110	Air heater	U-tube exchanger	Heater	Outlet temperature: 130°C Pressure drop: 0 atm	- Temperature based on the work of Nieder-Heitmann [154]
DR-100	Dryer	Atmospheric tray batch dryer	Dryer	Operation mode: continuous Dryer type: shortcut Pressure drop: 0 atm Heat duty: 0 Moisture specification basis: WET	- Conditions based on the work of Nieder-Heitmann [154]
M-103	Liquid mixing tank	Agitated tank-enclosed	Mixer	Pressure drop: 0 atm	
D-104	Air separation	Vertical process vessel	Flash2	Pressure drop: 0 atm Duty: 0	

Table D8 Stream table of process in Scenario I (Refined glycerol as carbon source) (cont.)

Stream	37	38	39	40	41	42	43	44	45	46
Temperature (°C)	5.4	25.0	130.0	3.7	3.7	3.8	3.8	3.8	3.8	3.8
Pressure (atm)	1.0	1.0	1.0	1.0	1.0	1.0	1.0	1.0	1.0	1.0
Mass vapor fraction	0.000	1.000	1.000	0.814	0.000	0.578	1.000	0.000	0.000	0.000
Total flow (kg/h)	4.52E+02	4.52E+02	4.52E+02	6.75E+02	2.28E+02	9.54E+02	5.52E+02	4.03E+02	3.99E+02	4.03E+00
Component Mass Fractions										
Glycerol	0.000	0.000	0.000	0.000	0.000	0.000	0.000	0.000	0.000	0.000
H ₂ O	0.004	0.000	0.000	0.003	0.000	0.005	0.000	0.011	0.011	0.011
NH ₃	0.000	0.000	0.000	0.000	0.000	0.000	0.000	0.000	0.000	0.000
O ₂	0.000	0.210	0.210	0.140	0.000	0.099	0.172	0.000	0.000	0.000
CO ₂	0.000	0.010	0.010	0.007	0.000	0.005	0.008	0.000	0.000	0.000
N ₂	0.000	0.780	0.780	0.522	0.000	0.369	0.638	0.001	0.001	0.001
DHA	0.005	0.000	0.000	0.003	0.000	0.005	0.000	0.012	0.012	0.012
GA	0.000	0.000	0.000	0.000	0.000	0.000	0.000	0.000	0.000	0.000
NaOH	0.000	0.000	0.000	0.000	0.000	0.000	0.000	0.000	0.000	0.000
Methanol	0.043	0.000	0.000	0.027	0.005	0.044	0.012	0.089	0.089	0.089
Acetone	0.447	0.000	0.000	0.298	0.005	0.472	0.169	0.887	0.887	0.887
NaCl	0.000	0.000	0.000	0.000	0.000	0.000	0.000	0.000	0.000	0.000
Tripalmitin	0.000	0.000	0.000	0.000	0.000	0.000	0.000	0.000	0.000	0.000
Microorganism	0.000	0.000	0.000	0.000	0.000	0.000	0.000	0.000	0.000	0.000
DHA (solid)	0.500	0.000	0.000	0.000	0.990	0.000	0.000	0.000	0.000	0.000

Table D9 Stream table of process in Scenario II (Crude glycerol as carbon source) (cont.)

Stream	37	38	39	40	41	42	43	44	45	46
Temperature (°C)	5.4	25.0	130.0	4.0	4.0	3.9	3.9	3.9	3.9	3.9
Pressure (atm)	1.0	1.0	1.0	1.0	1.0	1.0	1.0	1.0	1.0	1.0
Mass vapor fraction	0.000	1.000	1.000	0.813	0.000	0.571	1.000	0.000	0.000	0.000
Total flow (kg/h)	4.52E+02	4.52E+02	4.52E+02	6.75E+02	2.28E+02	9.65E+02	5.51E+02	4.14E+02	4.09E+02	4.14E+00
Component Mass Fractions										
Glycerol	0.000	0.000	0.000	0.000	0.000	0.000	0.000	0.000	0.000	0.000
H ₂ O	0.005	0.000	0.000	0.003	0.000	0.005	0.000	0.011	0.011	0.011
NH ₃	0.000	0.000	0.000	0.000	0.000	0.000	0.000	0.000	0.000	0.000
O ₂	0.000	0.210	0.210	0.140	0.000	0.098	0.172	0.000	0.000	0.000
CO ₂	0.000	0.010	0.010	0.007	0.000	0.005	0.008	0.000	0.000	0.000
N ₂	0.000	0.780	0.780	0.522	0.000	0.365	0.639	0.001	0.001	0.001
DHA	0.005	0.000	0.000	0.003	0.000	0.005	0.000	0.013	0.013	0.013
GA	0.008	0.000	0.000	0.006	0.000	0.009	0.000	0.021	0.021	0.021
NaOH	0.000	0.000	0.000	0.000	0.000	0.000	0.000	0.000	0.000	0.000
Methanol	0.043	0.000	0.000	0.027	0.005	0.045	0.012	0.089	0.089	0.089
Acetone	0.439	0.000	0.000	0.292	0.005	0.467	0.168	0.866	0.866	0.866
NaCl	0.000	0.000	0.000	0.000	0.000	0.000	0.000	0.000	0.000	0.000
Tripalmitin	0.000	0.000	0.000	0.000	0.000	0.000	0.000	0.000	0.000	0.000
Microorganism	0.000	0.000	0.000	0.000	0.000	0.000	0.000	0.000	0.000	0.000
DHA (solid)	0.500	0.000	0.000	0.000	0.990	0.000	0.000	0.000	0.000	0.000

Table D10 Description of unit operation in Scenario III

Unit	Process Description	Equipment type	Model	Operating Conditions	Design comment
S-100	Cation exchange resin	Vertical process vessel	Sep	NaCl 37 % separation Regeneration by 4 wt% HCl	- Conditions based on the work of Jittjant et al. [138]
S-101	Anion exchange resin	Vertical process vessel	Sep	NaCl 59 % separation Regeneration by 4 wt% NaOH	- Conditions based on the work of Jittjant et al. [138]
M-100	Liquid mixing tank	Agitated tank-enclosed	Mixer	Pressure drop: 0 atm	
E-100	Sterilization	Fixed tube sheet heat exchanger	Heater	Outlet temperature: 121°C Pressure drop: 0 atm	- Conditions based on the work of Jittjant et al. [138]
E-101	Feedstock cooler	Fixed tube sheet heat exchanger	Heater	Outlet temperature: 80°C Pressure drop: 0 atm	- The cost of equipment, installation and utilities are calculated to determine the optimal temperature.
E-102	Feedstock cooler	Fixed tube sheet heat exchanger	Heater	Outlet temperature: 30°C Pressure drop: 0 atm	- The cost of equipment, installation and utilities are calculated to determine the optimal temperature.
R-100	Fermentation	Agitated tank-enclosed and jacketed	RStoic	Temperature: 30°C Pressure drop: 0 atm Reaction: GLY + 0.003 NH ₃ + 0.620 O ₂ → 0.951 DHA + 0.004 GA + 0.016 MICROOR + 0.119 CO ₂ + 1.125 H ₂ O	- The reactor operates isothermally ($\Delta T > 15\%$ of T_{inlet}). - Reaction based on the work of Jittjant et al. [138] - The stoichiometric coefficients were employed to describe the reaction in fermenter. - Assumed 100 % conversion of glycerol
D-100	Gas separation	Vertical process vessel	Flash2	Pressure drop: 0 atm Duty: 0	
S-102	Microorganism removal	Tubular cross-flow filter	CFFilter	Pressure drop: 0 atm Solids to solid outlet: 1 Liquid load of solids outlet: 0.3	- Conditions based on the work of Nieder-Heitmann [154]

Unit	Process Description	Equipment type	Model	Operating Conditions	Design comment
E-103	Evaporator	Fixed tube sheet heat exchanger	Heater	Outlet temperature: 101.85°C Pressure drop: 0 atm	- Temperature was obtained from the design spec.
D-101	Evaporator	Vertical process vessel	Flash2	Pressure drop: 0 atm Duty: 0	
P-100	Pump	Centrifugal pump	Pump	Outlet pressure: 2.5 atm	
C-100	Water separation	Distillation column (Total condenser)	RadFrac	1 st stage pressure: 2 atm pressure drop: 0.5 atm Number of stages: 45 Feed stage: 22 Condenser: Total Reboiler: Kettle Distillate rate: 786.5 kg/h Molar reflux ratio: 0.0196	- Flash model was used to determine the bubble point pressure. - The shortcut distillation model (DSTWU) was used for preliminary specifications. The optimum distillate rate and molar reflux ratio were obtained from the design spec.
V-100	Valve	Pressure reducing valve	Valve	Outlet pressure: 1 atm	
E-106	Crystallization	U-tube exchanger	Heater	Outlet temperature: 5°C Pressure drop: 0 atm	- Temperature based on the work of Martinez-Gallegos et al. [196]
M-101	Liquid mixing tank	Agitated tank-enclosed	Mixer	Pressure drop: 0 atm	
CR-100	Crystallization	Oslo growth type crystallizer	Crystallizer	Temperature: 5°C Pressure: 1 atm DHA → DHACRYS (Dihydroxyacetone crystal: Solid) Solubility is concentration data with 78.96 gm/L at 5°C	- Solubility was obtained on the work of Martinez-Gallegos et al. [196]
S-103	Crystal separation	Vertical process vessel	Sep	DHACRYS 100 % separation	
E-107	Methanol recovery	U-tube exchanger	Heater	Outlet temperature: 99.58°C Pressure drop: 0 atm	- Temperature was obtained from the design spec.

Unit		Process Description		Equipment type		Model		Operating Conditions		Design comment
D-103	Methanol recovery	Vertical process vessel	Flash2	Pressure drop: 0 atm Duty: 0						
E-108	Methanol cooler	U-tube exchanger	Heater	Outlet temperature: 5°C Pressure drop: 0 atm						
M-102	Liquid mixing tank	Agitated tank-enclosed	Mixer	Pressure drop: 0 atm						
E-109	Acetone heater	U-tube exchanger	Heater	Outlet temperature: 5°C Pressure drop: 0 atm						
SW-100	Washer	Rotary drum filter	SWash	Liquid to solid mass ratio: 1					- Condition based on the work of Lari et al. [197]	
E-110	Air heater	U-tube exchanger	Heater	Outlet temperature: 130°C Pressure drop: 0 atm					- Temperature based on the work of Nieder-Heitmann [154]	
DR-100	Dryer	Atmospheric tray batch dryer	Dryer	Operation mode: continuous Dryer type: shortcut Pressure drop: 0 atm Heat duty: 0 Moisture specification basis: WET					- Conditions based on the work of Nieder-Heitmann [154]	
M-103	Liquid mixing tank	Agitated tank-enclosed	Mixer	Pressure drop: 0 atm						
D-104	Air separation	Vertical process vessel	Flash2	Pressure drop: 0 atm Duty: 0						

Table D11 Stream table of process in Scenario III (Treated glycerol as carbon source) (cont.)

Stream	43	44	45	46	47	48	49	50	51	52
Temperature (°C)	5.4	25.0	130.0	3.8	3.8	3.8	3.8	3.8	3.8	3.8
Pressure (atm)	1.0	1.0	1.0	1.0	1.0	1.0	1.0	1.0	1.0	1.0
Mass vapor fraction	0.000	1.000	1.000	0.814	0.000	0.578	1.000	0.000	0.000	0.000
Total flow (kg/h)	4.52E+02	4.52E+02	4.52E+02	6.75E+02	2.28E+02	9.54E+02	5.52E+02	4.03E+02	3.99E+02	4.03E+00
Component Mass Fractions										
Glycerol	0.000	0.000	0.000	0.000	0.000	0.000	0.000	0.000	0.000	0.000
H ₂ O	0.004	0.000	0.000	0.003	0.000	0.005	0.000	0.011	0.011	0.011
NH ₃	0.000	0.000	0.000	0.000	0.000	0.000	0.000	0.000	0.000	0.000
O ₂	0.000	0.210	0.210	0.140	0.000	0.099	0.172	0.000	0.000	0.000
CO ₂	0.000	0.010	0.010	0.007	0.000	0.005	0.008	0.000	0.000	0.000
N ₂	0.000	0.780	0.780	0.522	0.000	0.369	0.638	0.001	0.001	0.001
DHA	0.005	0.000	0.000	0.003	0.000	0.005	0.000	0.012	0.012	0.012
GA	0.000	0.000	0.000	0.000	0.000	0.000	0.000	0.000	0.000	0.000
NaOH	0.000	0.000	0.000	0.000	0.000	0.000	0.000	0.000	0.000	0.000
HCl	0.000	0.000	0.000	0.000	0.000	0.000	0.000	0.000	0.000	0.000
Methanol	0.043	0.000	0.000	0.027	0.005	0.044	0.012	0.089	0.089	0.089
Acetone	0.447	0.000	0.000	0.298	0.005	0.472	0.169	0.887	0.887	0.887
NaCl	0.000	0.000	0.000	0.000	0.000	0.000	0.000	0.000	0.000	0.000
Tripalmitin	0.000	0.000	0.000	0.000	0.000	0.000	0.000	0.000	0.000	0.000
Microorganism	0.000	0.000	0.000	0.000	0.000	0.000	0.000	0.000	0.000	0.000
DHA (solid)	0.500	0.000	0.000	0.000	0.990	0.000	0.000	0.000	0.000	0.000

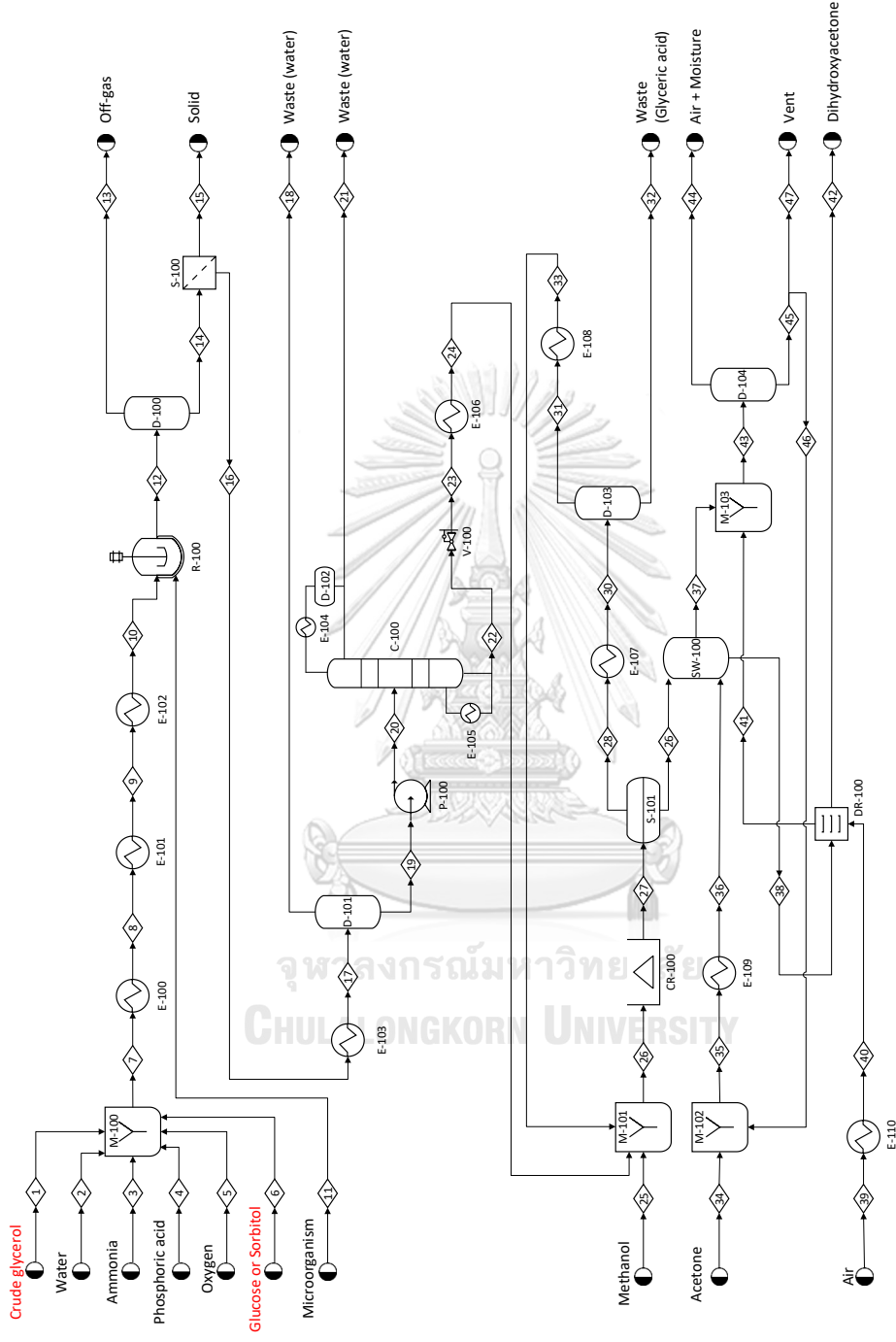


Figure D3 Process flow diagram of Scenarios IV and V

Table D12 Description of unit operation in Scenarios IV and V

Unit	Process Description	Equipment type	Model	Operating Conditions	Design comment
M-100	Liquid mixing tank	Agitated tank-enclosed	Mixer	Pressure drop: 0 atm	
E-100	Sterilization	Fixed tube sheet heat exchanger	Heater	Outlet temperature: 121°C Pressure drop: 0 atm	- Conditions based on the work of Lu et al. [55]
E-101	Feedstock cooler	Fixed tube sheet heat exchanger	Heater	Outlet temperature: 80°C Pressure drop: 0 atm	- The cost of equipment, installation and utilities are calculated to determine the optimal temperature.
E-102	Feedstock cooler	Fixed tube sheet heat exchanger	Heater	Outlet temperature: 30°C Pressure drop: 0 atm	- The cost of equipment, installation and utilities are calculated to determine the optimal temperature.
R-100	Fermentation	Agitated tank-enclosed and jacketed	RStoic	Temperature: 30°C Pressure drop: 0 atm Reaction: For Scenario IV GLY + 0.046 glucose + 0.002 NH ₃ + 0.78 O ₂ → 0.997 DHA + 0.0004 GA + 0.007 MICROOR + 0.277 CO ₂ + 1.28 H ₂ O For Scenario V GLY + 0.036 sorbitol + 0.019 NH ₃ + 0.78 O ₂ → 0.92 DHA + 0.043 GA + 0.098 MICROOR + 0.234 CO ₂ + 1.308 H ₂ O	- The reactor operates isothermally ($\Delta T > 15\%$ of T_{inlet}). - Reaction based on the work of Lu et al. [55] - The stoichiometric coefficients were employed to describe the reaction in fermenter. - Assumed 100 % conversion of glycerol
D-100	Gas separation	Vertical process vessel	Flash2	Pressure drop: 0 atm Duty: 0	
S-100	Microorganism removal	Tubular cross-flow filter	CFilter	Pressure drop: 0 atm	- Conditions based on the work of Nieder-

Unit	Process Description	Equipment type	Model	Operating Conditions	Design comment
				Solids to solid outlet: 1 Liquid load of solids outlet: 0.3	Heitmann [154]
E-103	Evaporator	Fixed tube sheet heat exchanger	Heater	Outlet temperature: 101.85°C Pressure drop: 0 atm	- Temperature was obtained from the design spec.
D-101	Evaporator	Vertical process vessel	Flash2	Pressure drop: 0 atm Duty: 0	
P-100	Pump	Centrifugal pump	Pump	Outlet pressure: 2.5 atm	
C-100	Water separation	Distillation column (Total condenser)	RadFrac	1 st stage pressure: 2 atm pressure drop: 0.5 atm Number of stages: 45 Feed stage: 22 Condenser: Total Reboiler: Kettle For Scenario IV Distillate rate: 772 kg/h Molar reflux ratio: 0.02 For Scenario V Distillate rate: 811 kg/h Molar reflux ratio: 0.02	- Flash model was used to determine the bubble point pressure. - The shortcut distillation model (DSTWU) was used for preliminary specifications. The optimum distillate rate and molar reflux ratio were obtained from the design spec.
V-100	Valve	Pressure reducing valve	Valve	Outlet pressure: 1 atm	
E-106	Crystallization	U-tube exchanger	Heater	Outlet temperature: 5°C Pressure drop: 0 atm	- Temperature based on the work of Martínez-Gallegos et al. [196]
M-101	Liquid mixing tank	Agitated tank-enclosed	Mixer	Pressure drop: 0 atm	

Unit	Process Description	Equipment type	Model	Operating Conditions	Design comment
CR-100	Crystallization	Oslo growth type crystallizer	Crystallizer	Temperature: 5°C Pressure: 1 atm DHA → DHACRYS (Dihydroxyacetone crystal: Solid) Solubility is concentration data with 78.96 gm/L at 5°C	- Solubility was obtained on the work of Martínez-Gallegos et al. [196]
S-101	Crystal separation	Vertical process vessel	Sep	DHACRYS 100 % separation	
E-107	Methanol recovery	U-tube exchanger	Heater	For Scenario IV Outlet temperature: 98.4°C Pressure drop: 0 atm For Scenario V Outlet temperature: 102.1°C Pressure drop: 0 atm	- Temperature was obtained from the design spec.
D-103	Methanol recovery	Vertical process vessel	Flash2	Pressure drop: 0 atm Duty: 0	
E-108	Methanol cooler	U-tube exchanger	Heater	Outlet temperature: 5°C Pressure drop: 0 atm	
M-102	Liquid mixing tank	Agitated tank-enclosed	Mixer	Pressure drop: 0 atm	
E-109	Acetone heater	U-tube exchanger	Heater	Outlet temperature: 5°C Pressure drop: 0 atm	
SW-100	Washer	Rotary drum filter	SWash	Liquid to solid mass ratio: 1	- Condition based on the work of Lari et al. [197]
E-110	Air heater	U-tube exchanger	Heater	Outlet temperature: 130°C Pressure drop: 0 atm	- Temperature based on the work of Nieder-Heitmann [154]

Unit	Process Description	Equipment type	Model	Operating Conditions	Design comment
DR-100	Dryer	Atmospheric tray batch dryer	Dryer	Operation mode: continuous Dryer type: shortcut Pressure drop: 0 atm Heat duty: 0 Moisture specification basis: WET	- Conditions based on the work of Nieder-Heitmann [154]
M-103	Liquid mixing tank	Agitated tank-enclosed	Mixer	Pressure drop: 0 atm	
D-104	Air separation	Vertical process vessel	Flash2	Pressure drop: 0 atm Duty: 0	

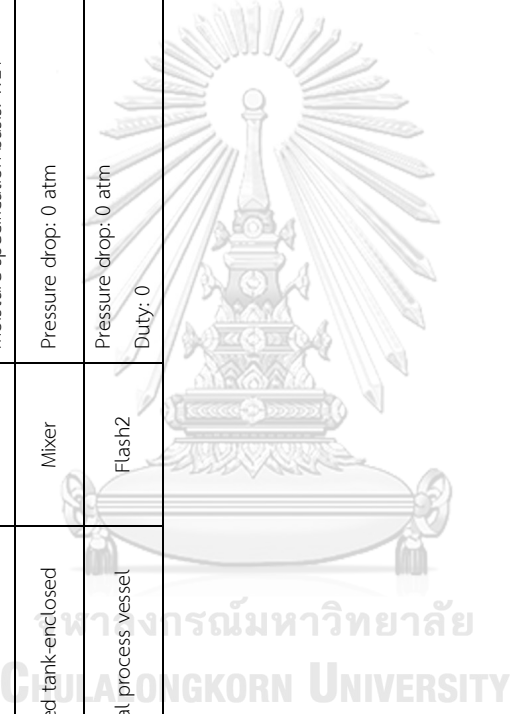


Table D13 Stream table of process in Scenario IV (cont.)

Stream	37	38	39	40	41	42	43	44	45	46	47
Temperature (°C)	5.4	5.4	25.0	130.0	3.7	3.7	3.8	3.8	3.8	3.8	3.8
Pressure (atm)	1.0	1.0	1.0	1.0	1.0	1.0	1.0	1.0	1.0	1.0	1.0
Mass vapor fraction	0.000	0.000	1.000	1.000	0.814	0.000	0.578	1.000	0.000	0.000	0.000
Total flow (kg/h)	2.79E+02	4.52E+02	4.52E+02	4.52E+02	6.75E+02	2.28E+02	9.54E+02	5.52E+02	4.03E+02	3.99E+02	4.03E+00
Component Mass Fractions											
Glycerol	0.000	0.000	0.000	0.000	0.000	0.000	0.000	0.000	0.000	0.000	0.000
H ₂ O	0.009	0.004	0.000	0.000	0.003	0.000	0.005	0.000	0.011	0.011	0.011
NH ₃	0.000	0.000	0.000	0.000	0.000	0.000	0.000	0.000	0.000	0.000	0.000
O ₂	0.000	0.000	0.000	0.000	0.000	0.000	0.000	0.000	0.000	0.000	0.000
CO ₂	0.000	0.000	0.210	0.210	0.140	0.000	0.099	0.172	0.000	0.000	0.000
N ₂	0.000	0.000	0.010	0.010	0.007	0.000	0.005	0.008	0.000	0.000	0.000
DHA	0.000	0.000	0.780	0.780	0.522	0.000	0.369	0.638	0.001	0.001	0.001
GA	0.010	0.005	0.000	0.000	0.003	0.000	0.005	0.000	0.012	0.012	0.012
NaOH	0.000	0.000	0.000	0.000	0.000	0.000	0.000	0.000	0.000	0.000	0.000
HCl	0.000	0.000	0.000	0.000	0.000	0.000	0.000	0.000	0.000	0.000	0.000
Methanol	0.086	0.043	0.000	0.000	0.027	0.005	0.044	0.012	0.089	0.089	0.089
Acetone	0.895	0.447	0.000	0.000	0.298	0.005	0.472	0.169	0.887	0.887	0.887
NaCl	0.000	0.000	0.000	0.000	0.000	0.000	0.000	0.000	0.000	0.000	0.000
Tripalmitin	0.000	0.000	0.000	0.000	0.000	0.000	0.000	0.000	0.000	0.000	0.000
Microorganism	0.000	0.000	0.000	0.000	0.000	0.000	0.000	0.000	0.000	0.000	0.000
DHA (solid)	0.000	0.500	0.000	0.000	0.000	0.990	0.000	0.000	0.000	0.000	0.000

Table D14 Stream table of process in Scenario V (cont.)

Stream	37	38	39	40	41	42	43	44	45	46	47
Temperature (°C)	5.4	5.4	25.0	130.0	3.8	3.8	3.8	3.8	3.8	3.8	3.8
Pressure (atm)	1.0	1.0	1.0	1.0	1.0	1.0	1.0	1.0	1.0	1.0	1.0
Mass vapor fraction	0.000	0.000	1.000	1.000	0.814	0.000	0.577	1.000	0.000	0.000	0.000
Total flow (kg/h)	2.81E+02	4.52E+02	4.52E+02	4.52E+02	6.75E+02	2.28E+02	9.56E+02	5.52E+02	4.05E+02	4.01E+02	4.05E+00
Component Mass Fractions											
Glycerol	0.000	0.000	0.000	0.000	0.000	0.000	0.000	0.000	0.000	0.000	0.000
H ₂ O	0.009	0.004	0.000	0.000	0.003	0.000	0.005	0.000	0.011	0.011	0.011
NH ₃	0.000	0.000	0.000	0.000	0.000	0.000	0.000	0.000	0.000	0.000	0.000
O ₂	0.000	0.000	0.000	0.000	0.000	0.000	0.000	0.000	0.000	0.000	0.000
CO ₂	0.000	0.000	0.210	0.210	0.140	0.000	0.099	0.172	0.000	0.000	0.000
N ₂	0.000	0.000	0.010	0.010	0.007	0.000	0.005	0.008	0.000	0.000	0.000
DHA	0.000	0.000	0.780	0.780	0.522	0.000	0.369	0.638	0.001	0.001	0.001
GA	0.010	0.005	0.000	0.000	0.003	0.000	0.005	0.000	0.012	0.012	0.012
NaOH	0.003	0.002	0.000	0.000	0.001	0.000	0.002	0.000	0.004	0.004	0.004
HCl	0.000	0.000	0.000	0.000	0.000	0.000	0.000	0.000	0.000	0.000	0.000
Methanol	0.086	0.043	0.000	0.000	0.027	0.005	0.045	0.012	0.089	0.089	0.089
Acetone	0.892	0.446	0.000	0.000	0.297	0.005	0.471	0.169	0.883	0.883	0.883
NaCl	0.000	0.000	0.000	0.000	0.000	0.000	0.000	0.000	0.000	0.000	0.000
Tripalmitin	0.000	0.000	0.000	0.000	0.000	0.000	0.000	0.000	0.000	0.000	0.000
Microorganism	0.000	0.000	0.000	0.000	0.000	0.000	0.000	0.000	0.000	0.000	0.000
DHA (solid)	0.000	0.500	0.000	0.000	0.000	0.990	0.000	0.000	0.000	0.000	0.000

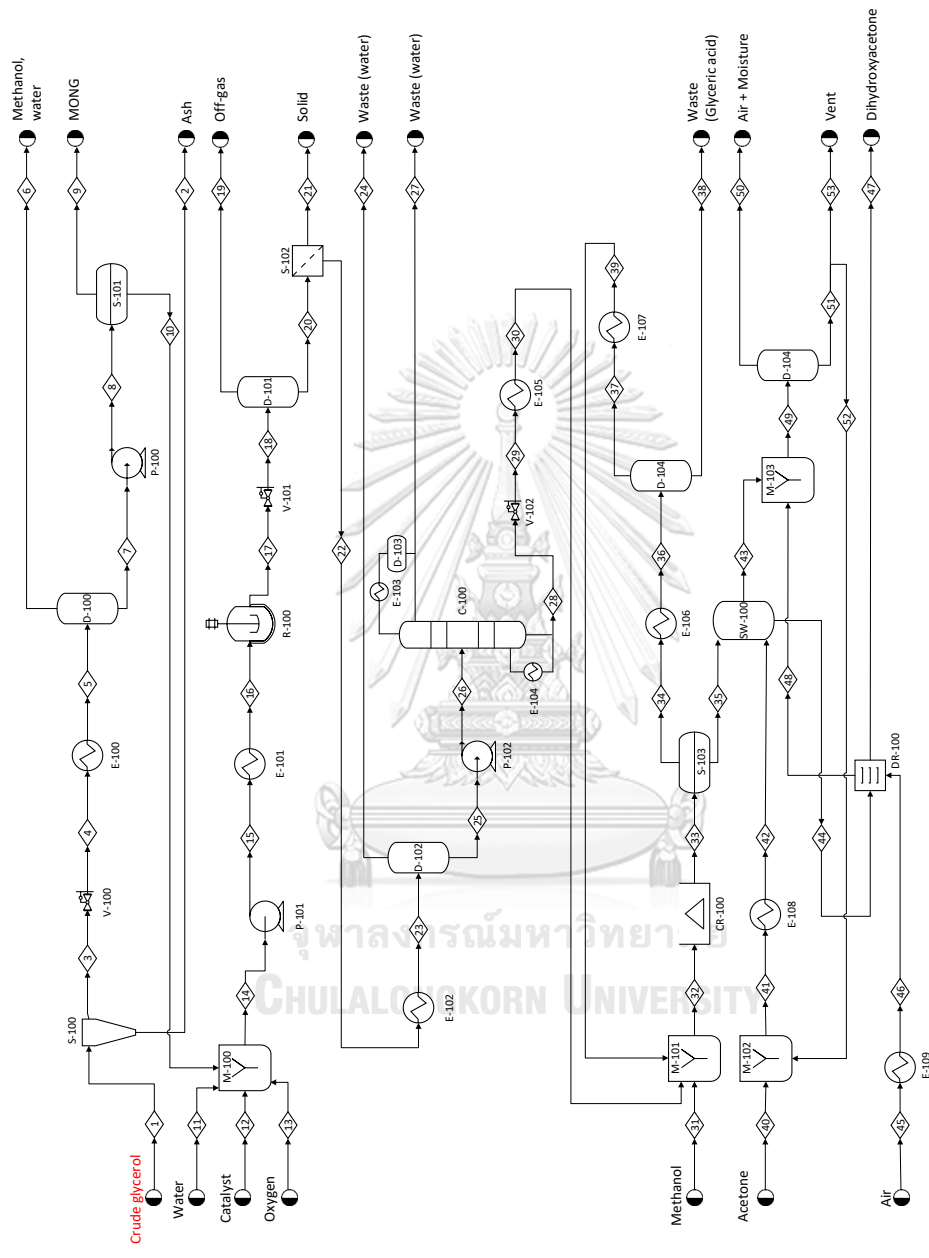


Figure D4 Process flow diagram of Scenario VI

Table D15 Description of unit operation in Scenario VI

Unit	Process Description	Equipment type	Model	Operating Conditions	Design comment
S-100	Ash removal	Splitter	SSplit	Split fraction MIXED stream: 0.99 CISOLID stream: 0.01	- Conditions based on the work of Ding [203]
V-100	Valve	Pressure reducing valve	Valve	Outlet pressure: 0.1 atm	- Pressure based on the patent of Chang [189]
E-100	Methanol and water separation	U-tube exchanger	Heater	Outlet temperature: 95°C Pressure drop: 0 atm	- Temperature based on the patent of Chang [189]
D-100	Gas separation	Vertical process vessel	Flash2	Pressure drop: 0 atm Duty: 0	
P-100	Pump	Centrifugal pump	Pump	Outlet pressure: 1 atm	
S-101	MONG removal	Vertical process vessel	Sep	MONG 99 % separation	- Removal data is performed based on the work of Ding [203]
M-100	Liquid mixing tank	Agitated tank-enclosed	Mixer	Pressure drop: 0 atm	
P-101	Pump	Centrifugal pump	Pump	Outlet pressure: 10 atm	- Pressure based on the work of Liu et al. [199]
E-101	Heating	Fixed tube sheet heat exchanger	Heater	Outlet temperature: 50°C Pressure drop: 0 atm Temperature: 50°C Pressure drop: 0 atm	- Temperature based on the work of Liu et al. [199]
R-100	Catalytic oxidation	Agitated tank-enclosed and jacketed	RStoic	Reaction: $GLY + 0.5 O_2 \rightarrow DHA + H_2O$ (100 % conversion of GLY) $DHA + 1.5 O_2 \rightarrow GCA + CO_2 + H_2O$ (29.4 % conversion of DHA) $GCA + O_2 \rightarrow OXA + H_2O$ (95.2 % conversion of GCA) $OXA + 0.5 O_2 \rightarrow 2 CO_2 + H_2O$ (99.3 % conversion of OXA)	- The reactor operates isothermally ($\Delta T > 15\%$ of T_{inlet}). - Reaction based on the work of Liu et al. [199]
V-101	Valve	Pressure reducing valve	Valve	Outlet pressure: 1 atm	

Unit	Process Description	Equipment type	Model	Operating Conditions	Design comment
D-101	Gas separation	Vertical process vessel	Flash2	Pressure drop: 0 atm Duty: 0	
S-102	Microorganism removal	Tubular cross-flow filter	CFilter	Pressure drop: 0 atm Solids to solid outlet: 1 Liquid load of solids outlet: 0.3	- Conditions based on the work of Nieder-Heitmann [154]
E-102	Evaporator	Fixed tube sheet heat exchanger	Heater	Outlet temperature: 101.85°C Pressure drop: 0 atm	- Temperature was obtained from the design spec.
D-102	Evaporator	Vertical process vessel	Flash2	Pressure drop: 0 atm Duty: 0	
P-102	Pump	Centrifugal pump	Pump	Outlet pressure: 2.5 atm	
C-100	Water separation	Distillation column (Total condenser)	RadFrac	1 st stage pressure: 2 atm pressure drop: 0.5 atm Number of stages: 45 Feed stage: 22 Condenser: Total Reboiler: Kettle Distillate rate: 781.7 kg/h Molar reflux ratio: 0.019	- Flash model was used to determine the bubble point pressure. - The shortcut distillation model (DSTWU) was used for preliminary specifications. The optimum distillate rate and molar reflux ratio were obtained from the design spec.
V-102	Valve	Pressure reducing valve	Valve	Outlet pressure: 1 atm	
E-105	Crystallization	U-tube exchanger	Heater	Outlet temperature: 5°C Pressure drop: 0 atm	- Temperature based on the work of Martinez-Gallegos et al. [196]
M-101	Liquid mixing tank	Agitated tank-enclosed	Mixer	Pressure drop: 0 atm	
CR-100	Crystallization	Oslo growth type crystallizer	Crystallizer	Temperature: 5°C Pressure: 1 atm DHA → DHACRYS (Dihydroxyacetone crystal:Solid) Solubility is concentration data with 78.96 gm/L at 5°C	- Solubility was obtained on the work of Martinez-Gallegos et al. [196]
S-103	Crystal separation	Vertical process vessel	Sep	DHACRYS 100 % separation	
E-106	Methanol recovery	U-tube exchanger	Heater	Outlet temperature: 102.2°C	- Temperature was obtained from the design spec.

Unit		Process Description		Equipment type		Model		Operating Conditions		Design comment	
D-104	Methanol recovery	Vertical process vessel	Flash2					Pressure drop: 0 atm			
E-107	Methanol cooler	U-tube exchanger	Heater					Pressure drop: 0 atm Duty: 0			
M-102	Liquid mixing tank	Agitated tank-enclosed	Mixer					Outlet temperature: 5°C Pressure drop: 0 atm			
E-108	Acetone heater	U-tube exchanger	Heater					Pressure drop: 0 atm Outlet temperature: 5°C			
SW-100	Washer	Rotary drum filter	SWash					Liquid to solid mass ratio: 1			- Condition based on the work of Lari et al. [197]
E-109	Air heater	U-tube exchanger	Heater					Outlet temperature: 130°C Pressure drop: 0 atm			- Temperature based on the work of Nieder-Heitmann [154]
DR-100	Dryer	Atmospheric tray batch dryer	Dryer					Operation mode: continuous Dryer type: shortcut Pressure drop: 0 atm Heat duty: 0 Moisture specification basis: WET			- Conditions based on the work of Nieder-Heitmann [154]
M-103	Liquid mixing tank	Agitated tank-enclosed	Mixer					Pressure drop: 0 atm			
D-105	Air separation	Vertical process vessel	Flash2					Pressure drop: 0 atm Duty: 0			

VITA

NAME	Piyawan Thanahiranya
DATE OF BIRTH	19 March 1996
PLACE OF BIRTH	Ratchaburi, Thailand
INSTITUTIONS ATTENDED	B.Eng. Chemical Engineering, Thammasat University
HOME ADDRESS	29 Moo.2, Cham Rae Sub-district, Photharam District, Ratchaburi, 70120
PUBLICATION	<p>1) Thanahiranya, P.; Charoensuppanimit, P.; Soottitantawat, A.; Arpornwichanop, A.; Thongchul, N.; Assabumrungrat, S., Sustainable process design of propionic acid production from glycerol: A comparative study of bio-based and petroleum-based technologies. ACS Sustainable Chemistry & Engineering. 2022, 10 (45), 14761-14774. DOI: 10.1021/acssuschemeng.2c03761.</p> <p>2) Thanahiranya, P.; Charoensuppanimit, P.; Sadhukhan, J.; Soottitantawat, A.; Arpornwichanop, A.; Thongchul, N.; Assabumrungrat, S., Succinic Acid Production from Glycerol by Actinobacillus succinogenes: Techno-economic, environmental, and exergy analyses. Journal of Cleaner Production. 2023, 404, 136927. DOI: 10.1016/j.jclepro.2023.136927.</p> <p>3) Thanahiranya, P.; Sadhukhan, J.; Charoensuppanimit, P.; Soottitantawat, A.; Arpornwichanop, A.; Thongchul, N., & Assabumrungrat, S., Sustainability Assessment of Dihydroxyacetone (DHA) Production from Glycerol: A Comparative Study between Biological and Catalytic Oxidation Routes. ACS Sustainable Chemistry & Engineering. 2023, DOI: 10.1021/acssuschemeng.3c05354</p>



จุฬาลงกรณ์มหาวิทยาลัย
CHULALONGKORN UNIVERSITY